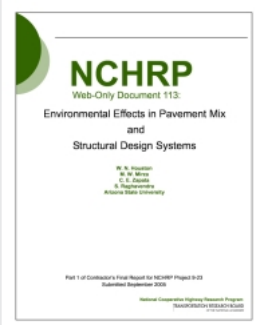

Environmental Effects in Pavement Mix and Structural Design Systems

DETAILS

0 pages | null | PAPERBACK

ISBN 978-0-309-43678-6 | DOI 10.17226/23244

AUTHORS

NCHRP

Web-Only Document 113:

Environmental Effects in Pavement Mix and Structural Design Systems

W. N. Houston
M. W. Mirza
C. E. Zapata
S. Raghavendra
Arizona State University

Part 1 of Contractor's Final Report for NCHRP Project 9-23
Submitted September 2005

National Cooperative Highway Research Program
TRANSPORTATION RESEARCH BOARD
OF THE NATIONAL ACADEMIES

ACKNOWLEDGMENT

This work was sponsored by the American Association of State Highway and Transportation Officials (AASHTO), in cooperation with the Federal Highway Administration, and was conducted in the National Cooperative Highway Research Program (NCHRP), which is administered by the Transportation Research Board (TRB) of the National Academies.

THE NATIONAL ACADEMIES

Advisers to the Nation on Science, Engineering, and Medicine

The **National Academy of Sciences** is a private, nonprofit, self-perpetuating society of distinguished scholars engaged in scientific and engineering research, dedicated to the furtherance of science and technology and to their use for the general welfare. On the authority of the charter granted to it by the Congress in 1863, the Academy has a mandate that requires it to advise the federal government on scientific and technical matters. Dr. Ralph J. Cicerone is president of the National Academy of Sciences.

The **National Academy of Engineering** was established in 1964, under the charter of the National Academy of Sciences, as a parallel organization of outstanding engineers. It is autonomous in its administration and in the selection of its members, sharing with the National Academy of Sciences the responsibility for advising the federal government. The National Academy of Engineering also sponsors engineering programs aimed at meeting national needs, encourages education and research, and recognizes the superior achievements of engineers. Dr. Charles M. Vest is president of the National Academy of Engineering.

The **Institute of Medicine** was established in 1970 by the National Academy of Sciences to secure the services of eminent members of appropriate professions in the examination of policy matters pertaining to the health of the public. The Institute acts under the responsibility given to the National Academy of Sciences by its congressional charter to be an adviser to the federal government and, on its own initiative, to identify issues of medical care, research, and education. Dr. Harvey V. Fineberg is president of the Institute of Medicine.

The **National Research Council** was organized by the National Academy of Sciences in 1916 to associate the broad community of science and technology with the Academy's purposes of furthering knowledge and advising the federal government. Functioning in accordance with general policies determined by the Academy, the Council has become the principal operating agency of both the National Academy of Sciences and the National Academy of Engineering in providing services to the government, the public, and the scientific and engineering communities. The Council is administered jointly by both the Academies and the Institute of Medicine. Dr. Ralph J. Cicerone and Dr. Charles M. Vest are chair and vice chair, respectively, of the National Research Council.

The **Transportation Research Board** is one of six major divisions of the National Research Council. The mission of the Transportation Research Board is to provide leadership in transportation innovation and progress through research and information exchange, conducted within a setting that is objective, interdisciplinary, and multimodal. The Board's varied activities annually engage about 7,000 engineers, scientists, and other transportation researchers and practitioners from the public and private sectors and academia, all of whom contribute their expertise in the public interest. The program is supported by state transportation departments, federal agencies including the component administrations of the U.S. Department of Transportation, and other organizations and individuals interested in the development of transportation. **www.TRB.org**

www.national-academies.org

TABLE OF CONTENTS

LIST OF FIGURES

LIST OF TABLES

ACKNOWLEDGMENTS

The research reported herein was performed under NCHRP Project 9-23 by the Department of Civil and Environmental Engineering at Arizona State University (ASU).

Dr. William N. Houston, Professor of Civil Engineering, ASU, was the principal investigator of the project and Dr. M. Waseem Mirza, Assistant Research Professor, ASU, was the co-investigator. The other authors of this report are Claudia E. Zapata, Faculty Research Associate at ASU and Suresh Raghavendra, former Research Assistant at ASU.

The preparation of this report was a team effort, with general supervision being provided by Professor Houston, Dr. Mirza, and Dr. Zapata. Major contributions were made by Suresh Raghavendra, Bonnie Whitley, and Yugantha Perera, Research Assistants; Dr. Matthew W. Witczak, Professor of Civil Engineering, ASU, and Project Coordinator; Dr. Norma F. Hubele, Professor of Industrial and Management Systems Engineering Department, ASU, and statistical consultant for the project; Gregg Larson, at ERES Consultants and programming consultant for the project; and Arianna Valle, Student Assistant.

ABSTRACT

It is well documented that environmental effects play a significant role in characterizing the material properties, which in turn affects the pavement performance. Studies under the Strategic Highway Research Program (SHRP) were carried out to study the age hardening characteristics of asphalt binders and mixes. As a result of this study, laboratory procedures American Association of State Highway and Transportation Officials, provisional protocols (AASHTO PP1-98 and PP2-99) were developed to study the hardening potential of asphalt binders and mixes. The approaches followed in these procedures are of great value for the ongoing research on pavement aging; however, due to the limited resources and time constraints under the SHRP program, these provisional procedures have certain limitations associated with them. Research study, National Cooperative Highway Research Program (NCHRP 9-23) was initiated to assess these limitations and if possible, enhance the predictive capabilities of these protocols.

Binders and field cores were obtained from LTPP sections and other sites across the United States. Original, laboratory-aged, and field-aged binders were characterized. Based on the findings, an alternate procedure to the AASHTO PP1-98 protocol is suggested and presented. The alternate procedure includes field aging conditions and volumetric properties of the mix. The model developed was calibrated and validated using the data obtained from the field cores. Parametric analysis was performed on the final model to ascertain the practicality of the output.

The assessment of the existing PP2-99 test protocol is also presented. Asphalt mix cores aged in the laboratory were tested for complex modulus. These modulus values were then compared to the modulus of the field cores, the age of which were known from the construction records. Due to the limited amount of data available, the PP2-99 protocol could not be improved, as it was the case for the PP1-98 protocol.

SUMMARY

This report documents and presents the results of the NCHRP 9-23 Project titled *Environmental Effects in Pavement Mix and Structural Design Systems.* The report has been divided into two parts. PART 1 presents the conclusions for the aging study and the work done under Tasks 2 and 7 presented below. PART 2 contains the findings for the moisture study, which comprises the work done under Tasks 4 and 5. PART 1 is presented in the following document, while PART 2 waits for final preparation details and will be presented shortly to the panel members.

Task 2 comprises the literature review on the development and validation of the Superpave mix conditioning procedures. Under Task 2, literature review was carried out in details and work by several researchers in the area of asphalt aging was identified. Wherever possible, data was extracted from the existing research studies that were considered useful for the current research work. Major effort was devoted to summarize the work done under the SHRP program. Under the SHRP program the major areas of concentration were to study both the chemical and physical changes that occur during the construction phase as well as during the in-service life of the pavement. What was concluded under the SHRP program is that both the chemical and physical properties can be used to characterize the age hardening behavior of asphalt binders and may be highly correlated. In this research work, only physical changes were considered to assess the age hardening characteristics of asphalt binders.

Task 7 objective was to conduct laboratory testing on the binders and field mixes to verify the following provisional protocols: AASHTO PP1-98, Standard Practice for Accelerated Aging of Asphalt Binder Using a Pressurized Aging Vessel, PAV and AASHTO PP2-99, Standard Practice for Mixture Conditioning of Hot Mix Asphalt.

The report is organized into 12 major chapters, which describe the general study approach adopted and the research findings:

- Chapter 2: Literature Review.
- Chapter 3: Correction Factor for Binder Recovery.
- Chapter 4: Verification of PP1-98 Protocol.
- Chapter 5: Improvement of the PP1-98 Protocol and Model Development.
- Chapter 6: Calibration of the Expanded PP1 Model with Field Data.
- Chapter 7: Validation of the Expanded PP1 Model with Field Data.
- Chapter 8: Parametric Study of the Expanded PP1 Equation.
- Chapter 9: Conclusions and Recommendations for Future Research Work on PP1 Protocol.
- Chapter 10: Verification of PP2-99 Protocol.
- Chapter 11: Analysis and Correlation of Laboratory Aged and Field Aged Cores Data.

- Chapter 12: Conclusions and Recommendations for Future Research Work on PP2-99 Protocol.

The conclusions of this research study can be found in two different chapters: Chapter 9 presents the conclusions and recommendations for future research work on PP1-98 protocol while Chapter 12 presents the conclusions and recommendations for future research work on PP2-99 protocol.

INTRODUCTION AND RESEARCH APPROACH

PROBLEM STATEMENT

The satisfactory design of a pavement mix and structural configuration for a layered pavement system requires the execution of numerous challenging tasks and must usually be done in an iterative mode. Two important aspects of this process are the use of a computational model to quantify environmental effects for the design period and translating changes in temperature and moisture contents into changes in moduli and other physical properties, including aging effects.

The Version 2.6 of the Integrated Climatic Model (ICM) was subjected to calibration and validation under this project. The ICM is a one-dimensional coupled heat and moisture flow model developed for the FHWA and adopted in the Guide for New and Rehabilitated Pavement Analysis and Design developed under NCHRP 1-37A project. The model is intended to predict or simulate the changes in behavior and characteristics of pavement and unbound materials in conjunction with environmental conditions over several years of operation. The research work presented in this report was intended to calibrate and validate the ICM version 2.6 moisture and temperature predictive capabilities and to develop practical guidelines for selecting ICM input data sets.

Environmental conditions play a significant role in the change of pavement material properties and hence the pavement response. This was also observed by several research studies including the work done under SHRP A-005 and SHRP A-002 studies.

The SHRP A-005 study clearly showed the environmental effect on the age hardening characteristics of asphalt binders (AAPT 1995 – "Development of Global Aging System for Short and Long Term Aging of Asphalt Cements). The importance of climatic conditions on the age hardening characteristics of the asphalt mixes was illustrated. Other factors considered were the volumetric properties (air voids), and the depth below the pavement surface. Furthermore, the model developed takes into account the temperature susceptibility of the binder.

In addition to the work done under SHRP A-005, work under SHRP A-002 resulted in the development of two provisional test methods to study the age hardening properties of asphalt binders (AASHTO Designation: PP1-98, Standard Practice for Accelerated Aging of Asphalt Binder Using a Pressurized Aging Vessel, PAV) and for the mixes (AASHTO Designation: PP2-99, Standard Practice for Mixture Conditioning of Hot Mix Asphalt, HMA). These two provisional procedures are associated with certain limitations and work was needed to verify the guidelines presented in these provisional protocols.

This research evaluated aging effects from two standpoints. First, the ICM-predicted temperatures were validated, because of the great importance of temperature in the asphalt aging process. Second, protocols for accelerated aging such as PP1-98 and PP2-99 were evaluated to find out if they correctly simulated changes in mechanical

properties, such as moduli, and if these changes occurred in periods of time which corresponded to those of the natural-aged prototype asphalt mixes.

CURRENT KNOWLEDGE

Integrated Climatic Model

The earlier versions of the ICM were comprised of three major components:

1. The Infiltration and Drainage Model (ID Model) developed at the Texas A&M University;
2. The Climatic-Materials-Structural Model (CMS Model) developed at the University of Illinois; and,
3. The Cold Regions Research and Engineering Laboratory (CRREL) Frost Heave and Thaw Settlement Model (CRREL Model) developed at the United States Army CRREL.

The ICM output includes temperature, moisture content, and freeze/thaw depths throughout the entire pavement profile, and can be applied to either asphalt concrete (AC) or Portland cement concrete (PCC) pavements. Modifications to the ICM have spanned the last decade (Lytton et al., 1990, Larson and Dempsey, 1997). In July 1999, the latest available version of the ICM was Version 2.1, as developed by Larson and Dempsey at the University of Illinois. Version 2.1 was nominated for use in the Superpave performance model and the *Mechanistic-Empirical Pavement Design Guide*. An ASU research team headed by Dr. M. Witczak initiated a series of checks on the predictive accuracy of the ICM Version 2.1 for ten LTPP SMP sites in 1999. The agreements between predicted and TDR measured moisture contents were judged unsatisfactory and the ASU research team was commissioned to develop a set of modifications to the ICM, aimed at increasing its predictive accuracy. Initially, the ASU team developed the following modifications:

1. Use of new functional fits for the SWCCs;
2. Use of new relationships between the SWCCs and material index properties;
3. Use of new hydraulic conductivity functions for saturated (k_{sat}) and unsaturated (k_{unsat}) materials; and
4. Employment of equilibrium moisture content as an input value.

In consideration of these findings, the question arose as to whether it was appropriate to input the equilibrium moisture in the general case, because, for example, these equilibrium moisture contents would typically not be known for new pavement construction where instrumentation is unavailable. Thus, it was ultimately concluded that the ICM should, in fact, be required to predict the equilibrium moisture contents. The incorporation of these modifications into the ICM code improved the predictive ability of moisture contents. However, the emphasis for this first study was on predicting seasonal oscillations about the equilibrium or mean moisture contents. It was later found that these seasonal oscillations were typically fairly minor, in the absence of open cracks in the pavement.

A major goal of the NCHRP 9-23 project was to evaluate if the improvements were adequate and if further improvements would be necessary. The decisions on how to make any needed improvement were based on the results of sampling and testing at the LTPP sites. The recommendations made from the moisture study part are included in this dissertation. The asphalt aging study part is in progress and recommendations are to be made once the results are analyzed.

Moisture Content Changes

Moisture content changes that occur after construction of the pavement section fall into one of three categories:

1. Increase or decrease from the initial condition (typically near optimum) to the equilibrium or "average" condition,
2. Seasonal fluctuation about the average or normal moisture condition due to infiltration of rainfall through cracks in the bound layer(s) and due to fluctuations in groundwater table in the absence of freeze/thaw, and
3. Variations in moisture content due to freeze/thaw.

Recent studies (Witczak et al., 2000) have shown that the effect on resilient moduli, M_R, due to categories 1 and 3 can be quite significant. However, category 2, i.e., seasonal changes in moisture in the absence of freeze/thaw, were found to produce typically insignificant changes in M_R. As a consequence of this finding, it was tentatively decided for the *Mechanistic-Empirical Pavement Design Guide* to assume that there are no cracks in newly-constructed pavements and that the GWT does not fluctuate during the design period. After making this simplifying assumption, the role of the ICM with respect to moisture content was the prediction of changes under categories 1 and 3.

The research team of the NCHRP Project 1-37A carried out a limited validation study (Witczak et al., 2000) of the ICM with data from ten LTPP SMP sections. However, the comparison between the ICM-predicted and the TDR-measured moisture contents was made in this study before the finding that seasonal changes in moisture content in the absence of freeze/thaw produced negligible changes in M_R had been made. Therefore, the comparisons were repeated as a part of the NCHRP Project 9-23, which was directed at the full data set from all the LTPP SMP sections. In this project, the emphasis was placed on prediction of the changes from the initial condition to the equilibrium condition and on freeze/thaw effects.

It is apparent that the prediction of moisture content alone is not a justifiable end. It is the effect of moisture changes on the mechanical properties of the pavement layers, such as M_R, that is of primary interest. Therefore, in order to decide if a given level of predictive accuracy on moisture content is acceptable or not, it is necessary to translate a typical error in moisture content into a typical error in modulus or another mechanical property.

Effects of Temperature

Temperature serves as the link between the environmental effects on unbound layers and bound layers. Temperature changes directly control freezing and thawing, which in turn produces dramatic changes in the M_R of unbound layers. Moduli of bound layers, particularly asphaltic layers, are likewise directly controlled by temperature, which also controls thermal cracking of the pavement. Furthermore, temperature and time couple to produce aging effects. Thus, temperature is a key variable in all of these processes which control the response of pavement sections to traffic loads, and the ICM is to be required to predict temperature.

RESEARCH OBJECTIVES

The objectives of this research project were to:

1. Validate the Version 2.6 of the ICM developed in NCHRP Project 1-37A with data from the Long Term Pavement Performance Seasonal Monitoring Program (LTPP SMP) and other field experiments.
2. Develop practical guidelines for selecting ICM input data sets.
3. Verify the estimated period or rate of aging simulated by the current Superpave binder and hot mix asphalt (HMA) conditioning procedures – AASHTO provisional practices PP1-98 and PP2-99 – with data from LTPP Specific Pavement Studies (SPS) and other field experiments.
4. Revise the current conditioning procedures as necessary for their use with the materials characterization test and model under development in NCHRP 9-19 project for the Superpave performance model system.

RESEARCH APPROACH

To accomplish the objectives described above, the NCHRP Project 9-23 was divided into three phases. The tasks within each phase are shown below.

PHASE I

- Task 1: Experiment Design for the Calibration and Validation of the Version 2.6 of the ICM
- Task 2: Literature Review on the Development and Validation of the Superpave Mix Conditioning Procedures
- Task 3: Preparation of the Interim Report Presenting the Results of Phase I

PHASE II

- Task 4: Validation of the ICM with the Full LTPP SMP Data Set
- Task 5: Sensitivity Analysis of the Fully Validated ICM
- Task 6: Preparation of the Interim Report Presenting the Results of Phase II

PHASE III

- Task 7: Experiments to Verify the Estimates of Rate of Aging Simulated by AASHTO PP1-98 and PP2-99 Test Procedures

Task 8: Preparation of Final Report

Task 1: Experiment Design for Calibration and Validation of the ICM Version 2.6

Task 1 required the preparation of a detailed, statistically based experiment design for the calibration and validation of the version 2.6 of the ICM. The experiment design began with the identification of the material and climatic input data needed for thorough analyses.

Task 2: Literature Review on the Development and Validation of the Superpave Mix Conditioning Procedures

This task included a critical review of the development of the Superpave mix conditioning procedures PP1-98 and PP2-99 that were developed to study the age hardening characteristics of the asphalt mixes.

Task 3: Preparation of the Interim Report in Summarizing Tasks 1 and 2

An interim report that documented the research performed in Phase I and included details of the work planned for Phases II and III was prepared and submitted to the NCHRP panel.

Task 4: Validation of the ICM with the LTPP SMP Data Set

Task 4 required the execution of the experiment developed under Task 1. This encompassed the calibration and validation of the ICM with the LTPP SMP data set and other data sets as may be found useful. This validation was an iterative process. The ICM was used in its current form for prediction, for the first iteration. Given that the predictive accuracy had room for improvement, then all available information and research findings available to date were used to develop a list of modifications to the ICM. These modifications were made and comparative runs were repeated until acceptable accuracy was achieved.

Task 5: Sensitivity Analysis of the Validated ICM

This task included a sensitivity analysis of the fully validated ICM. In other words, after the ICM predictions were made to be as accurate overall as was practical, a sensitivity analysis of the output variables to the input variables was completed. This quantification involved varying the input variables through a multi-factor designed experiment over their reasonable ranges and mapping the corresponding output variable ranges. This sensitivity analysis was important because rational decisions needed to be made relative to the time and money that should be spent in maximizing the quality of the input data. An informed basis was needed for deciding which input variables could be selected from a range of default values versus those inputs which should be project-specific or based on actual tests on materials from the project.

Task 6: Preparation of the Interim Report Presenting the Results of Phase II

An interim report that documented the research performed in Phase II was planned in Task 6. Given the delay in the research schedule, the Interim Report was not submitted to the NCHRP panel and instead, was delivered as part of the preliminary draft of the final report.

Task 7: Experiments to Verify the Estimates of Rate of Aging Simulated by AASHTO PP1-98 and PP2-99 Test Procedures

The objective of this task was to conduct laboratory testing on the binders and field mixes to verify PP1-98 and PP2-99 test procedures.

Task 8: Preparation of Final Report

The present document is the preliminary draft report. The final report will be submitted to the NCHRP panel once the revisions and recommendations from the panel are incorporated. The final report will summarize the findings and conclusions drawn during the study.

ORGANIZATION OF THE REPORT

The report was divided into two parts. PART 1 presents the conclusions for the aging study and the work done under Task 7. PART 2 contains the findings for the moisture study, which comprises the work done under Tasks 4 and 5. PART 1 is presented in the following document, while PART 2 waits for final preparation and will be presented shortly to the panel members.

PART I

CALIBRATION OF PP1-98 (AASHTO DESIGNATION PP1-98: STANDARD PRACTICE FOR ACCELERATED AGING OF ASPHALT BINDER USING A PRESSURIZED AGING VESSEL) AND PP2 (AASHTO DESIGNATION PP2-99: STANDARD PRACTICE FOR MIXTURE CONDITIONING OF HOT MIX ASPHALT) PROTOCOLS

CHAPTER 1

INTRODUCTION

BACKGROUND

In the last fifty to sixty years, a significant amount of research has been focused on the use and behavior of asphalt cements within pavement applications. It is well documented that environment plays a significant role in characterizing the paving material properties as a function of time, which in turn affects the pavement performance. The major environmental factors that affect material properties include temperature and moisture changes with time.

Properties of unbound materials that include both coarse-grained and fine-grained soils are heavily dependent on moisture and temperature. Temperature becomes more significant in areas subjected to frost action, wherein the water in the unbound material freezes and thaws. This freezing and thawing greatly influences the material response and hence the pavement performance[1].

In case of asphalt mixes, work done under the Strategic Highway Research Program, SHRP A-005 clearly showed the environmental effect (temperature) on the age hardening characteristics of asphalt binders[2]. The study concluded that higher mean annual air temperatures result in relatively higher rate of aging compared to the cooler climates[3]. The study also showed the effect of other parameters such as volumetric properties and the location of the asphalt layer in the pavement system on asphalt mix aging. Higher air voids results in higher oxidation and hence more stiffening of the asphalt mix. Asphalt layers that are located deeper in the pavement system do not come in direct contact with air; as a result, the oxidation of the binder in these layers is reduced. Therefore, the stiffening of the asphalt mix is inversely proportional to the depth at which it is located in the pavement system[4]. On the other hand, moisture does not have any significant effect on the aging properties of asphalt mixes. However, moisture may result in stripping phenomenon, which will eventually affect the durability.

Hardening, or aging of the original asphalt binder, due to the plant mix/laydown process (short-term aging) and normal in-situ aging (long-term aging) are extremely complex phenomena because of the numerous factors that influence the rate of aging. While the mechanism of aging is complex, its impact on pavement performance is generally understood. The short and long term aging processes result in the hardening of the asphalt binder with time. Thus, overall response i.e., dynamic modulus of the asphalt mixture also gradually increases in rigidity with time[1].

As the asphalt mix becomes more rigid with the aging process, an increased susceptibility to cracking and fracture occurs. This hardening of the asphalt cements (mixture) aids in the development of several distress types, which may ultimately lead to the failure of the pavement system[5]. Typical distresses that result from the aging of the asphalt include,

1. Disintegration
2. Fracture
    a. Fatigue cracking
    b. Thermal cracking

Disintegration may be viewed as a non-load associated cracking failure due to random, irregular surface cracking, which is brought on by the brittle nature of the asphalt cement due to the aging/oxidation process.

Fracture of the pavement system due to repetitive load or fatigue cracking may be accelerated due to the aging process. As the asphalt ages, the dynamic modulus, or stiffness of the mix increases. This increased stiffness will result in increased levels of tensile stress in the asphalt layer and hence result in accelerated load-induced fracture.

The increased stiffness due to aging can also be responsible for the accelerated growth of thermal fracture (transverse cracks) in a pavement system. Thermal fracture distress is associated with extremely cold temperatures that cause thermal stresses to be induced in the asphalt layer. Once these thermal stresses exceed the tensile strength of the layer, a transverse crack is developed across the paving lane. Therefore, as the asphalt ages, the mix stiffness is increased resulting in larger tensile stresses causing transverse cracks. Due to this immense effect that aging of asphalt has on the pavement performance, it becomes extremely important to simulate the field aging in the laboratory, study the properties of the aged-asphalt and incorporate them suitably in the mix design.

Work on age hardening properties was carried out under the Strategic Highway Research Program, SHRP A-003A to simulate the field aging in the laboratory. As a result of the work done under SHRP, laboratory procedures were developed to simulate the hardening potential of asphalt binders and mixes. The two procedures developed were: *American Association of State Highway and Transportation Officials, AASHTO Designation: PP1-98, Standard Practice for Accelerated Aging of Asphalt Binder Using a Pressurized Aging Vessel, PAV* for the asphalt binders, and *AASHTO Designation: PP2-99, Standard Practice for Mixture Conditioning of Hot Mix Asphalt, HMA* for the mixes[(6)]. The approaches followed in these procedures are of great value for the ongoing research on pavement aging; however, due to the limited resources and time constraints under the SHRP program, these provisional procedures developed have certain limitations.

NCHRP 9-23, *Environmental Effects in Pavement Mix and Structural Design Systems,* research study was initiated to verify the work done under SHRP and to provide conclusions on the significance of limitations associated with the existing protocol. Overcoming these limitations would involve the validation of these procedures with respect to their capability of predicting the age hardening characteristics of asphalt binders and mixes. To achieve this objective, laboratory tests were conducted on the binders and field cores obtained from LTPP and other sites across the United States at Arizona State University, Advanced Pavement Laboratory.

RESEARCH OBJECTIVE

The standard testing procedure under the existing PP1-98 protocol requires binder samples to be tested at the following conditions:

- Asphalt binder aged using T240 (RTFOT)
- PAV aging time = 20 hrs
- Air pressure = 2.10 MPa
- Aging temperature = 100°C or 110°C as a function of climate

The standard testing procedure under the existing PP2-99 protocol requires asphalt mix to be tested at the following conditions:

- Asphalt mix aged in the forced draft oven
- Aging time = 5 days
- Aging temperature = 85°C

The major limitations associated with the existing protocols can be summarized as follows:

1. PP1-98 protocol specifies the use of two PAV temperatures and PP2-99 protocol specifies the use of only one oven-aging temperature to represent a wide range of mean annual air temperatures (*MAAT)*. The *MAAT* in USA alone varies approximately from 35°C to 75°C. This wide range, coupled with the fact that PP1-98 protocol fails to specify a clear "cut-off" for the climatic conditions represented by each one of the PAV aging temperatures currently used, becomes a clear limitation.
2. The standard PP1-98 protocol represents the expected aging of the binder in a period of 5 to 10 years and PP2-99 protocol represents the expected aging of the mix in a period of 5 to 7 years. Two problems arise with this specification:
    a) The range is wider than desired, and
    b) Prediction of aging at any other time during the life of the pavement is not possible under the limited conditions of the current protocols.
3. The laboratory conditions are similar for every single binder. However, the aging potential depends on the binder type, which has to be accounted for in the protocols.
4. The aging estimated by the protocols does not account for volumetric properties, in particular variation in air-voids, which has a significant influence on oxidative aging[7].

The objective of this research study was to assess the aforementioned limitations associated with the aging protocols and to develop, if possible, a methodology to overcome these limitations to the maximum possible extent.

The main objective of this research study can be summarized as follows: to verify and improve the estimated period or rate of aging simulated by the current Superpave binder conditioning procedures – AASHTO provisional practice PP1-98 and PP2-99.

ORGANIZATION OF THE REPORT

The report is organized into 12 major chapters, which describe the general study approach adopted. A brief review of these chapters and the work accomplished in each one of them is presented to aid the reader to become familiar with the processes used to develop the final model in this study.

Chapter 2	Literature Review
Chapter 3	Correction Factor for Binder Recovery
Chapter 4	Verification of PP1-98 Protocol
Chapter 5	Improvement of the PP1-98 Protocol and Model Development
Chapter 6	Calibration of the Expanded PP1 Model with Field Data
Chapter 7	Validation of the Expanded PP1 Model with Field Data
Chapter 8	Parametric Study of the Expanded PP1 Equation
Chapter 9	Conclusions and Recommendations for Future Research Work on PP1 Protocol
Chapter 10	Verification of PP2-99 Protocol
Chapter 11	Analysis and Correlation of Laboratory Aged and Field Aged Cores Data
Chapter 12	Conclusions and Recommendations for Future Research Work on PP2-99 Protocol

Literature Review

This chapter presents the review of the literature pertaining to the asphalt aging process and procedures and binder extraction and recovery. In the later stages of the study, extraction and recovery of binders from field cores were adopted. Therefore, different extraction / recovery procedures and their relative merits and demerits are discussed.

Correction Factor for Binder Recovery

In this chapter, an experimental study to develop a correction factor to account for the changes in the binder viscosity that may occur due to the extraction and recovery procedures is presented.

Verification of the Current PP1-98 Protocol

This chapter presents the verification of the existing PP1-98 test procedure. The PP1-98 Protocol is designed to simulate five to ten years of oxidative aging that occurs in asphalt binders during pavement service. Binders aged in the laboratory were tested for viscosity. These viscosity values were then compared to the viscosity of the extracted binders from the field cores, the age of which were known from the construction records. The protocol was verified based on comparisons between lab aged and field aged binders.

Improvement of the PP1-98 Protocol and Model Development

This chapter presents a methodology to improve the existing PP1-98 test procedure. The current protocol specifies that one aging condition (another for desert conditions), one aging time (20 hours), and one confining pressure (2.1 MPa) represent five to ten years of aging in the field for all climatic conditions. Furthermore, no account is made for the volumetric properties of the asphalt mix. In order to increase the predictive capabilities and to overcome some of the limitations in the current protocol, an improved model was developed. This model is specific to the binder type and is based on field aging conditions.

Calibration of the Expanded PP1 Model with Field Data

This chapter presents the calibration of the expanded PP1 model using the field data. Field cores were obtained from three different agencies: MnRoad, WesTrack, and ADOT. Binders from these cores were extracted and submitted to DSR testing. Using the aging equation, the viscosity of the binders was predicted for the given set of field aging conditions. The predicted viscosity was then compared with the measured viscosity. Based on the comparison, the model was calibrated to fit the field data available.

Validation of the Expanded PP1 Model with Field Data

This chapter discusses the validation of the expanded PP1 model using the LTPP field database. The procedure followed in this task was similar to that followed in the calibration phase. The cores in this phase were taken from eight LTPP sites. The field aging conditions were obtained from the database *DATAPAVE*. However, the binders were not obtained from these sites, and the RTFO viscosities were generally not available from the database. Therefore, the RTFO viscosities were estimated using the A-VTS values obtained from the *Mechanistic-Empirical Pavement Design Guide*[8]. The viscosities obtained from these cores were used to validate the expanded model.

Parametric Study of the Expanded PP1 Equation

This chapter presents the sensitivity analysis of all the parameters involved in the PP1 Equation. A matrix covering the possible range of input values were used to generate the output. Based on the output generated, the constraints to be applied on the input parameters were determined.

Conclusions and Recommendations for Future Research Work on PP1 Protocol

This chapter presents the final study conclusions and recommendations for future work on PP1 Protocol.

Verification of PP2-99 Protocol

This chapter presents the verification of the existing PP2-99 test procedure. The PP2-99 Protocol is designed to simulate five to seven years of oxidative aging that occurs in asphalt mixes during pavement service. Asphalt mix cores aged in the laboratory were tested for complex modulus. These modulus values were then compared to the modulus

of the field cores, the age of which were known from the construction records. The protocol was verified based on the comparison between lab aged and field aged cores.

Analysis and Correlation of Laboratory Aged and Field Aged Cores Data

This chapter explains the methodology adopted to improve the existing PP2-99 test procedure. The current protocol specifies that one aging temperature (85° C) and one aging time (5 days) represent five to seven years of aging in the field for all climatic conditions. Also, no account is made for the volumetric properties of the asphalt mix. The data presented in this chapter points the fact that aging depends on environmental conditions and volumetric properties.

Conclusions and Recommendations for Future Research Work on PP2-99 Protocol

This chapter presents the final study conclusions and recommendations for future work on PP2-99 Protocol.

CHAPTER 2

LITERATURE REVIEW

INTRODUCTION

Asphalt and asphalt-based materials are of particular interest to engineers because of their desirable cohesive and thermo-mechanical properties, resistance to weathering, ease of processing and their comparatively low cost. It is a substance that imparts controllable flexibility for use in most instances and is usually resistant to most acids, alkalies, and salts. At ordinary atmospheric temperatures it is in a solid to semi-solid state, but liquefies at high temperatures. Because of these properties, asphalt is used for a great variety of purposes. For 1999, the estimated total production of HMA in the United States was close to 550 million tons, with a value nearly to $20 billion. This material was produced by an estimated 1,100 producer firms in approximately 3,600 HMA plants and placed by thousands of paving contractor firms. Among the various uses of asphalt, the major one is by the road paving industry. Out of 2.3 million miles of paved road in the United States, 94 percent are surfaced with asphalt[9].

This huge network of asphalt pavements in the US obviously involves a very big investment and requires a considerable challenge to keep these roads/highways in a serviceable condition. Without question, the durability of asphalt cement is a major factor that determines the life of asphalt pavement, and needs considerable attention. In general terms, durability is the resistance to change in property with time and traffic. When considering the asphalt pavements, it is known that changes in the original properties of asphalt do take place during construction and in-service. The amount of change in binder properties during construction and during the service life of the pavement defines the asphalt mix durability. This change in asphalt mix properties during the service life of the pavement directly affects the pavement performance. That is, in order to have desirable field performance; it is important to ensure, that the asphalt material not only has the necessary properties at the time of placement, but also during the service life of the pavement which defines the long-term durability.

Historically, it has been observed that many asphalt pavements exhibit poorer performance than they were designed for. One of the problems encountered with these pavements is the poor durability or excessive change in material properties with time. When considering asphalt pavements, change in material properties in terms of physical properties refers to the change in hardening characteristics of the binder. The hardening results in brittleness and makes the asphalt mix stiffer with time. This increase in rigidity under the applied traffic load and volume changes due to the seasonal variation in temperatures may produce stresses that lead to the development of cracks in the pavement layer. This development of cracks progresses with time as the asphalt binder becomes harder and harder. Consequently, the cracks developed reduce the structural capacity of the pavement and the pavement starts to deteriorate at a higher rate.

Looking at the phenomenon of hardening or aging and its relationship to the durability of asphalt cement, it is important to realize that both the ultimate hardening and the rate of hardening are concerns of asphalt technologists. Thus, the discussion in this chapter will be directed towards the evaluation and characterization of those properties that may be responsible for aging of the binder. Before discussing the aging phenomena of asphalt cement, it is important to first understand the basic fundamental properties of asphalt cement that are most commonly used in aging studies and how they affect the aging of asphalt binders.

FUNDAMENTAL ASPHALT CEMENT PROPERTIES

Asphalt cement is a black sticky material, which is solid or semisolid at ordinary atmospheric temperature, and readily liquefies upon heating, by dissolving it in petroleum solvent or by emulsifying it. It is either obtained in a natural form (very minor) or as a constituent of the petroleum refinery process (major). A major constituent of all asphalt is bitumen, which is composed primarily of complex hydrocarbon molecules, but also contains other atoms, such as oxygen, nitrogen and sulfur.

Among the several properties of asphalt cement, one of the most significant is its thermo-plasticity, i.e., it liquefies as it is heated and hardens as it is cooled. From liquid to solid state, asphalt behavior changes drastically and its flow properties are characterized as Newtonian, Pseudo-plastic, Dilatant, Bingham plastic and Thixotropic. This special combination of characteristics and flow properties is the fundamental reason why asphalt is used very extensively as a paving material. However, these properties are unique for a given asphalt type. In order to understand and describe asphalt behavior under different conditions, several measures, based upon physical and chemical properties, are used. These physical and chemical measures used by the asphalt researcher and engineers are discussed in the following sections.

Chemical Composition of Asphalt Cements

The chemical analysis of asphalts has always been a challenge for the asphalt chemists because of the chemical complexity and the wide variety of molecular types and structures present. In general the molecules in asphalt cement are characterized by relatively high molecular weight that imparts special characteristics to the asphalt cement and eventually to the asphalt mixes used for pavement construction. The amount and the ratio of different molecules that defines the chemical composition in the final asphalt product depend upon number of factors. Among the other factors, the main source of variation is the crude-oil source. This chemical composition imparts characteristics behavior to asphalt cement that is the thermo-plasticity and durability. As mentioned earlier, one of the factors that define the durability is the age hardening characteristics of asphalt cement.

Before discussing the age hardening characteristics of the asphalt binders and it relationship to the chemical composition, a brief discussion on the fundamental (chemical) behavior is presented.

Asphalt Chemistry

When we talk about the chemistry, the basic unit is the atom. An atom consists of a nucleus that contains protons and neutrons, that is surrounded by a "cloud" of electrons. The number of protons (positive charge) and electrons (negative charge) is equal within the atom. The electrons surrounding the atom can interact with other atoms to form molecules. There are several ways the atoms can interact with each other and form "bonds". Different type of bonding is formed depending upon the interactions of the electrons. When two or more atoms share the electrons, we call them covalent bonds. The covalent bonding between the atoms is usually very strong and requires lot of energy to be broken. The number of electrons that can be shared is unique to each type of atom. Since atoms of carbon can share up to four electrons, many different types of molecules can be formed, and long chains or rings of atoms are possible. For a single covalent bond, each atom contributes a single electron. The single bond between hydrogen (H) and carbon (C) atoms is represented as C-H. In case of two electron sharing as in the case of carbon (C) and oxygen (O), covalent double bond is formed and is represented as: C=O.

Chemist often refers asphalt as a hydrocarbon, which simply means that it is composed primarily of atoms of carbon and hydrogen. In fact, asphalts used for paving contain between 90 and 95 weight percent hydrogen and carbon atoms. The remaining 5 to 10 percent of the atoms in the asphalt consist of two types[(10)]:

- heteroatoms
- metals

The heteroatoms are nitrogen, oxygen, and sulfur. These atoms are called heteroatoms ("hetero" meaning different) because they can replace carbon atoms in the asphalt molecular structure. These heteroatoms contribute to many of asphalt's unique chemical and physical properties by forming associations between molecules. Both the kind and amount of heteroatoms present in a given asphalt are function of both the crude oil(s) from which the asphalt was produced and the state of aging of the asphalt.

The heteroatoms, especially, sulfur play an important role in the aging of asphalt because they are more chemically reactive than hydrogen or carbon, and can be oxidized, or incorporate oxygen, more easily than the hydrocarbons. When asphalt oxidizes, two main products are formed:

Sulfur atoms (S) are oxidized to sulfoxide (S=O)
Carbon (C) is oxidized to carbonyl (C=O)

The oxidation of the sulfur and carbon atom within the asphalt molecule results in the oxidative aging. This oxidative aging is the main cause of the long-term aging of asphalt binders. The amount of oxidative aging with time is related to the hardening as will be shown in the later part of this chapter.

The last group of atoms that asphalt contains in addition to hydrocarbons and heteroatoms are the metals. These are atoms such as vanadium, nickel, and iron that are present in very small quantities in the asphalt, usually less than 1 percent and may play an important role in the aging process. The amount of metals present in the asphalt is usually indicative of the crude source from which the asphalt was refined[10].

The three types of atoms; hydrocarbons, heteroatoms, and metals are all combined in the asphalt in a wide range of different molecules such as Aliphatic, Cyclic, Aromatic and are shown in Figure 1. As mentioned earlier, these molecules are the result of the formation of strong covalent bonds. These molecules can then interact with one another and forms molecular bonding, which is much weaker compared to the covalent bonding. These types of molecular interactions are important to chemists and asphalt technologists because they are responsible for determining many of asphalt's physical properties. The molecular bonding in the asphalt cement can be categorized into three types of "weak" bonds and are shown in Figure 2:

- pi-pi bonding
- hydrogen (or polar) bonding
- Van der Waals forces

In the case of a pi-pi bonding, the aromatic molecules (shown in Figure 1) form stacks of molecules due to their flat shape, and the electrons in the aromatic rings interact with one another to form pi-pi bonds. This pi-pi interaction is unique to aromatic molecules and leads to some interesting physical and chemical properties. Graphite is commercially important because its aromatic rings form flat sheets of molecules that can easily slide around on top of one another, giving it the slippery properties that make it such an excellent dry lubricant.

The second form of bonding is the hydrogen bonding. In this case the molecules containing heteroatoms are generally polar (have unevenly distributed electrical charges) and play an important role in affecting asphalt's physical properties by interacting with other molecules through the formation of hydrogen bonds. This occurs when a heteroatom on one molecule interacts with a hydrogen atom next to a heteroatom on a different molecule. This is illustrated in Figure 2. In this illustration the carboxylic acid group is interacting with the sulfoxide group on the molecule below it. This interaction is shown as a dotted line to signify that the bond is relatively weak when compared with the covalent bonds holding the atoms of the two molecules together. In general, two heteroatoms are required for the formation of hydrogen bonds. Research to date indicates that the heteroatoms play a crucial role in determining the physical properties of asphalt cements. Thus, hydrogen bonding is probably the most important of the forms of weak molecular interactions.

Van der Waals forces are the last form of weak interactions between molecules that are important in asphalt chemistry. In this type of very weak bonding, long chains of aliphatic hydrocarbons (such as hexane in Figure 1, but with more carbon atoms)

intertwine and are weakly held together. This type of bonding is dependent on the amount and type of aliphatic molecules in given asphalt, just as pi-pi bonding will depend on the amount and type of aromatic molecules, and hydrogen bonding depends on the number of heteroatoms.

As mentioned above, all of these types of bonds are weak and are easily broken by heat or stress. They will form again when the molecules cool or the stress is removed. This property of formation and breaking of weak bonds between the asphalt molecules is the key to understanding the physical properties of asphalt. It explains why asphalt is a free-flowing liquid at temperatures above about 250° F, where virtually all the molecules exist as individual entities (weak bonding breaks at high temperatures). It is also important to remember that the bonds between atoms that form the molecules such as those shown in Figure 1 are called covalent bonds and are not broken or reformed during the processes which normally take place in asphalt. The covalent bonds between atoms are 10 to 100 times stronger than the weak bonds between molecules.

Molecular and Fractional Level

The chemistry of asphalt discussed in the previous section clearly justifies as asphalt being a very complex material in terms of chemical composition. Characterizing asphalt at the molecular level requires analyzing complex mixture of heteroatoms that form the molecule of asphalt cement ranging in size from molecular weights of several hundred to several thousand. The relative proportion of heteroatoms depends upon the type and the source of asphalt, which defines the behavior of asphalt. Table 1 shows the typical proportion of heteroatoms from four asphalt sources. The table shows that carbon and hydrogen are the major constituents of the asphalt molecule but vary with different asphalt source. Other heteroatoms and metals, though present in small amounts, impart functionality and polarity to the molecules, which greatly influence the physical properties of the asphalt. Large differences in the proportional distribution of heteroatoms exist between different sources of asphalt making the molecular structure very complex. This, in turn, makes the determination of asphalt composition by molecular components separation very difficult, if not impossible, by present-day techniques.

The second approach (fractional level) is generally the preferred analysis scheme of asphalt chemists to simplify the chemical structure of asphalt cement. At this level, molecules are grouped together to form a fraction of asphalt. While several schemes have been developed to group the molecules into different fractions, it is important to realize that all the fractionation schemes separate asphalt into less complex and more homogeneous fractions. The fractions obtained are, in themselves, still complex mixtures since they contain a complex undefined proportion of heteroatoms or molecules. This scheme reduces the accuracy of prediction of the chemical structure of asphalt, which will directly influence the characterization of asphalt cement properties. However, several research studies have shown that the fractional separation is often sufficiently definitive to provide useful information to describe the complex nature of asphalt cement.

A variety of fractional distribution techniques are available, with some more complex than others. These separation schemes can be classified into five general types based on the procedure used[11]:

1. Partitioning with Partial Solvents
2. Selective Adsorption Desorption
3. Chemical Precipitation
4. Gel Permeation Chromatography (GPC)
5. Infrared Spectroscopy

Partitioning with Partial Solvents[13]

This technique separates the asphalt fractions based upon the polarity of the constituent. In general, asphalt is treated with increasingly polar solvents, which will result in a series of fractions with decreasing polarity. Three main fractional constituents (asphaltics, paraffinics and cyclics) obtained from this technique are shown in Figure 3(a)). This is not a widely used technique because the fractions obtained are not distinctively different.

Selective Adsorption Desorption[14]

This is the most widely used technique used by asphalt researchers. The flow of the scheme is shown in Figure 3(b). Asphalt is divided into four main constituents. In the first step, asphaltene, which is an insoluble substance, is separated based upon its insolubility in a non-polar paraffinic solvent. The remaining petrolenes (maltenes) fraction, which is dissolved in paraffinic solvent is then adsorbed on a chromatography column and sequentially separated with increasing polarity. The remaining constituents obtained after the asphaltene separation are:

1. Saturates
2. Naphthene Aromatic
3. Polar Aromatic

The typical physical characteristics observed for the above fractions are shown in Table 2. It shows that two of the fractions are found to be liquid and two solids. The liquid portion acts as a plasticizer for the solid proportions of asphalt. A higher percentage of the solid portion results in a more viscous grade asphalt. As mentioned earlier, at the elemental level, heteroatoms are found in different proportions in asphalt, and as a consequence, the fractions formed from these heteroatoms appear in very different proportions. Typical relative proportions of these fractions for the asphalt obtained from three crude sources are shown schematically in Figure 4. The proportions of these fractions separate the behavior asphalts from one another. In addition, the figure also shows the change in physical properties with the change in the chemical composition. The relationship between the chemical and physical properties is discussed in the later part of this chapter.

Chemical Precipitation[16]

This fractional distribution technique is based upon the chemical reactivity of asphalt with sulfuric acid. The schematic of chemical precipitation is shown in Figure 3(c). After asphaltenes are separated using precipitation, the remaining asphalt is then separated in fractions by different concentrations of sulfuric acid. Eighty-five (85) percent sulfuric acid is used to separate most polar components, including most of the basic and non-basic nitrogen compounds and many of the oxygenated molecules. Ninety-eight (98) percent is next used to precipitate the 1st acidaffins fraction, which contain unsaturated hydrocarbons. Lastly, sulfuric acid containing 30 percent SO_3, is used to separate less reactive components, called 2nd acidaffins. The final remaining fraction is called paraffins.

Gel Permeation Chromatography (GPC)

Gel Permeation Chromatography, also referred to as exclusion chromatography, is used to separate the constituents of asphalt on the basis of the molecular size rather than the type of chemical fraction. Analysis in this technique is based upon separating different molecular weights into distinct groups of molecular gradation. The GPC possesses pores of various known diameters. Asphalt mixed with a solvent such as tetra-hydrofuron is poured through the different size pores. A schematic profile of asphalt molecular size gradation obtained from GPC is shown in Figure 5. The x-axis is the time required for the molecule to emerge from the system and the y-axis is the representation of the concentration of asphalt molecules in solution. The time required for elution is related to the molecular size and the molecules are eluted in decreasing molecule sizes. Thus, in the figure shown, the molecule size decreases from left to right. The area under the curve is divided into eight groups, which may range from three to as high as ten groups depending upon the accuracy desired. A large number of groups would probably provide more accuracy, but would be too cumbersome to analyze. The molecular size distributions achieved are then used in describing the asphalt behavior.

Infrared Spectroscopy

This technique is used extensively for investigation of molecular structure and the analysis of functional groups. The technique is based upon the absorption of electromagnetic wave energy. The absorption of electromagnetic energy is recorded as a function of wavelength, specific groups of atoms in molecules giving rise to specific absorption bands whose wavelengths fall within a definite range regardless of the composition of the remainder of the molecules. The amount of absorption of the specific band of wavelength determines quantitatively the functional group present in the substance being analyzed.

The study of available literature shows that it is not important to analyze the entire range of the wavelength absorption spectrum. Only specific ranges of wavelengths are important to characterize the functional group for asphalt durability studies. Typical functional groups used in asphalt durability studies include: anhydride, carboxylic acid and ketone[17]. The absorption region of these groups lies between wavenumbers (reciprocal of wavelength) 1600 cm^{-1} and 1900 cm^{-1}. The amount of absorption of

electromagnetic energy by these groups reflects the behavior of asphalt. A typical absorption profile as a function of the wavenumber is shown in Figure 6.

Physical Properties of Asphalt Cements

The previous section on the chemical composition clearly shows the complexity of characterizing asphalt cement both on the molecular and fractional level. However, at the fractional level the complexity is much less compared to the molecular level. Because of this most of the researcher in the paving industry have opted to characterize asphalt based upon the physical properties. For most engineering and construction purposes, the physical characteristics of asphalt cements are usually used in specifications. It will be shown later in this chapter that the physical characteristics are related to the chemical composition and any change in chemical properties is reflected on the physical properties. The main physical measures used are by the paving industry are:

1. Consistency (flow properties)
2. Purity
3. Safety

Consistency

Consistency is used to describe the viscosity or the degree of fluidity of asphalt at a specific temperature. It is important to use a specific temperature when comparing the consistencies for different asphalts. This is because asphalt is a thermo-plastic material and its flow properties highly depend upon the temperature. At cold temperatures it is hard and behaves like an elastic material, whereas at high temperatures it is more viscous and flows under the action of gravity. The following are common, standard tests for measuring the consistency of asphalt.

1. Dynamic Shear Modulus (G*)
2. Viscosity
3. Penetration
4. Softening point

Dynamic Shear Modulus (DSM)

The DSM is intended for determining the linear visco-elastic properties of asphalt binders required for specification testing and is not intended as a comprehensive procedure for the full characterization of the visco-elastic properties of asphalt binder. The Dynamic Shear Rheometer (DSR) is the standard test method (AASHTO TP5-98) for determining the DSM and is applicable both to un-aged and aged asphalt binders.

The two properties obtained using the DSR are the complex shear modulus, G* and the phase angle. The G* is defined as the ratio calculated by dividing the absolute value of the peak-to-peak shear stress, τ, by the absolute value of the peak-to-peak shear strain, γ. The phase angle, δ, is the angle in radian between a sinusoidally applied strain and the resultant sinusoidal stress in a controlled strain testing mode, or between applied stress and resultant strain in a controlled stress testing mode.

The test can be carried out at various temperatures and frequencies. Oscillatory loading frequencies using this standard can range from 1 to 100 rad/s using a sinusoidal waveform. Specification testing is performed at a test frequency of 10 rad/s. The test temperatures for this test is related to the temperature experienced by the pavement in the geographical area for which the asphalt binder is intended. The complex shear modulus obtained at a specific frequency and temperature is an indicator of the stiffness or resistance of asphalt binder to deformation under load. The complex shear modulus and the phase angle define the resistance to shear deformation of asphalt binder in the linear visco-elastic region. Other linear visco-elastic properties such as the storage modulus (G'), or the loss modulus (G"), can be calculated from the complex modulus and the phase angle. The loss modulus (G") is a measure of the energy dissipated during each loading cycle.

Viscosity

Standard viscosity measurements are generally conducted at two major temperatures: 60°C (140°F) and 135°C (275°F) for most specifications. The 60°C (140°F) temperature typifies the maximum asphalt pavement temperature in service, whereas 135°C (275°C) generally represents mixing and lay-down temperatures for hot asphalt.

The viscosity test at 60°C (140°C) is generally carried out by capillary tube viscometers (ASTM D2171). Two commonly used viscometers are the Asphalt Institute Vacuum Viscometer and the Cannon-Manning Vacuum Viscometer. However, viscosity at 135°C (275°F) is commonly estimated by Zeitfuchs cross arm viscometer.

Penetration

The penetration test (ASTM D5) is an empirical measure of asphalt consistency. In this test, a needle with a standard weight is allowed to bear on the surface of asphalt cement for a given specified time. The distance, in units of 0.1 mm, which the needle penetrates into the asphalt cement, is the penetration measurement. The test can be carried out over a wide range of temperatures. However, if the test temperature is not specifically mentioned, the ASTM recommends the test to be done at 25°C (77°F) with 100 grams of load for 5 seconds. Other conditions may be used for special testing, such as the following:

Temperature, °C (°F)	Load, gms	Time, sec.
0 (32)	200	60
4 (39.2)	200	60
46.1 (115)	50	5

Softening Point

A softening point test is used to determine the temperature at which the fluidity of asphalt begins (ASTM D36). The softening point (or sometimes called the Ring and Ball Temperature) is important because it denotes an equi-viscous point for all asphalt

materials. Samples of asphalt loaded with steel balls are confined in brass rings suspended in a beaker of water, glycerin or ethylene glycol at 25 mm (1 inch) above the metal plate. The liquid is then heated at a prescribed rate. As the asphalt softens, the balls and the asphalt gradually sink towards the plate. At a moment the asphalt touches the plate, the temperature of water is determined and this is designated as the ring and ball (T_{RB}) softening point of asphalt.

Purity

The solubility test (ASTM D2042) is a measure of the purity of asphalt. Bitumen is a major constituent of asphalt and is 99.5 percent soluble in carbon disulfide (CS_2). Thus the percent of asphalt dissolved in carbon disulfide determines the purity of the asphalt cement in question.

Safety

The temperature at which asphalt fumes ignite generally defines the safety aspects of asphalt. Combustible fumes are produced by asphalt upon heating and specifications usually require that asphalt fumes produced upon heating should not catch fire up to at least 175°C (374°F). The Flash Point test (ASTM D92) is normally used to check the combustibility of asphalt as a function of temperature. In this test, asphalt is heated gradually. The temperature at which the fumes released from the asphalt ignite is defined as the flash point.

Relationship Between Chemical and Physical Properties

A brief overview of the chemical and physical properties of asphalt cement is presented in the previous sections. Both of these properties are used to characterize the behavior of asphalt cement, however, for specification purposes, physical properties are commonly used. This is because of the ease of measuring the physical properties and interdependence of physical properties on the chemical composition. The dependence occurs because each chemical fraction does possess a unique set of physical characteristics. Table 3 shows the physical characteristics of the chemical fractions considered in Corbett-Swarbrick procedure (Selective Adsorption-Desorption). The relative percentage of each fraction then defines the physical characteristics of the overall asphalt.

Table 3 shows that both saturates and naphthene-aromatic are liquid and have low viscosities compared to solid polar aromatic and asphaltene. It is important to note that all asphalts will have consistencies between the extremes defined by these fractions, in which the saturates and naphthene-aromatic are liquids acting as plasticizers for the solid polar aromatic and asphaltenes. No viscosity data for asphaltenes are reported in Table 3, because they have extremely large viscosities and cannot be determined with currently available equipment[18].

Another important observation made in the literature is that the relationship between chemical and physical properties is highly temperature dependent. This implies that two

asphalts, having the same viscosity at a given temperature with different chemical composition, may not have equivalent consistencies at other temperatures. This is because the chemical fractions of asphalt cement play a significant role in defining the temperature susceptibility. This can be explained by the study conducted by Corbett[15]. Figure 4 shows asphalt from three crude sources having different chemical fractions but the same consistency at 140°F (2000 Poises). However, different consistencies at other temperatures will occur because of the chemical fractions, each having different temperature susceptibilities and combined in different proportions. This combined "asphalt system" will result in a different temperature susceptibility of the overall asphalt. Figure 7 shows the temperature susceptibility concept schematically for the three asphalts shown in Figure 4. It shows that all three asphalt have the same viscosity at 140°F but different viscosities at other temperatures. Asphalt A shows the greatest change in viscosity with temperature change and is considered to be a highly temperature susceptible material compared to asphalts C and E.

MECHANISM OF ASPHALT HARDENING

Asphalt durability can be defined as the resistance to change from the original properties of the asphalt caused by construction process and in-service use. The ability of asphalt to resist change is related to the type and source of asphalt cement, which in tern depends upon the chemical composition. This change in the fundamental material properties in terms of physical and chemical properties is primarily caused by: (1) oxidation, which results in a change in structure and chemical composition, and (2) the loss of volatile oils. The loss of volatile oil is not considered a significant factor contributing towards hardening of asphalt cement for most paving grade asphalts. However, chemical restructuring and oxidation are known to be major factors contributing towards hardening (aging) of asphalt cement.

As mentioned earlier, both chemical and physical changes take place during the oxidation aging by reaction with atmospheric oxygen. It was found that this hardening is the result of the oxidation of certain asphalt molecules with the formation of highly polar and strongly interactive chemical fraction containing oxygen. Some of the most important fractional groups formed during oxidation are shown in Figure 8. The figure shows that the main oxygen groups formed during oxidative aging are; anhydride, carboxylic acid, ketone and sulfoxide. The amount of oxidation is related to the age hardening characteristics and can be measured by the chemical fractional techniques mentioned earlier. Peterson[17] has shown graphically the formation of these functional groups as a function of time, when the asphalt is cured in an oven at 45°C. This is shown graphically in Figure 9 for modified asphalt marketed as Chemkrete. Asphalt oxidized in the laboratory shows the change in the formation of ketone and anhydrides as the aging progresses. It is evident from the figure that the rate of formation of oxidized groups is higher initially and decreases as the time progresses. Formation of anhydrides and ketone is the major cause of the hardening of asphalt cement since they are the major constituents of the polar aromatic and the asphaltenes. As mentioned earlier, polar aromatic and asphaltenes are the solid constituents of asphalt, and an increase in these fractions will result in an increase in the viscosity of asphalt cement. In a similar study by Plancher[12], he studied the change in the chemical

fractions after Rolling Thin Film Oven (RTFO) test. Chemical fractions were analyzed by infrared spectroscopy and the results are presented in Table 4. The data represent averages for four different mixes. The data show that ketone and sulfoxide are major oxidation products formed during the oxidation aging; carboxylic acids and anhydrides are formed in small quantities.

Based upon the fractional composition of the asphalt as explained earlier, chemists and researchers have used these fractions to define the age hardening characteristics of asphalt binder. In Traxler and Schweyer[19], the asphalt is dissolved in n-butanol and insoluble materials are removed (also shown schematically in Figure 3(a). The insoluble materials are referred as "asphaltics". Next the acetone is added and the insoluble materials, called the saturates (S) or the parafinics are separated from the acetone soluble materials, which are called cyclics (C). In the later study, Traxler[20] further split the asphaltics into asphaltenes (A) and resins (R) based upon solubility in n-heptane. Based upon his findings, Traxler defined coefficient of dispersion "X" as (R+C)/(A+S) to characterize asphalt binder. A higher value of "X" indicates a better state of dispersion and is related to asphalt hardening.

In addition to the work done by Traxler, Rostler[21] has defined the asphalt durability by Rostler durability parameter ($N+A_1/P+A_2$) and the ratio of N/P (Figure 3(c)). In his approach n-pentane is used to separate the asphaltenes from the other four components. The other four components are nitrogen bases "N", first acidaffins as "A_1", second acidaffins as A_2 and the finally paraffins as "P". Generally, asphalts with high Rostler parameters and high N/P ratios have good physical properties mainly because high values of these parameters indicate aromaticity in the asphalt and consequently, highly solubilized asphaltenes. On the other hand, because the Rostler durability parameter is the ratio of the most reactive species to the least reactive species (neglecting asphaltenes), a high value of the Rostler durability parameter also indicates a tendency to react, and thus age[22].

Additional work on the chemical by Corbett [14, 23] suggests a shift in aromatic components (naphthene aromatics, NA and polar aromatics, PA) to asphaltenes. That is during the aging process, asphaltenes increase while napthene aromatics and polar aromatics decreases. The naphthene aromatics change to polar aromatics and then turn to asphaltenes. This is also shown schematically in Figure 10. Results in Figure 10 are for two depths. It shows that the changes were greater in the binder from the 1/8 in. top layer than in the binder from the ¼ in. in depth. This indicates that hardening changes are more pronounced at or near the surface of the pavement because of greater exposure to air, sunlight, and other atmospheric factors. Similar results were obtained by the work by Bullin, et al.[22]. Figure 11(a) shows the asphaltene production in the PA fractions aged at 95°C and 0.2 atmospheric oxygen, whereas, Figure 11(b) shows the increase in asphaltene content for five NA fractions aged at 100°C and 0.2 atmospheric. The increase in the asphaltene content will result in an increase in the hardness of the asphalt binder.

In addition to the fractional components, research was also concentrated on the development of the corbonyl content or the carbonyl area with the increase in the oxidation phenomena. Figure 12 is the FT-IR spectra of SHRP AAA-1 before and after oxidative aging. As the

aging progresses, the band representing oxygen – containing functionalities are intensified, with those of carbonyl group and the sulfoxide group increasing the most.

Carbonyl content or carbonyl area (CA) as measured by FT-IR was used as a measurement of oxidation. The sulfoxide band (near wavenumber 1000 cm^{-1}) increases very sharply during the early period of oxidation and then grows much more slowly. This is because sulfoxide is the product of sulfur oxidation, which happens rapidly at the beginning of the oxidative aging and then reaches a pseudo-steady state[11, 24]. Because of this, it is not suggested to use sulfoxide band for long-term aging. On the other hand the conbonyl band (near wavenumber 1700 cm^{-1}) grows with age. More importantly, numerous data have shown the linear relationship between carbonyl area and long-term aging. This is also shown in Figure 13 for the thirteen conditions shown in Table 5 for the SHRP AAA-1 binder.

Lau et al.[25] showed that at 20 atm oxygen pressure and at temperatures from 140-200 ^{o}F, the carbonyl formation rate becomes constant after an initial more rapid rate. The constant chemical rate will then vary as the exponent of the reciprocal absolute temperature. The rate of reaction is then given by this constant times a function of reactant concentrations. At the conditions in the POV, oxygen pressure is constant, and the actual oxygen uptake by the asphalt is so small compared with the number of available reaction sites, that effectively the reactant concentration are constant. If the rate of oxidation can be considered proportional to the growth rate in carbonyl area, then at temperature T:

$$\frac{dA}{d\theta} \sim k \sim \exp(-E/RT) \tag{2.1}$$

Where:

CA = carbonyl area,
k = the rate constant,
θ = time,
E = a constant energy of activation unique to the reaction taking place, and
R = gas constant (1.987 cal/g mol K).

From this equation:

$$\ln k \sim \frac{E}{R}\left(\frac{1}{T}\right) \tag{2.2}$$

Hence, one would expect a plot of k versus (1/T) to be linear.

Lunsford[26] expanded equation 2.1 to:

$$k = A' P^{\alpha} \exp(-E/RT) \tag{2.3}$$

to include the effect of oxygen pressure. In the constant rate region, carbonyl area CA as a function of time is:

$$CA = CA_o + k\,t \tag{2.4}$$

The above equations show the change in the carbonyl area as a function of time. However, this change in the chemical composition due to oxidation directly affects the physical properties of the binders. Typical trends obtained on the SHRP AAA-1 binder for the viscosity and the carbonyl area are shown in Figure 14. Figure clearly shows the increase in the viscosity with an increase in the carbonyl area for different aging conditions. In the literature the slope of log of viscosity to carbonyl area was defined as the hardening susceptibility, HS. HS is asphalt dependent and has been determined to be independent of aging temperature below 113°C [24, 25]. No literature discussion exists as to whether HS is aging pressure dependent, although the samples studied by Petersen et al[24] were aged at different pressures.

FACTORS AFFECTING AGE HARDENING

The hardening of asphalt binders occurs in two major stages. These stages are:

1. Plant hot mix and laydown operation
2. Long term in-service hardening

The basic cause of the hardening during the first stage (Short Term Aging - STA) is mainly due to volatilization and oxidation, whereas, oxidation is the major factor for the second stage (Long Term Aging - LTA). Several factors are responsible for the change in binder properties during these two stages. Some of these factors are controllable while others are uncontrollable. A brief discussion of the effect of these factors on the aging hardening characteristics of as asphalt binders is discussed below.

Plant Hot Mix and Laydown Operation

It is a generally accepted fact that a considerable amount of hardening occurs in the mixing and laydown operation in a relatively short period of time. This may amount to 10 to 30% of the total ultimate hardening of asphalt cement. The major factors responsible for hardening during the mixing operation are:

1. Plant Operation
    a. Mixing temperature
    b. Mixing time
    c. Mix composition
    d. Asphalt type
    e. Plant type
2. Laydown Operation
    a. Delay incurred in compaction after laydown
    b. Rate of cooling

Of all the factors mentioned above, the mixing temperature and the type of asphalt cement, are considered to be most important elements responsible for the short term hardening of asphalt cement. Plant mixing temperatures typically range from 275 to 350°F. Higher temperatures usually result in higher loss of volatile material in the binder and also accelerate the oxidation phenomena.

As mentioned earlier, an increase in the ketone fraction is the result of the hardening process and the major portion of ketone is found in the asphaltene fraction. Peterson[11] showed that asphaltenes are brittle solids at normal temperatures and are indeed quite unreactive at ordinary temperatures because their solid, highly structured state reduces molecular mobility, which, in turn, reduce reaction to oxygen. However, when asphaltenes are heated, their mobility and thus their reaction to oxygen increases. This process results in the formation of ketone and consequently, hardens the asphalt.

Bright[27] showed the effect of mixing temperature on percent retained penetration in Figure 15. It was concluded, that the percent-retained penetration decreases about 2 percent for each 10°F increase in the mixing temperature until a mix temperature of 340°F is obtained. At temperatures in excess of 340°F, the rate of decrease in retained penetration become more excessive.

In addition to the mixing temperature, the type of asphalt (ie. asphalt grade) is critical to the hardening phenomenon. Softer (low viscosity) asphalts are more prone to change compared to harder (high viscosity) grade asphalts. However, it is important to realize that higher temperatures during mixing and laydown are usually required for harder grade asphalts. Thus, this shows a direct link between the asphalt grade and the mixing temperature. This is also evident from Asphalt Institute specifications for mixing asphalt. The Asphalt Institute criteria requires that the mixing should be done between 150 to 190 centistokes and compaction be accomplished between 250-310 centistokes for all asphalt cement types. Thus higher temperatures are required to achieve these consistency limits for higher-grade asphalts.

Mixing time refers to the time it takes to mix the aggregate with asphalt cement. Longer mixing time will result in greater hardening of the asphalt cement if all other variables are kept constant. Greater hardening is due to the fact that asphalt is exposed to a high temperature (275-350°F) for a longer time period, which result in more loss of volatile material and also more oxidation. In contrast to long-term aging, mix composition does not have a significant effect upon the hardening of asphalt cement. This was also concluded by Bright[27] based upon three different types of mixes used in the plant mix operation.

The effect of plant type upon asphalt hardening has resulted in no significant effect. Bright[27] compared the results of hardening for plants from different manufacturers. His conclusions were: "*there appeared to be no clear cut evidence that the type of plant had appreciable effect on hardening*". The results obtained from his study for four plants are

shown in Figure 16. Lund[28] compared the hardening results between drum mixer and batch plants. He concluded there was a significant difference (at 90% level) between the two types, with the drum mixer resulting in a lower hardening of asphalt cement.

The mix/laydown and compaction operation is generally carried out in a short period of time after the plant mixing. However, delays in compaction may result in a greater hardening of the asphalt mix. This may also result in increased hardening, to greater depths below the pavement surface, if the asphalt is left in a loose state on the pavement or in the plant for a longer duration. However, in general it can be stated that, for all practical purposes, aging during the laydown operation is generally insignificant because the process is carried out in a relatively short time period. As such the plant mix and laydown operation can be considered as a one-stage process for short-term aging.

Rate of cooling refers to the amount of time required by the asphalt concrete mix to achieve atmospheric temperature. Bright[27], based on a laboratory study concluded "samples of paving mixtures that were cooled slowly in air showed approximately the same penetration loss at 300^{o}F and approximately 20 percent greater penetration loss at 400^{o}F than those quenched in water". Based on his findings it can be concluded that asphalt mixtures laid during cooler periods of the year may result in lesser hardening compared to the mixtures compacted during the warmer summer time period.

In summary, all the factors discussed do have some effect on the hardening phenomenon during the mix/laydown process. Unfortunately, not enough knowledge is currently available to quantitatively evaluate the impact of each parameter upon the consistency temperature shift from the original asphalt cement properties to those obtained at the mix/laydown conditions.

Long Term In-Service Aging

Long-term aging of asphalt cement, like the short-term age hardening process, is also the result of oxidation of the asphalt cement. Based upon numerous historic research studies, it has been shown that most of the hardening of asphalt takes place in the first 2-3 years. Major factors that contribute towards the rate of in-service hardening are:

1. Mix Type
2. Climatic Effects
3. Asphalt Type

Mix Type

The distribution of hardening within a layer of asphalt concrete is influenced by several properties of the as compacted asphalt mixture. Pavements with lateral cracking and high air voids have a greater degree of hardening and oxidation than un-cracked pavements with low air voids[29]. Thus asphalt recovered at some selected age with high air void content will be harder compared to the same asphalt with less air voids. Another important finding from the prior study noted was that air void content did not appear to be the only factor affecting the rate of hardening. Other factors, such as asphalt film

thickness in combination with air voids, need to be considered. It can be logically concluded that asphalt in the compacted asphaltic mixture which is in direct contact with the air will harden by oxidation at a much faster rate than the one not in direct contact with the air. Based on this assumption, it can be stated that if the film thickness of the asphalt coating on the aggregate is greater (due to a greater asphalt content), a longer time will be required for the entire thickness of the asphalt film to become hard.

The importance of air voids was also documented by a study done by the California Department of Transportation. The effect of air voids was studied on fabricated briquettes. The effect of voids shown in Figure 17, indicate a definite increase in hardening as the void percentage increases. It is important to keep in mind that the initial air voids play a dominating role but the rate of change of air voids as a function of time (due to traffic densification) is a very important factor to consider. The higher rate of reduction of air void over the thickness of the pavement will have a lower hardening rate compared to pavements which show a slower rate of reduction of air voids.

Climatic Effects

At present, fundamental environmental factors that influence asphalt aging are not clearly understood. Some of the major factors that influence the aging phenomenon of asphalt are:

1. Temperature Conditions
    a. Mean annual air temperature
    b. Maximum monthly air temperature
2. Cloud Cover
3. Radiation
4. Precipitation

The relative importance and how these variables interact are not well understood at this time. However, most researchers agree that mean annual air temperature is a good overall indicator of the climate influence in the study of the hardening process. A study carried out in Australia clearly indicated the importance of climate on the hardening process. The study concluded that the rate of thermal oxidation was approximately doubled for every 10°C (18°F) rise in temperature[3].

Kemp[30] shows the effect of weathering on fabricated briquettes. The change in absolute viscosity at 77°F for four climatic regions as a function of time is shown in Figure 18. The results clearly indicate an increase in the hardening rate in warmer climate.

Asphalt Type

This factor refers to the stiffness (viscosity) of asphalt cement after the mixing/laydown of the pavement. Asphalt with lower viscosities, were found to increase in viscosity more rapidly than asphalt with high viscosities. That is, the relative percent change at any time is greater for softer grade asphalt as compared to harder grade asphalt.

Field Hardening of Asphalt Cement

As discussed in the previous sections, hardening/aging of asphalt binder occurs in two stages. The second stage of hardening, which is also referred to as the long-term hardening phenomena occurs primarily due to the environmental conditions, with the largest in-service change in the properties of the binder occurring during the first 2-3 years of the service life of the pavement.

Confining our discussion to the physical properties of asphalt cement, it is not incorrect to state that a decrease in penetration and an increase in viscosity occur during the aging phenomenon. Figure 19 shows the trend in the rate of change in the consistency during mixing (short term) and in the service life (long term) of the nine pavement sections at the Zaca Wigmore constructed in California in 1954[31]. The curves have the normal expected shape with a rather rapid increase in hardening during first 16-20 months, and a definite decrease in hardening rate thereafter. It is important to note that the rate of hardening for all the sections varies considerably although all asphalts were of a 200-300 penetration grade. The different rates of hardening can be due to the different initial air void contents and the change in void content during the service life. However, the rate of hardening under similar weathering and pavement conditions is also influenced by the asphalt source.

EFFECT OF AGING AND ITS RELATION TO PAVEMENT PERFORMANCE

Performance can be defined as how well the pavement is performing its intended function as a function of time. In other words, it is a level of serviceability of a given pavement system. With the current practice, Present Serviceability Index (PSI) is used to measure the serviceability level of the pavement system. This is a subjective measure and is based upon the condition of the pavement. It is measured on a scale of 0 to 5, where 0 represents a very poor pavement with 5 being an excellent pavement. Typical plots of serviceability for two pavements A and B are shown in Figure 20. The decrease in serviceability level as a function of traffic/time is due to the deterioration of the pavement. The area under the serviceability curve represents the performance of the pavement. The greater area under the curve represents the higher level of performance, i.e., pavement B in the figure has a higher performance compared to the performance of pavement A. Thus, for a poor pavement the appearance of the distress will be rapid, which will then result in a lower performance level. The development of the distress or the performance of the pavement depends upon a large number of factors. However, binder properties are not the only cause of the development of the distress, they are considered to be the very important to the overall performance of any flexible pavement system.

The following primary distress types are typically considered by pavement engineers to study the performance of asphalt pavement.

1. Cracking
    a. Thermal Cracking
    b. Fatigue Cracking

2. Rutting (Permanent Deformation)
3. Moisture Damage

Cracking

Fracture of the asphalt pavement layer is the most important distress that may result from the hardening of asphalt cement. This is due to the fact that cracking of the asphalt cement is directly related to large (high) stiffness of the asphalt mixture. Cracking in the pavement is categorized as thermal or fatigue cracking.

Thermal Cracking

Development of thermal cracking in any material requires two obvious situations: (1) contraction (shrinkage) of some or all components of the concrete, and (2) stiffening of the mix to a point at which viscous flow cannot occur at a rate high enough to relieve the strain caused by the contraction. Asphalt cements are temperature susceptible, visco-elastic materials and their rheological properties depend upon the stiffness. As the environment temperature changes due to seasonal variations, expansion and contraction take place to release the stresses. Within the mix, since the aggregate effectively has no viscous flow (at any service temperature), the ability to flow and hence avoid cracking must be totally within the visco-elastic binder. However, aggregates may have various coefficients of thermal expansion and thus contribute differentially to pavement contraction. Therefore, variations in aggregate may have an effect on the overall problem of thermal cracking. If the binder is presumed totally responsible for the creep properties, then some chemical property or set of properties of the binder is responsible for the variation in flow properties among different asphalts.

For a new pavement the temperature stresses that are developed are released mainly due to the viscous flow of the asphalt mix. As the asphalt hardens its behavior changes from viscous to elastic behavior and becomes stiffer and more brittle. Thus, if the asphalt experiences a temperature drop, the thermal stress produced will exceed the tensile strength of the material and a crack will form. The development of such cracks increases as the hardening progresses. This will ultimately lead to a complete failure of the pavement system.

Fatigue Cracking

Fatigue of asphalt concrete is a result of repeated loads applied to the asphalt pavement. It is a fundamental fact that the fatigue life of the pavement is a function of the stiffness (modulus) of the asphalt mix. This is illustrated by the Asphalt Institute[32] fatigue procedure of asphalt pavements. The fatigue relationship is as follows:

$$N_f = 18.4 \times (4.32 \times 10^{-3} \times \varepsilon_t^{-3.29} \times E^{-0.854}) \quad (2.5)$$

Where:

N_f = number of repetitions to failure,

ε_t = horizontal tensile strain,
E = elastic modulus of asphalt mix.

The modulus values used are directly a function of the stiffness of the binder. Since, with aging, the viscosity of the asphalt increases, it results in a greater stiffness of the asphalt mix. This will result in a reduced life because of the lack of flexibility in the aged mat of the surface layer.

Numerous researchers have studied cracking phenomena related to asphalt hardening. Hubbard and Gollomb[33] reported a study showing the effect of asphalt hardening on the development of cracks in the asphalt pavements. They concluded that pavements having a penetration range between 26-51 were rated good to excellent, whereas pavements having penetrations below 26 were rated as poor. Another study by Lewis[34] summarized the correlation between pavement cracking and the performance. This is shown in Table 6. The study concluded that even though the performance results were greatly scattered, the relationship of asphalt properties to performance for various sources is in fair agreement. The effect of environment is evident in the Arizona and Cuba studies.

Kandhal[35] reported the change in asphalt properties and their relation to cracking. Figure 21 shows the trends of hardening for four sections in Pennsylvania (1961-1962). It shows that the cracking in the pavement occurs when the consistency of asphalt reaches a certain value regardless of the mix properties and original asphalt grade. The different rates of drop in penetration or increases in viscosity are the result of the differences in the air voids used in the four sections.

Rutting (Permanent Deformation)

Rutting of asphalt concrete pavements is primarily caused by permanent deformation of any layer in the structural system. This deformation is either caused by consolidation (volume change) or due to the shear flow (no volume change) in the pavement layer. An increase in stiffness of the asphalt concrete causes an increase in the rutting resistance of the pavement. Thus, aging of the asphalt cement binder results in a stiffer mix, which theoretically improves the rutting resistance of the pavement.

Permanent deformation of asphalt-aggregate mixes can be affected by asphalt type or by aggregate type and mix characteristics. It generally occurs at high temperatures because of shear stresses in the upper part of the pavement surface.

Moisture Damage

Moisture damage is a major concern in the performance study of the asphalt pavements. The aggregate-asphalt bond is weakened in the presence of water, which will result in the stripping of asphalt cement from the aggregate and the pavement shows localized structural failures. This phenomenon is accelerated as the hardening progresses.

Numerous studies (A-003B in particular) have demonstrated that moisture damage that causes loss of adhesion is primarily associated with aggregate. Classifying moisture damage susceptibility from the chemistry of only the binder is probably a minor effect. However, work under the SHRP program relates the carbonyl content with the moisture damage. More damage resulted into more oxidized asphalt.

IMPORTANCE OF AGING FOR PAVEMENT SPECIFICATIONS

In general, it is essential that short-term aging of mixtures in the field be controlled and that long-term aging not be excessive. While it is important to note that short-term aging in the field can be controlled through mixture specifications and by appropriate quality assurance, long-term aging is more uncertain.

Short-Term Aging

Alternative approaches in the mixture specifications are:

1. Setting limits of stiffness achieved after a short-term aging procedure relative to an un-aged condition. A factor of 2 may be a suitable upper limit; preliminary studies suggest this might cause a level of asphalt aging similar to that in the thin film oven test.
2. Establishing design levels of fatigue, rutting, or thermal cracking performance for the beginning of the life of a project and ensuring that these levels are met. Some projects may require only that permanent deformation to be controlled; specific requirements will depend on the pavement structure. The new *Mechanistic-Empirical Pavement Design Guide* for flexible pavement (NCHRP 1-37A) is based upon the aging that occurs during the short-term and long-term aging. Controlling or limiting the hardening during mixing and laydown operation will have significant effect on the overall pavement performance.

Long-Term Aging

The extent of long-term aging will depend on the amount of short-term aging that occurs. Mixtures that undergo relatively little short-term aging are more susceptible to long-term aging. Hence, a specification for long-term aging is meaningful only if the short-term aging in the field is controlled. As with short-term aging, alternative approaches exist:

1. Setting limits relative to an un-aged condition. A lower limit is necessary to ensure adequate deformation resistance, and an upper limit to ensure adequate fatigue and thermal cracking resistance. These limits could be established by engineering judgment. An example would be to limit the aging to a factor of between 3 and 4. Excessive aging will be prone to cracking and revealing of the asphalt layer.
2. Establishing design levels for fatigue, etc., after a period of 10 years (i.e., long-term aging) and ensuring that these levels are met. This is analogous with the second approach for short-term aging.

3. Use models for aging, stiffness, fatigue, deformation, and thermal cracking to estimate limits for aging on a project-by-project basis. The process is used in the new *Mechanistic-Empirical Pavement Design Guide* (NCHRP 1-37A) for the design of flexible pavement structures. The software developed can be used to study the effect of aging on rutting and fatigue as a function of asphalt layer thickness and material type.

Quality Assurance

Knowledge of the extent of short and long-term aging gives the assurance at the time of design and also during the construction about the service life of a pavement. A simple approach would be to estimate the hardening potential at the time of design using available aging models. In addition, verification of the hardening potential can be done by comparing the stiffness of the un-aged and aged mix just after construction. The aging index could be used as an indicator to estimate the service life.

AGING PREDICTION METHODOLOGIES

With the current state of knowledge, the prediction of age hardening characteristics can be broadly categorized into two groups. These are:

1. Laboratory Aging Tests
2. Aging Predicted Equations

Both of the above methodologies are discussed in the following sections.

Laboratory Aging Tests

A variety of methods have been used by several researchers and agencies to study the aging characteristics of asphalt during the mixing/laydown (short term) and in-service (long term) process. Unfortunately, no satisfactory test for estimating field hardening is generally accepted or in general use, because of the limitation attached to each test procedure. The available laboratory test will fall into following categories:

1. Binder Testing
    a. Short Term Aging
    b. Long Term Aging
2. Mix Testing
    a. Short Term Aging
    b. Long Term Aging

Binder Testing

Since the beginning of the use asphalt cement, hardening properties of the asphalt binder has been a major factor. In order to determine the hardening potential both during the mix/laydown operation as well as during the service life, several test procedures were introduced in the last century. The test procedures developed can be grouped into following categories:

1. Extended Heating Procedures
   - Thin Film Oven Test (TFOT)
   - Shell Microfilm Test
   - Rolling Thin Film Oven Test (RTFOT)
   - Rolling Microfilm Oven Test (RMFO)
   - Tilt-Oven Durability Test (TODT)
   - Thin Film Accelerated Aging Test (TFAAT)
2. Oxidation Tests
   - Air Blowing
   - Pressure Oxidation
3. Ultraviolet and Infrared Light Treatment

Extended Heating Procedures

Under the extending heating methods the most commonly used aging tests are the Thin-Film Oven (TFO) and Rolling Thin-Film Oven (RTFO). The Thin Film Oven-TFO (ASTM - D1754) is not a test, but a procedure to harden asphalt to a condition that approximates the condition occurring in a normal, hot mix facility. The change in mass or consistency before and after the procedure is an indication of the durability of asphalt cement. The test is made by placing a 50 ml sample on a 140 mm diameter and 10 mm deep pan. The asphalt layer is about 3mm deep. The sample is rotated, approximately 5 to 6 revolutions per minute in an oven at 163^{o}C (325^{o}F) for 5 hours. The mass loss in weight of the test sample is expressed as percentage of the original weight. The asphalt is then subjected to consistency measurements. The apparatus is shown in Figure 22(a).

The main objective of the Rolling Thin Film Oven-RTFO (ASTM - 2872) test is the same as the TFO test. In this test a specified amount of sample is poured into a bottle, which rotates at a specified rate at 163^{o}C (325^{o}F). The rotation of the bottle continues to expose a fresh film of asphalt cement. Once each rotation, the orifice of the sample bottle passes before an air jet. Heated air from the jet purges accumulated vapors from the sample bottle. The asphalt obtained after the RTFO is used for specification compliance with AR-viscosity graded series. The apparatus is shown in Figure 22(b).

Another test that is worth mentioning is the Thin Film Accelerated Aging Test (TFAAT). Petersen[36] and his coworkers have developed a modification of the RMFO to provide a 4 g sample of asphalt; a practical size for further testing. A temperature of 235^{o}F (113^{o}C) was used for 72 hours. As background to the test development, Petersen notes that many asphalts exhibit volatile loss in the TFOT and RTFOT in excess of what is typically lost during the lower temperature long-term aging in the field. He notes that Corbett and Merz[23], in analysis of asphalts used in the Michigan Test Road observed virtually no change in the asphalt saturate fraction (which contains the potentially volatile asphalt components) after 18 years of pavement service. He also notes that with regard to the TFOT and RTFOT, "the level of oxidative aging and hardening in the tests is much less than what occurs during field aging, reflecting only the aging that occurs during hot-plant mixing.

Oxidation Tests

The two methods under the oxidation tests are; air blowing and pressure oxidation. In case of air blowing, air is blow at the asphalt at 425°F (229°C) at a rate of 1/3 ft^3/min (0.0091 m^3/min) for 15 minutes. Penetration and ductility were measured before and after aging, and asphalts retaining higher values were judged superior.

In case of pressure oxidation, it is a two-stage test to simulate: hardening during mixing and hardening during service life. TFOT without modification is used to simulate the first stage and pressure oxidation is used for the second stage. The work on pressure oxidation is reported by Lee[37]. Figure 23 shows sample data from his study and the correlation between laboratory data and field data. Lee found that the development of aging followed a hyperbolic model.

Ultraviolet and Infrared Light Treatment

Vallerga et al.[38] reported on studies using both ultraviolet (UV) and infrared (IR) light to age asphalt films in TFOT containers. The ultraviolet treatment was found to be most effective in terms of changes in penetration softening point and ductility of the asphalts treated. Details of the work can be found in reference 38.

Mix Testing

Less work has been done with laboratory aging of mixtures than with binder studies. One of the biggest huddles was the extraction of the binder to study the effect of aging. However, the development of an accepted procedure for extracting and recovering asphalt from mixtures (Abson Recovery) no doubt influenced subsequent research, since many of the early studies on mixture aging involve tests on recovered asphalt.

Test procedures that were developed to study the age hardening characteristics of mixes can be grouped into following categories.

1. Extended Heating Procedure
2. Oxidation Test
3. Ultraviolet/Infrared Treatment

Extended Heating Procedures

Similar to the binder testing the loose or compacted mix samples are exposed to extended periods of heating. Once the asphalt mix sample is aged, the aged properties are determined by one of the procedures.

1. The hardening properties of asphalt cements can be determined either by measuring the mix properties such as the compressive strength or resilient modulus of laboratory oven-aged, molded specimens.
2. Extracting binder from the mix and comparing consistencies of un-aged and recovered asphalt.

Plancher et al.[11] also used an oven aging procedure on 1 in. thick by 1-1/2 in. diameter samples (25 mm by 40 mm) as a part of a study to evaluate the effect of lime on oxidative hardening of asphalt. It was found that the resilient modulus (measured with a diametric test configuration) of lime-treated mixtures was changed less than no treated mixtures by the aging process.

Hugo and Kennedy[39] describe a method of oven aging of mixture briquettes at 212°F (100°C). This procedure is similar to an Australian standard (Standards Association of Australia, 1980). This procedure was carried out for 4 and 7 days in a dry atmosphere and in an atmosphere of 80% relative humidity, due to the need to assess a project located close to the ocean. Asphalt was recovered for viscosity determination from 4 in. (100 mm) samples cored from laboratory- produced slabs to determine the age hardening characteristics of the mix.

Von Quintus et al.[40] have published the findings from the second phase of the study to develop an Asphalt Aggregate Mixture Analysis System (AAMAS). They investigated the use of forced-draft oven aging to simulate short-term hardening. They compared the recovered versus initial penetration and viscosity ratios for asphalts used in each of the five projects, for both field and laboratory aging. Von Quintus et al. discounted the possibility of using the TFOT or RTFOT to age the asphalt first, and then prepare laboratory mixtures, because this would be time consuming. In case of the long term aging Von Quintus et al. also investigated "long-term environmental aging". A forced draft oven was investigated with the following conditions:

1. Place six compacted specimens in the oven at 140°F (60°C) for 2 days, then remove three specimens.
2. Increase the temperature to 225°F (107°C) and age the remaining three specimens for 5 days.

Also, a pressure oxidation treatment was investigated, with three compacted specimens conditioned for 5 or 10 days at 140°F (60°C) and 100 psi. Von Quintus et al. recommend the oven aging approach over the pressure oxidation approach.

Oxidation Tests

Kumar and Goetz[41] describe a study of the effects of film thickness, voids and permeability on asphalt hardening in an asphalt-aggregate mixtures. Their method of hardening the mix involved "pulling" air through a set of compacted specimens at a constant head of 0.02 in. of water. The low head was used to avoid turbulence in the airflow through the specimen. The specimens were maintained at 140°F (60°C). The test was interrupted at periods of 1, 2, 4, 6 and 10 days and the samples tested in simple creep to study the age hardening characteristics.

Kim et al.[42] utilized pressure oxidation to age laboratory compacted samples representative of Oregon mixtures. Samples were subjected to oxygen at 100 psi and 140°F (60°C) for 0, 1, 2, 3 and 5 days. The effects of aging were evaluated by resilient modulus

and fatigue life determined by the diametric test. The modulus results for the three mixtures evaluated are shown in Figure 24. Data are plotted in terms of modulus ratio is defined as:

$$modular\ ratio = \frac{modulus\ of\ aged\ mixture}{modulus\ of\ unaged\ mixture} \tag{2.6}$$

Ultraviolet/Infrared Treatment

Hveem, Zube and Skog[43] presented a comprehensive description of various tests and specifications for paving grade asphalts. This included an infrared weathering test for Ottawa sand mixtures. The mixtures were tested in a "semi-compacted state". The infrared radiation was controlled to give a constant mass temperature of 140°F (60°C) and an air stream at 105°F (41°C) was maintained across the specimen.

Hveem et al. describe a calibration procedure to determine the number of hours required in the weathering test to correspond to field aging. This procedure utilized a shot abrasion test to evaluate the aged mixtures. The authors "state with some confidence" that 1000 hrs of exposure in the weathering machine is approximately equal to 5 years field aging.

Other researchers including Kemp and Predoehl[30] also utilized an "actinic light weathering test", ant the was conducted with the following conditions:

1. 35°C (95°F)
2. 18 hrs
3. 1000 MW/cm^2 of 3660 Angstrom actinic radiation

Hugo and Kennedy[39] evaluated the effect of UV-radiation on mixtures obtained from laboratory prepared slabs and freshly constructed field projects. Tia et al.[43] conducted an extensive laboratory study, which included developing aging methods by heat and ultraviolet light.

Aging Predicted Equations

Several regression equations have been developed in the past to characterize the age hardening characteristics of the asphalt mixes. Among these studies, the most comprehensive work was done by Mirza and Witczak[1] to characterize short and long term aging behavior. A brief discussion of the work done is presented below. It is worth noting that the equations developed are currently being used by the *Mechanistic-Empirical Pavement Design Guide* (NCHRP 1-37A) for flexible pavements to characterize the asphalt mixes.

The conceptual approach used to develop the global aging system is shown schematically in Figure 25. Figure 25(a) shows an asphalt surface layer for a typical pavement section. The depth at any point within the asphalt pavement layer is defined by "z" (ie. z=0 refers to surface, z=h_{ac} refers to the bottom of asphalt layer). Figure 25(b) shows the change in

asphalt properties with depth and time at a specific pavement temperature. The three lines shown on the figure define the three major conditions of the asphalt binder that occur during the life of the pavement system. The asphalt properties at these three stages can be categorized as:

1. Original (as refined) Properties
2. Mix/Laydown Properties (t = 0)
3. Field Aged Properties (t > 0)

Line #1 refers to the original (as refined) properties of the asphalt cement before it is used within the pavement surface. This original viscosity can be visualized as a constant value with depth. Line #2 refers to the mix/laydown condition (t=0), a condition at construction laydown. A constant viscosity with depth is used in the analysis, however a shift from the original viscosity is the result of hardening that occurs during the mixing and laydown operation. This shift (increase) in viscosity represents the short-term aging phenomena. Line #3 represents the field-aged properties of asphalt binder at any time (t>0) after the mix/laydown process. As shown in the figure, this change in viscosity is not uniform with depth below the pavement surface. This is because long-term aging (hardening) of the asphalt cement is mainly due to the oxidation process. The higher oxidation near the surface is due to the fact that asphalt is in direct contact with circulating air and direct solar radiation and this effect decreases rapidly with depth and becomes negligible at a few inches below the pavement surface. In addition, pavement temperatures at/near the pavement surface generally result in a wide temperature variation but also show a significant attenuation with depth. These changes will then result in a non-uniform viscosity with depth as shown by Line #3.

In order to determine the change in asphalt cement properties from the original to mix/laydown and then to field aged conditions, two separate set of equation were developed. The solution technique and the methodology used in accomplishing the above two phases are discussed in the following section.

Original to Mix/Laydown Condition

The following regression model was developed to predict the short term aging influence upon the original (refined) asphalt cement viscosity.

$$\log\log \eta_{t=0} = a_o + a_1 \log\log \eta_{orig}$$
$$a_o = (0.054405 + 0.004821\ x\ code) \qquad (2.7)$$
$$a_1 = (0.972035 + 0.010886\ x\ code)$$

Where:

$\eta_{t=0}$ = mix/laydown viscosity (cp) at temperature T_R (Rankine)
η_{orig} = original viscosity (cp) at temperature T_R (Rankine)
Code = hardening resistance (code=0 for average)

The hardening resistance (HR) is mathematically defined as the ratio of log-log mix/laydown viscosity to log-log original viscosity. The code value is used to account for the chemical composition and the selection of this value can be made by the user's previous experience with local plant/materials from the following table.

Mix/Laydown Hardening Resistance	Suggested Range	Code Value
Excellent to Good	HR <= 1.030	-1
Average	1.030 < HR <= 1.075	0
Fair	1.075 < HR <= 1.100	1
Poor to Very Poor	HR > 1.100	2

Mix/Laydown (t=0) to Field Aging (t>0)

The viscosities obtained at mix/laydown condition are then used to predict the in-situ time dependent properties (long term aging effect) of the asphalt binder by the following relationship:

$$\log\log \eta_{aged} = \frac{\log\log \eta_{t=0} + A\ x\ t}{1 + B\ x\ t} \tag{2.8}$$

Where

$$A = -0.004166 + 1.41213\ x\ C + C\ x \log(Maat) + D\ x \log\log \eta_{t=0}$$

$$B = 0.197725 + 0.068384\ x \log C$$

$$C = 10^{274.4946 - 193.831\ x \log(T_R) + 33.9366\ x \log(T_R)^2}$$

$$D = -14.5521 + 10.47662\ x \log(T_R) - 1.88161\ x \log(T_R)^2$$

η_{aged} = aged viscosity (centipoise),
$\eta_{t=0}$ = viscosity at mix/laydown (centipoise),
Maat = mean annual air temperature (^oF),
T_R = temp in Rankine ($^oR = ^oF + 459.7$).

Air Voids Adjustment Factor

Since limited information was available on the influence of air void content upon the general long-term aging model, this variable was not included in the final aging model. However, an adjustment factor that takes into effect the influence of air voids upon the aged viscosity ($\log\log \eta_{aged}$) is given below.

$$F_v = \frac{1 + 1.0367\ x\ 10^{-4}\ x\ VA\ x\ t}{1 + 6.1798\ x\ 10^{-4}\ x\ t} \tag{2.9a}$$

$$\log\log \eta'_{aged} = F_v\ x\ \log\log \eta_{aged} \tag{2.9b}$$

In this equation, "VA" is the air voids expressed in percentage at time, "t". The prediction of air voids at any time is obtained by the regression equation.

$$VA = \frac{VA_{orig} + 0.0111\,x\,t - 2}{1 + 4.24x10^{-4}\,xtxMaat + 1.169x10^{-3}\,x\frac{t}{\eta_{orig,77}}} + 2 \qquad (2.10)$$

$\eta_{orig,77}$ is viscosity at 77°F and is expressed in terms of Mega-Poise and VA_{orig} is the original (initial) air voids expressed in percentage.

Viscosity Depth Relationship

It is to be noted that the long-term aging model (equation 2.8) represents the in-situ viscosity at a depth of 0.25 inch from the surface. This is also shown in Figure 25(b). Point "A" on the figure shows the depth at which the aged viscosity predictions are made using equation 2.8. The viscosity at other depths may be obtained by the following relationship.

$$\eta_{aged,z} = \frac{\eta_{aged}\,x\,(4 + A) - A\,x\,\eta_{t=0}\,(1 - 4\,x\,z)}{4\,x\,(1 + A\,x\,z)} \qquad (2.11a)$$

$$A = 23.82\,x\,\mathrm{Exp}^{(-0.0308\,x\,Maat)} \qquad (2.11b)$$

The above equations provide the age hardening properties of the asphalt binder as a function of time and the environmental conditions. The mix properties are then obtained by the equation given in Figure 26. As can be seen the equations requires an aged viscosity values to estimate the aged mix modulus. The equation is a function of bitumen properties and the aggregate gradation.

AASHTO STANDARDS FOR AGE HARDENING CHARACTERIZATION

Under the Strategic Highway Research Program (SHRP), significant amount of effort was spent on characterizing the age hardening behavior both for the asphalt binder and the asphalt mix. Based upon the work done under SHRP A-002 and SHRP A-003, provisional AASHTO protocols PP1-98 and PP2-99 were developed. A brief overview of the work done is presented below.

AASHTO Designation PP1-98: Standard Practice for Accelerated Aging of Asphalt Binder Using a Pressurized Aging Vessel (PAV)

This practice covers the accelerated aging (oxidation) of asphalt binders by means of pressurized air and elevated temperature. The test method is intended to simulate in-

service oxidative aging of asphalt binders and is intended for use with residue from AASHTO T 240 (RTFOT). The test provides an estimate of the physical or chemical properties of asphalt binder after five to ten years of in-service aging in the field.

The concept presented by the test is excellent; however, the key is the accuracy or the confidence level in the prediction of the property change. Because of the limitations associated with the test, a verification study is needed. The limitations associated with PP1-98 protocol are:

1. For asphalt binders of different grades or from different sources, there is no unique statistical correlation between the aging time and temperature in this test and in-service pavement age and temperature. Therefore, for a given set of in-service climatic conditions, it is not possible to select a single PAV aging time and temperature that will accurately predict the properties of all asphalt binders after a specific set of in-service exposure conditions.
2. The relative degree of hardening of different asphalt binders varies at different aging temperatures in the PAV. Therefore, two asphalt binders may age similarly at one temperature, but age differently at another temperature.

AASHTO Designation PP2-99: Standard Practice for Mixture Conditioning of Hot Mix Asphalt (HMA)

This practice describes the procedures for the short and long-term aging of uncompacted and compacted hot mix asphalt (HMA). Similar to the PP1-98 protocol, this procedure is associated with certain limitations as listed below.

1. In case of the short-term conditioning, the test procedure does not account for mixing process (batch or continuous) and time.
2. For the long-term aging, in contrast to PP1-98, this method does not account for the climatic effects on the age hardening characteristics. This is important because different mixes will result in different age hardening characteristics depending upon the aging (environmental) temperature.

No link is established between the conditioning time and the age hardening characteristics of the mix. The test only provides relative comparison between the mixes for specific environmental and traffic conditions.

AGING OF ASPHALT BINDER

Bell, 1989, discussed short-term aging and long-term aging associated with volatilization and oxidation, respectively[47]. The Superpave asphalt binder specifications address these two major mechanisms of asphalt binder aging. Short and long-term aging are addressed through the use of the RTFO and PAV aging procedures, respectively.

Short-Term Aging

Changes in asphalt binder characteristics that occur during the mixing, lay down, and compaction processes were associated with short-term aging. In 1940, Lewis and

Welborn introduced the TFO test for differentiating volatility and hardening characteristics of asphalts[47]. In 1963 Hveem, Zube, and Skog introduced the RTFO test in specifications for the CALTRANS[47]. Bell, 1989, summarized the test methods that have been used to simulate the short-term aging on asphalt binders[47]. He identified six test methods:

1. Thin film oven test
2. Shell microfilm test
3. Rolling thin film oven test
4. Rolling microfilm oven test
5. Tilt-oven durability test and
6. Thin film accelerated aging test

Initially, The Rolling Thin Film Oven (ASTM D 2872) and Thin Film Oven (ASTM D 1754) tests were both being utilized for short-term aging in the Superpave asphalt binder specifications[47]. The same authors stated that further investigation of these test methods were discontinued and "attention was given to long-term field aging which is not addressed in the current specifications". In the final version of the PG specification, the RTFO test was selected to approximate short-term aging. The RTFO was selected for the following reasons: temperature can be controlled more precisely, more samples can be aged in a relatively shorter time, and modified binders can be tested without "skin over"[47].

Long-Term Aging

Asphalt binders age due to two major mechanisms: volatilization or short-term aging and oxidation or long-term aging. The in-service or long-term aging of asphalt binders represent slow, longer term oxidation[47]. Due to relatively moderate in-service temperatures, long-term volatilization is slow. Thus, the in-service aging or long-term aging is mainly related to oxidation of asphalt binders. In the Superpave asphalt binder specifications, long-term aging is represented by the PAV test, which reflects both the chemical and physical changes of asphalt binders in-service [47].

The PAV test is intended to approximate five to ten years of in-service aging. However, several factors affect in-service aging, which could influence this approximation[47]. These factors are: local climatic conditions, aggregate type, absorption, mixture type, asphalt film thickness, air-void content, traffic loading, and asphalt chemical composition.

In reviewing previous efforts to select a long-term aging test, the PAV test was adopted for Superpave because it is a relatively fast and simple procedure.

Concerns Related to Superpave Asphalt Binder Specifications

Short-Term Aging

Anderson and Kennedy in 1993 reported, "Aging or hardening of asphalt cement occurs during mixing and lay down process and during service. The existing methods, the Thin

Film Oven Test (TFOT) ASTM D 1754 and Rolling Thin Film Oven Test (RTFOT) ASTM D 2872, were reviewed and questions were raised with regard to the calibration of these methods for different plants, operating conditions, asphalt sources, and aggregate types. An in-depth study to validate and cross-correlate the two test methods was considered, however, a comprehensive evaluation of TFOT test and RTFOT test methods would have consumed a disproportionate amount of the available resources. Therefore, further study of the two methods was discounted and attention was given to long-term field aging, which is not addressed in the current specifications. In order to simplify the specification, the rolling thin film oven test was chosen as the single test for the new Superpave asphalt binder specification.

The RTFOT test can be completed more rapidly than TFOT test, the RTFOT test is preferable for polymer-modified binders, and there is less between-laboratory variability for the RTFOT test than for TFOT test. Hence the RTFOT test was chosen in preference to the TFOT test. If both the RTFOT and TFOT tests were retained in the Superpave asphalt binder specification the net effect would have been to double the number of grades because different asphalt cements and different asphalt binders respond differently to the two tests"[47].

In 1989 Nelson and Wood reported that the TFO test was not severe enough to simulate the mixing stage for the asphalt cements, which were extracted/recovered from loose mixes used in their study[47]. These results were from mixtures produced in both drum-dryer and batch plants. Professor Leonard Wood indicated, "the local limestone and/or dolomite aggregates have an adverse affect on aging of asphalt cements due to their chemical compositions and adsorption"[47]

R. G. Hicks, F. N. Finn, C. L. Monismith and R. B. Leahy, in 1994 reported, "Aging of asphalt alone, and subsequent testing does not appear to be adequate to predict mix performance because of the apparent mitigating effect aggregate has on aging." The authors added, "The aging of certain asphalts is strongly mitigated by some aggregates but not by others. This appears to be related to the strength of chemical bonding (adhesion) between the asphalt and aggregate"[47]

Bell, 1989 also expressed concern about aging the neat (original) asphalt. He stated that asphalt binders age differently in a binder-aggregate mixture[47].

Long-Term Aging

The pressure aging vessel (PAV) was developed as part of the SHRP research program to simulate long-term aging of asphalt binders. However, there is concern that the PAV aging fails to predict in-service aging. Many researchers have an opinion that the PAV fails to predict 4, 8, or 15 years of in-service aging[47]. Climatic conditions in particular play a very important role in this regard. Harrigan, et al, 1993, reported, "This method is designed to simulate oxidative aging that occurs in the asphalt binders during pavement service. Residue from this test may be used to estimate physical or chemical properties of an asphalt binder after five to ten years of aging in the field. For asphalt binders of

different grades or from different sources there is no unique correlation between the aging time and temperature in this test and in-service pavement age and temperature. Therefore, for a given set of in-service climatic conditions, it is not possible to select a single PAV aging time and temperature that will predict the properties of all asphalt binders after a specific set of in-service exposure conditions"[47].

Similar statements can also be found in 1995 and 1996 AASHTO Provisional Standards[47]. Moreover, Andersen, et al, 1994, stated, "It is beyond the scope of this study to establish a quantitative relationship between laboratory-aging parameters (aging temperature-time) and field aging parameters that include service temperature-time as well as mixture variables"[47]. Citing some examples, they conclude that the relation between aging conditions in the PAV and conditions in the field is not very simple and the role of climate and the equivalency of the PAV aging should be evaluated relative to local pavement climate.

Branthaver et al, 1994, reported, "The results of the TFO-PAV aging conducted at temperatures of 60°, 70°, and 80°C (140°, 158°, and 176°F) indicated that the maximum temperature to which the pavement is exposed is an important factor in determining the eventual hardening of the pavement. The results showed that asphalts have widely ranging responses to rather small changes in temperature that occur in the pavement service temperature range. An aging test used to predict long-term durability of an asphalt layer or pavement must take into consideration the climate to which pavement will be exposed.

It was also found that aging of any asphalt was characterized by a response to one predominant factor, which differed among asphalts. This was not surprising because aging is a combination of oxidation, loss of volatiles, and response of the system to the first two factors. At present the findings of the statistical analysis is that aging of asphalt will probably have to be measured and cannot be predicted by simple methods"[47].

BINDER EXTRACTION AND RECOVERY

It is necessary to understand the error associated with the extraction and recovery process. This is important since the validation of the PP1-98 protocol is highly dependent upon the extraction of binder from the field cores. The extracted binder will be used for measuring the physical properties in the hot mix or in the pavement samples. It is important that the recovered asphalt is a true representation of the binder in the mix or the field cores.

It has been well documented in the literature that the properties of binder may change to some extent during the recovery process and a significant amount of variability exists in the test results between laboratories. This can be seen in the American Association of State Highway and Transportation Officials' (AASHTO) inter-laboratory proficiency tests in which various laboratories analyze pavement specimen provided by AASHTO for several properties, including asphalt content and viscosities of two different but similar asphalt mixtures. Figure 27[48], shows the results from 62 laboratories used in this study.

Points inside the box lie within one standard deviation of the mean and diagonal line represents perfect inter-laboratory reproducibility. The standard deviation of viscosities in these tests ranged from 25 to 42 percent. Unfortunately, the extraction methods were not specified and vary considerably between laboratories. It is likely that the error in the extracted asphalt samples stems due to the following reasons:

1. Asphalt in not completely or consistently extracted from the aggregate,
2. Residual solvent is left in the asphalt after recovery, and
3. Reaction of asphalt while in solution, sometimes called solvent aging, can alter the properties during both extraction and recovery.

Each of the above mentioned problems have been evaluated in the past by several researchers. Some of the above mentioned problems are more critical in the extraction phase whereas, the others are important during the recovery phase. In addition, these are also highly dependent upon the type of extraction and recovery procedures. At present, laboratories use several extraction and recovery processes. Some of the most common processes accepted by the paving industry are discussed below.

Extraction Methods

The two commonly used approaches for the extraction is the centrifuge and the reflux methods (usually in the form of ASTM D-2172, method A and B respectively). Other methods include vacuum extraction and sonification methods, but used infrequently.

Incomplete extraction and solvent aging are two major problems to consider when selecting an extraction method. Although all procedures have problems to some extent, some have more than the others. As an example, the reflux method exposes the asphalt to solvent at elevated temperature for a long period of time. This has been shown to cause considerable hardening caused by reactions that the asphalt undergoes when it is in dissolved state. The reaction even occurs at room temperature and the reaction rate increases exponentially with temperature and are constant over time. Under these circumstances, it is desirable to minimize these variables so as to limit the reaction that occurs during the extraction process. ASTM has also warned that the reflux method (D-2172B) should not be used when asphalt properties are to be measured.

The ASTM D2172 Method A typically leaves 2 to 4 percent of asphalt on the aggregate when trichloroethylene (TCE) is the extraction solvent. Modification of Method A by adding 15 percent ethanol to TCE in later washes and mixing thoroughly during each wash removes about half of the strongly absorbed material that method A leaves behind. However, ASTM D2172B, seems to have poor solvent contacting and leaves much more un-extracted asphalt.

The choice of extraction solvent is important in determining how much of the asphalt is extracted by a given method. However, for this research study we were more interested in the quality of the binder extracted rather than the quantity. The use of additional 15 percent ethanol was found to be very useful for hard-to-extract asphalts. It is believed

that most of the absorbed binder that is hard to extract usually have higher viscosity since it comes in direct contact with the aggregate during the mixing process, which is at a relatively high temperature. This resulted in an absorbed binder to become part of the aggregate and does not act as the binder in the asphalt mix. It is the effective binder (non-absorbed) that is more important for pavement performance and not the absorbed binder.

Burr, et al.[48] in their comparison work showed the effect of solvent on the extraction process. The comparison was carried out between the following extraction methods.

- SHRP Method
- ASTM D2172A
- ASTM D2172B

The results of the comparison are shown in Table 7 and are graphically shown in Figures 28 and 29[48]. The symbol ETOH in Table 7, and Figures 28 and 29 represents 15% ethanol that is added with the solvent during the extraction process. In this table the samples were obtained from two sites (Tex 21/77 and Young Bros. Pavement). Table 7 shows the solvents used with each extraction process. In addition, the table shows the extracted viscosities, amount of strongly adsorbed material recovered and the total amount of solvent used. The adsorbed asphalt was obtained by soaking the aggregate in 400 ml of TCE/15 percent ETOH. After four days of soaking the solvent was filtered from the aggregate samples.

The results obtained showed that the SHRP method and the modified method ASTM D2172A yielded similar average viscosities and had comparable precision. However, the Method B (using TCE) and Modified Method B (using toluene or toluene/ethanol) extraction resulted in lower viscosities in all cases and generally less reproducible.

It was concluded that the extracted viscosities varied directly with solvent strength, contacting efficiency, and the volume of the solvent used in the extraction. Another very important conclusion made was that the viscosities were not however, related to the amount of strongly absorbed material that could be recovered from the aggregate after extraction. This was an important conclusion for this project, since the main objective was to study the properties of the binder and not the estimation of asphalt content. Any remaining strongly absorbed binder is not going to affect the results and need not to be extracted, since it will not be a factor that affects the viscosities of the extracted binder.

Binder Recovery from Solvent

After the extraction process, the next step is the recovery of the binder from the solvent. Typically, removal of solvent is carried out by Abson method, ASTM D1856 or by rotary evaporation. The Abson method (ASTM D1856) removes solvent by distillation with the aid of CO_2 purge. The rotary evaporation, also termed as Roto-vap method, uses a rotary evaporator to mix the solution and a vacuum and vent gas to vaporize and sweep away solvent. Both methods are associated with problem of incomplete solvent removal

because the prescribed reaction times and temperatures do not guarantee complete solvent removal. Higher temperatures and longer distillation time for maximum removal may result in hardening of the binder and is dependent upon the binder type. The removal of the entire quantity of solvent is very important since even low solvent concentration in asphalt (about 0.2 percent) is enough to cause significant change in physical properties.

Burr et al. studied the extraction and solvent removal effects on viscosity during solvent removal process for three situations. Tank (AC –20) and oven aged (rolling thin-film oven test, RTFO) asphalts were dissolved in TCE at room temperature and solvent removal was initiated within 1 hour. The refluxed sample was a mixture of approximately 25 weight-percent tank asphalt (AC-20) in TCE that was refluxed for 4 hours at 200°F before initiating solvent removal. The reflux procedure simulated the conditions of hot extraction method such as ASTM D2172, Method B.

Figure 30[(49)], shows the effects of the recovery procedure on the hardening of asphalt binder for the three conditions. It can be observed that considerable amount of softening occurs by even small amount of solvent. The other important observation was the different degrees of residual hardening when reaching zero-solvent concentration for different asphalts and situations. It was observed that the tank asphalt typically hardened 5 to 10 percent above their original values. This effect probably resulted from a loss of volatile components during recovery. This phenomenon was not observed for RTFO sample, since the volatile material was lost during short-term hardening. In addition, it was also observed that the hardening index increased for binder left in the solvent for extended period of time. The results are shown in Figure 31[(49)].

Additional experiments were carried out on both the Abson and Roto-vap solvent removal methods for the purpose of evaluating their effectiveness in removing solvents. The typical trends observed are shown in Figure 32 and Figure 33[(49)]. It was observed that the Abson method, taken to its standard recovery time, can leave enough solvent to produce significant softening, especially for larger quantities of recovered material and for hardened asphalt such as those obtained from aged pavement cores. Increasing the temperature of the solvent removal and recovery time can reduce residual solvent concentration, although the previously mentioned solvent hardening effects must be considered.

Burr in his work on solvent extraction also concluded that Roto-vap method appears to be less consistent and less reproducible than the Abson method, but it may have some advantages for solvent removal.

Burr et al. made the final recommendation regarding Abson and Roto-vap procedure. According to them for the Abson procedure at 325°F, the minimum recovery time (after the last drop) for 50-grams sample is about 25 minutes. For 100 grams sample, 380°F will remove solvent within 20 min. For the Roto-vap procedure, 15 min past the last drop was adequate at 325°F.

TEST PROCEDURES USED IN THIS STUDY

Superpave asphalt binder test methods and the associated equipment that were used to carry out the experimental work in the study are discussed in this section. The purpose of each test, the significance and the description of the test method, as standardized by the AASHTO are discussed and outlined. Additionally, the description and the significance of the adopted Superpave asphalt binder equipment are also presented in this section. The Superpave asphalt binder tests include Dynamic Shear Rheometer (DSR), (AASHTO – TP5), Rolling Thin Film Oven Test (RTFOT), (AASHTO – T240), Pressure Aging Vessel (PAV), (AASHTO – PP1-98), and binder extraction and recovery procedure, (SHRP B – 006).

Dynamic Shear Rheometer (DSR) Test, AASHTO – TP5

Purpose and Significance of Use

The DSR test, (AASHTO – TP5, 1993, 1994, and 1995) measures the rheological characteristics of an asphalt binder and the phase angle. These characteristics represent the viscous and elastic behavior of the asphalt binder. A sample of asphalt is sandwiched between two parallel disks. The sample is subjected to oscillation through a fixed rotation. The DSR test is performed at temperatures associated with intermediate and high pavement service temperatures. Superpave asphalt binder specifications utilize DSR results to assess two criteria, rutting at elevated service temperatures and fatigue at intermediate service temperatures.

Concept of Operation

Figure 34 shows the BOHLIN DSR equipment. A similar device was used to characterize the asphalts in this study. The DSR test can be explained as follows.

An asphalt disk is sandwiched/placed between the DSR plates, as shown in Figure 35. Figure 35 also shows the two plates; the upper plate oscillates and the lower plate is fixed. The oscillating plate rotates through a fixed angle following a sine function and the applied torque is measured, as shown in Figure 36. The equations used to compute the complex shear modulus and phase angle using the DSR test results are as follows (Figure 37 illustrates the DSR measurements):

The complex shear modulus is computed as follows:

$$\tau = 2T/\pi r^3$$
$$\gamma = \theta r/h$$
$$G^* = (\tau_{max} - \tau_{min})/(\gamma_{max} - \gamma_{min})$$

Where,

T = maximum applied torque
R = radius of the sample

θ = rotational angle
h = sample height
τ = shear stress, and
ω = angular frequency.

The phase angle is computed as the time lag between the applied shear stress and resulting shear strain, as shown in Figure 37.

The DSR test is either conducted in a constant-stress mode or a constant-strain mode. In the constant-stress mode, a fixed torque is applied and the rotation of the upper plate is measured. In the constant-strain mode, the upper plate is rotated by a fixed amount and the resulting torque is measured.

DSR Test Procedures

The DSR test can be summarized as follows. Asphalt is heated until sufficiently fluid to pour. The asphalt is poured into a silicon mold, the use of which minimizes specimen trimming. The asphalt is left in the mold to cool. The distance between the upper and lower plate (Gap) is adjusted to 1 mm for tests on original or RTFO aged asphalts and 2 mm for PAV aged asphalts. Subsequently, the specimen is mounted between the parallel plates and excess asphalt is trimmed. Tests are computer controlled and depending on the type of DSR device, tests can be conducted in the constant stress mode or constant strain mode. The complex shear modulus and phase angle are reported.

DSR Device Description

A computer and associated software are used to control the test and data acquisition. Either water or air heating/cooling system controls the temperature during the DSR. Rotation torque is applied by an electric motor. Stress and/or strain is measured, recorded, and used as a feedback to control the test.

Short-term Aging RTFO Test, AASHTO T240

Purpose and Significance of Test

The Rolling Thin Film Oven test (RTFOT), (AASHTO – T240, 1995), is performed on the original asphalt binder to simulate the effects of the construction process on the asphalt binder (mixing, laydown and compaction). In the early 1960s, CALTRANS introduced the RTFO for its proposed aged-residue viscosity grading system. An RTFO is shown in Figure 38.

Concept of Operation

Glass jars are filled with 35 grams of asphalt binder and placed in the RTFO rack. While the RTFO sample rack is rotated, a jet of air is blown into the sample jars. This air along with elevated temperature (163ºC) and test duration of 80 minutes causes the asphalt binders to age. Figure 38 shows the jet nozzle, bottle rack, and an RTFO jar. Figure 39 illustrates the schematic/concept of operation of the RTFO test.

RTFO Test Procedure

The RTFO test can be described as follows. An asphalt sample is heated until sufficiently fluid to pour. The heated asphalt is poured into glass jars (35 +/- 0.5 gram). The contents of two jars are used to determine mass loss, which is limited to 1.0% in the Superpave specifications. The jars are heated in the RTFO oven (163°C) for 80 +/- 5 minutes. After the test duration, the asphalt residue is poured into one container to ensure homogeneity. The asphalt in the container can be used for either testing or additional aging in the Pressure Aging Vessel.

Long-term Aging PAV Test, AASHTO – PP1-98

Purpose and Significance of the Test

The Pressure Aging Vessel (PAV) test, (AASHTO – PP1-98, 1995), is performed on the RTFO conditioned binder to simulate long-term in-service aging (five to ten years). The PAV test does not consider different mix parameters that affect in-service aging such as aggregate type, air-voids, and film thickness.

Concept of Operation

The PAV test utilizes both temperature and pressure to simulate in-service aging. To accelerate test time while the pressure is maintained at 2.1 MPa, three different temperatures (90, 100, or 110°C) are used depending on asphalt binder grade and expected in-service environmental conditions. The asphalt ages as a result of the high temperature and pressure. This process causes the oxidation process to be accelerated. Figure 40 illustrates the PAV equipment.

PAV Test Procedure

A schematic of the PAV is shown in Figure 41. The PAV test procedure can be described as follows. An RTFO aged asphalt sample is heated until sufficiently fluid to pour. 50 +/- 0.5 grams of binder is poured into each Thin Film Oven (TFO) pan. TFO pans are placed in a pan holder. Subsequently, the pan holder is placed in the aging vessel. Figure 42 shows the aging vessel, TFO pans, and TFO pan holder. The pressure line and temperature monitoring devices are then connected to the pressure vessel. The PAV oven temperature is allowed to equilibrate at the test temperature. Pressure in the vessel is increased to 2.1 MPa over ten minutes. The asphalt binder is aged over a twenty-hour test period. The pressure is released slowly over a ten-minute period at the completion of the test. The TFO asphalt pans are placed in a vacuum degasser oven for a period of thirty minutes to release any trapped air. The aged asphalt is then poured into tins for future testing (DSR).

PAV Device Description

Major components of the PAV can be described as follows. The pressure vessel holds the TFO pans and TFO pan holder. A pressure line is connected to the pressure vessel that maintains the pressure constant throughout the test. A temperature probe that

measures the temperature inside the pressure vessel is also attached. The entire assembly is held in PAV oven.

Extraction of Asphalt Binders from Field Samples, SHRP B – 006

Purpose and Significance of Use

The extraction and recovery procedure, (SHRP B – 006, 1995), is performed to extract and recover asphalt binder from bituminous field samples. Subsequently, physical and/or chemical tests can be performed on the extracted and recovered asphalt. The asphalt content of the field samples can also be determined as a result of this procedure. However, it is not recommended to use the remaining aggregate for sieve analysis.

Concept of Operation

HMA samples (field cores or loose mixtures) are repeatedly washed using solvents. Filters are used throughout the test to recover aggregate fines. A rotary evaporator is used to distill the asphalt under vacuum. Finally, nitrogen is introduced to "drive-off" any remaining traces of solvents. Figure 43 shows a schematic of the SHRP extraction procedure.

Extraction and Recovery Procedure

The extraction and recovery procedure can be described as follows. HMA samples are heated and placed in a high-speed centrifuge. The HMA is repeatedly washed with solvent. The resulting solution is distilled in a rotary evaporator. Nitrogen is introduced to drive-off remaining traces of solvents. The recovered asphalt is poured into containers for subsequent testing.

Table 1
Elemental Analysis of Representative Petroleum Asphalts[12]

Element	Asphalt			
	B-2959 (Mexican)	B-3036 (Ark.-La.)	B-3051 (Boscan)	B-3602 (Calif.)
Carbon (%)	83.77	85.78	82.90	86.77
Hydrogen (%)	9.91	10.19	10.45	10.94
Nitrogen (%)	0.28	0.26	0.78	1.10
Sulfur (%)	5.25	3.41	5.43	0.99
Oxygen (%)	0.77	0.36	0.29	0.20
Vanadium (ppm)	180	7	1,380	4
Nickel (ppm)	22	0.4	109	6

Table 2
General Characterization of Each of the Four Generic Fractions Found in Bitumen[14]

Fraction	Color	Density (gm/cc)	Flow Character
Saturates	Colorless	0.87	Liquid
Napthene-Aromatics	Yellow to Red	0.98	Liquid
Polar-Aromatics	Black	1.07	Solid
Asphaltenes	Brown to Black	1.15	Solid

Table 3
Physical Properties of Chemical Fractions[18]

Fraction	Asphalt			
	Saturates	Naphthene-Aromatics	Polar Aromatics	Asphaltenes
Penetration @ 77°F	300+	300+	0	0
Softening Point, °F	66	76	170	375
Density @ 20 °F	0.89	0.99	1.05	1.15
Color	White	Yl. – Rd.	Blue	Br. – Bl.
Kin. Vis @ 100 °F	174	2777	2×10^{10}	*
Kin. Vis @ 210 °F	22	64	1.1×10^{5}	*
Kin. Vis @ 275 °F	12	20	2.1×10^{5}	*
Kin. Vis. Index	131	61	-117	*
Ab. Vis. @ 77 °F	140	3100	1.1×10^{10}	*
Ab. Vis. @ 140 °F	0.8	22	1.0×10^{6}	*
Physical State	Liquid	Liquid	Solid	Solid

* Above the level of detection

Table 4
Changes in Chemical Composition During Rolling Thin Film Oven (RTFO) Test [12]

Asphalt	Concentration, moles/liter				
	Ketones	Carboxlic Acid	Dicarboxylic Anhydrides	2-Quinolone type	Sulfoxide
B-2952					
Original	0.015	*	0.0014	0.003	0.015
Aged	0.310	*	0.0030	0.003	0.160
B-3036					
Original	0.021	*	0.0014	0.001	0.022
Aged	0.300	*	0.0030	0.001	0.200
B-3051					
Original	0.017	0.014	0.0030	0.009	0.010
Aged	0.340	0.018	0.0030	0.007	0.150
B-3602					
Original	0.045	0.060	*	0.011	0.015
Aged	0.490	0.075	0.0090	0.010	0.100

* Above the level of detection

Table 5
The Aging Conditions for Figure 3.13[22]

Condition	Temperature	Oxygen Pressure
C1	170°F (349.8 K)	20 atm
C2	180°F (355.4 K)	20 atm
C3	180°F (355.4 K)	10 atm
C4	190°F (360.9 K)	20 atm
C5	190°F (360.9 K)	0.2 atm
C6	200°F (366.5 K)	0.2 atm
C7	210°F (372.0 K)	0.2 atm
C8	140°F (333.2 K)	20 atm
C9	140°F (333.2 K)	0.2 atm
C10	150°F (338.7 K)	0.2 atm
C11	160°F (344.3 K)	0.2 atm
C12	170°F (349.8 K)	0.2 atm
C13	180°F (355.4 K)	0.2 atm

Table 6
Correlation of Pavement Condition with Physical Properties of Recovered Bitumen[34]

Source of Data	Location of Pavement	Condition of Pavement	Recovered Penetration at 77°F
Stattuck	Detroit, Mich.	Very Good Good Badly Cracked	20+ 20+ 20-
Thomas	Minnesota	Good Fair Poor	41 26 20
Hubbard and Gollomb	Ohio, Mich., N.Y., Ind., D.C.	Sound Prone to Crack Cracking Type	30+ 30- 20-
Vokac	Ohio, Pa., Md., Va., Mo., Ill., Ind., Mich., N.Y., N.J., D.C.	Sound Prone to Crack Cracking Type	25+ 18-25 18-
Powers	Arizona	Good Cracked	10+ 10-
Public Roads Administration	Cuba	Good Cracked	9 5

Table 7
Comparison of Extraction Methods

Sample	Method	Viscosity - 60°C (kPa)	Un-extracted Asphalt (% of Total)	Total Solvent Used (ml)
Tex 21/77	SHRP: Toluene, Toluene/ETOH	2.51	1.4	2575
		2.62	1.0	3915
		2.36	1.0	2910
		2.77	0.6	3800
		2.60	-	3100
	Average	2.57	1.0	3260
	Modified Method A: Toluene, Toluene/ETOH	2.83	5.2	3085
		3.03	3.8	2985
		2.71	-	3230
	Average	2.86	4.5	3100
	Modified Method B: Toluene, Toluene/ETOH	0.541	11.4	N/A
		0.655	11.7	N/A
		1.335	-	N/A
	Average	0.844	11.6	N/A
Young Bros. Pavement	SHRP: Toluene, Toluene/ETOH	95.0	1.66	3000
		90.3	1.34	3000
		88.2	1.26	3000
	Average	91.2	1.42	3000
	SHRP: TCE, TCE/ETOH	95.4	1.48	3000
		115.0	1.21	3000
		114.0	1.37	3000
	Average	108.0	1.35	3000
	Modified Method A: Toluene, Toluene/ETOH	93.7	1.60	3000
		90.6	2.04	3000
		91.8	2.00	3000
	Average	92.0	1.88	3000
	Modified Method B: Toluene	65.6	1.37	N/A
		62.2	1.16	N/A
	Average	63.9	1.27	N/A
	Method B: TCE	67.4	1.75	N/A
		80.4	1.80	N/A
	Average	73.9	1.78	N/A

- Indicates data not determined

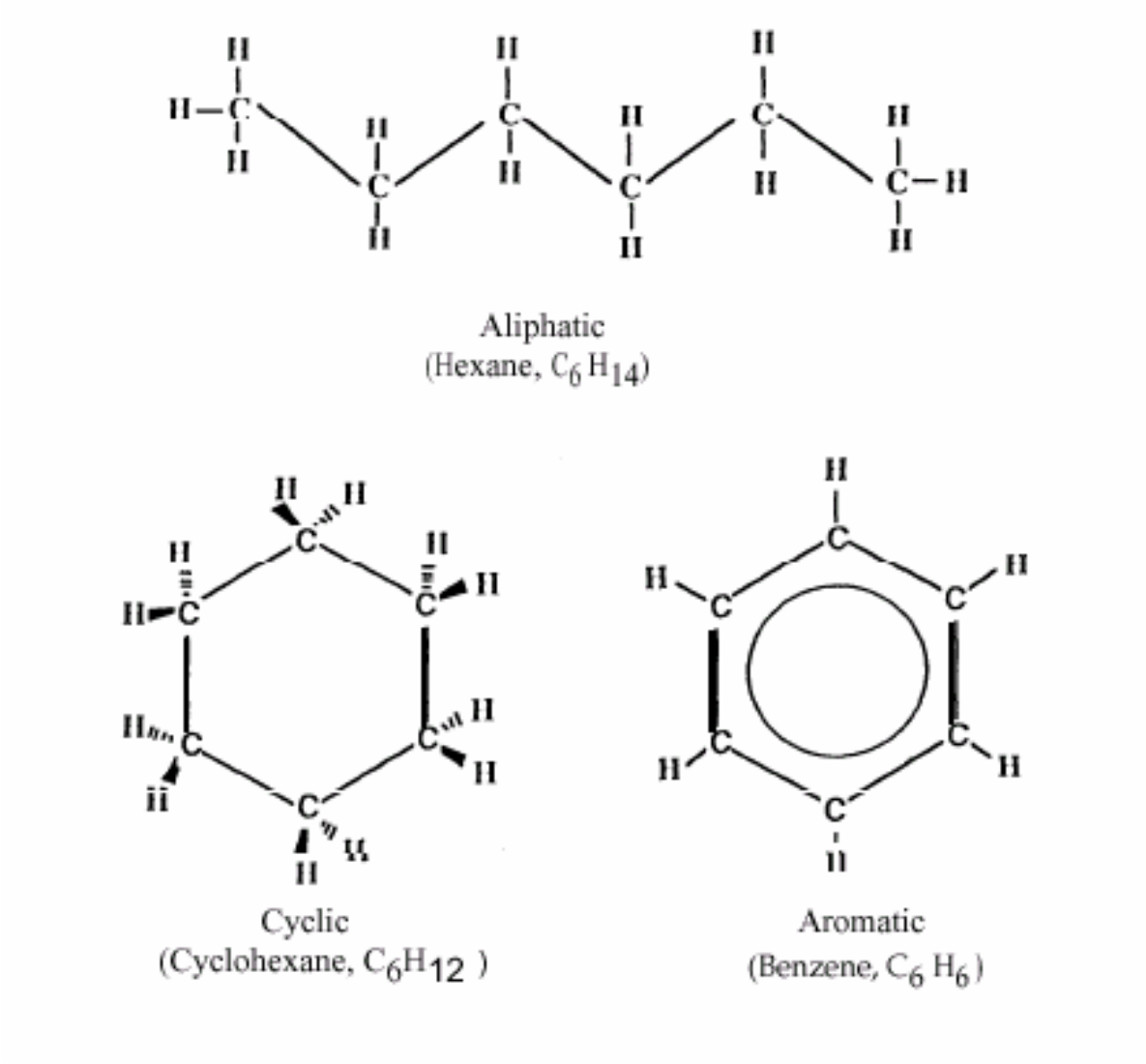

Figure 1
Types of Molecules in Asphalt[10]

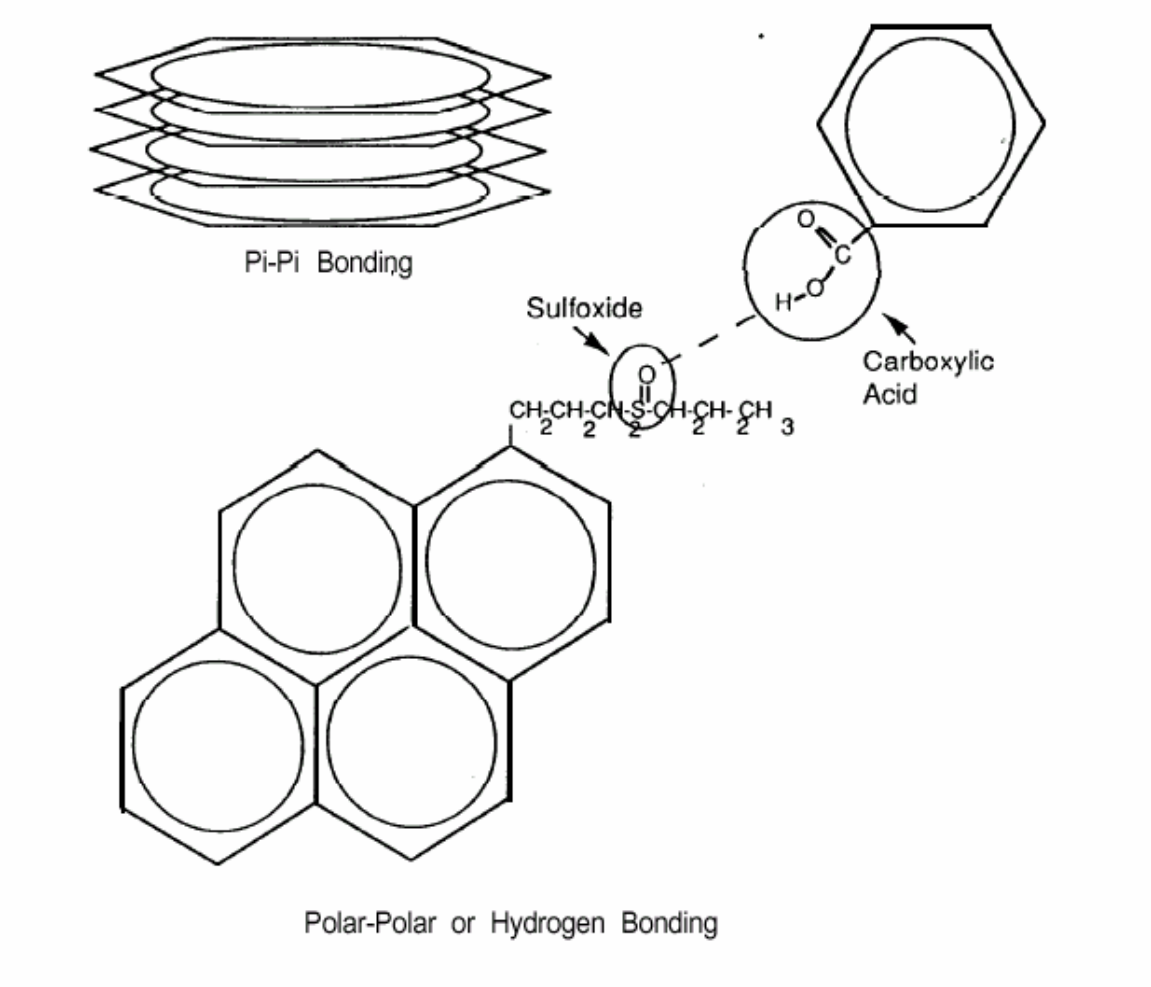

Figure 2
Types of Molecular Bonding in Asphalt *(10)*

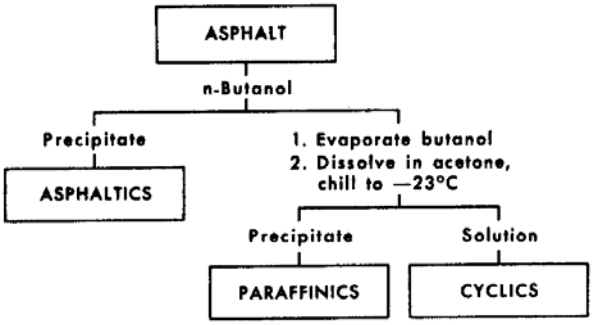

(a) Partition with Partial Solvents

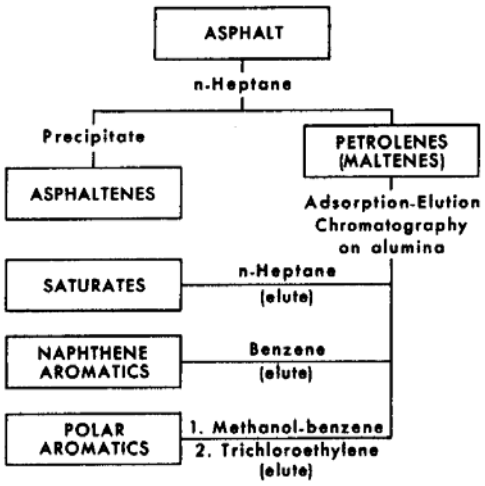

(b) Selective Adsorption Desorption

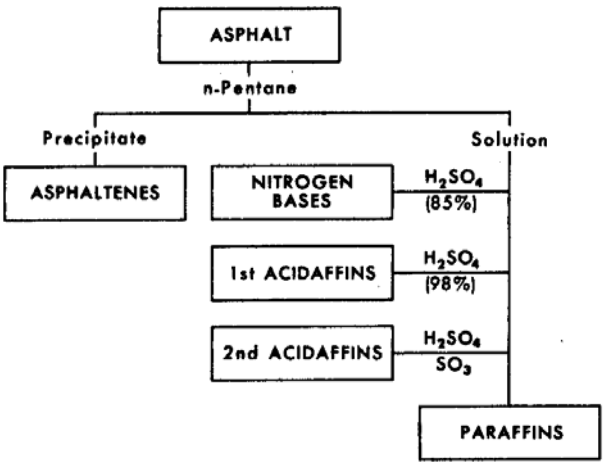

(c) Chemical Precipitation

Figure 3
Flow Diagram Showing Three Commonly Used Fractionation Schemes[(11)]

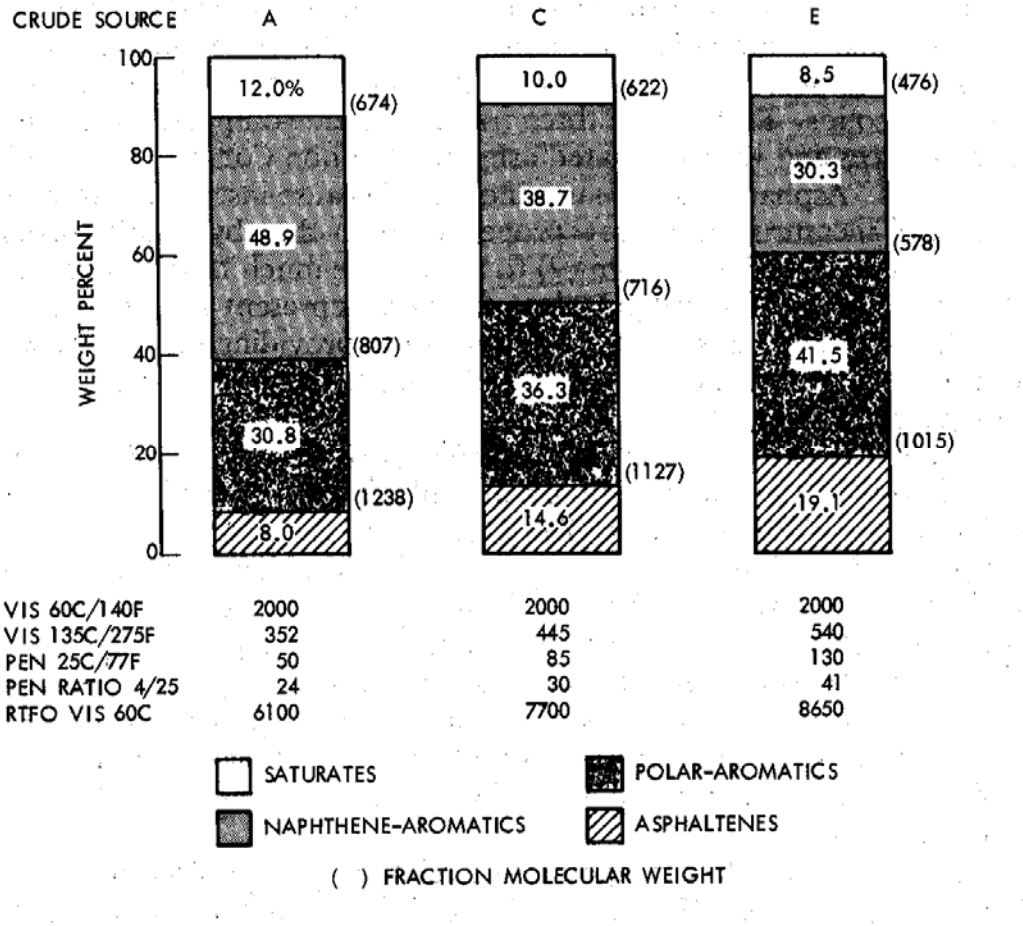

Figure 4
Typical Properties of Chemical Fractions Observed in Three Crude Sources[15]

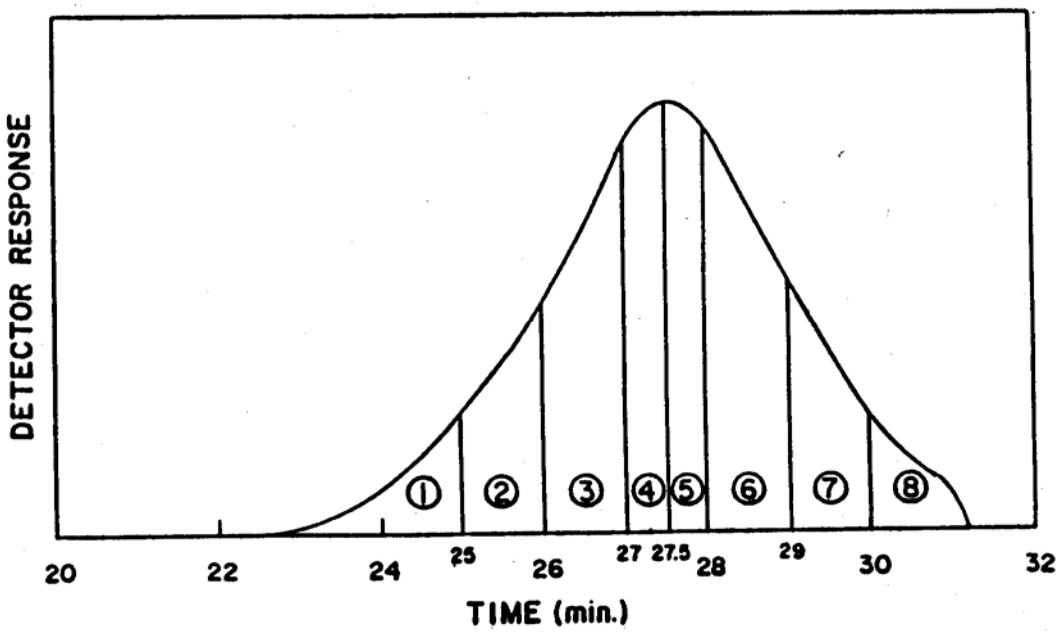

Figure 5
Typical Schematic Output Profile from Gel Permeation Chromatography

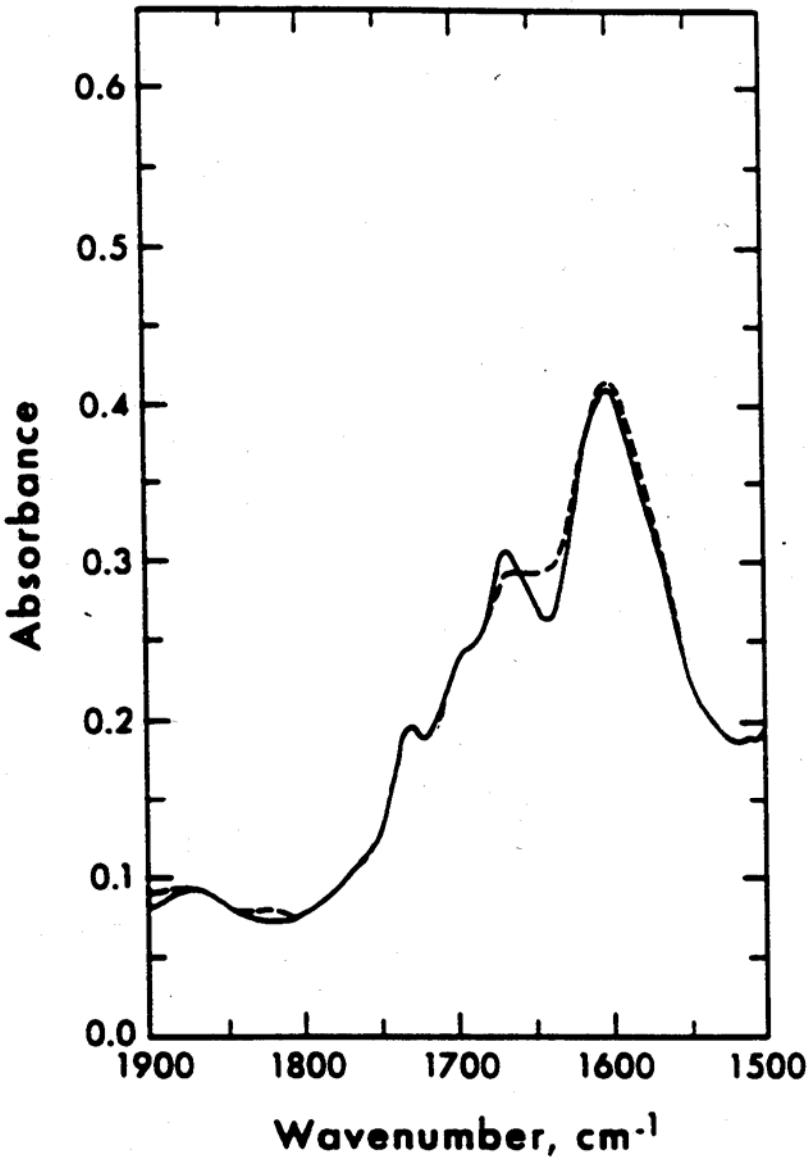

Figure 6
Typical Infrared Spectra Profile Used in Functional Group Analysis[16]

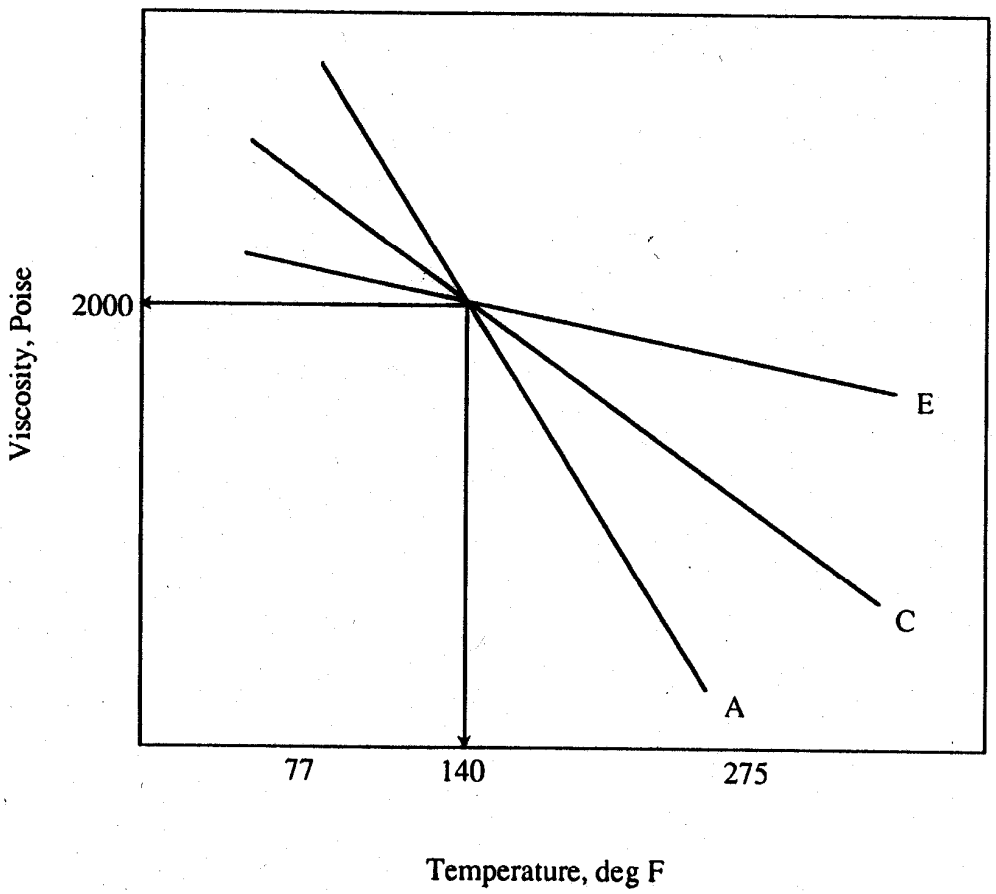

Figure 7
Illustration of Temperature Susceptibility Behavior of Three Types of Asphalts

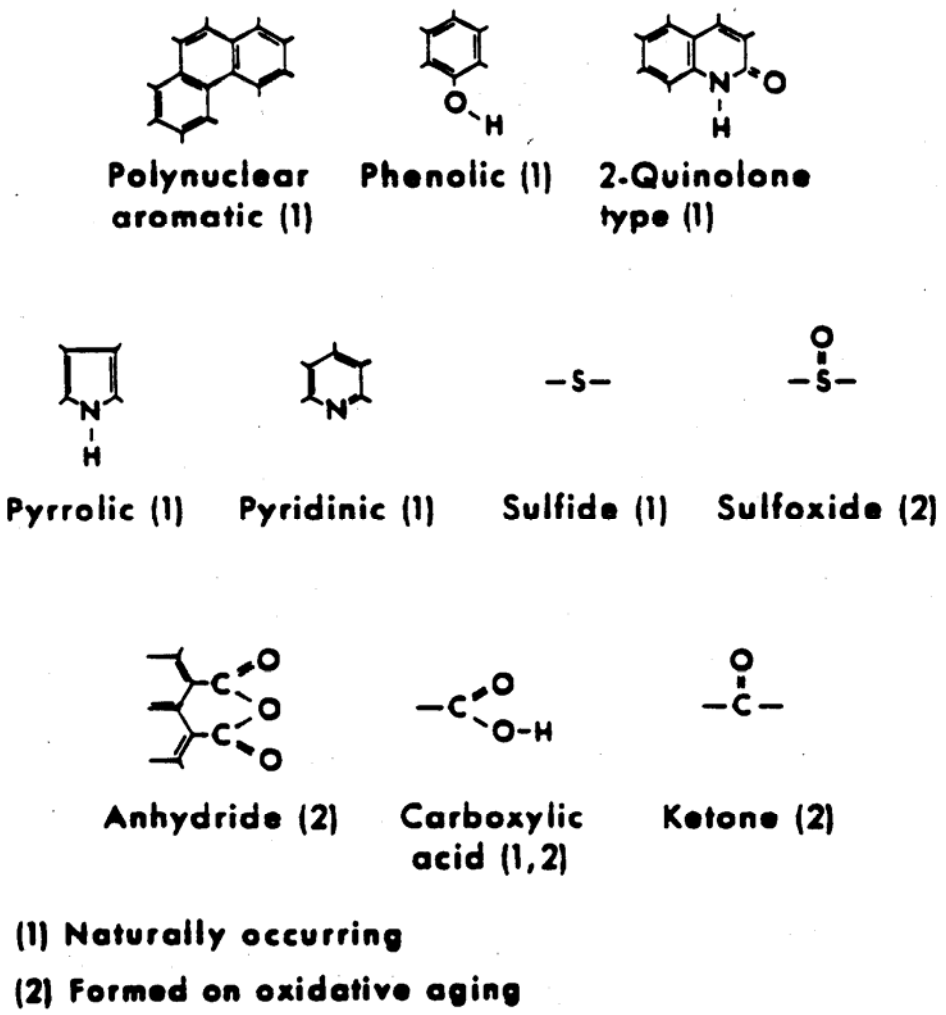

Figure 8
Important Chemical Functionalities Present in Asphalt Molecules[17]

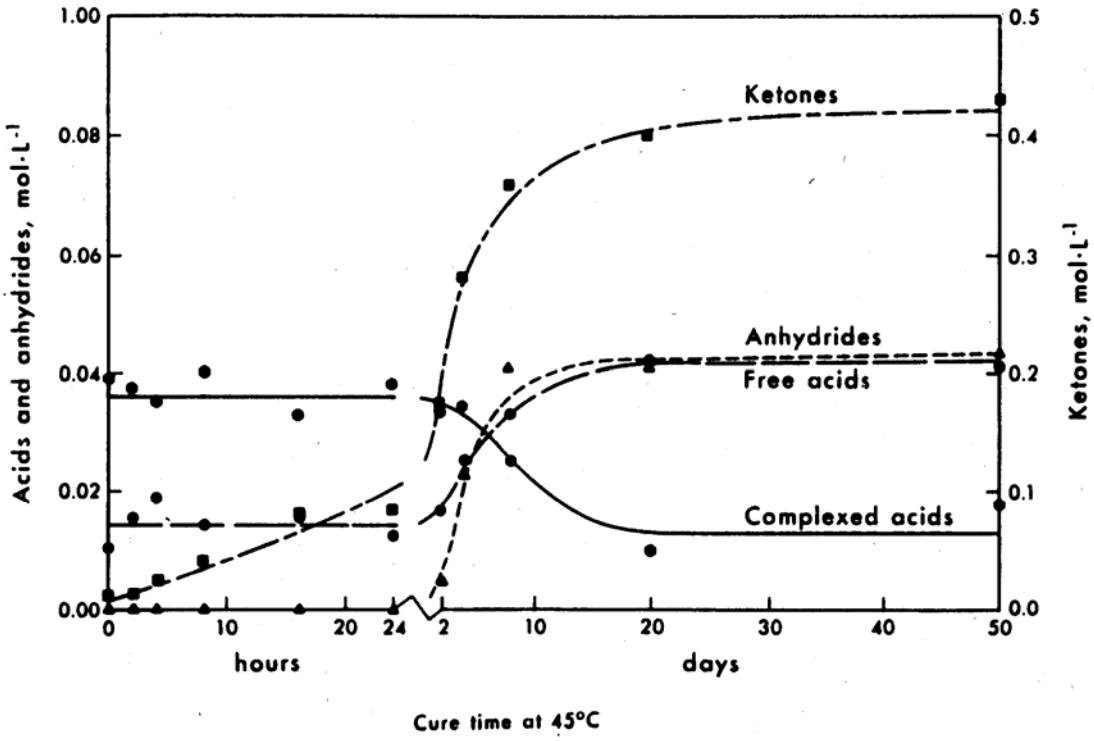

Figure 9
Changes in Chemical Functionality During Cure of Asphalt Cement[17]

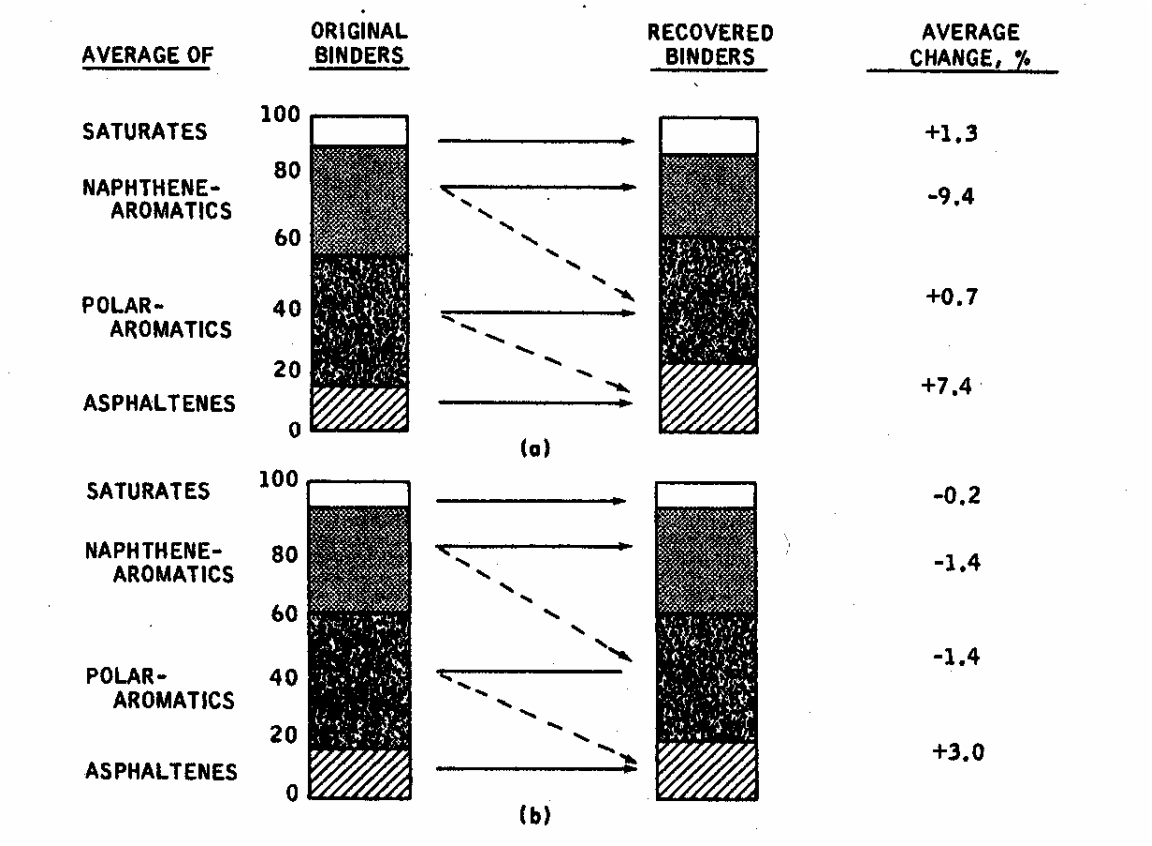

Figure 10
Mechanism of Change for (a) Top 1/8 in. Layer (b) ¼ in. Minus Layer

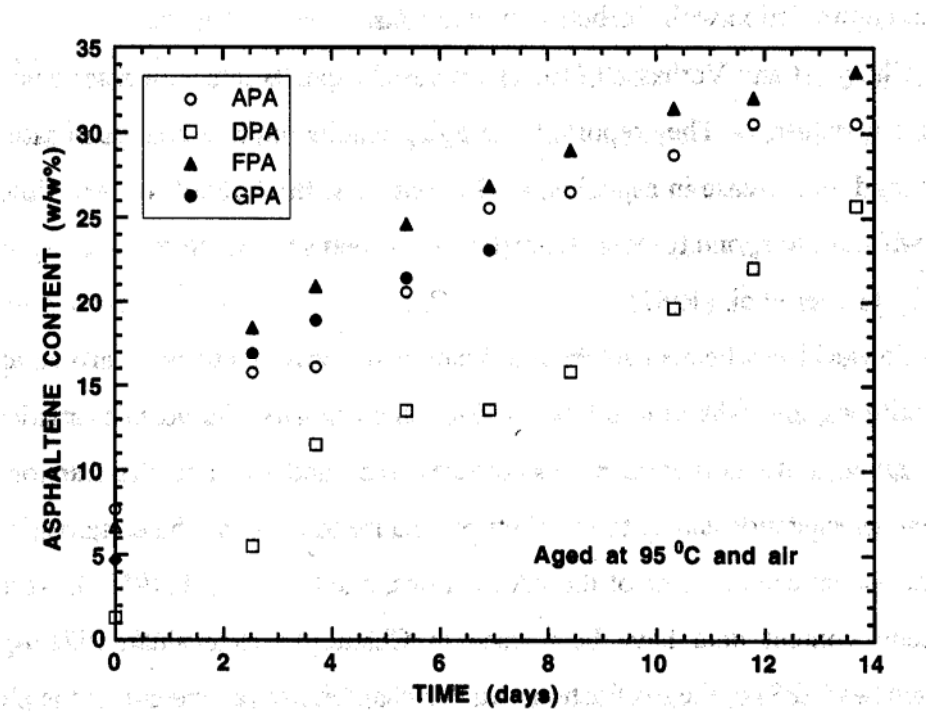

(a)

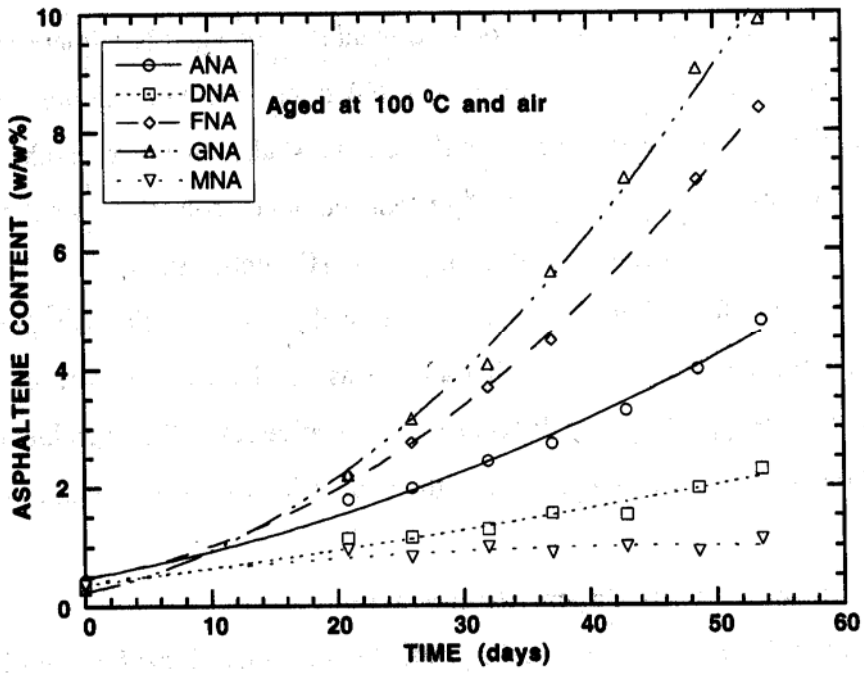

(b)

Figure 11
Asphaltene Production in Aged PA Fraction (a) and Asphaltene Production in Aged NA Fractions (b)

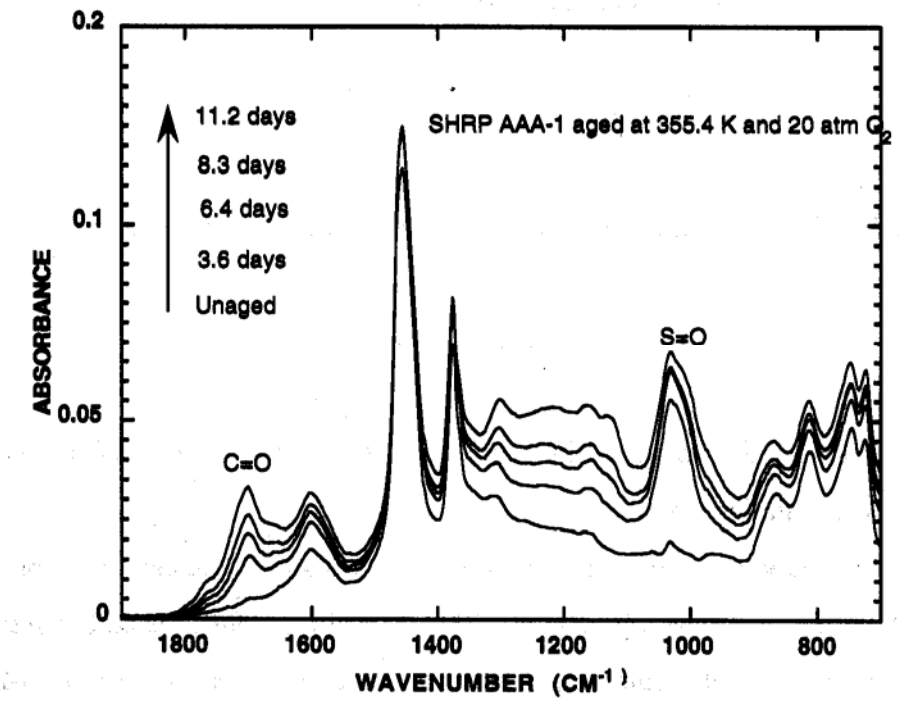

Figure 12
FTIR Spectra of Unaged and Aged SHRP AAA-1[(22)]

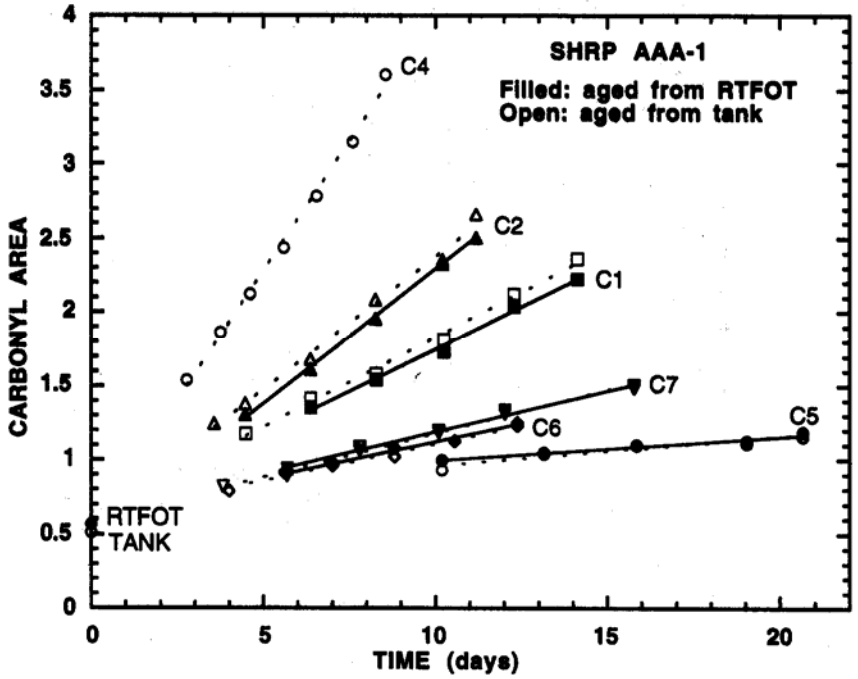

(a) SHRP AAA-1 C1-C7

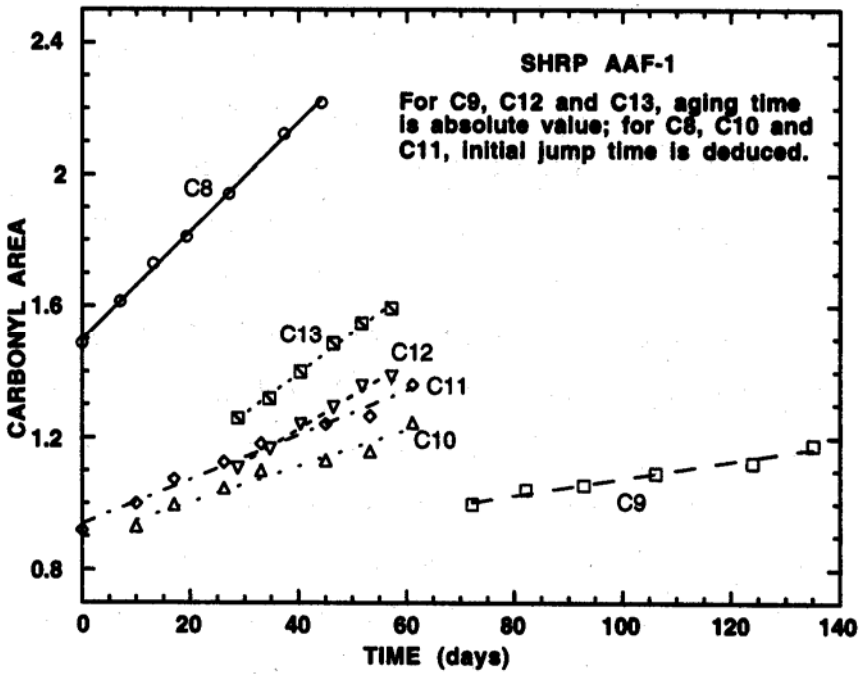

(b) SHRP AAA-1 C8-C13

Figure 13
Carbonyl Area vs. Aging Time

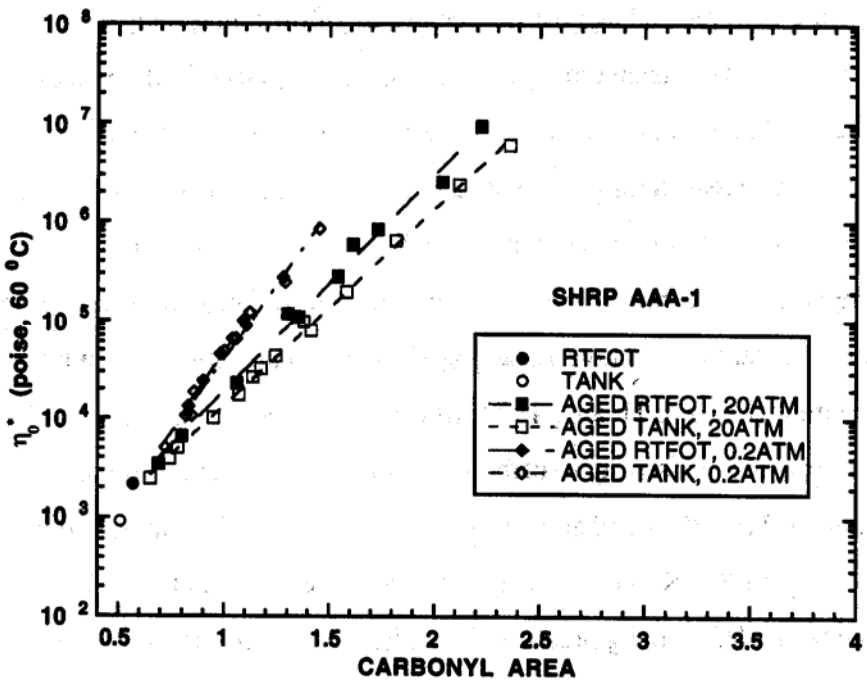

Figure 14
Relationship between Binder Viscosity and Carbonyl Area[22]

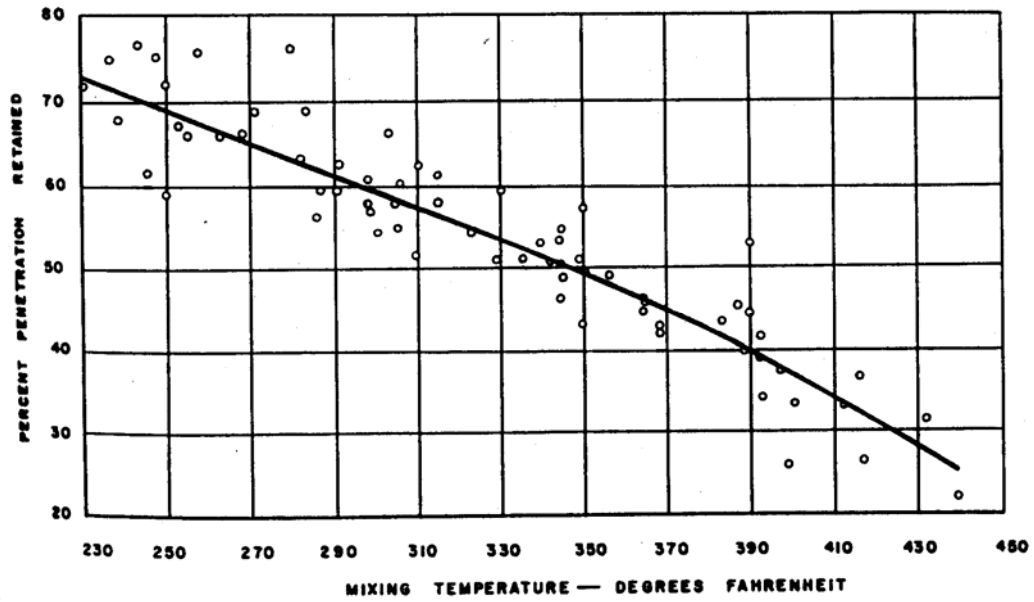

Figure 15
Relationship between Mixing Temperature and the Change in Penetration During Mixing Operation[27]

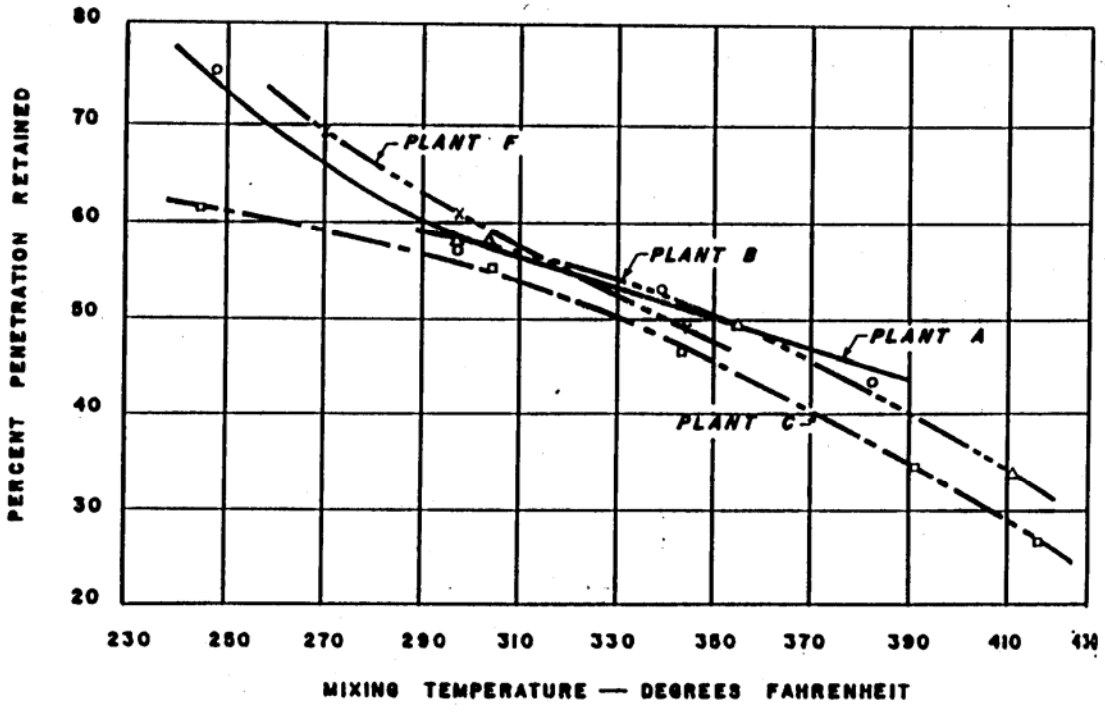

Figure 16
Percent Penetration Retained as a Function of Plant Type[27]

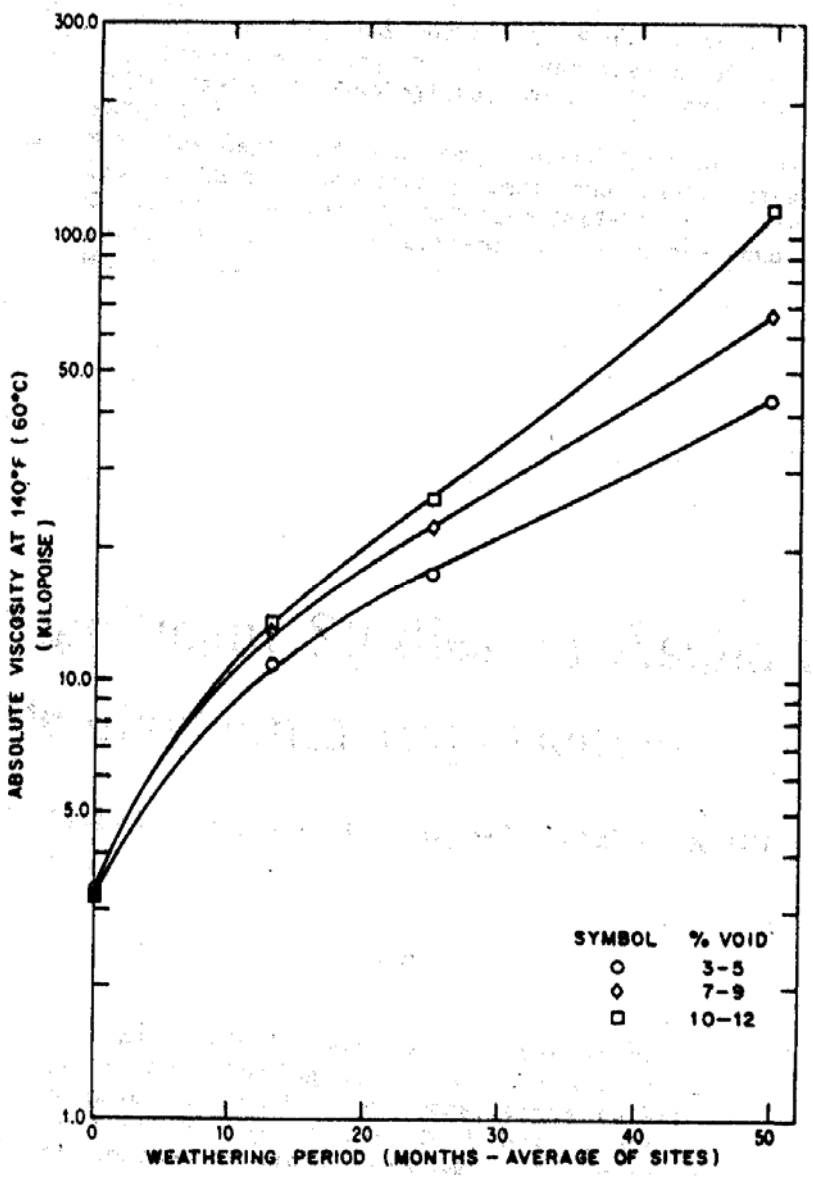

Figure 17
Effect of Air Voids on Hardening Properties[30]

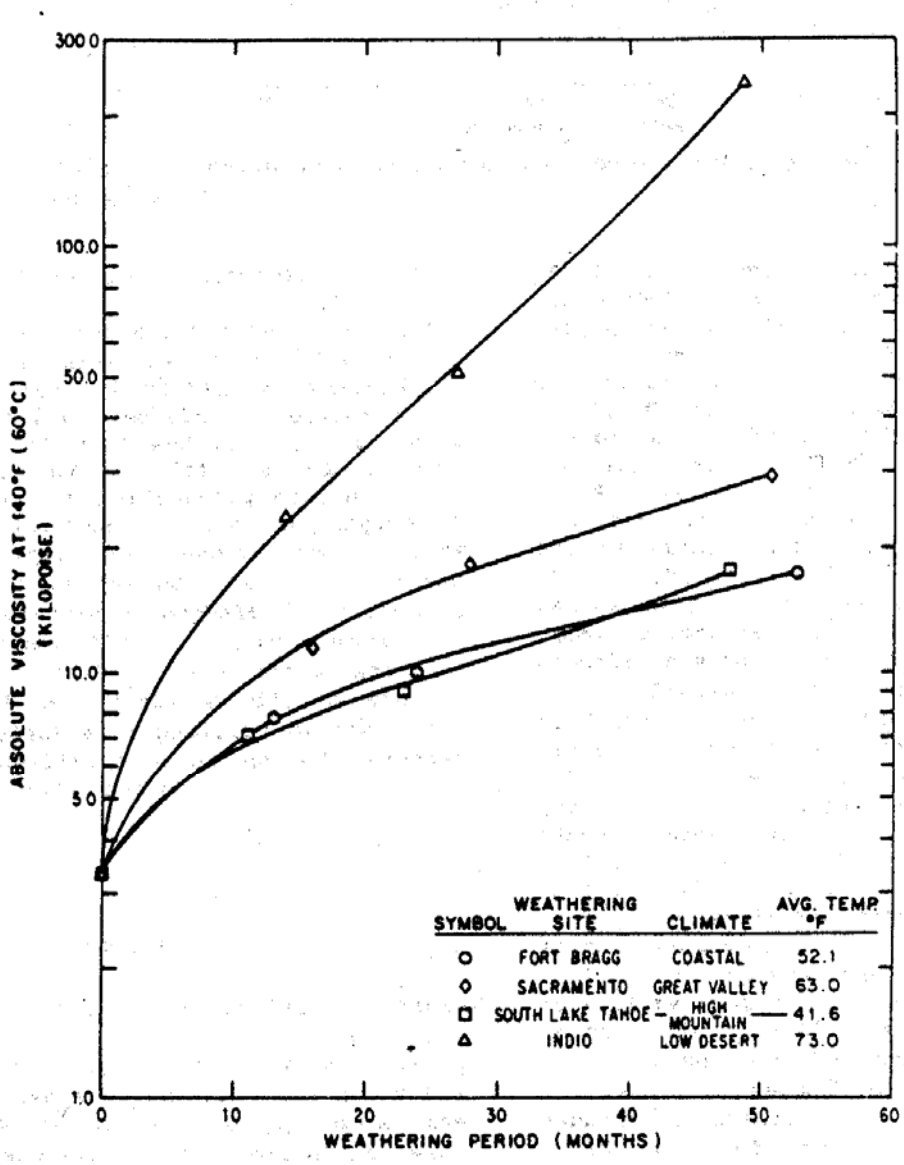

Figure 18
Effect of Climatic on Hardening Properties[30]

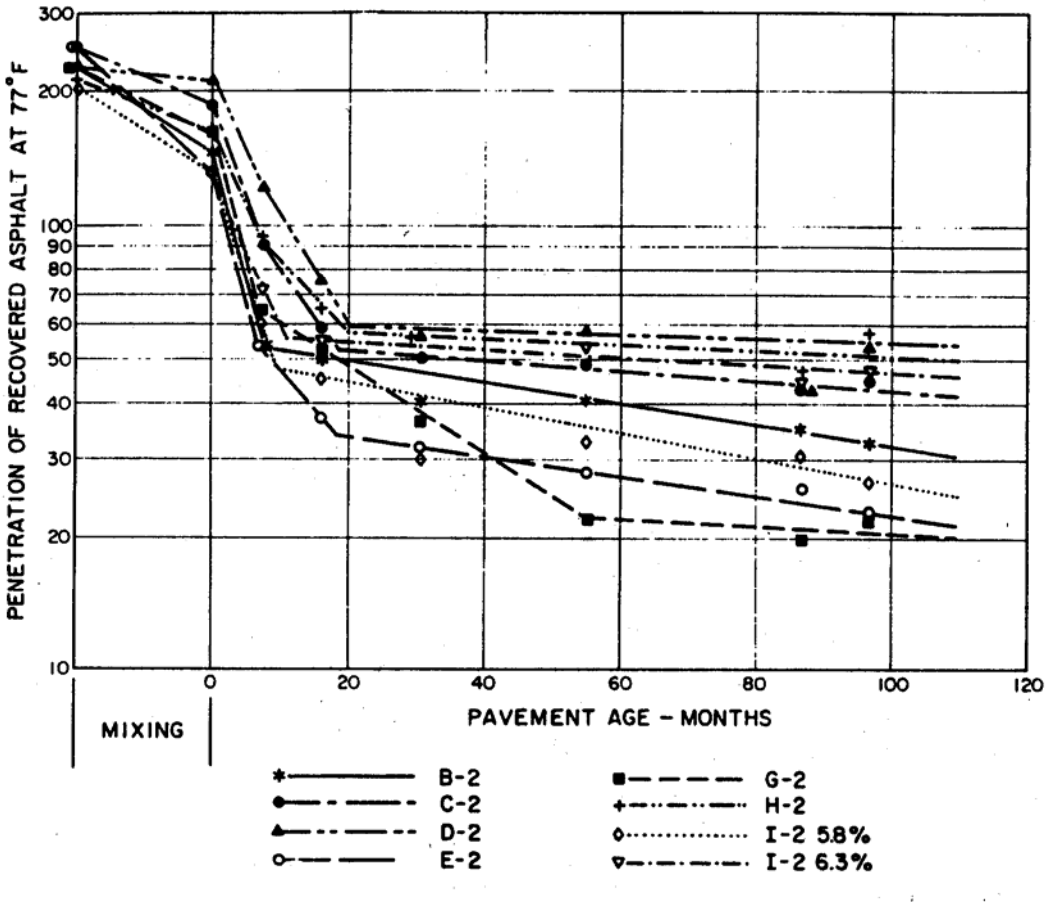

Figure 19
Hardening of 200-300 Paving Grade Asphalt at Zaca Wigmore Project[31]

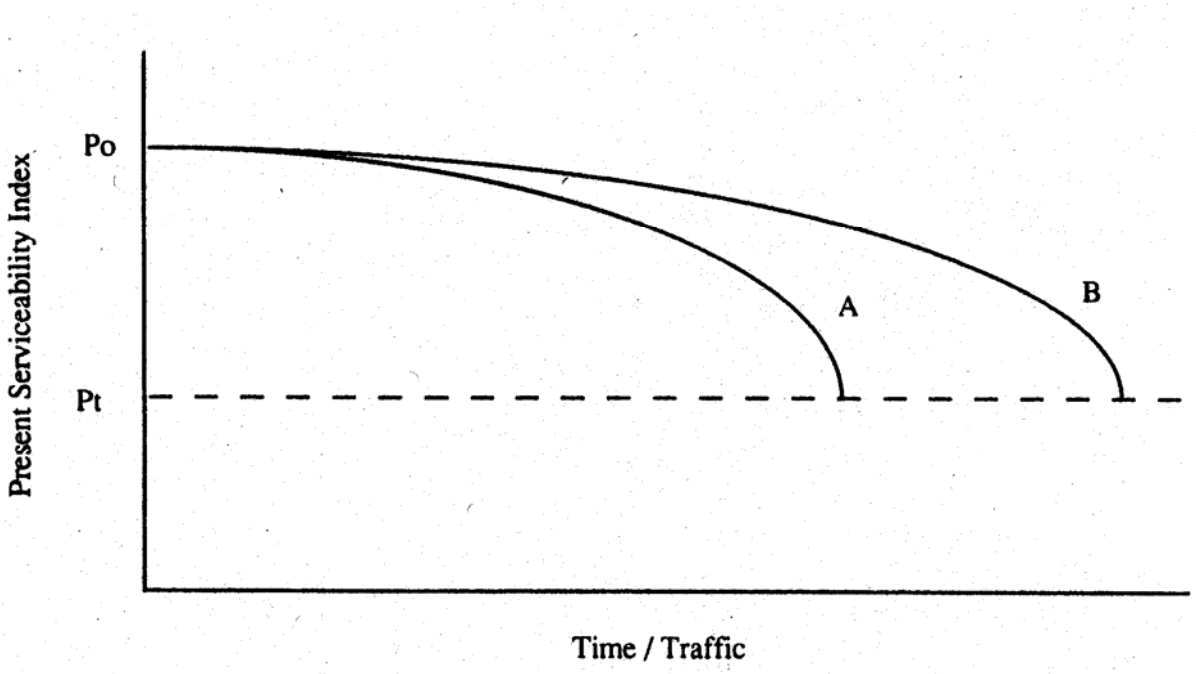

Figure 20
Typical Schematic Plot for Change in Serviceability as a Function of Time

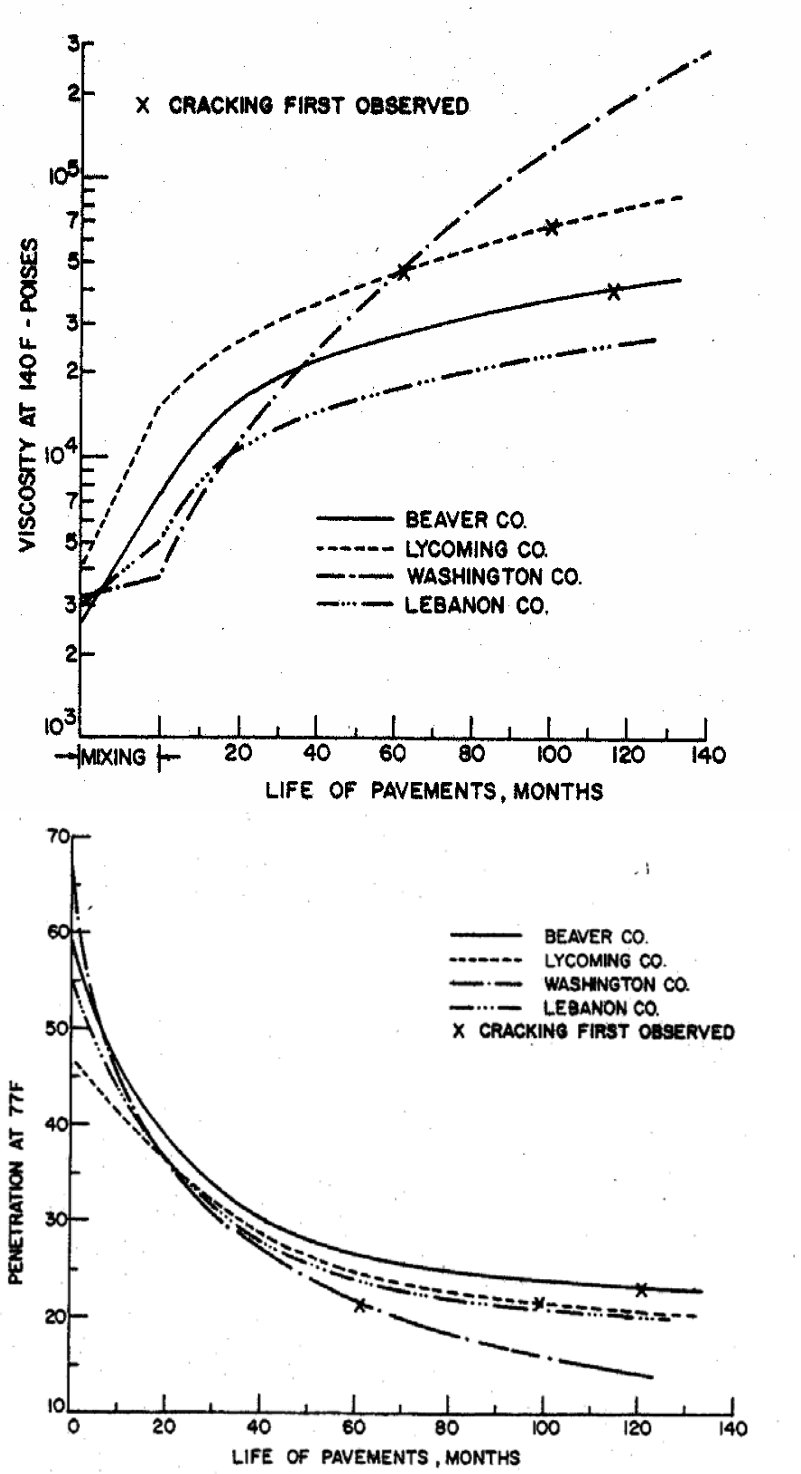

Figure 21
Change in Consistency of Asphalt as a Function of Time[35]

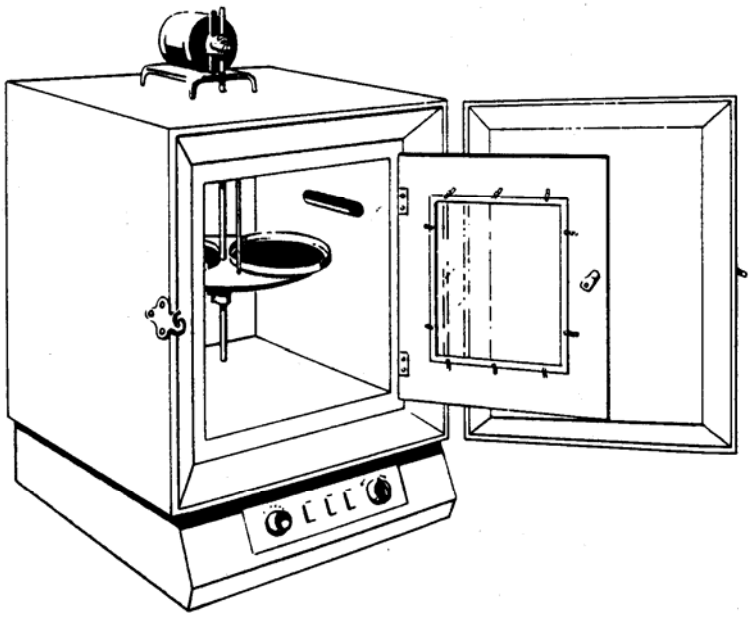

(a) Thin Film Oven (TFO)

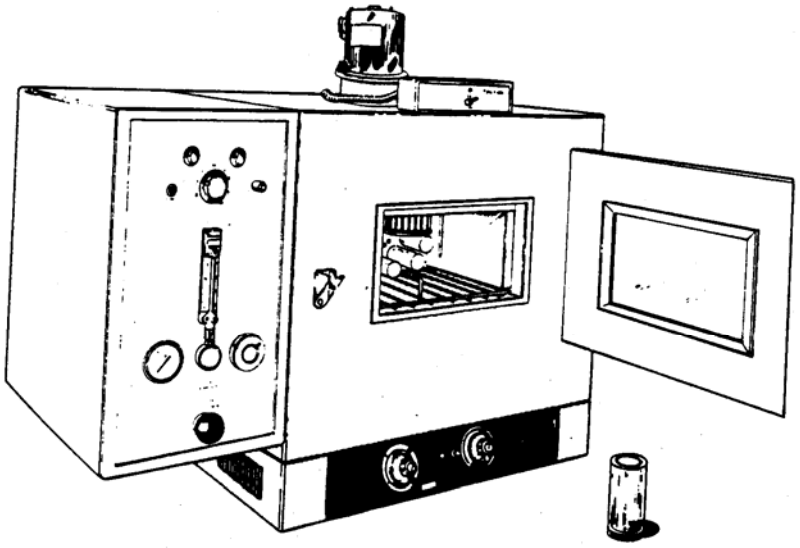

(b) Rolling Thin Film Oven (RTFO)

Figure 22
Laboratory Age Hardening Process

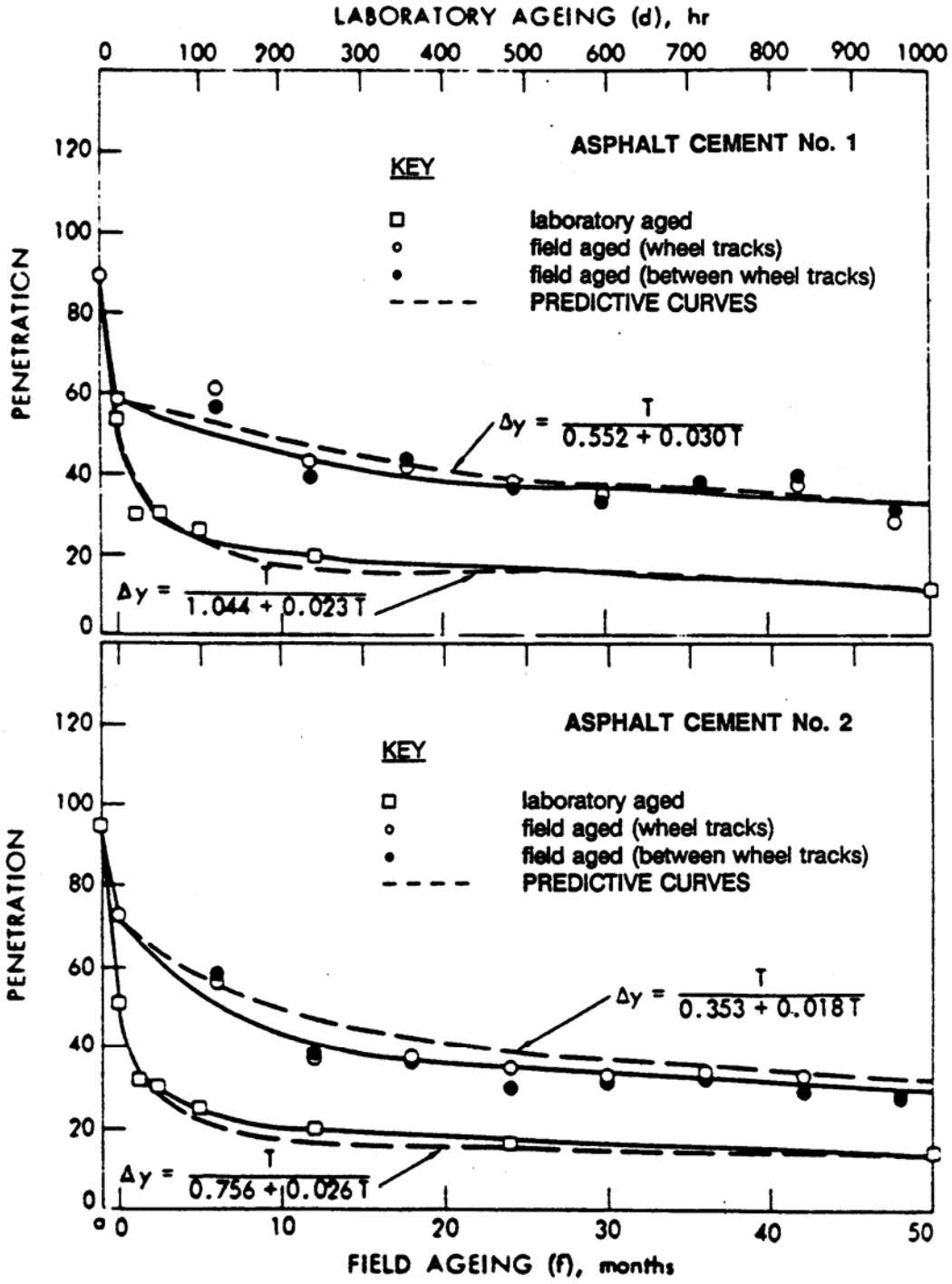

Figure 23
Penetration versus Time of Aging[37]

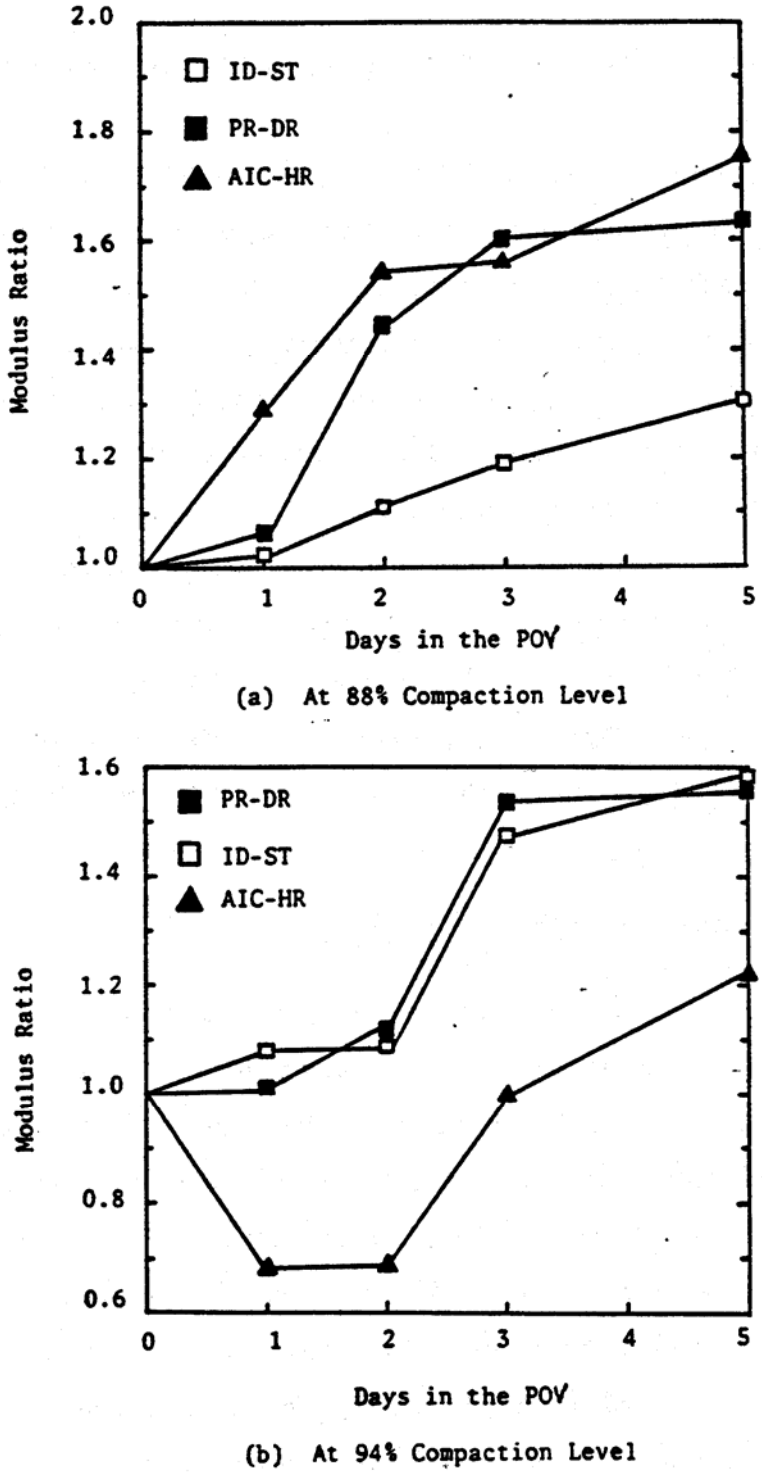

Figure 24
Aging Modulus Ratios for Three Asphalt Mixtures[42]

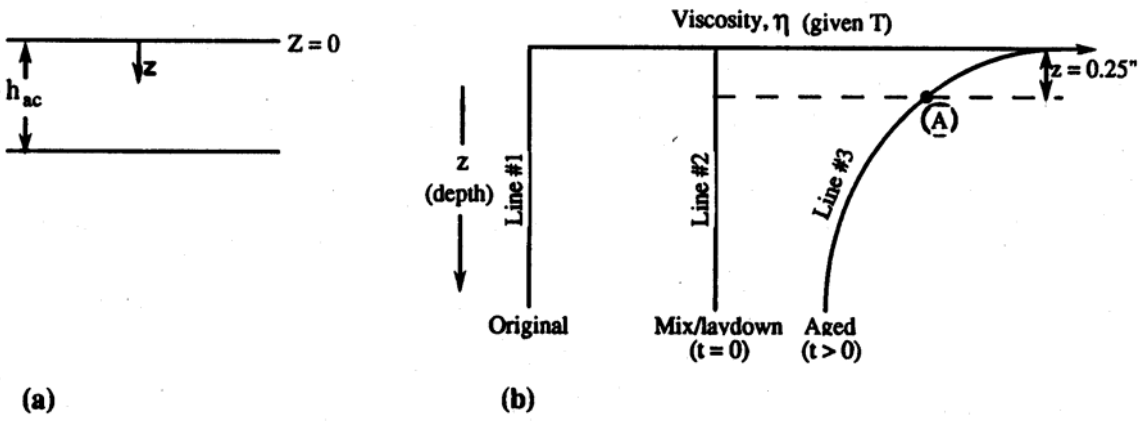

Figure 25
Typical Viscosity-Depth Relationship as a Function of the Time at a Given Temperature (a) Asphalt Layer Cross Section (b) Three Stage Viscosity Change Process with Depth

$$\log E = -1.249937 + 0.029232 \cdot p_{200} - 0.001767 \cdot (p_{200})^2 - 0.002841 \cdot p_4 - 0.058097 \cdot Va - 0.802208 \cdot \frac{Vb_{eff}}{(Vb_{eff} + Va)} +$$

$$+ \frac{3.871977 - 0.0021 \cdot p_4 + 0.003958 \cdot p_{38} - 0.000017 \cdot (p_{38})^2 + 0.005470 \cdot p_{34}}{1 + e^{(-0.603313 - 0.313351 \log(f) - 0.393532 \log(\eta))}}$$

Where the variables represent:

E	Asphalt Mix Dynamic Modulus, in 10^5 psi
η	Bitumen viscosity in 10^6 poise (at any temperature, degree of aging)
f	Load frequency in Hz
Va	% air voids in the mix, by volume
Vb_{eff}	% effective bitumen content, by volume
p_{34}	% retained on the ¾ inch sieve, by total aggregate weight (cumulative)
p_{38}	% retained on the 3/8 inch sieve, by total aggregate weight (cumulative)
p_4	% retained on the No. 4 sieve, by total aggregate weight (cumulative)
p_{200}	% passing the No. 200 sieve, by total aggregate weight

Figure 26
Revised Dynamic Modulus Predictive Equation(45)

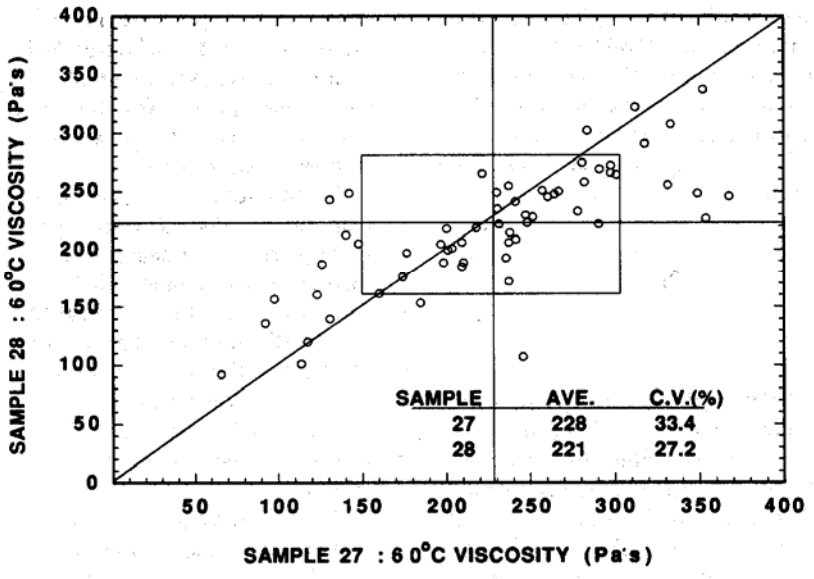

Figure 27
Results from the AASHTO Materials Reference Laboratory Proficiency Sample Program. Samples 27 and 28 are Replicates.

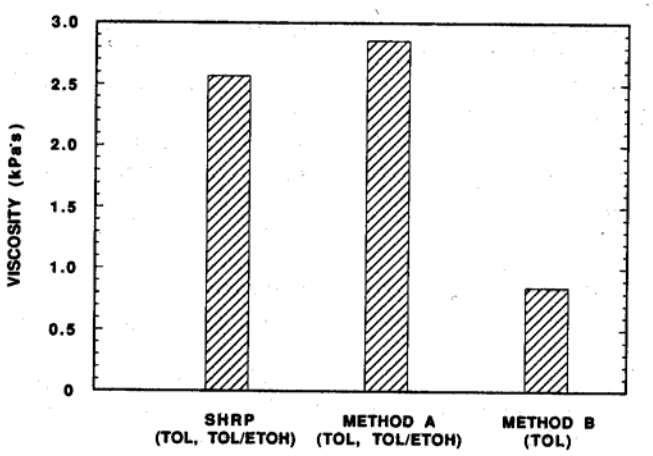

Figure 28
Average Viscosities of Asphalt Binder Extracted from Tex 21/77 Samples Using Various Extraction Methods.

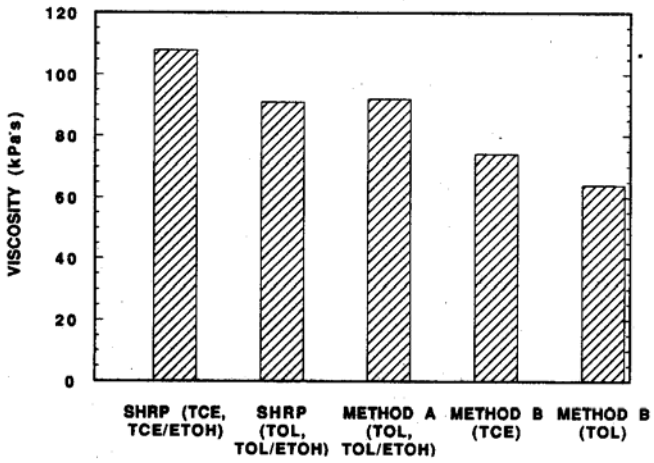

Figure 29
Average Viscosities of Asphalt Binder Extracted from Young Brothers Samples Using Various Extraction Methods.

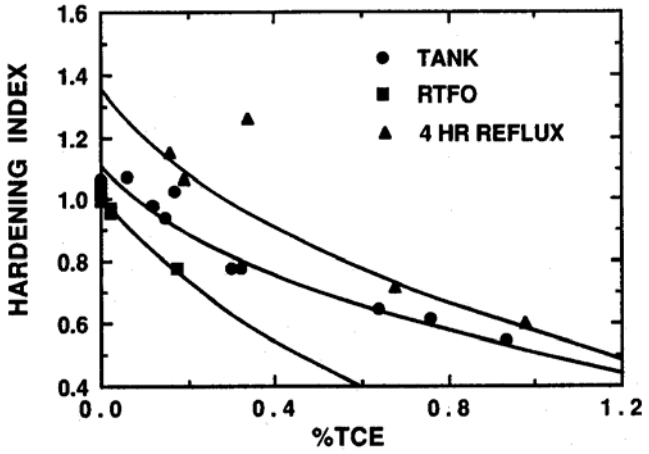

Figure 30
Removal of Solvent and Resulting Changes in Asphalt Viscosity.

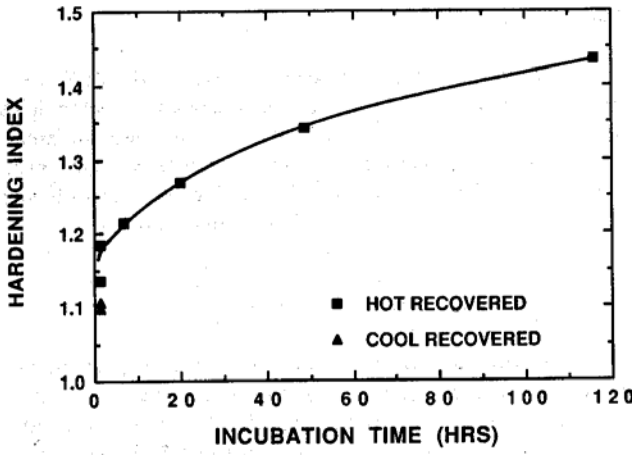

Figure 31
Hardening of Asphalt in TCE at Room Temperature for Extended Periods of Incubation Time Prior to Hot Recovery.

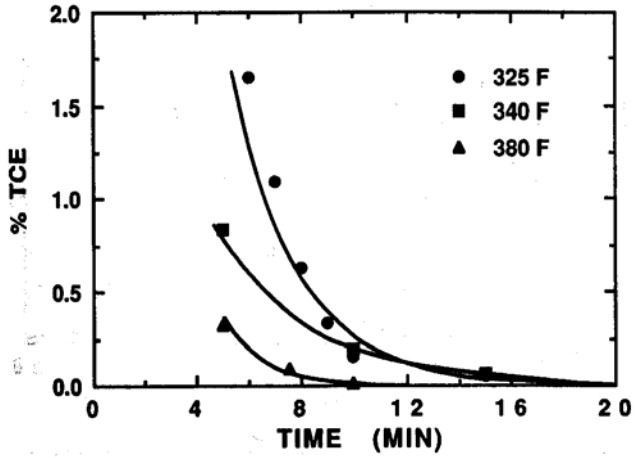

Figure 32
Residual Solvent Concentrations versus Abson Recovery Time at Three Temperatures for a Tank (AC-20) Asphalt.

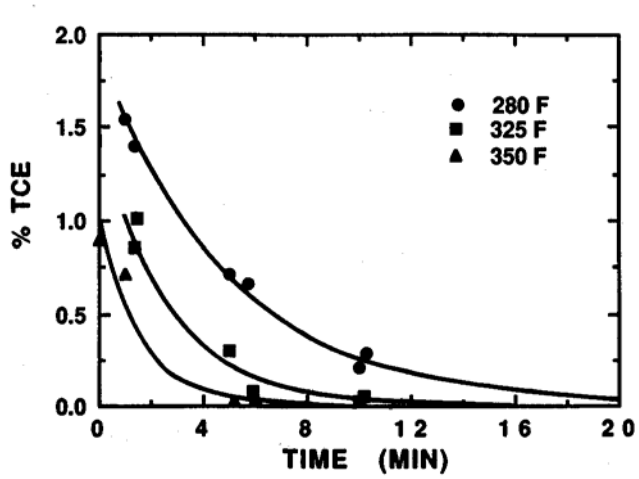

Figure 33
Residual Solvent Concentrations versus Roto-Vap Recovery Time at Three Temperatures for an AC-20 Asphalt.

Figure 34
The BOHLIN DSR

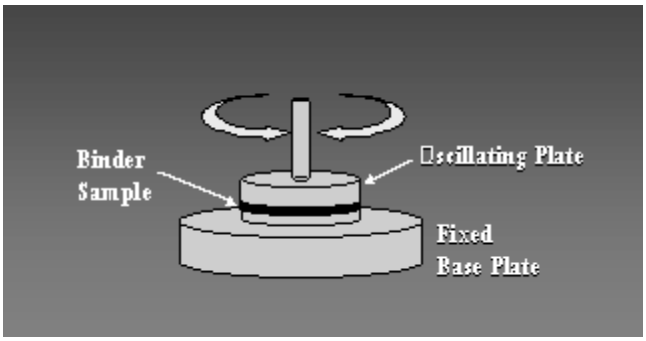

Figure 35
Schematic of the DSR Equipment.

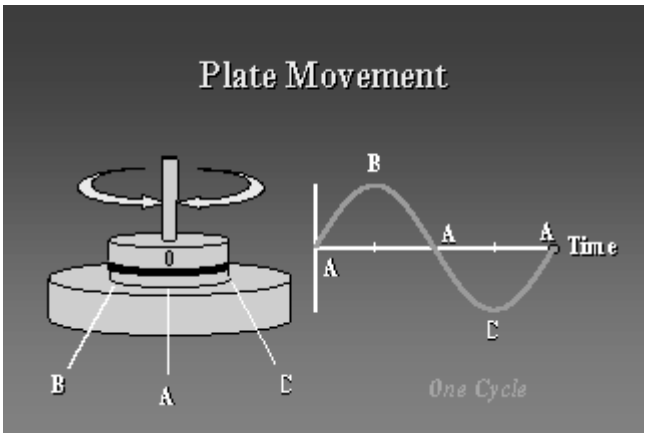

Figure 36
Schematic of the DSR Plate Movement.

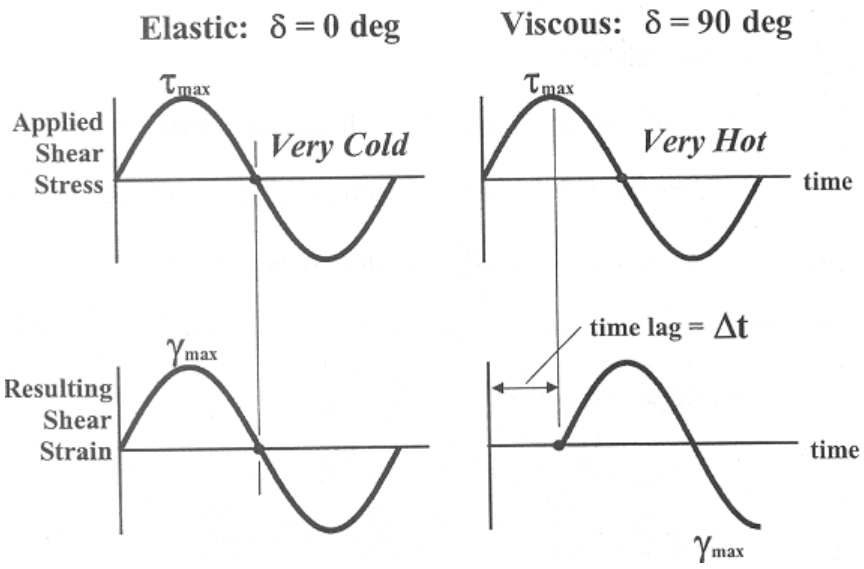

Figure 37
DSR Measurements

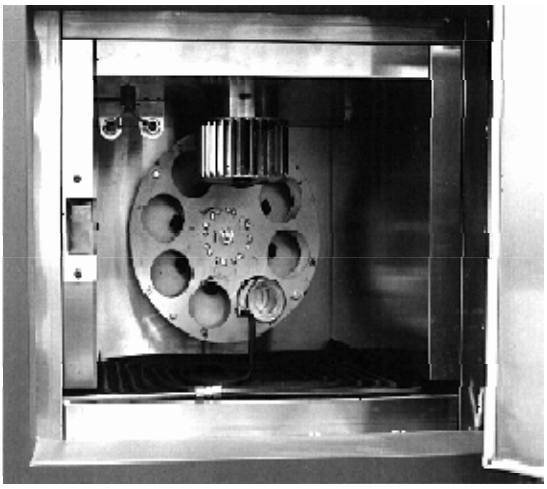

Figure 38
Rolling Thin Film Oven, RTFO – Short-Term Aging

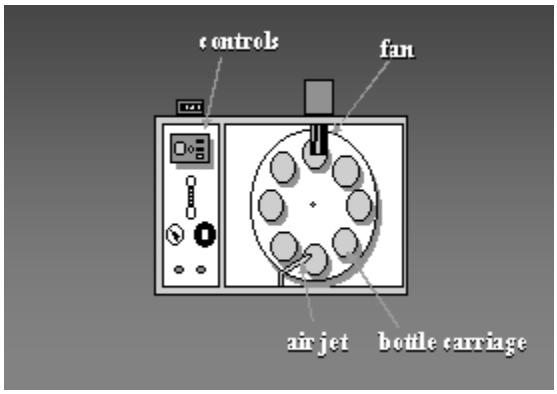

Figure 39
Schematic/Concept of Operation of RTFO

Figure 40
Pressure Aging Vessel, PAV – Long-Term Aging

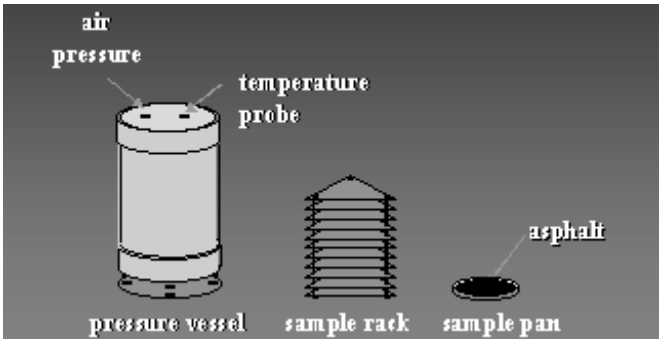

Figure 41
Schematic of the PAV

Figure 42
Pressure Vessel, TFO Pans, and TFO Pan Holder

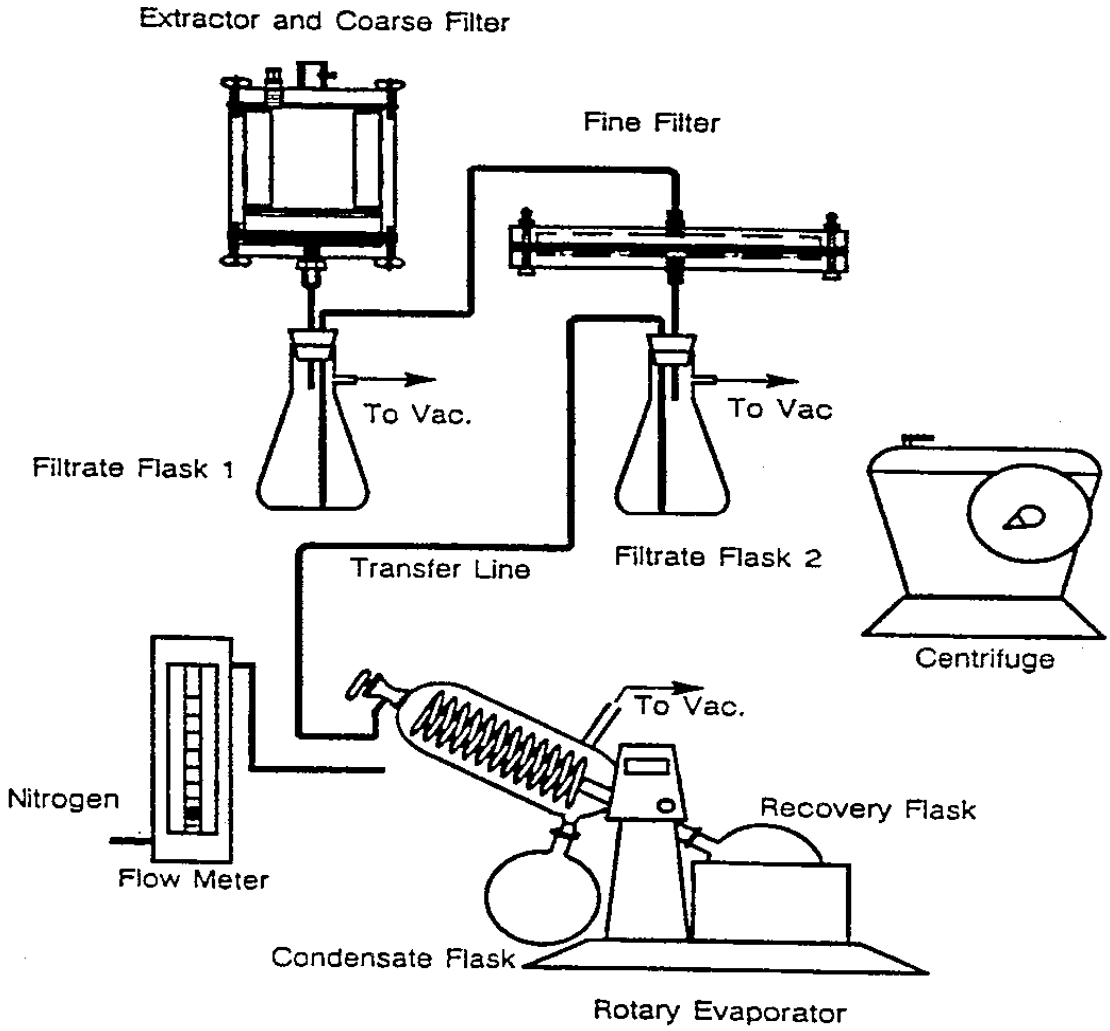

Figure 43
Schematic of the SHRP Extraction Procedure

CHAPTER 3

CORRECTION FACTOR FOR BINDER RECOVERY

INTRODUCTION

For the calibration and validation of the PP1-98 protocol, binders from the field cores need to be extracted and recovered for comparison. It has been well documented in the literature that the properties of the binder may change to some extent during the recovery process. The research team, well aware of the potential problems with the extraction and recovery procedures, developed a plan to minimize the error due to the extraction process. Because of the inherent problems associated with the binder extraction and recovery as cited in the literature, an experimental study was initiated to develop a correction factor to account for the changes in the binder viscosity that may occur due to the extraction and recovery procedures.

The correction factor to be developed was intended only for the recovery procedure in order to study the effect of the solvent. This is because solvent type was found to be the major factor contributing to the change in the properties of the binder during the recovery process (see *Chapter 2, Literature Review*).

Other factors such as the aging of binder may also contribute to the changes that occur during the recovery process. However, the intention is to minimize the laboratory effect, namely, the effects due to the equipment type, type of solvent, and the method used for the recovery process, and then to apply the experimentally determined correction factor.

MATERIALS USED

To account for the effect of extraction on different binder grades and aging conditions, all the binders used in the calibration phase of the project were used to develop the correction factor. The three PAV aging temperatures were 90°C, 100°C, and 110°C. The binders used in this study were:

1. ADOT AC-30 (Arizona)
2. ADOT AC-40 (Arizona)
3. MnRoad AC-20 (Minnesota)
4. MnRoad AC-120/150 (Minnesota)
5. WesTrack AC-20 (Nevada)

LABORATORY TESTING PROGRAM

In order to achieve the above objective, the following test sequence was adopted:

1. The correction factors were developed only for binders previously aged in the PAV, due to the fact that extractions were carried out on aged cores obtained from the field.

2. In order to account for different aging times in the field, binders were aged at three temperatures in the PAV: 90°C, 100°C, and 110°C.
3. DSR testing was carried out on each binder at each aged condition before it was mixed with the solvent for the recovery process.
4. The aged binders were mixed with the solvent and the mixture was subjected to the recovery process.
5. The extracted binders were then characterized using the DSR testing.

The DSR test results on the un-extracted (aged) binder (step 2) were compared with the DSR results on the extracted binder (Step 5) and the comparison was used for the development of correction factors for different aging conditions and binder types.

LABORATORY RESULTS

The DSR testing results obtained from aged binders (step 2) and recovered binders (step 5) are tabulated in Table 8.

The comparison plot of log log viscosity of the aged (un-extracted) binder versus log log viscosity of the recovered binder for ADOT AC-40 is shown in Figure 44. It can be observed from Figure 44 that the viscosity values lie on the equality line. This trend was observed in the 5 binders at all PAV aging conditions used in this study. A comparison plot of all the binder viscosities at all PAV aging conditions is shown in Figure 45.

In order to determine the significance of the difference between the aged binder viscosity and the recovered binder viscosity, the modulus of the asphalt mix was calculated using equation 3.1 developed by Witczak et al[50]. The modulus was calculated using the aged binder (un-extracted) and recovered binder viscosity results and keeping the rest of the parameters in equation 3.1 constant (values shown in parenthesis).

$$\log E^* = -1.249937 + 0.02932\rho_{200} - 0.001767(\rho_{200})^2 - 0.002841\rho_4 - 0.058097V_a - 0.802208\left(\frac{V_{beff}}{V_{beff}+V_a}\right) + \frac{3.871977 - 0.0021\rho_4 + 0.003958\rho_{38} - 0.000017(\rho_{38})^2 + 0.005470\rho_{34}}{1+e^{(-0.603313-0.313351\log(f)-0.393532\log(\eta))}} \quad (3.1)$$

Where,

E^* = Dynamic modulus, 10^5 psi
η = Bitumen viscosity (aged or extracted), 10^6 Poise
f = Loading frequency, Hz; (10 Hz)
V_a = Air void content, %; (7%)
V_{beff} = Effective bitumen content, % by volume; (10.8%)
ρ_{34} = Cumulative % retained on the 19-mm sieve; (0.1%)
ρ_{38} = Cumulative % retained on the 9.5-mm sieve; (23.9%)
ρ_4 = Cumulative % retained on the 4.76-mm sieve; (59.8%)

ρ_{200} = % passing the 0.075-mm sieve; (6.4%)

Figures 46 and 47 show the plots of modulus values calculated using the un-extracted binder viscosity versus the modulus calculated from the recovered binder viscosity. The results are shown in arithmetic and log scale respectively.

An error analysis was carried out on the viscosity values obtained from un-extracted (aged) and recovered binders. The plot of percentage difference in viscosities of un-extracted (aged) and recovered binders vs. un-extracted binder viscosity is shown in Figure 48. The frequency distribution of the percentage differences is shown in Figure 49.

It can be observed from Figures 46 and 47 that all the modulus values plot on the equality line. Furthermore, it can be observed from Figure 48 that the average error is 2.9 %.

CONCLUSION

It can be concluded that a correction factor is not necessary, as the differences in viscosity values obtained from un-extracted (aged) binders and recovered binders were found to be insignificant for all practical purposes. Therefore, no correction factor was applied to the extracted binder viscosity results.

Table 8
DSR Results of Aged and Recovered Binders

Binder	Temp (C)	log T (R)	Viscosity cP					
			PAV 90	Recovered	PAV 100	Recovered	PAV 110	Recovered
ADOT AC-40	25	2.729732	460730000	422320000	469770000	442870000	449690000	440390000
	45	2.757927	71160000	63887000	97298000	78305000	120950000	105200000
	65	2.784403	3333000	3060900	4717600	4162000	7581300	6611100
	85	2.809358	216930	194590	310060	288010	512440	481300
ADOT AC-30	25	2.729732	-	-	299810000	280950000	343810000	363450000
	45	2.757927	-	-	40424000	46934000	78020000	84306000
	65	2.784403	-	-	3174400	3571600	7435200	8489700
	85	2.809358	-	-	247820	267310	622620	711060
MnRoad AC-20	25	2.729732	213660000	189790000	2036642169	242700000	285020000	285820000
	45	2.757927	14008000	12395000	29000654	19252000	32050000	39040000
	65	2.784403	818860	724970	1157115	1141600	2309000	2991200
	85	2.809358	64244	66295	96777	95024	208570	264960
MnRoad AC-120/150	25	2.729732	149470000	4859300	803836388	139820000	223720000	183390000
	45	2.757927	8034100	7058100	12316269	8318100	20301000	15932000
	65	2.784403	440870	389050	530383	491060	1430100	1154400
	85	2.809358	45253	38351	47754	41853	118940	114010
WesTrack AC-20	25	2.729732	283730000	240440000	2851303883	284990000	356280000	350980000
	45	2.757927	15725000	15901000	30096502	22192000	40966000	42857000
	65	2.784403	739240	768350	1000863	1169400	2336600	2678500
	85	2.809358	63138	58310	75112	94434	175340	208490

- Data not available

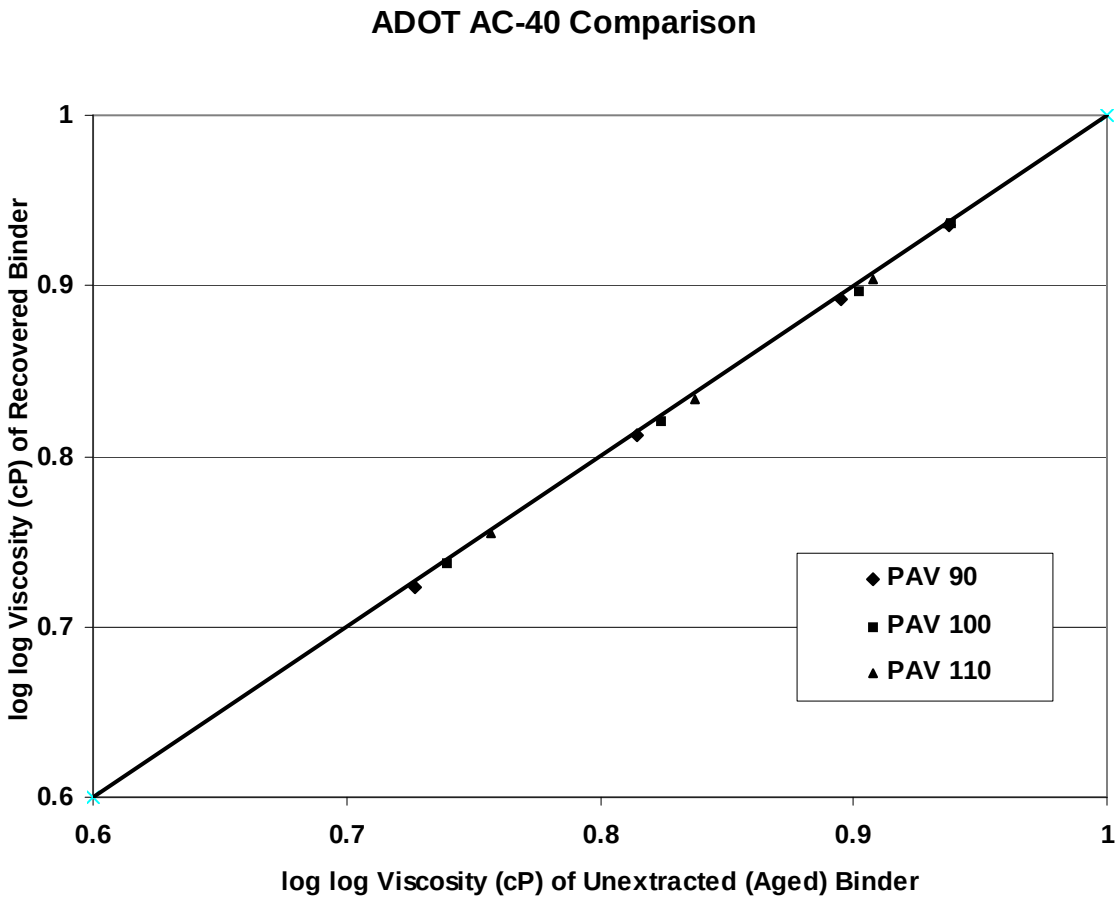

Figure 44
Viscosity Comparison for ADOT AC-40

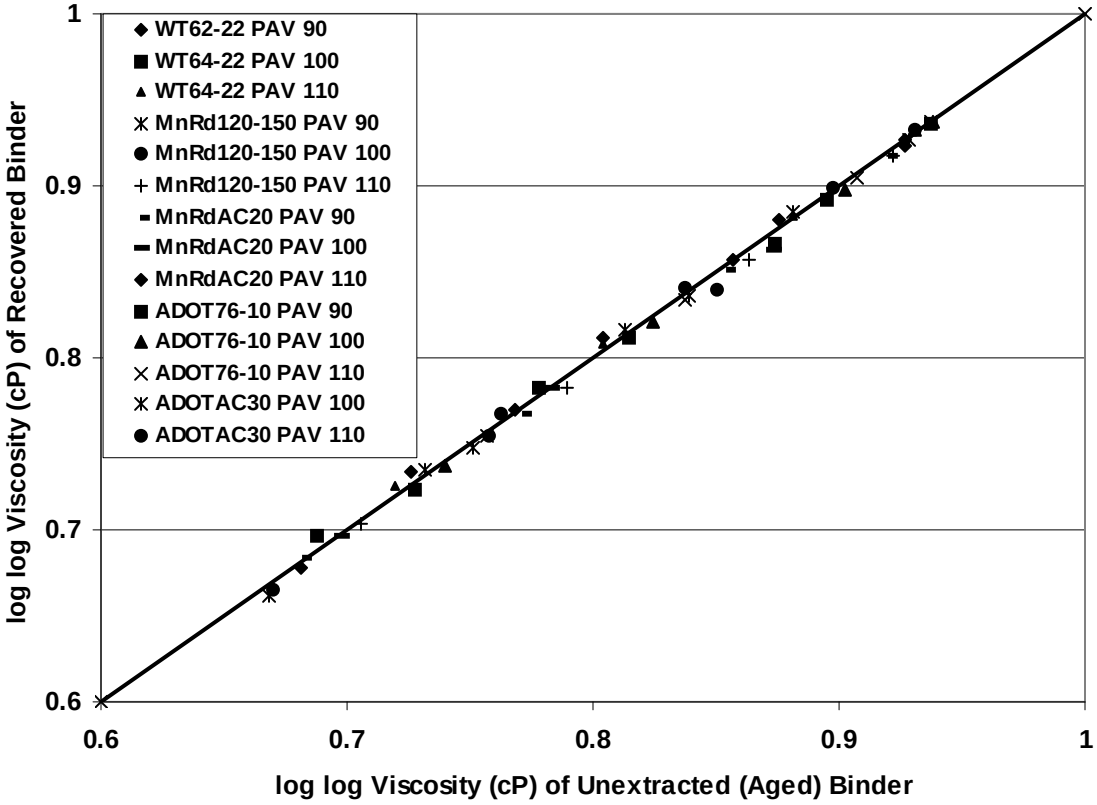

Figure 45
Viscosity Comparison for all Binders

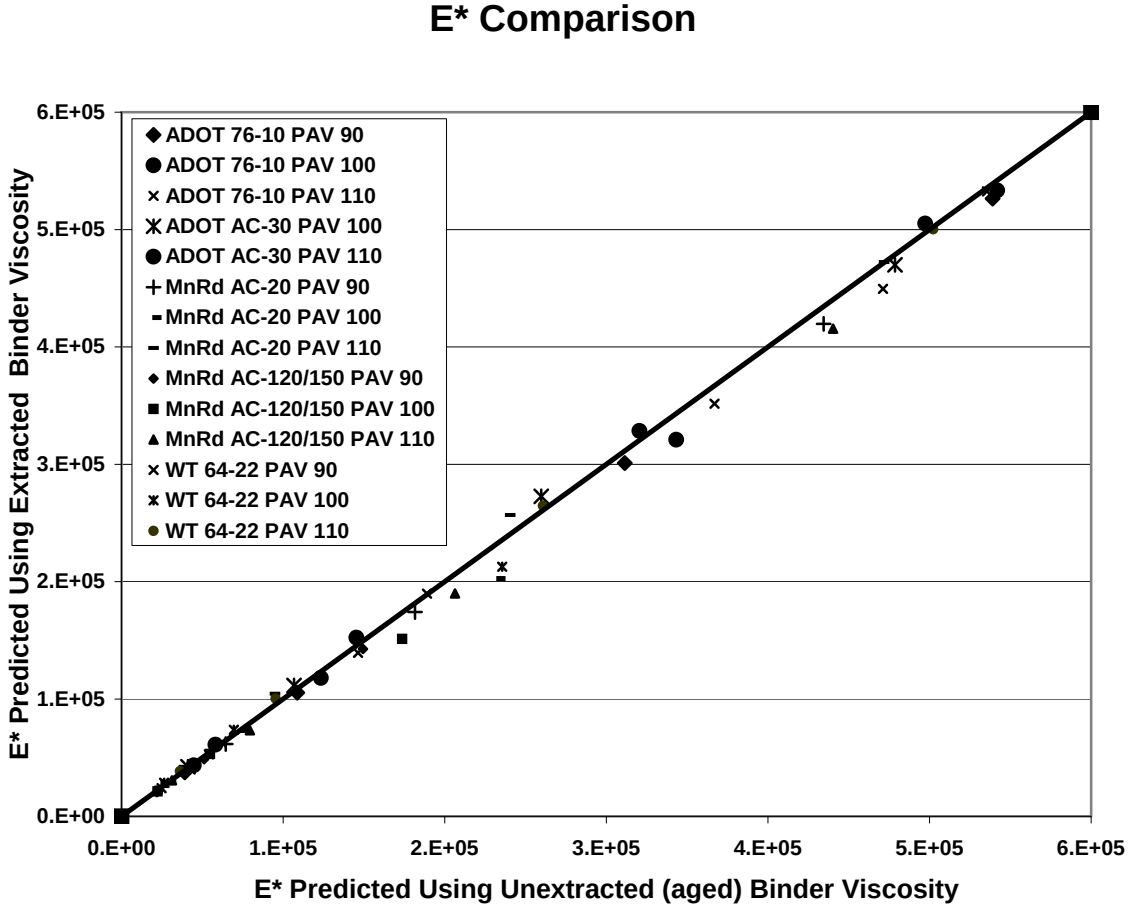

Figure 46
Modulus Comparison for All Binders in Arithmetic Scale

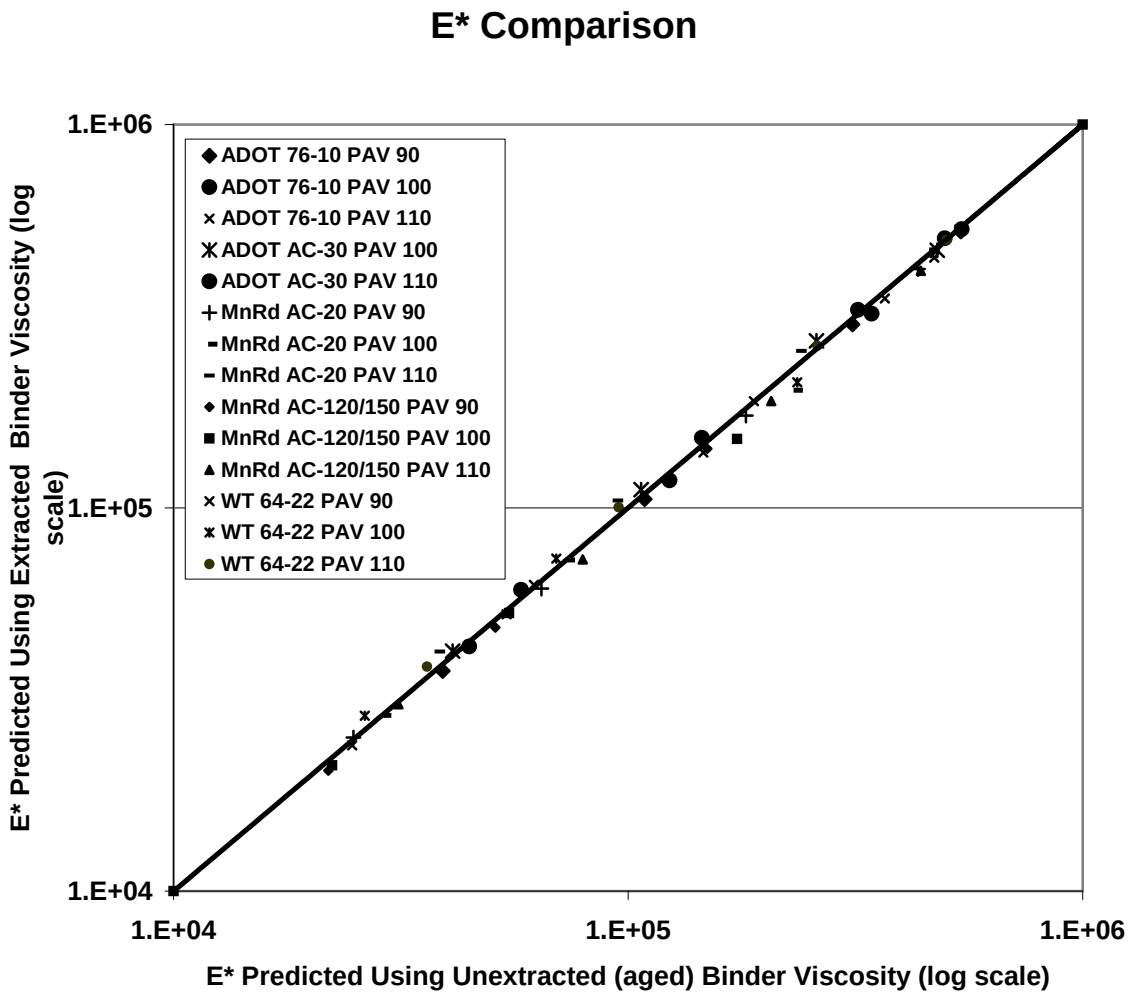

Figure 47
Modulus Comparison for All Binders in Log Scale

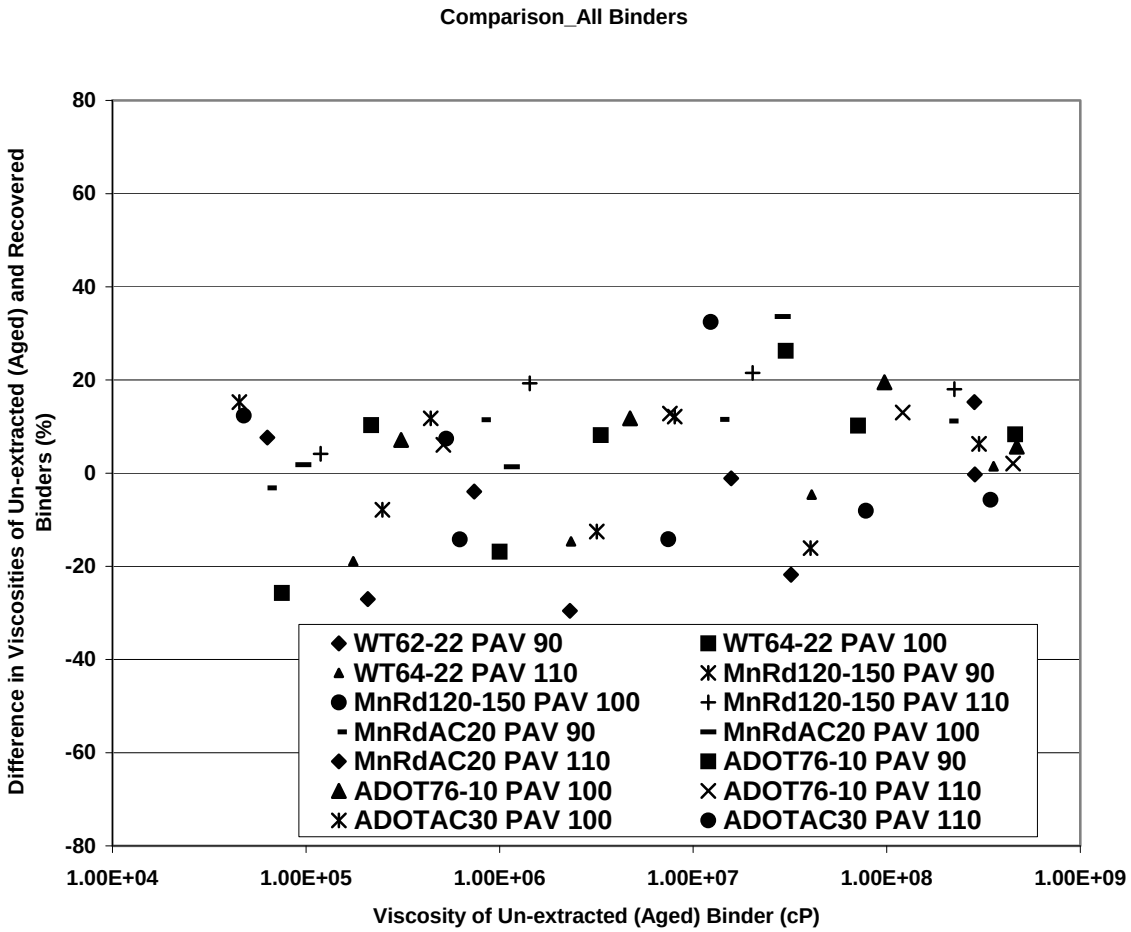

Figure 48
Plot of Percentage Difference in Viscosities of Un-Extracted (Aged) and Recovered Binders vs. Un-Extracted Binder Viscosity

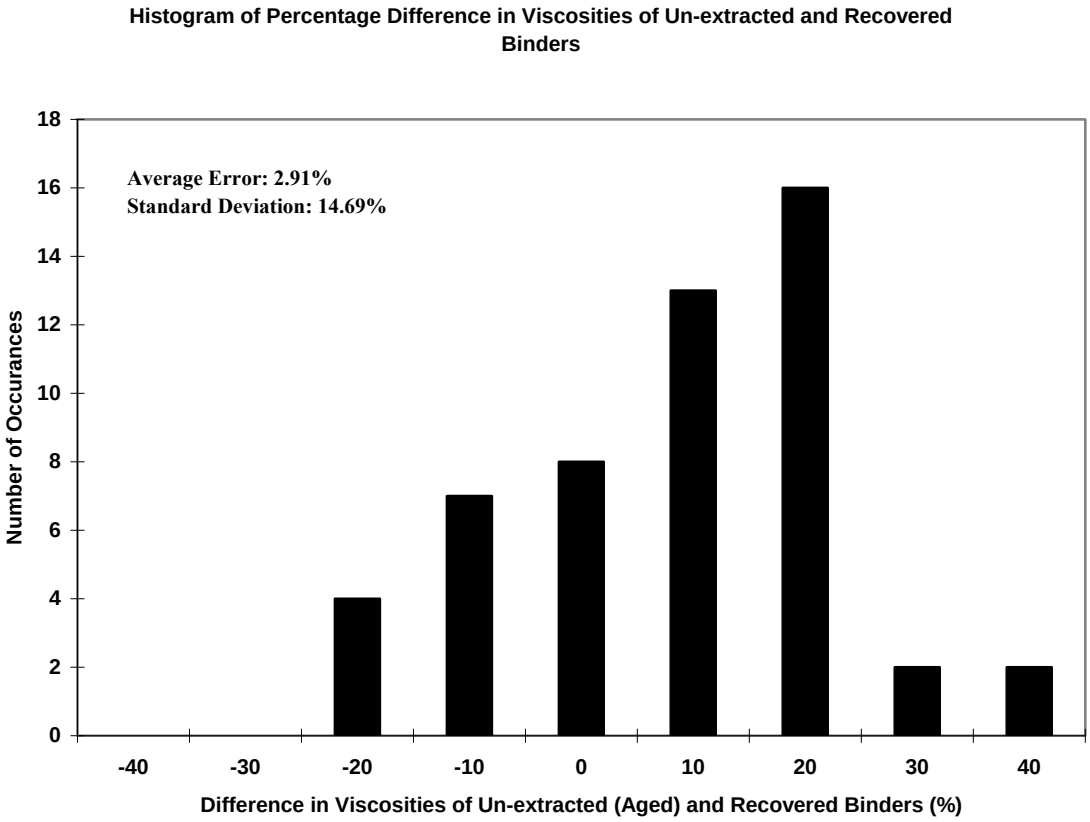

Figure 49
Frequency Distribution of Percentage Difference in Viscosities of Un-Extracted (aged) and Recovered Binders

CHAPTER 4

VERIFICATION OF PP1-98 PROTOCOL

AASHTO DESIGNATION PP1-98: STANDARD PRACTICE FOR ACCELERATED AGING OF ASPHALT BINDER USING A PRESSURIZED AGING VESSEL (PAV)

INTRODUCTION

AASHTO Designation PP1-98 covers the standard practice for accelerated aging (oxidation) of asphalt binders by means of pressurized air and at elevated temperature. The test method is intended to simulate in-service oxidative aging of asphalt binders and for use with residue from AASHTO T240 (RTFOT). The test provides an estimate of the change in the physical or chemical properties of asphalt binders after five to ten years of in-service aging in the field.

CURRENT CONDITIONS FOR THE PP1-98 PROTOCOL

The standard testing procedure under the existing PP1-98 protocol requires asphalt samples to be tested at the following conditions:

- Asphalt binder aged using T240 (RTFOT)
- PAV aging time = 20 hrs
- Air pressure = 2.10 MPa
- Aging temperature = 100°C or 110°C as a function of climate

APPROACH

The following approach was adopted to verify the existing protocol:

1. Binders and field cores were obtained from the field sites.
2. Binders were aged in RTFO and PAV at three aging temperatures (90°C, 100°C, 110°C).
3. DSR testing was carried out on the aged binders.
4. A-VTS plots were developed using the viscosity values obtained from DSR testing.
5. Field cores of 10-inch and 6-inch diameter were obtained from existing pavements.
6. Binder was extracted and recovered from these field cores.
7. Extracted field-aged binder was subjected to DSR testing to obtain field-aged viscosity values.
8. Field-aged viscosity values were plotted on the corresponding A-VTS plots.
9. The PAV temperature corresponding to the filed-aged viscosity was noted and compared with the existing protocol.

10. Field aging conditions such as mean annual air temperature (*MAAT*) and aging time were previously known for these cores.
11. Observations and conclusions were made based on the plots.

These steps are explained in detail in the following sections.

LABORATORY TESTING ON BINDER

Three binders were obtained from three different sites across the country:

1. ADOT AC-30 (Arizona)
2. MnRoad AC-20 (Minnesota)
3. WesTrack AC-20 (Nevada)

The DSR testing was carried out at a sweep of four temperatures (25°C, 45°C, 65°C, and 85°C) on original, RTFO and PAV aged binders. The viscosity values obtained from the DSR testing were used to develop A-VTS plots as shown in Figure 50.

Figure 50 shows that the viscosity values at lower temperatures tend to converge. Similar trend was observed in all the DSR tests conducted, both on PAV-aged binders and on field-aged (extracted) binders shown in the following section. This phenomenon can be attributed to the fact that at low temperatures, the viscosity of the binder increases and tends to converge to an ultimate value irrespective of the PAV aging condition. For this reason, viscosity values at 25°C were considered to be outliers and were discarded in further analysis. This resulted in relatively parallel A-VTS lines and improved R^2 values.

DSR TEST RESULTS ON LABORATORY AGED BINDERS

The DSR test results and the A and VTS values of the laboratory-aged (PAV aged) binders obtained after the elimination of viscosity results at 25°C are summarized in Tables 9 to 11. The A-VTS plots obtained from the data presented in Tables 9 to 11 are shown in Figures 51 to 53, respectively.

LABORATORY TESTING ON RECOVERED BINDER FROM FIELD CORES

In order to verify the PP1-98 protocol, field cores and binders were obtained from the following sites:

Kingman, Arizona

Kingman site is located on Highway 93 near Chloride and is about 9 years old. It has a dense graded mix with 4.5% asphalt by weight.

- Field Aging time: 9 years
- Binder type: AC-30
- *MAAT*: 62.6°F

MnRoad, Minnesota

The Minnesota Road Research Project is the world's largest and most comprehensive outdoor pavement laboratory. It is located 40 miles northwest of Minneapolis/St. Paul. The Sections selected were 16 and 18. Section 16 has 197 mm HMA layer and 711 mm base. Section 18 has base courses of 229 mm and 305 mm and 197 mm HMA layer.

- Field Aging time: 9 years
- Binder type: AC-20
- *MAAT*: 46.2°F

WesTrack, Nevada

WesTrack is located at Nevada Automotive Test Center (NATC), 60 miles southeast of Reno and 35 miles from Carson City. The climate is dry, no frost penetration, although the LTPP database has catalogued this site as dry and subject to freezing action.

The sections selected in WesTrack were 12, 15 and 16. These sections were designed for 4% 8% and 12% air voids, respectively. Also they are of fine and fine-plus gradation type.

- Field Aging time: 7 years
- Binder type: AC-20
- *MAAT*: 54.4°F

The field cores obtained were of 6-inch diameter and of varying heights exceeding 6 inches. From these cores, sub-cores of 4-inch diameter and 6-inch height were obtained. These cores were sliced into layers as shown in Figure 54. Binder was extracted separately from these layers and DSR testing was conducted on the extracted binder. Three cores were taken from each site. Two of these cores were used for extraction and recovery. This resulted in one replicate for each binder extraction and DSR testing on the field-aged binders.

DSR TEST RESULTS ON FIELD-AGED BINDER

The DSR test results on the field-aged binder are as shown in Table 12. Results from the Table 12 were used to obtain the A-VTS plots for the field-aged binders extracted at various depths. The A-VTS plots are as shown in Figures 55 to 60.

DATA ANALYSIS

It can be observed from the graph that viscosity values at all three depths, plotted nearly on top of each other, i.e. there is no difference in the viscosity values obtained at different depths in the pavement, for all practical purposes. This trend was observed for all the binders extracted from the field cores. Therefore, for the verification study, the average viscosity of the binder extracted from the top layer (1-inch thickness) was considered to be representative of the site.

Viscosity values obtained from the field-aged binder DSR tests, on the binder extracted from the top layer of the field cores were plotted on the corresponding laboratory-aged binder DSR results (A-VTS plots) as shown in Figures 61 to 63.

It can be observed from Figures 61 to 63 that the viscosity trend of the field-aged binder followed that of the laboratory-aged binder. Therefore, field-aged binder viscosity was calculated at a reference temperature (65°F) and used for comparison. Viscosity of the field-aged binder at 65°F was calculated and plotted on the corresponding A-VTS plots of the laboratory-aged binder. From this comparison, a particular PAV aging temperature was chosen to simulate the field aging at a known set of field aging conditions.

Field-aged viscosities at 65°F were plotted on the A-VTS plots as shown in Figures 64 to 66. The results of the comparison are summarized in Table 13 and Table 14.

RESULTS AND CONCLUSIONS

As it can be observed from the comparison tables, for Kingman, Arizona site with a *MAAT* of 62.6°F and 9 years aging time, the field-aged viscosity corresponded to a PAV aging temperature of 101°C. This is in accordance with the current PP1-98 protocol. However, for the MnRoad Cells 16 and 18 with a *MAAT* of 46.2°F and 9 years aging time, the field-aged viscosity corresponded to PAV aging temperatures of 95°C and 89°C, respectively. This observation is in accordance with the fact that binders do not undergo as much aging in lower temperatures as they do at higher temperatures. Therefore, to accommodate the lower *MAAT*s in the field, a lower PAV aging temperature might be included in the PP1-98 protocol.

For WesTrack Sections 15 and 16, the field-aged viscosity corresponded to PAV 109°C and 110°C respectively and for Section 12, it was 72°C. This might be due to the fact that sections 15 and 16 have higher air voids than section 12. It can also be observed that WesTrack binder in Sections 15 and 16 has aged more than the ADOT binder in spite of having lower *MAAT* and lower aging period. This might be a result of the difference in the binder grades. WesTrack binder is softer than the ADOT binder and hence, undergoes higher degree of aging than the ADOT binder.

Similar trends were observed in the analyses conducted at the other two DSR test temperatures (65ºC and 85ºC) also. Results from the analysis conducted at 60ºC are reported in Table 15. Absolute viscosity of the binders is reported at a standard temperature of 60ºC. Therefore, 60ºC was selected as the standard analysis temperature.

Based on the observations made from the analyses conducted, the following conclusions were drawn.

1. A lower PAV aging temperature (90°C) than those specified in the existing protocol (100°C, 110°C) might be needed to simulate the aging in colder regions (lower *MAAT*).

2. Binder grade (stiffness) and mix air voids are important factors to be considered when deciding the PAV aging temperature.
3. Other PAV aging conditions such as aging time (currently 20 hours) and pressure (currently 2.1 MPa) might be altered to simulate the aging in the field of lower air void mixes at colder regions.

Table 9
DSR Results for ADOT AC-30 Binder

Temperature (C)	Viscosity (Pas)	A	VTS	R^2
ADOT AC-30 - Original				
45	3534.2	10.512	-3.5155	1.0000
65	191.48			
85	20.818			
ADOT AC-30 - RTFO				
45	9429.6	10.178	-3.3845	0.9999
65	497.04			
85	46.885			
ADOT AC-30 - PAV 90				
45	37512	9.3111	-3.0564	0.9970
65	2478.2			
85	187.17			
ADOT AC-30 - PAV 100				
45	40424	8.8794	-2.8991	0.9955
65	3174.4			
85	247.82			
ADOT AC-30 - PAV 110				
45	78020	8.0864	-2.6057	0.9941
65	7435.2			
85	622.92			

Table 10
DSR Results for MnRoad AC-20 Binder

Temperature (C)	Viscosity (Pas)	A	VTS	R^2
MnRoad AC-20 - Original				
45	2046.9	10.818	-3.6324	1.0000
65	114.14			
85	12.728			
MnRoad AC-20 - RTFO				
45	5491.9	10.651	-3.5615	1.0000
65	265.67			
85	26.333			
MnRoad AC-20 - PAV 90				
45	14008	10.08	-3.3445	0.9982
65	818.86			
85	64.244			
MnRoad AC-20 - PAV 100				
45	29000	10.265	-3.4055	1.0000
65	1157.1			
85	96.777			
MnRoad AC-20 - PAV 110				
45	32050	8.8909	-2.9057	0.9983
65	2309			
85	208.57			

Table 11
DSR Results for WesTrack AC-20 Binder

Temperature (C)	Viscosity (Pas)	A	VTS	R^2
WesTrack AC-20 - Original				
45	2097.7	10.924	-3.6708	0.9999
65	107.59			
85	12.399			
WesTrack AC-20 - RTFO				
45	4577.6	10.699	-3.5809	1.0000
65	225.82			
85	22.837			
WesTrack AC-20 - PAV 90				
45	15725	10.286	-3.4186	0.9998
65	739.24			
85	63.138			
WesTrack AC-20 - PAV 100				
45	30096	10.836	-3.6122	1.0000
65	1000.8			
85	75.113			
WesTrack AC-20 - PAV 110				
45	40966	9.5574	-3.1451	0.9983
65	2336.6			
85	175.34			

Table 12
DSR Test Results on Extracted Field Aged Binder

Temperature (C)	log T (R)	Top		Middle		Bottom	
		Viscosity (Pas)	loglog Visc (cP)	Viscosity (Pas)	loglog Visc (cP)	Viscosity (Pas)	loglog Visc (cP)
ADOT-Kingman-1							
45	2.757927	63162	0.89212	52024	0.887404	55449	0.888959
65	2.784403	3808.3	0.818274	3134.7	0.812659	3565.6	0.816383
85	2.809358	239.9	0.730785	219.8	0.727706	214.62	0.726863
ADOT-Kingman-2							
45	2.757927	56485	0.88941	53936	0.888285	57930	0.890024
65	2.784403	3683.2	0.817316	3313.3	0.814265	3826	0.818407
85	2.809358	228.4	0.729059	202.39	0.724783	226.35	0.728742
MnRoad Cell-16-1							
45	2.757927	18409	0.8612374	17000	0.8591653	17513	0.8599401
65	2.784403	944.81	0.7763629	857.36	0.7732863	886.18	0.7743361
85	2.809358	76.368	0.6886788	65.03	0.6824261	63.748	0.6816452
MnRoad Cell-16-2							
45	2.757927	18319	0.8611102	19199	0.8623269	17148	0.8593913
65	2.784403	973.34	0.777301	957.47	0.7767829	882.6	0.7742077
85	2.809358	77.534	0.6892638	75.837	0.6884092	66.537	0.683323
MnRoad Cell-18-1							
45	2.757927	13416	0.8529447	12857	0.851817	11527	0.8489103
65	2.784403	766.64	0.7697163	614.35	0.7625597	590.36	0.7612599
85	2.809358	61.141	0.6800029	55.037	0.6758383	52.071	0.6736287
MnRoad Cell-18-3							
45	2.757927	14201	0.8544469	14210	0.8544636	12095	0.8501931
65	2.784403	772.34	0.7699537	694.92	0.7665567	586.77	0.7610605
85	2.809358	63.225	0.6813217	64.09	0.6818552	49.36	0.6714853
WesTrack Section-12-1							
45	2.757927	8385.9	0.8403288	6893.5	0.834957	10423	0.8462129
65	2.784403	395.58	0.7479735	322.95	0.7410834	468.21	0.7536168
85	2.809358	36.38	0.659047	30.016	0.6510213	42.463	0.6653944
WesTrack Section-12-3							
45	2.757927	10145	0.8454858	6734.5	0.8343129	10911	0.8474409
65	2.784403	477.84	0.7542935	302.54	0.7388426	480.9	0.7545054
85	2.809358	38.935	0.6618449	29.82	0.6507453	42.732	0.6656516
WesTrack Section-15-4							
45	2.757927	41483	0.8818336	36509	0.8786596	32185	0.8755042
65	2.784403	1973	0.7990045	1723.9	0.7949418	1445.7	0.7895862
85	2.809358	137.24	0.7107502	111.84	0.7031707	99.092	0.6986258

Table 12 – Cont'd

Temperature (C)	log T (R)	Top		Middle		Bottom	
		Viscosity (Pas)	loglog Visc (cP)	Viscosity (Pas)	loglog Visc (cP)	Viscosity (Pas)	loglog Visc (cP)
WesTrack Section-15-6							
45	2.757927	43035	0.882742	33881	0.8767925	34044	0.8769127
65	2.784403	2043.8	0.8000595	1593.1	0.7925488	1543.3	0.7915819
85	2.809358	147.66	0.7134286	107.03	0.7015253	103.52	0.700273
WesTrack Section-16-7							
45	2.757927	41604	0.8819057	37298	0.8791926	43745	0.8831461
65	2.784403	1924.3	0.798255	1741.8	0.7952541	2036.3	0.7999496
85	2.809358	130.87	0.7090018	122.56	0.7065769	142.36	0.7120928
WesTrack Section-16-8							
45	2.757927	50089	0.8864762	38191	0.8797815	36708	0.8787952
65	2.784403	2429.9	0.8052009	1697.4	0.794473	1683.6	0.7942258
85	2.809358	163.98	0.7172369	118.18	0.7052258	111.84	0.7031707

Table 13
Summary of the Comparison Results at 65ºC

Binder	Section	loglog Viscosity (cP) @ 65ºC				Field Age (years)	*MAAT* (F)
		PAV 90	PAV 100	PAV 110	Field Core		
AC-30	ADOT-KM	0.8007497	0.8071364	0.8310803	0.8111672	9	62.6
AC-20	MnRd - 16	0.7675632	0.7827146	0.8002593	0.7737159	9	46.2
	MnRd - 18				0.7664439	9	46.2
AC-20	WT - 12	0.7672389	0.7781784	0.8001732	0.7494311	7	54.4
	WT - 15				0.7959783	7	54.4
	WT - 16				0.7978829	7	54.4

Table 14
Summary of the Comparison Results at 65ºC

Binder	Section	Field Age (years)	*MAAT* (F)	loglog Viscosity (cP) @ 65ºC		% Change in loglog Viscosity Due to Aging
				Original	Field Core	
AC-30	ADOT-KM	9	62.6	0.7228085	0.8111672	12.22
AC-20	MnRd - 16	9	46.2	0.7039305	0.7737159	9.91
	MnRd - 18	9	46.2		0.7664439	8.88
AC-20	WT - 12	7	54.4	0.7017209	0.7494311	6.80
	WT - 15	7	54.4		0.7959783	13.43
	WT - 16	7	54.4		0.7978829	13.70

Table 15
Summary of the Comparison Results at 60ºC

Binder	Section	loglog Viscosity (cP) @ 60°F					Corresponding PAV Temp
		RTFO	PAV 90	PAV 100	PAV 110	Field Core	
AC-30	ADOT-KM	0.7760822	0.8206224	0.8258914	0.8479372	0.8313784	101
AC-20	MnRd - 16	0.7573879	0.7891996	0.8047456	0.8190570	0.7953659	95
	MnRd - 18					0.7881968	89
AC-20	WT - 12	0.7514960	0.7893547	0.8015466	0.8205196	0.7723899	72
	WT - 15					0.8173721	109
	WT - 16					0.8193699	110

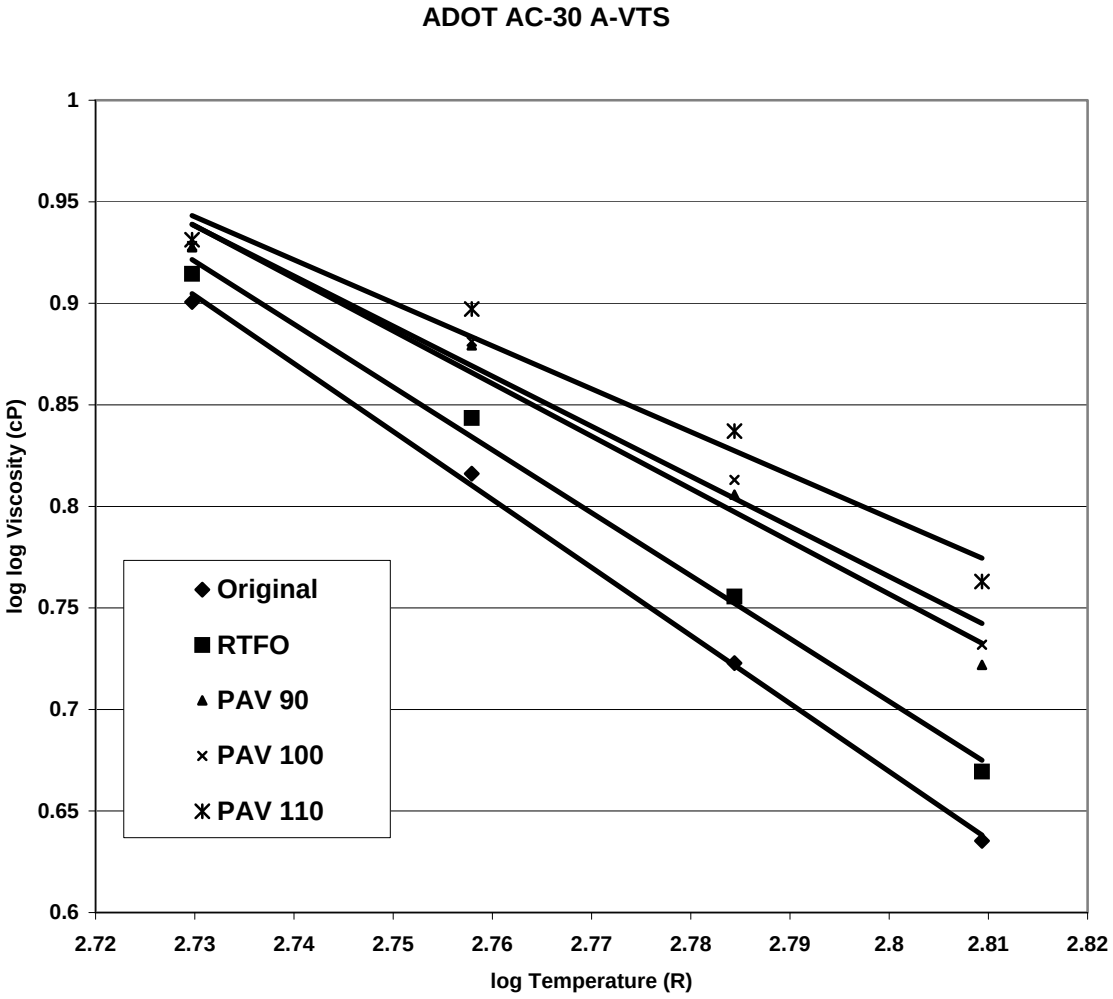

Figure 50
A-VTS Plots for ADOT AC-30

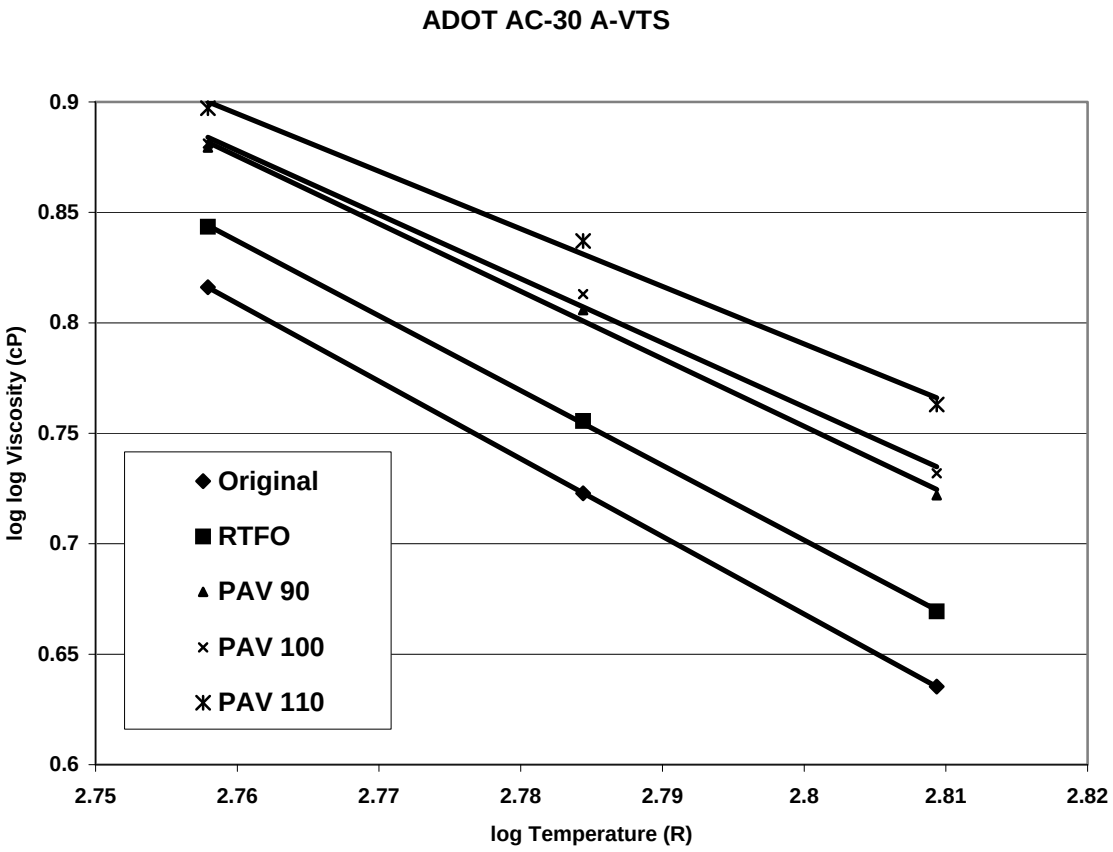

Figure 51
A-VTS Plots for ADOT AC-30 Binder

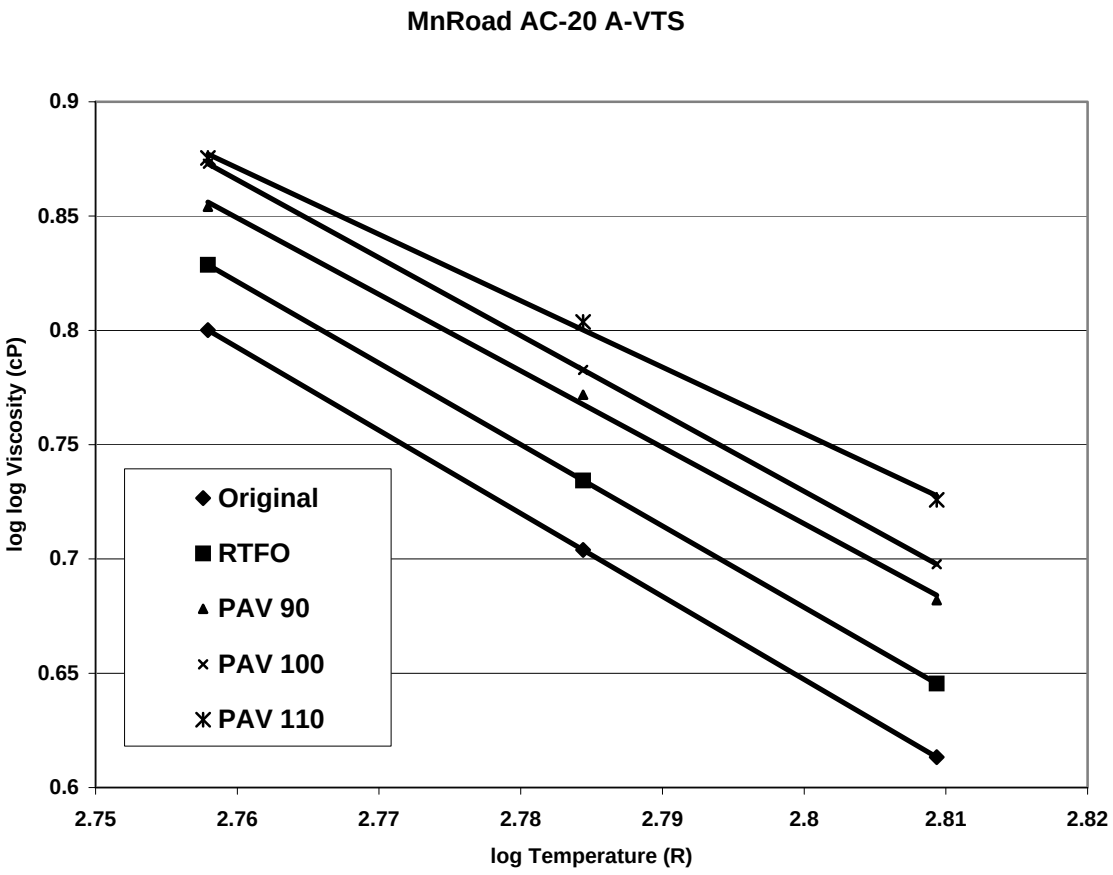

Figure 52
A-VTS Plots for MnRoad AC-20 Binder

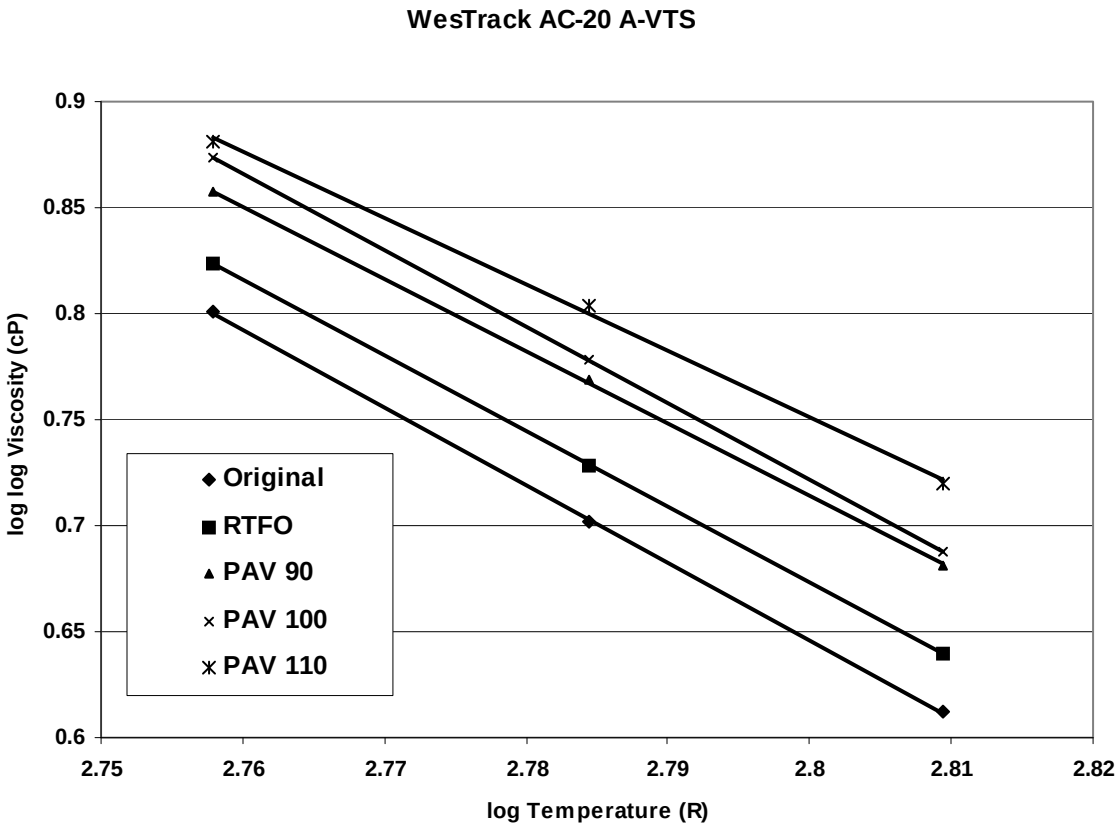

Figure 53
A-VTS Plots for WesTrack AC-20 Binder

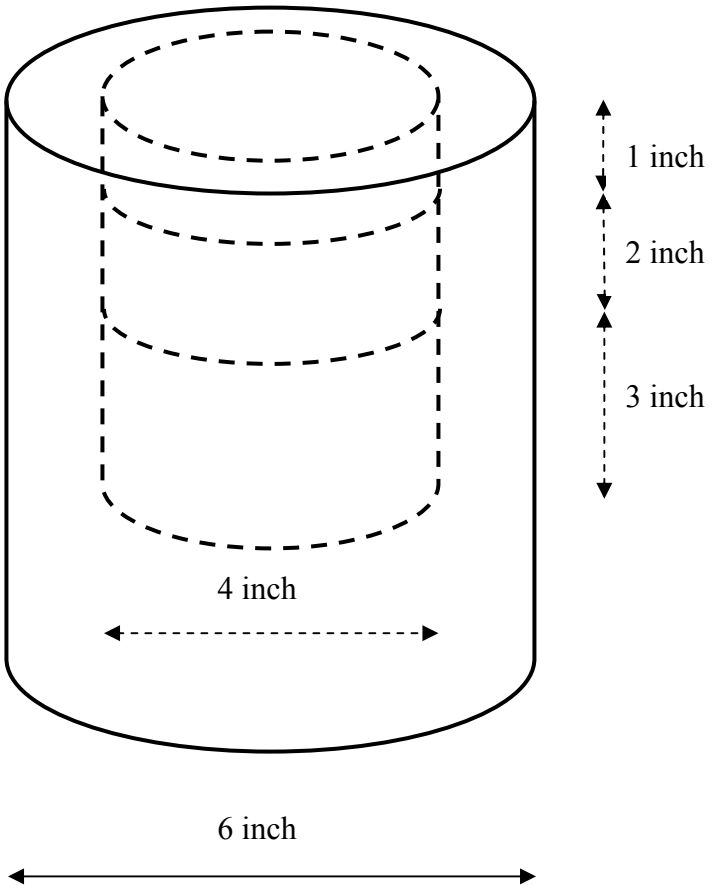

Figure 54
Sketch of Sub-Cored and Sliced Field Core

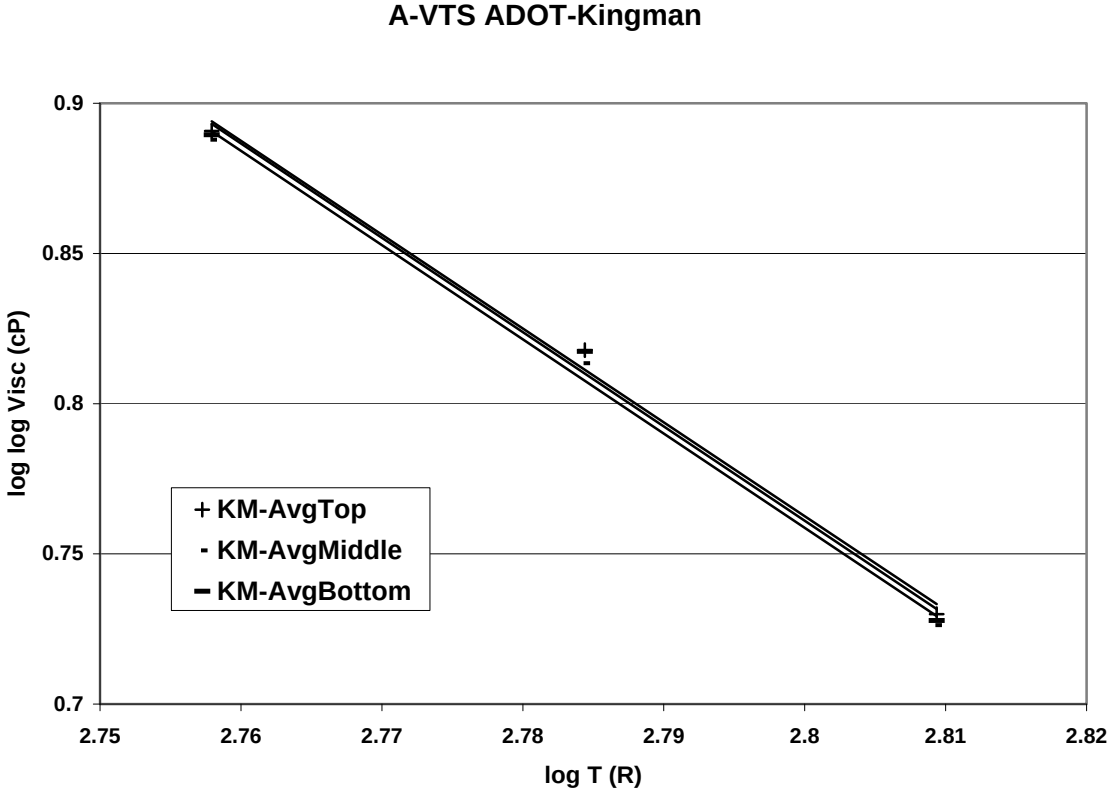

Figure 55
A-VTS for ADOT Kingman Field Core

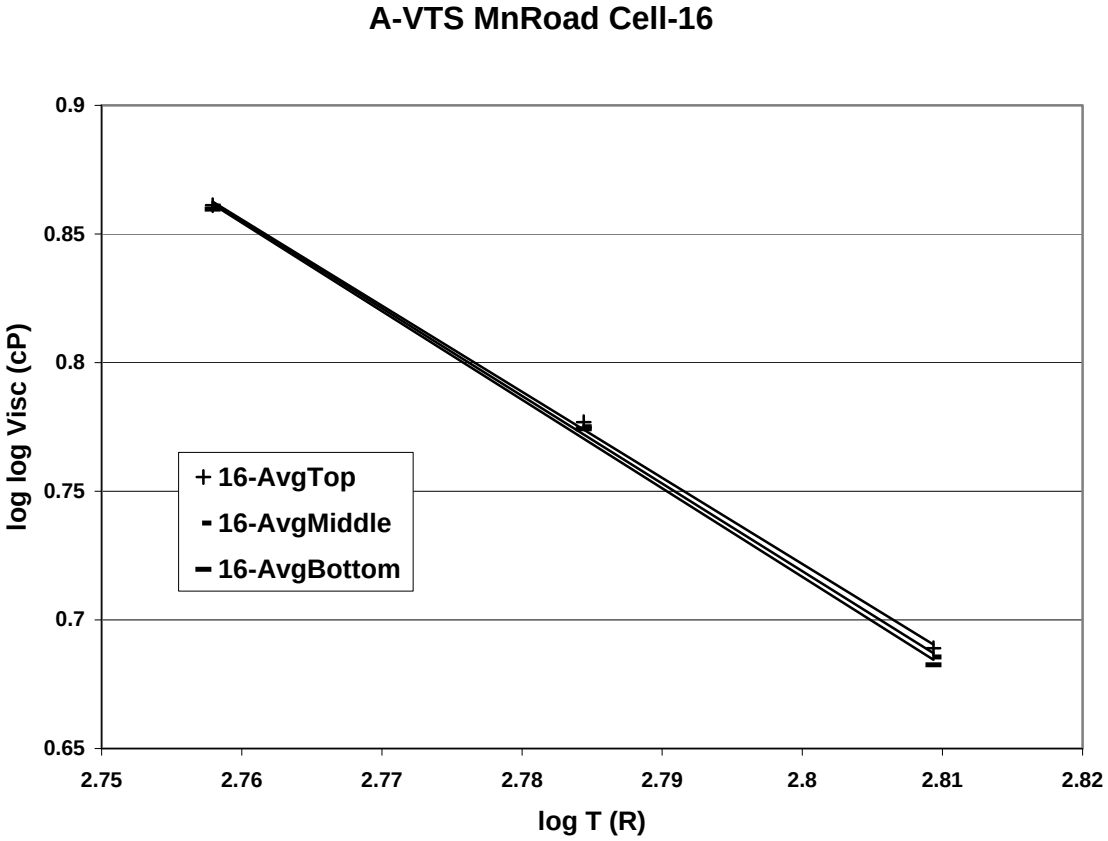

Figure 56
A-VTS for MnRoad Cell-16 Field Core

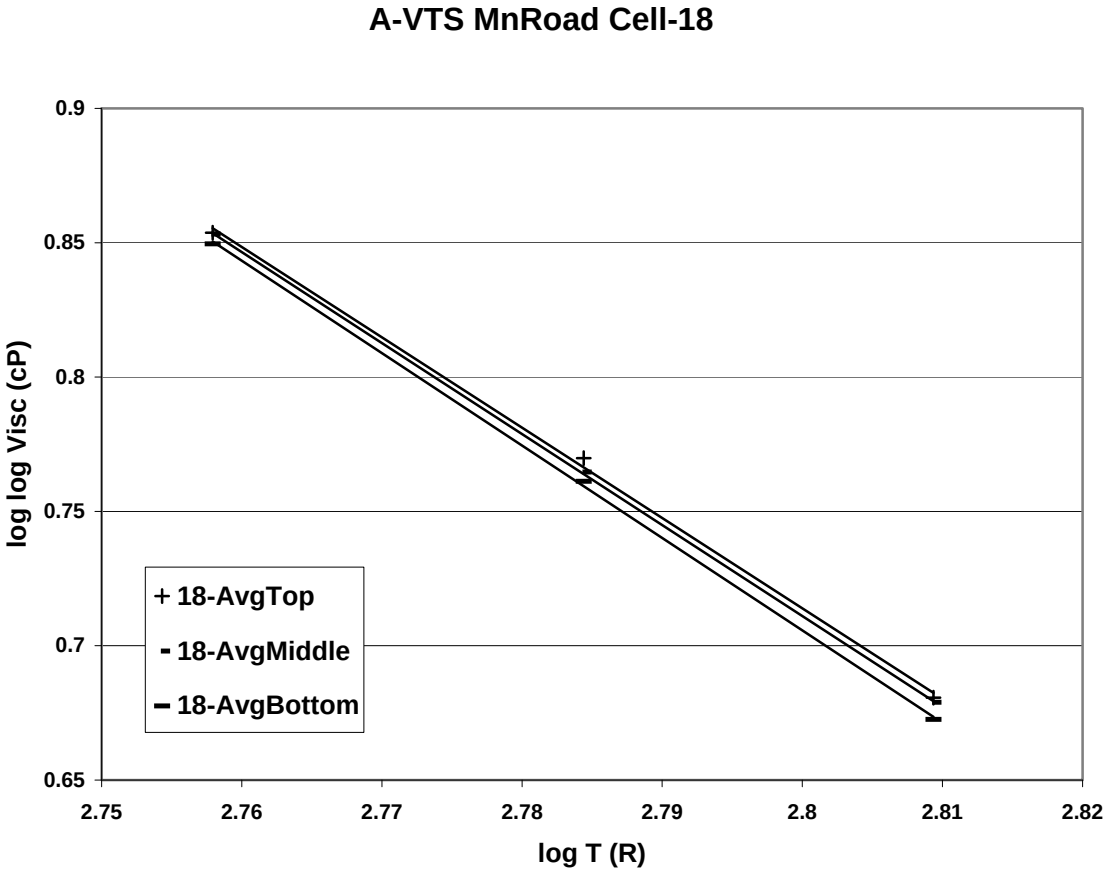

Figure 57
A-VTS for MnRoad Cell-18 Field Core

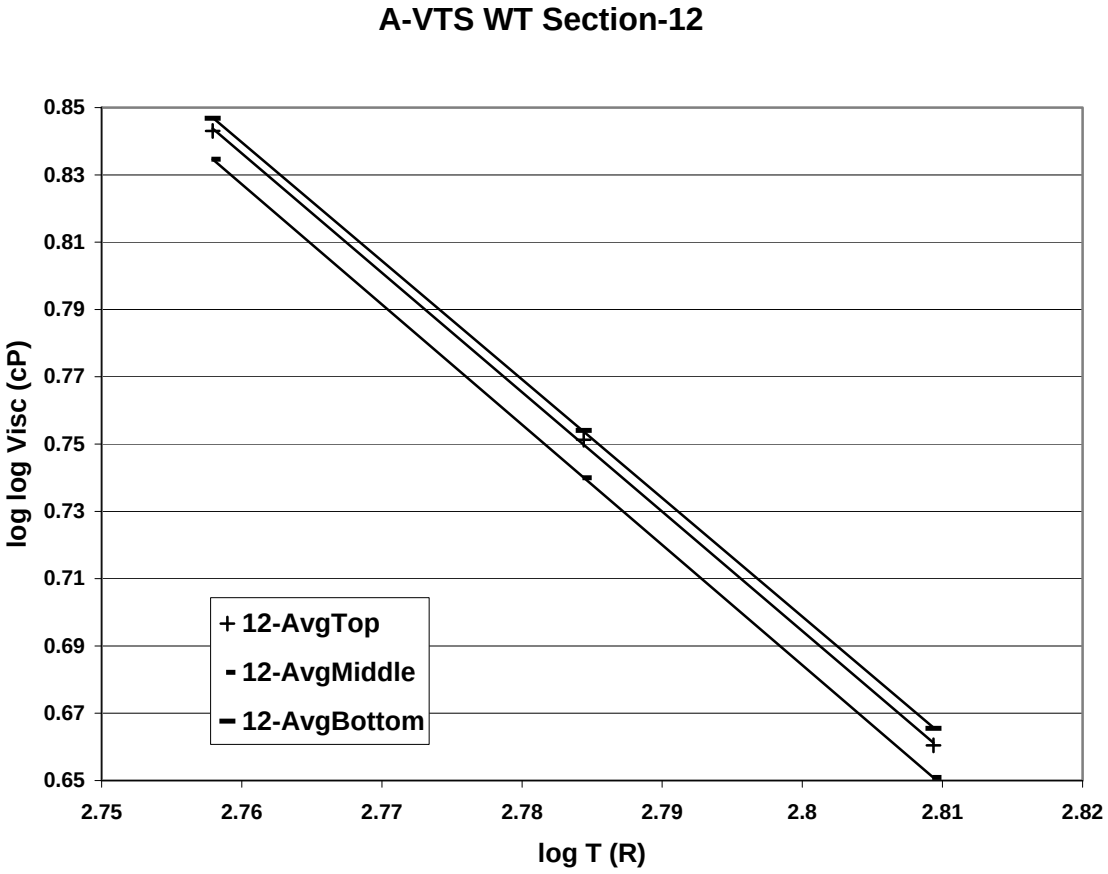

Figure 58
A-VTS for WesTrack Section 12 Field Core

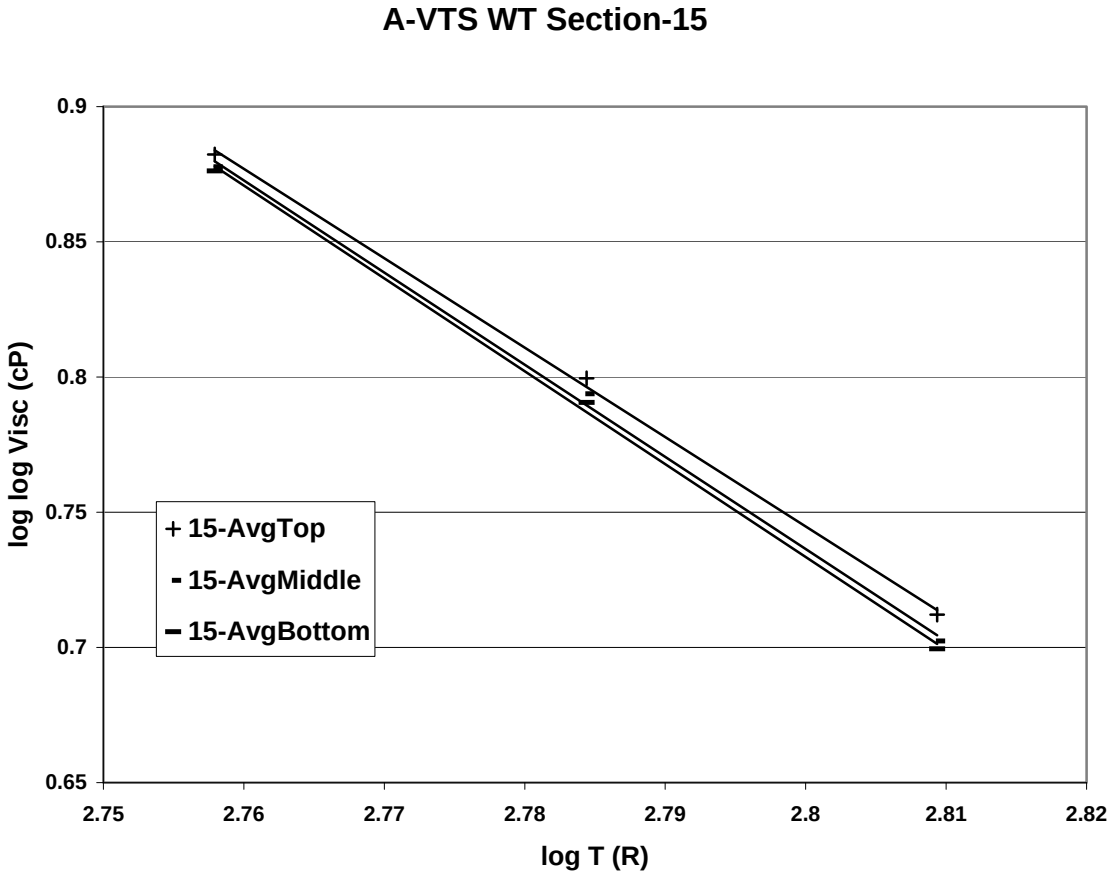

Figure 59
A-VTS for WesTrack Section 15 Field Core

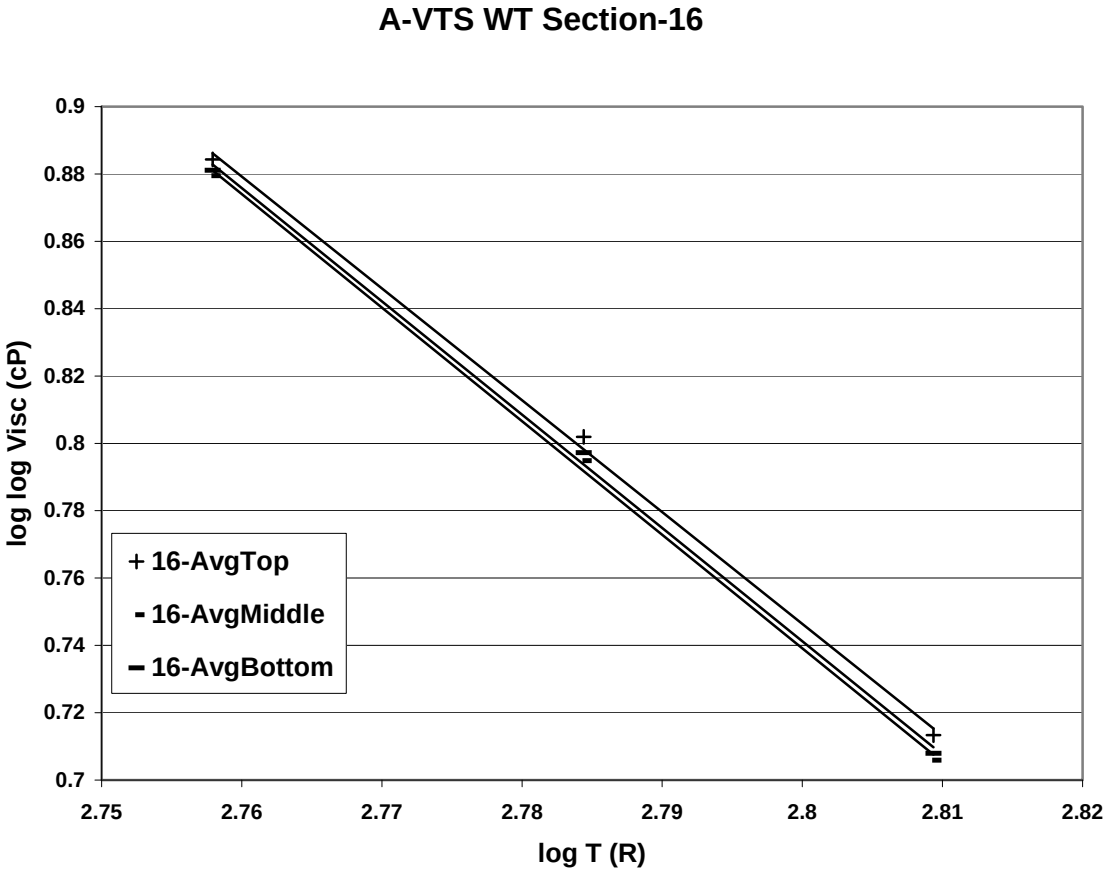

Figure 60
A-VTS for WesTrack Section 16 Field Core

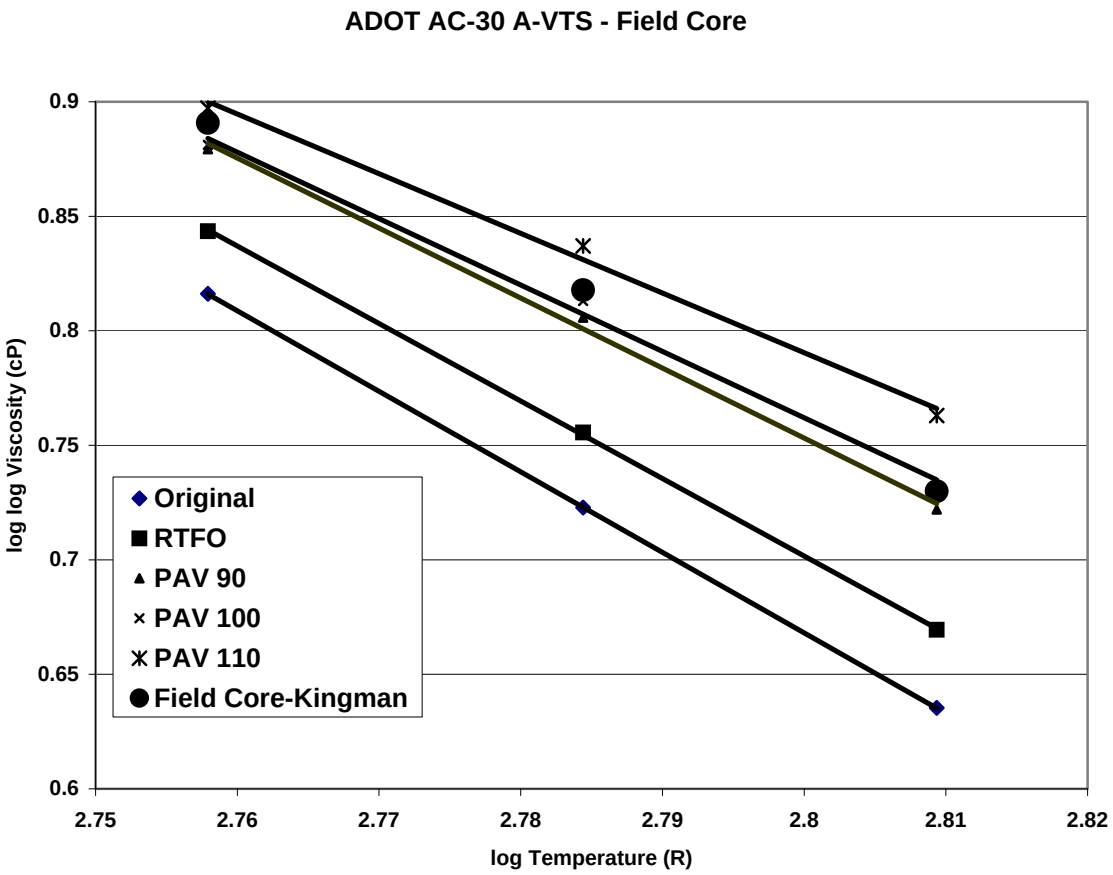

Figure 61
Field Viscosity Plotted on Top of Laboratory Aged Binder A-VTS Plots for ADOT AC-30 Binder

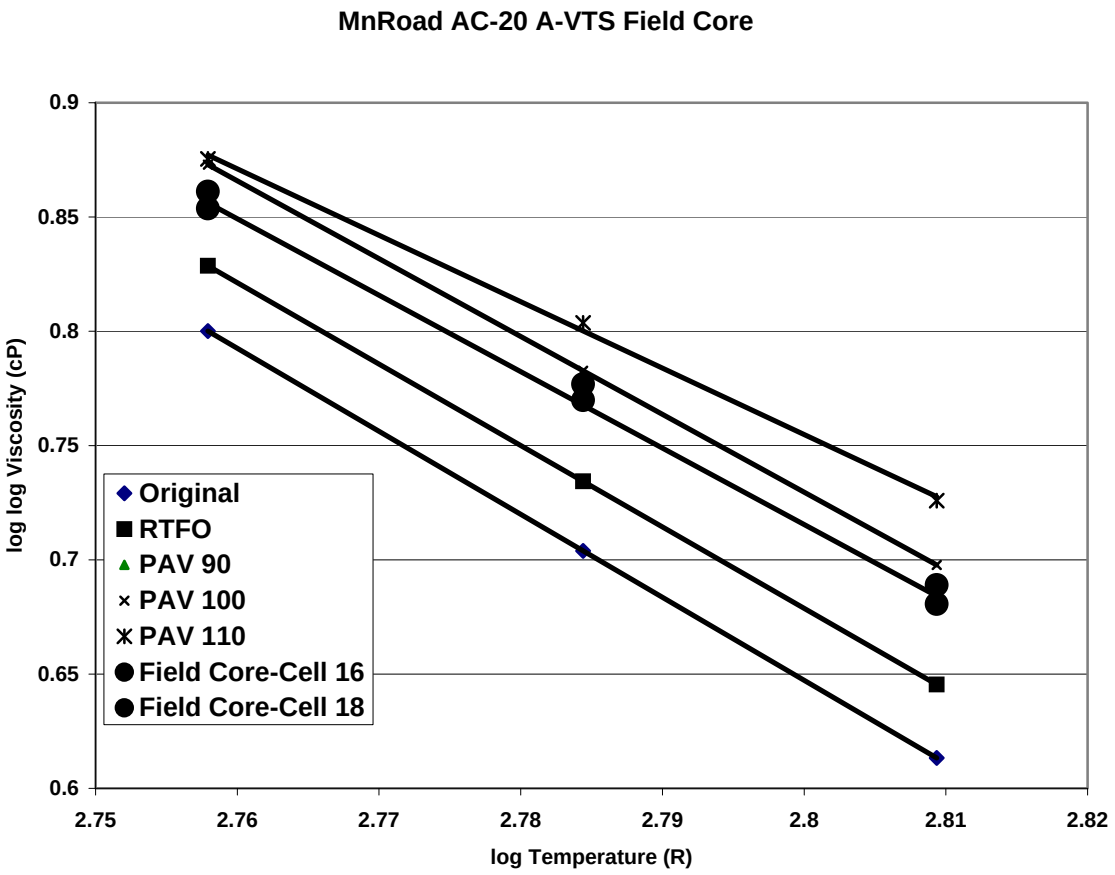

Figure 62
Field Viscosity Plotted on Top of Laboratory Aged Binder A-VTS Plots for MnRoad AC-20 Binder

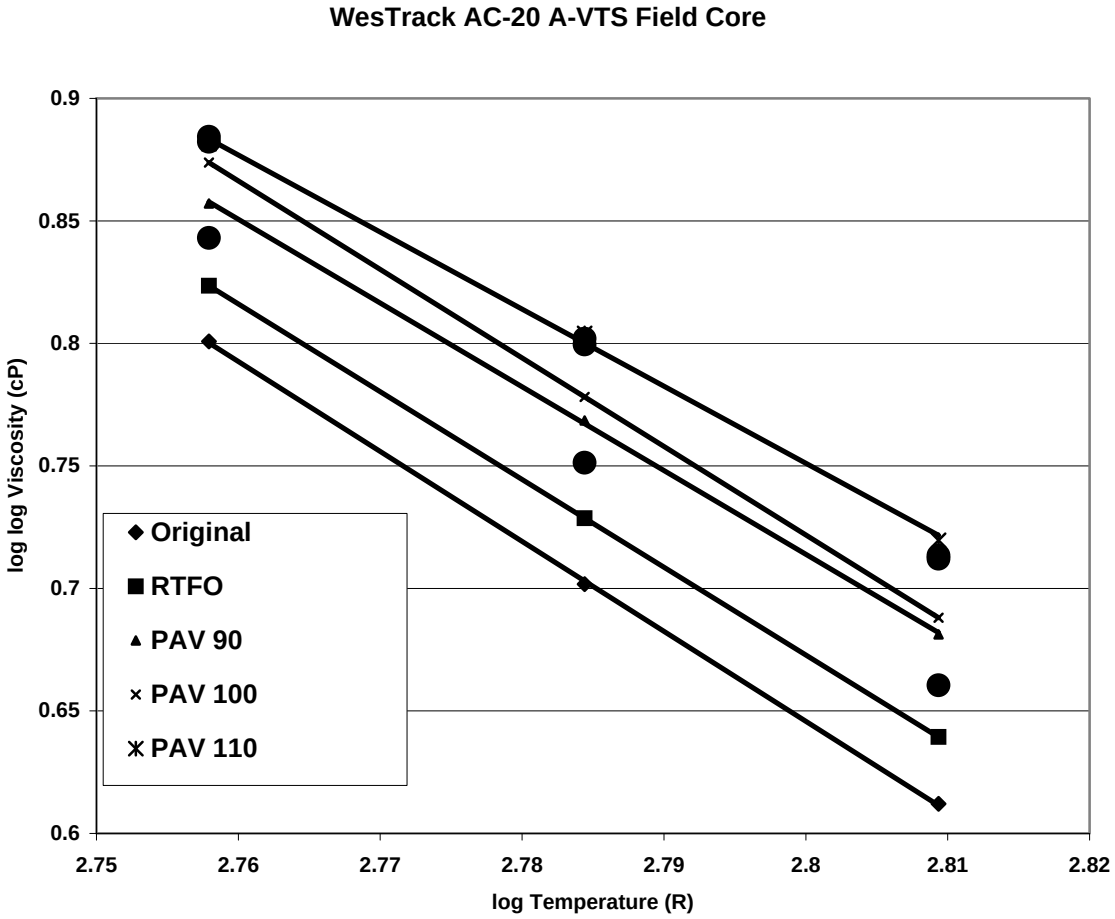

Figure 63
Field Viscosity Plotted on Top of Laboratory Aged Binder A-VTS Plots for WesTrack AC-20 Binder

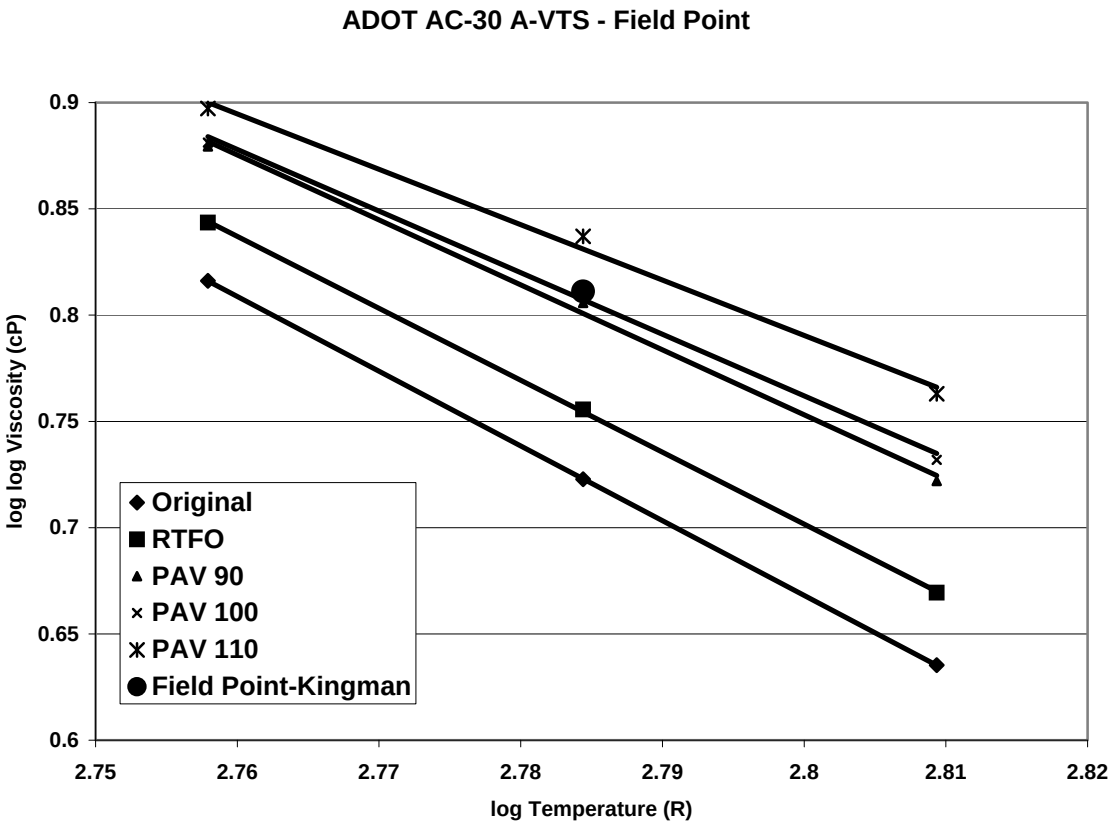

Figure 64
Field-Aged Viscosity at 65°F on A-VTS Plots for ADOT AC-30

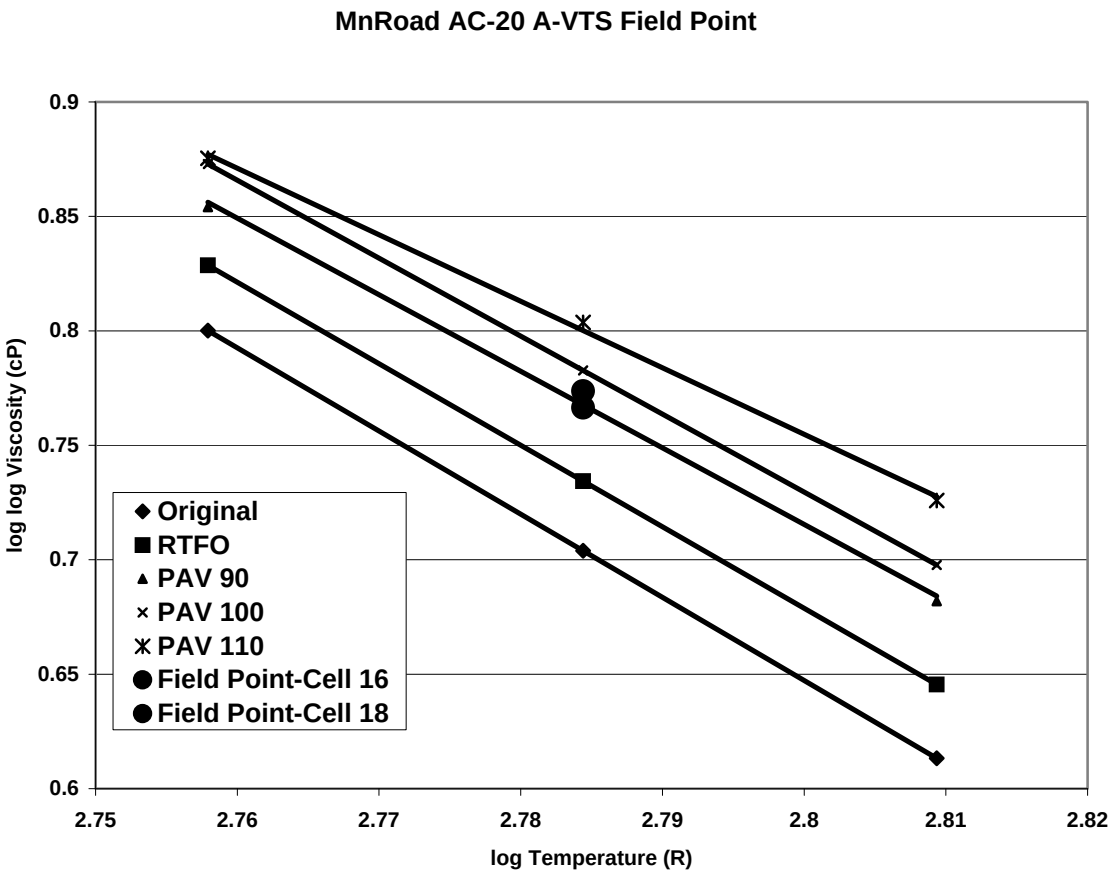

Figure 65
Field-Aged Viscosity at 65°F on A-VTS Plots for MnRoad AC-20

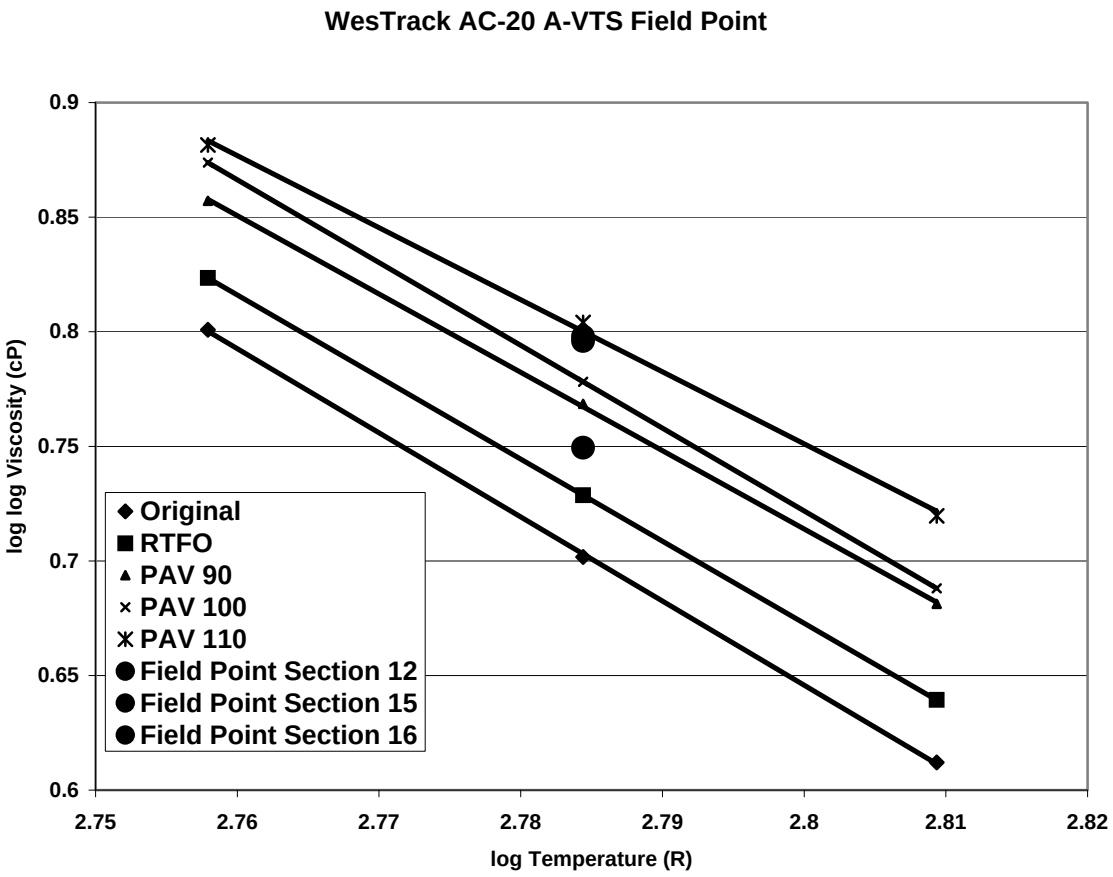

Figure 66
Field-Aged Viscosity at 65°F on A-VTS Plots for WesTrack AC-20

CHAPTER 5

IMPROVEMENT OF THE PP1-98 PROTOCOL AND MODEL DEVELOPMENT

INTRODUCTION

From the verification study of the PP1-98 Protocol presented in *Chapter 4*, it is evident that the concept presented under this protocol is good; nevertheless, it has some limitations. These limitations relate to the user's ability to predict the age hardening behavior of asphalt binders in the field, under different *MAAT* and volumetric properties, using the PP1-98 Protocol.

CURRENT CONDITIONS FOR THE PP1-98 PROTOCOL

The standard testing procedure under the existing PP1-98 protocol requires asphalt samples to be tested at the following conditions:

- Asphalt binder aged using T240 (RTFOT)
- PAV aging time = 20 hrs
- Air pressure = 2.10 MPa
- Aging temperature = 100°C or 110°C as a function of climate

According to the existing protocol, two PAV temperatures (100°C for general conditions and 110°C for desert conditions) along with one aging time (20 hours) and one air pressure (2.1 MPa) are sufficient conditions to represent 5 to 10 years of aging in the pavement for all climatic conditions. However, it is well documented in the existing literature that environmental conditions play a significant role in the hardening of asphalt pavements as documented in *Chapter 2, Literature Review*. Based on the findings, it would not be surprising if the above range of laboratory conditions were found to be insufficiently broad to include the wide range of climatic conditions found in the filed.

LIMITATIONS OF THE EXISTING PROTOCOL

The major limitations associated with the existing PP1-98 protocol can be summarized as follows:

1. The protocol specifies the use of only two PAV temperatures to represent a wide range in *MAAT*. The *MAAT* in USA alone varies from 35°C to 75°C approximately. This wide range, coupled with the fact that the protocol fails to specify a clear "cut-off" for the climatic conditions represented by each one of the PAV aging temperatures currently used, becomes a clear limitation.
2. The standard PP1-98 protocol represents the expected aging of the binder in a period of 5 to 10 years. Two problems arise with this specification:

    a. The 5 – 10 years range is wider than desired, and

   b. Prediction of aging at any other time during the life of the pavement is not possible under the limited conditions of the current protocol.

3. The PP1-98 laboratory conditions are similar for every single binder. As shown in the literature review, the relative degree of hardening of different asphalt binders varies at different aging temperatures in the PAV. Therefore, two asphalt binders may age similarly at one temperature, but age differently at another temperature.
4. The aging estimated by the protocol does not account for field mix condition viz. air-voids.

In order to overcome these limitations of the current PP1-98 protocol, it was decided to pursue a laboratory and field testing program that would result in an improved protocol, in terms of predictive capability.

MATERIALS COLLECTED

In order to accomplish the objectives of this research study, the following original (un-aged) binders were obtained from three agencies across the country.

- **ADOT AC-30**
  PG: 64 – 16
  Location: I-40 in Kingman, Arizona
- **ADOT AC-40**
  PG: 76 – 10
  Location: I-10 in Perryville, Arizona
- **MnRoad AC-20**
  PG: 64 – 22
  Location: Cell 16, 18, MnRoad, Minnesota
- **MnRoad AC-120/150**
  PG: 58 – 28
  Location: Cell 21, MnRoad, Minnesota
- **WesTrack AC-20**
  PG: 64 – 22
  Location: Section 12, 15, and 16, WesTrack, Nevada

APPROACH

The following approach was adopted for the improvement of PP1-98 Protocol and model development:

1. Original binders were obtained from ADOT, MnRoad and WesTrack.
2. Binders were aged in RTFO and PAV at three aging temperatures (90°C, 100°C and 110°C).
3. DSR testing was carried out on the aged binders.

4. A-VTS plots were developed using the viscosity values obtained from DSR testing.
5. Laboratory-aged viscosity at any desired PAV temperature and binder temperature were obtained from the A-VTS plots.
6. Aged viscosities at various aging times and field aging conditions were estimated using the predictive equation developed by Mirza and Witczak[1].
7. The predicted viscosity values from step 6 were plotted on the corresponding A-VTS plots at a reference temperature of 65ºC.
8. Aging time required in the field to simulate the laboratory aging at three PAV aging temperatures were obtained from the plots.
9. PAV aging temperatures were plotted against the corresponding field aging times at different *MAAT*s for all binders.
10. Using these plots, a relationship was developed between PAV aging temperature and field aging time, as a function of *MAAT* and binder type.

These steps are explained in detail in the following sections.

LABORATORY TESTING PROGRAM

In order to account for the variations in aging time and differences in environmental conditions, in the field, testing in the PAV was carried out at three different temperatures: 90°C, 100°C and 110°C. The standard pressure of 2.10 MPa and aging time of 20 hours were maintained constant in the laboratory program. The assumption built into this procedure was based on the expectation that the PAV temperature would account for most of the variables that affect aging in the field i.e., higher PAV temperature will represent greater aging times and warmer climates and lower PAV temperature will represent lesser aging times and colder climates.

The other two factors, viz., pressure and aging time might have also served well in representing different aging conditions. However, the selection of temperature as a variable was based on the following two reasons:

1. Availability of Existing Data: A significant amount of PAV data was available from previous research studies. These data were used in this research study.

2. Testing Practicality: It was more practical to suggest changing one parameter to account for different environmental and aging conditions than changing several parameters at a time. Suggesting a change in the pressure along with the temperature would have resulted in a more complicated model that might not have been necessary. Furthermore, it might not have resulted in a significantly more accurate model. It was believed that changing the temperature alone could adequately account for different environmental and aging conditions.

As stated earlier, three temperatures (90°C, 100°C, 110°C) were selected for PAV aging. The material property that was tested for was the viscosity (η) of the asphalt binder obtained from the Dynamic Shear Rheometer (DSR) test. The viscosity values were

obtained at a sweep of four temperatures (25°C, 45°C, 65°C and 85°C) to define the temperature susceptibility of the asphalt binders. This was considered important because similar grade asphalts are sometimes suspected to have different temperature susceptibilities, i.e., two asphalts might have the same properties at one temperature, but different properties at other temperatures.

LABORATORY TESTING ON BINDER

The DSR testing was carried out at a sweep of four temperatures on the original (un-aged), RTFO, and three PAV aged binders. As mentioned in *Chapter 4, Verification of PP1-98 Protocol*, the viscosity values at 25°C were subsequently eliminated from consideration after concluding that this temperature was too low and viscosities were too high to be reliably measured.

The DSR results and the A and VTS values of the laboratory-aged (PAV-aged) binders are summarized in Tables 16 to 20. The A-VTS plots obtained from the data presented in Tables 16 to 20 are shown in Figures 67 to 71.

VISCOSITY PREDICTION FROM EQUATION DEVELOPED BY PREVIOUS RESEARCH

Equations 5.1 and 5.2 developed by Mirza and Witczak[1], were used in the prediction of viscosities at various aging times and *MAAT*s. These equations were developed based on the results obtained from 40 field projects and are considered to give fairly accurate predictions of the aged viscosity. The *MAAT*s for all the sites were obtained from the *Mechanistic-Empirical Pavement Design Guide*.

$$\log\log\eta_{aged} = \frac{\log\log\eta_{t=0} + A \cdot t}{1 + B \cdot t} \tag{5.1}$$

$$\eta_{ult} = \frac{A}{B} \tag{5.2}$$

Where,

$$A = -0.004166 + 1.41213C + C\log(MAAT) + D\log\log\eta_{t=0}$$

$$B = 0.197725 + 0.068384\log C$$

$$C = 10^{274.4946 - 193.831\log(T_R) + 33.9366\log(T_R)^2}$$

$$D = -14.5521 + 10.47662\log(T_R) - 1.88161\log(T_R)^2$$

η_{aged} = aged viscosity in the field (centipoises)
$\eta_{t=0}$ = viscosity at mix/lay-down (centipoises)
η_{ult} = ultimate viscosity at a given set of field conditions
$MAAT$ = mean annual air temperature (F)
T_R = reference binder temperature in Rankine (R = F+459.7),
t = aging time in the field (months).

The predicted viscosities from equation 5.1 were plotted on the corresponding A-VTS plots at a log temperature (R) of 2.785, which corresponds to 65ºC (intermediate value of the temperature range at which the DSR testing was carried out), as shown in Figures 72 to 76. The ultimate viscosity for a particular *MAAT* and binder type combination is obtained from equation 5.2.

DATA ANALYSIS

Figures 72 to 76 show the predicted viscosities plotted on the A-VTS plots for all the binders at a *MAAT* of 40°F. Similar plots were developed at *MAAT*s ranging from 40°F to 70°F. Based on these plots, aging time required in the field to simulate the PAV aging at 90°C, 100°C and 110°C were predicted at several *MAAT*s. The predicted field aging times, in months, were plotted against the PAV aging temperatures. These plots are shown in Figures 77 to 81.

Based on the plots shown in Figures 77 to 81, the relationship between field aging time (months) and PAV aging temperature (°C) can be expressed in the form of the following general equation,

$$T_{PAV} = a_i . \ln(t_{aging}) + b_i \tag{5.3}$$

Where,

T_{PAV} → PAV Aging Temperature (C)
t_{aging} → Field Aging Time (months)
a_i, b_i → Correlation parameters for binder *i*, which are dependent on *MAAT* and η_{RTFO}

OPTIMIZATION OF THE MODEL

Step-wise regression analysis was conducted on the parameters *a* and *b* to ascertain the relative significance of the parameters. RTFO binder viscosity at a reference temperature of 65ºC was used to be consistent with the prior analysis. As a result, the following general equation was obtained.

$$T_{PAV} = \left(2.960435 + 0.183085 \times \left(\log\log \eta_{RTFO,65^oC}\right)^2 \times MAAT\right) \times \ln(t_{aging}) + 111.4301 - 82.7266 \times \left(\log\log \eta_{RTFO,65^oC}\right)^2 \tag{5.4}$$

Equation 5.4 gives the relation between PAV aging temperature and field aging time. By inputting Mean Annual Air Temperature in the field, RTFO Viscosity of the binder at 65°C and one of the two parameters (PAV aging temperature or Field aging time), the remaining parameter can be estimated.

In order to ascertain the effect of test temperature on the model development, similar analyses were carried out at other DSR test temperatures: 45ºC and 85ºC. At 45ºC, the

aged viscosities obtained from the predictive equation (equation 5.1) did not follow the general trend observed in the field. The aged viscosities predicted at this temperature decreased with increase in aging time and reached values below RTFO viscosity. This results might be attributed to the fact that at low temperatures, the binder is in a semi-solid state and the predictive equation might not give accurate prediction. Therefore, the model was developed only at 85ºC. This model is shown in equation 5.5.

$$T_{PAV} = \left(4.123608 + 0.167497 \times \left(\log\log \eta_{RTFO,85^oC}\right)^2 \times MAAT\right) \times \ln(t_{aging}) + 100.5881 - 72.0344 \times \left(\log\log \eta_{RTFO,85^oC}\right)^2 \quad (5.5)$$

An error analysis was conducted to ascertain the difference in PAV aging temperatures estimated from equations 5.4 and 5.5. The average difference in PAV aging temperatures estimated from the two equations was found to be 0.59ºC. The standard deviation was found to be 1.64ºC. Figure 82 shows the plot of the difference in PAV aging temperatures obtained from analyses at 65ºC, and 85ºC vs. aging time. Figure 83 shows the frequency distribution of the difference in the estimated PAV aging temperatures obtained from equations 5.4 and 5.5.

Based on the error analysis, it was concluded that there is no significant effect of the analysis temperature (DSR test temperature) on the prediction of PAV aging temperature. Therefore, the standard temperature of 60ºC (absolute viscosity) was used to develop the model. The model developed at this temperature is shown in equation 5.6.

$$T_{PAV} = \left(2.132432 + 0.193560 \times \left(\log\log \eta_{RTFO,60^oC}\right)^2 \times MAAT\right) \times \ln(t_{aging}) + 109.9632 - 78.2945 \times \left(\log\log \eta_{RTFO,60^oC}\right)^2 \quad (5.6)$$

Figure 84 shows the error analysis conducted on equation 5.6. It can be observed that the average error and standard deviation were found to be 0.03ºC and 3.20ºC respectively.

SUMMARY OF THE DEVELOPMENT OF THE MODEL

1. Age binders at 90, 100 and 110°C in the PAV
2. From A-VTS plots (Figures 67 to 71), pickoff $\eta_{aged,\ lab}$ at any desired PAV temperature, at a binder temperature of 65°C
3. Use equation 5.1 to estimate $\eta_{aged,\ field}$ as a function of *MAAT*, aging time, η_{RTFO} and binder temperature
4. Set $\eta_{aged,\ lab} = \eta_{aged,\ field}$ to obtain $T_{PAV} = f(t_{field}, a, b)$ (Figures 77 to 81), where, *a* and *b* are function of *MAAT* and binder type
5. Quantify *a* and *b* in terms of *MAAT* and $\eta_{RTFO@65^oC}$ using step-wise regression analysis to get, $T_{PAV} = f(t_{field}, MAAT, \eta_{RTFO@65^oC})$ (equation 5.4), where, T_{PAV} = Predicted PAV temperature to achieve $\eta_{aged,\ lab} = \eta_{aged,\ field}$

Table 16
DSR Results for ADOT AC-30 Binder

Temperature (C)	Viscosity (Pas)	A	VTS	R^2
ADOT AC-30 - Original				
45	3534.2	10.512	-3.5155	1.0000
65	191.48			
85	20.818			
ADOT AC-30 - RTFO				
45	9429.6	10.178	-3.3845	0.9999
65	497.04			
85	46.885			
ADOT AC-30 - PAV 90				
45	37512	9.3111	-3.0564	0.9970
65	2478.2			
85	187.17			
ADOT AC-30 - PAV 100				
45	40424	8.8794	-2.8991	0.9955
65	3174.4			
85	247.82			
ADOT AC-30 - PAV 110				
45	78020	8.0864	-2.6057	0.9941
65	7435.2			
85	622.92			

Table 17
DSR Results for ADOT AC-40 Binder

Temperature (C)	Viscosity (Pas)	A	VTS	R^2
ADOT AC-40 - Original				
45	12035	10.826	-3.6172	1.0000
65	468.29			
85	41.076			
ADOT AC-40 - RTFO				
45	28373	10.429	-3.4648	0.9998
65	1156.8			
85	87.926			
ADOT AC-40 - PAV 90				
45	71160	9.8863	-3.2595	0.9984
65	3333			
85	216.93			
ADOT AC-40 - PAV 100				
45	97298	9.626	-3.1624	0.9984
65	4717.6			
85	310.06			
ADOT AC-40 - PAV 110				
45	120950	8.9961	-2.9319	0.9965
65	7581.3			
85	512.44			

Table 18
DSR Results for MnRoad AC-120/150 Binder

Temperature (C)	Viscosity (Pas)	A	VTS	R^2
MnRoad AC-120/150 - Original				
45	1128.2	11.331	-3.825	1.0000
65	62.166			
85	7.0429			
MnRoad AC-120/150 - RTFO				
45	2306.9	10.714	-3.5934	1.0000
65	129.19			
85	14.378			
MnRoad AC-120/150 - PAV 90				
45	8034.1	10.018	-3.3281	1.0000
65	440.87			
85	45.253			
MnRoad AC-120/150 - PAV 100				
45	12316	10.531	-3.51	1.0000
65	530.38			
85	47.755			
MnRoad AC-120/150 - PAV 110				
45	20301	9.3477	-3.0754	0.9974
65	1430.1			
85	118.94			

Table 19
DSR Results for MnRoad AC-20 Binder

Temperature (C)	Viscosity (Pas)	A	VTS	R^2
MnRoad AC-20 - Original				
45	2046.9	10.818	-3.6324	1.0000
65	114.14			
85	12.728			
MnRoad AC-20 - RTFO				
45	5491.9	10.651	-3.5615	1.0000
65	265.67			
85	26.333			
MnRoad AC-20 - PAV 90				
45	14008	10.08	-3.3445	0.9982
65	818.86			
85	64.244			
MnRoad AC-20 - PAV 100				
45	29000	10.265	-3.4055	1.0000
65	1157.1			
85	96.777			
MnRoad AC-20 - PAV 110				
45	32050	8.8909	-2.9057	0.9983
65	2309			
85	208.57			

Table 20
DSR Results for WesTrack AC-20 Binder

Temperature (C)	Viscosity (Pas)	A	VTS	R^2
WesTrack AC-20 - Original				
45	2097.7	10.924	-3.6708	0.9999
65	107.59			
85	12.399			
WesTrack AC-20 - RTFO				
45	4577.6	10.699	-3.5809	1.0000
65	225.82			
85	22.837			
WesTrack AC-20 - PAV 90				
45	15725	10.286	-3.4186	0.9998
65	739.24			
85	63.138			
WesTrack AC-20 - PAV 100				
45	30096	10.836	-3.6122	1.0000
65	1000.8			
85	75.113			
WesTrack AC-20 - PAV 110				
45	40966	9.5574	-3.1451	0.9983
65	2336.6			
85	175.34			

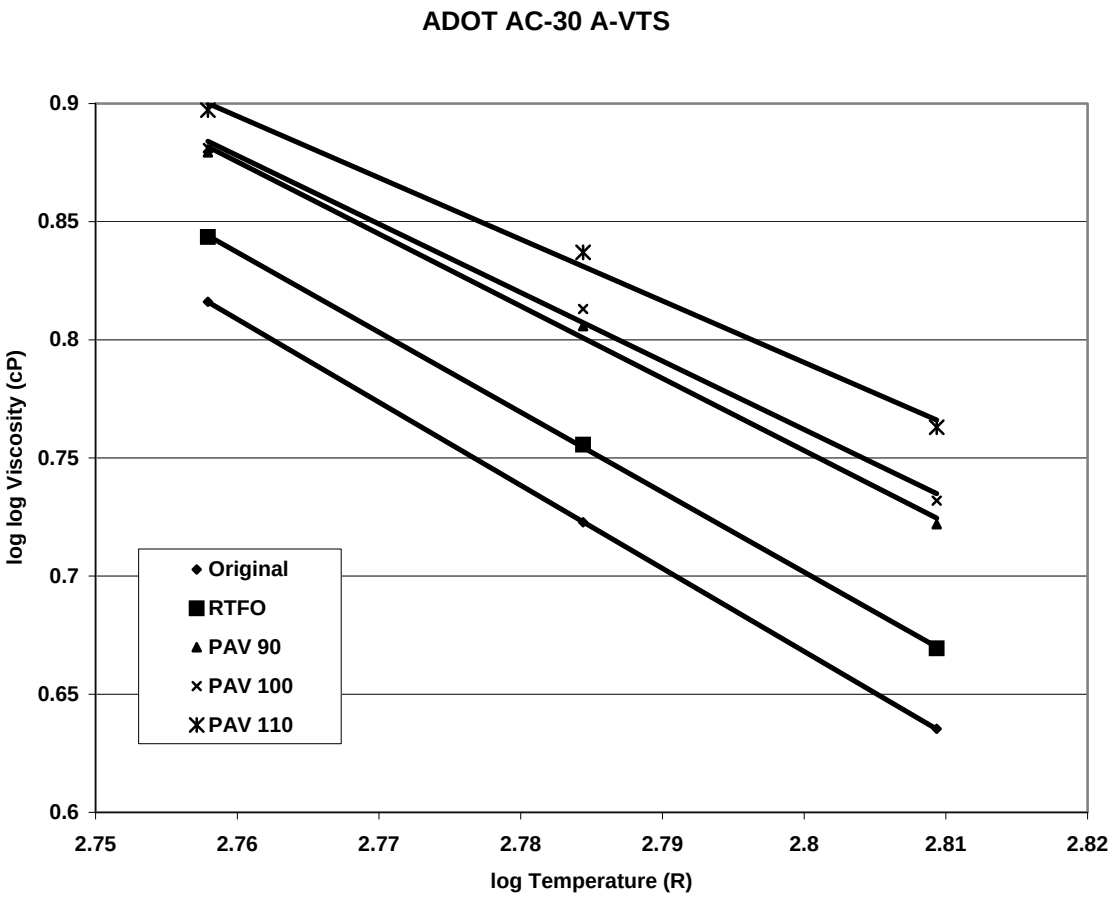

Figure 67
A-VTS Plots for ADOT AC-30 Binder

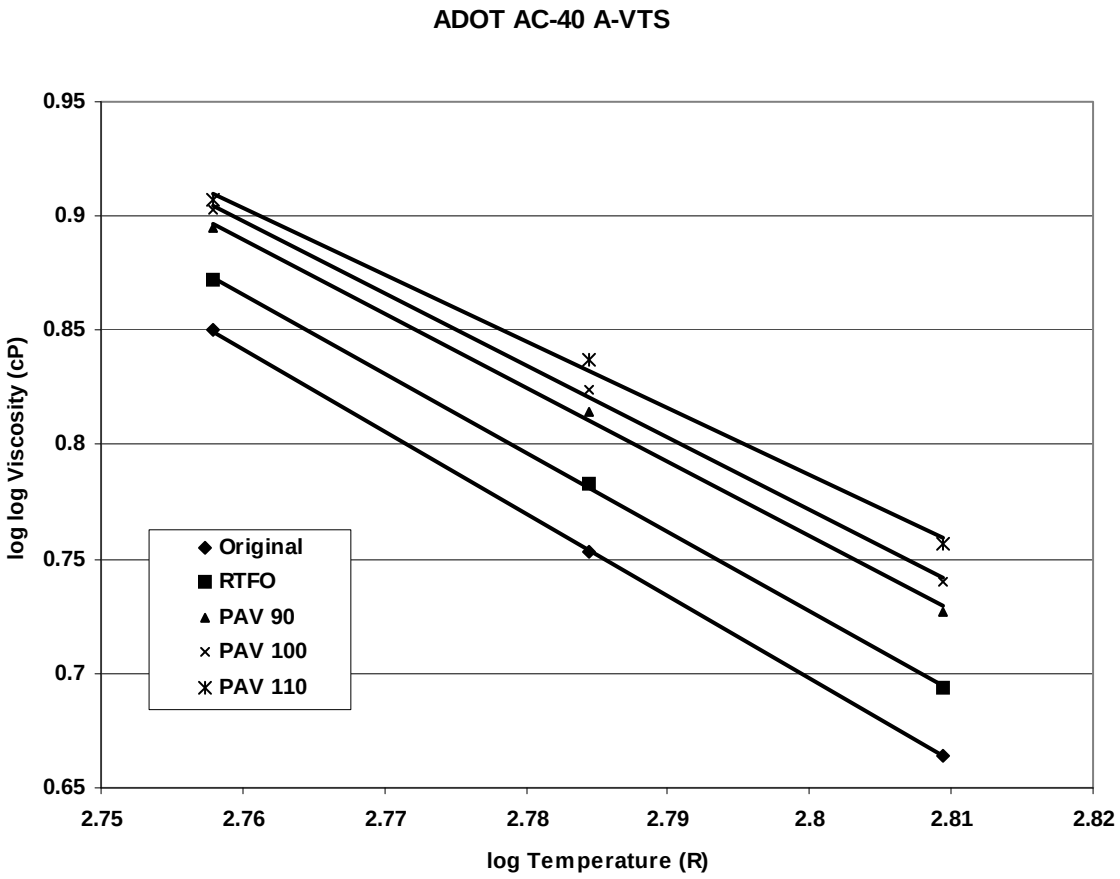

Figure 68
A-VTS Plots for ADOT AC-40 Binder

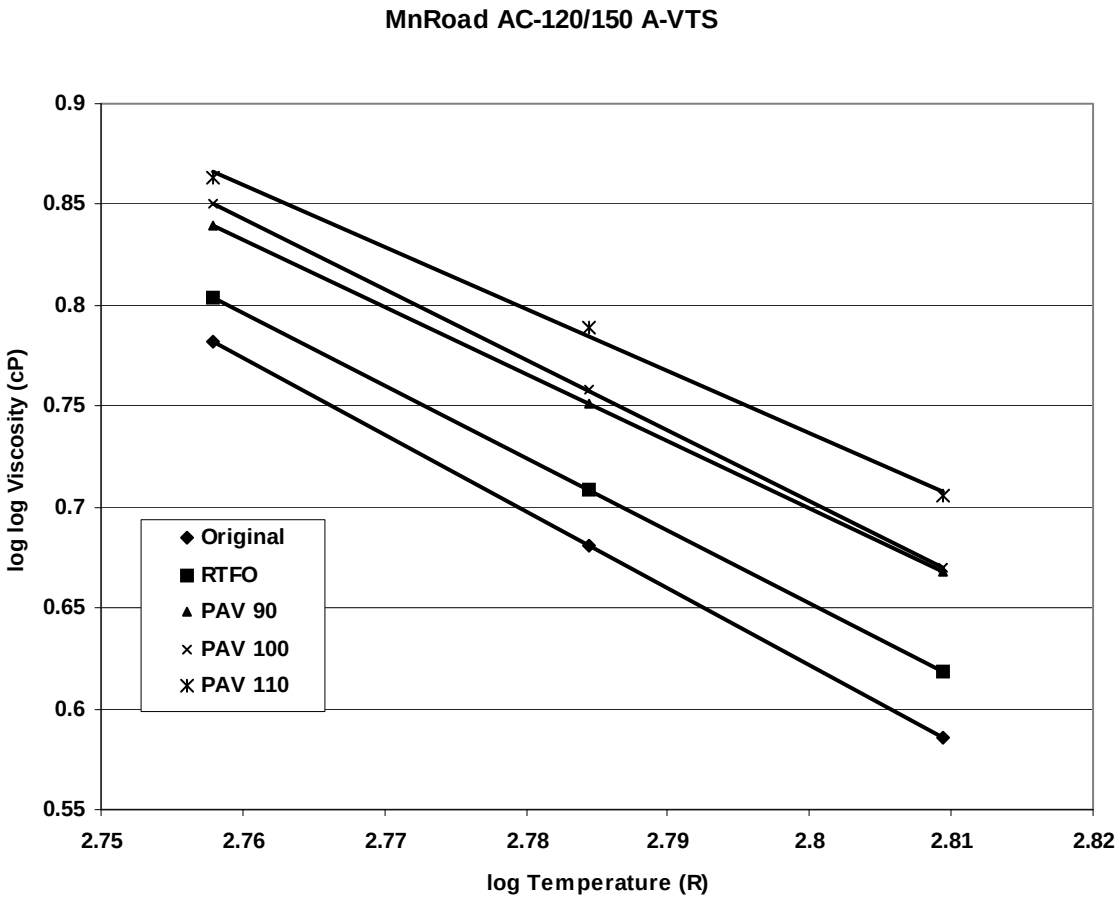

Figure 69
A-VTS Plot for MnRoad AC-120/150 Binder

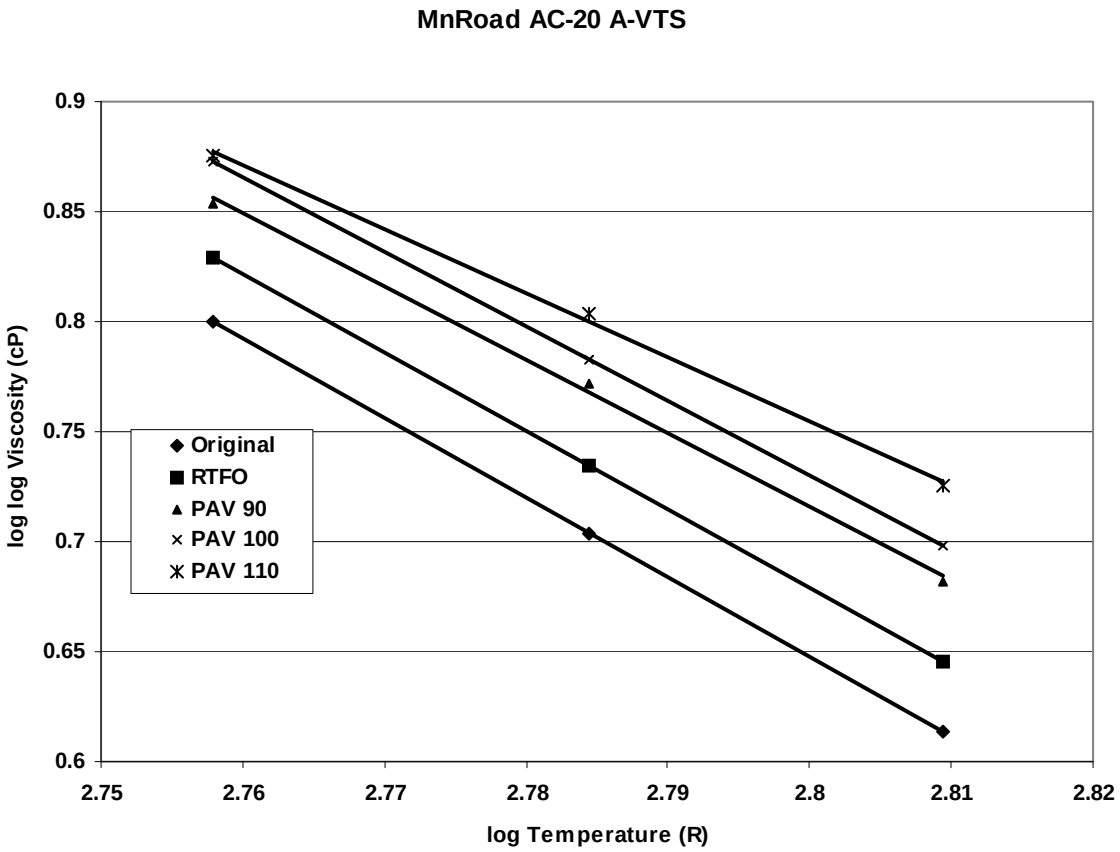

Figure 70
A-VTS Plot for MnRoad AC-20 Binder

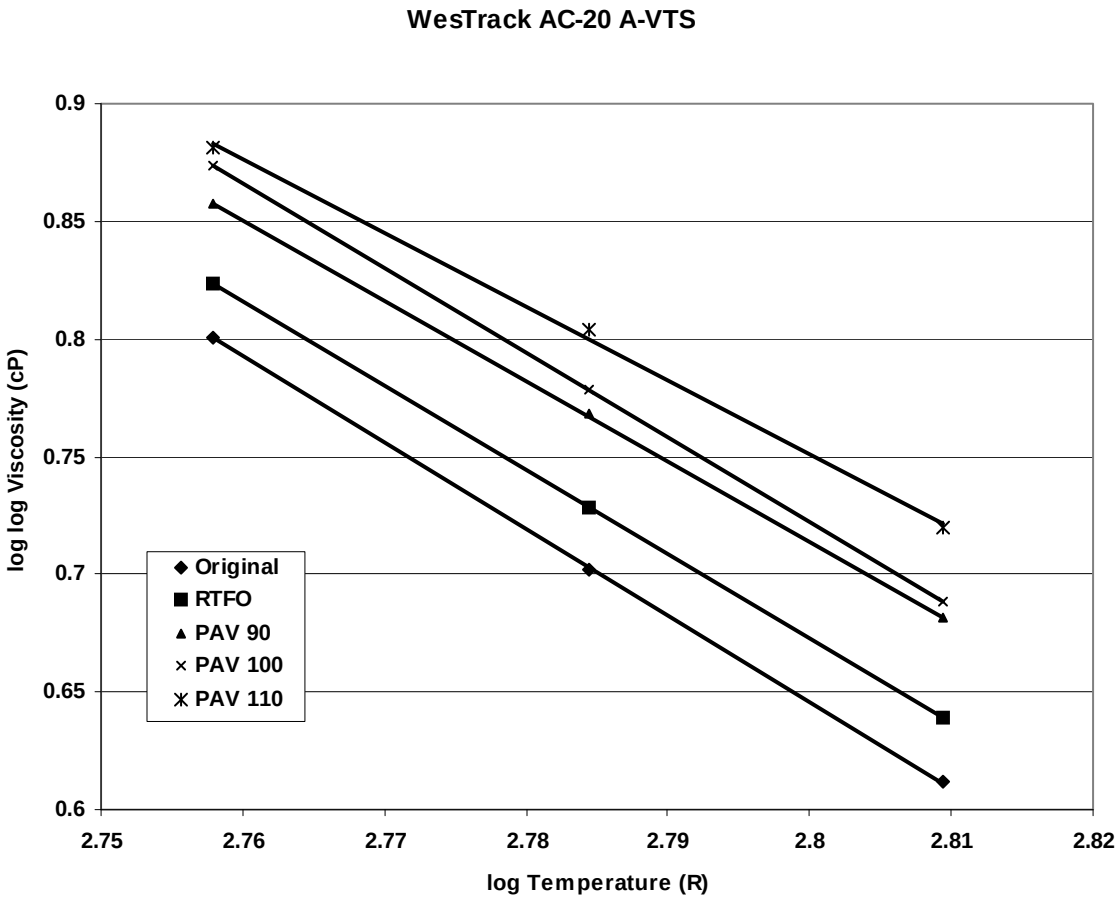

Figure 71
A-VTS Plot for WesTrack AC-20 Binder

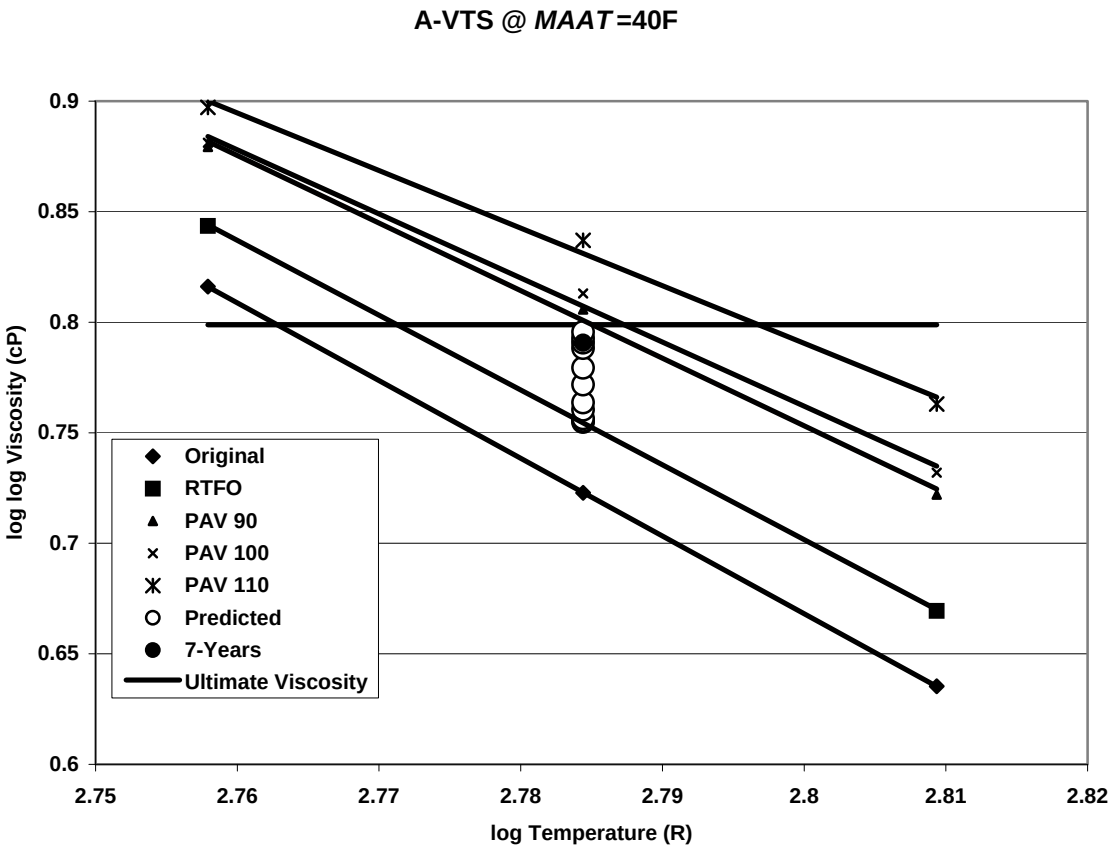

Figure 72
Predicted Viscosities Plotted on A-VTS Plots for ADOT AC-30

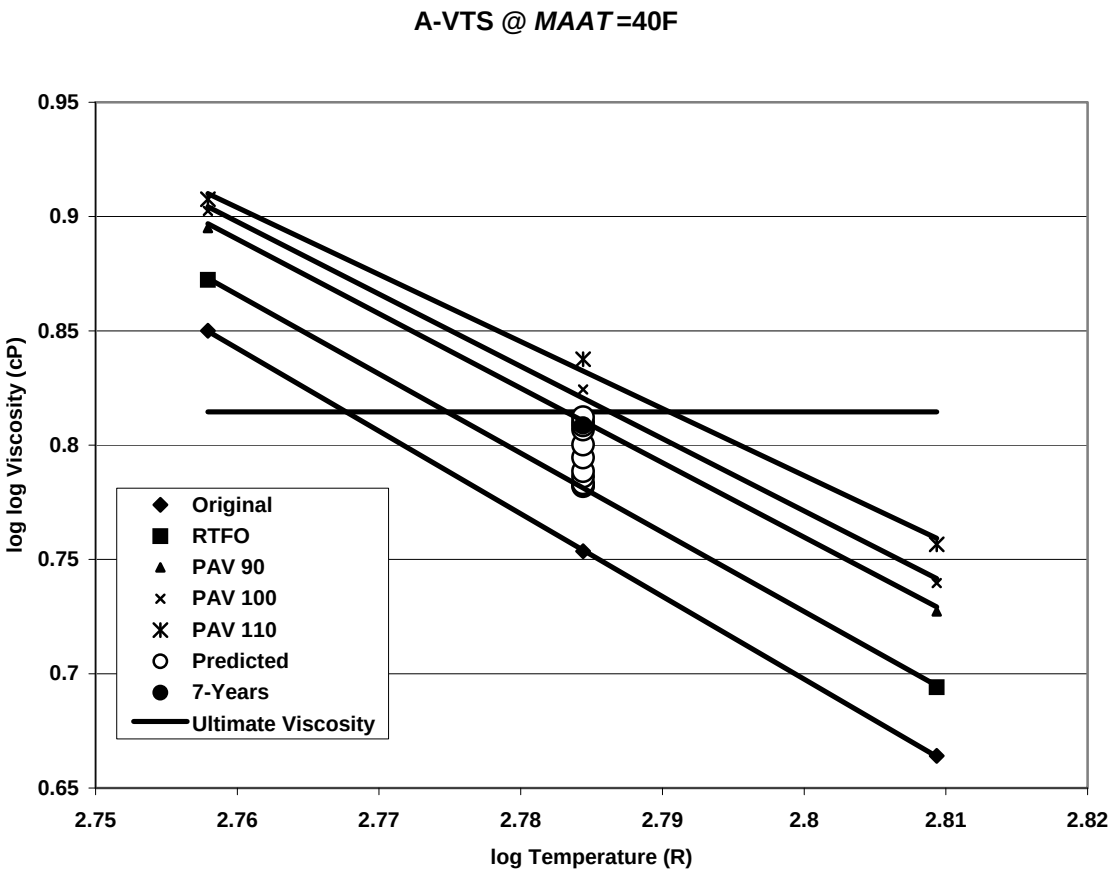

Figure 73
Predicted Viscosities Plotted on A-VTS Plots for ADOT AC-40

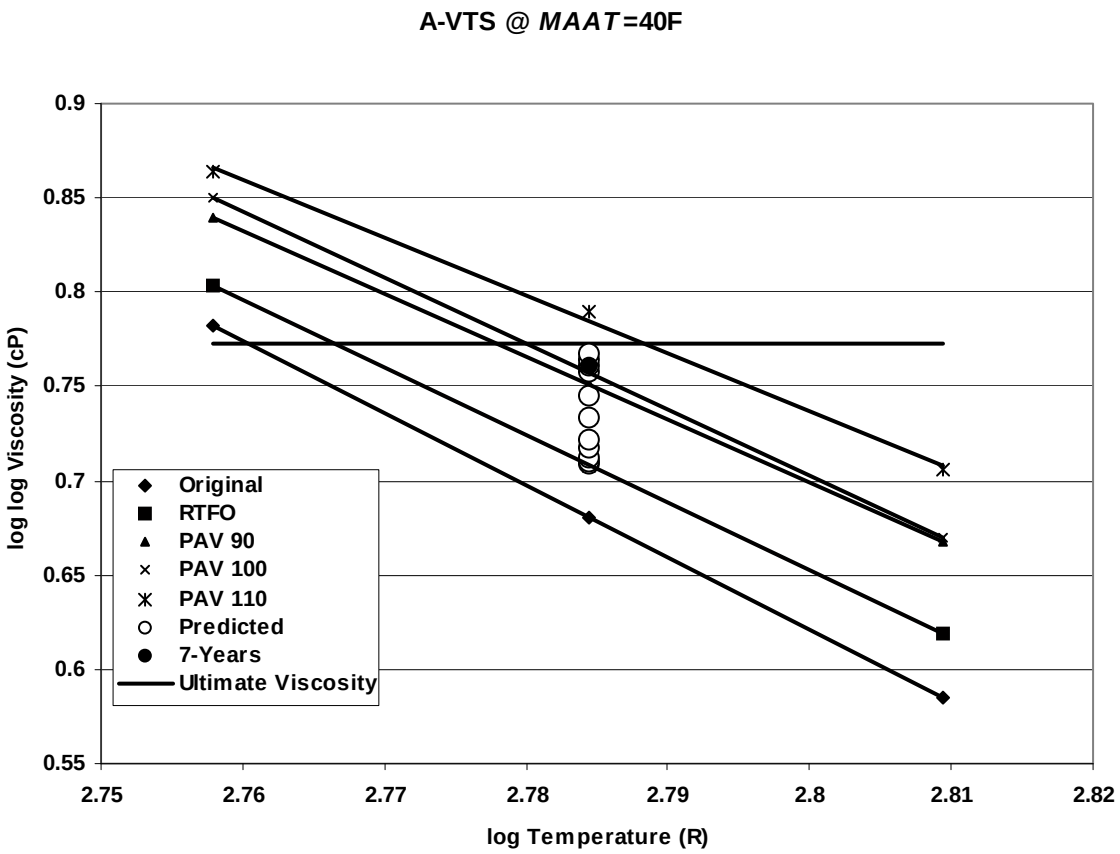

Figure 74
Predicted Viscosities Plotted on A-VTS Plots for MnRoad AC-120/150

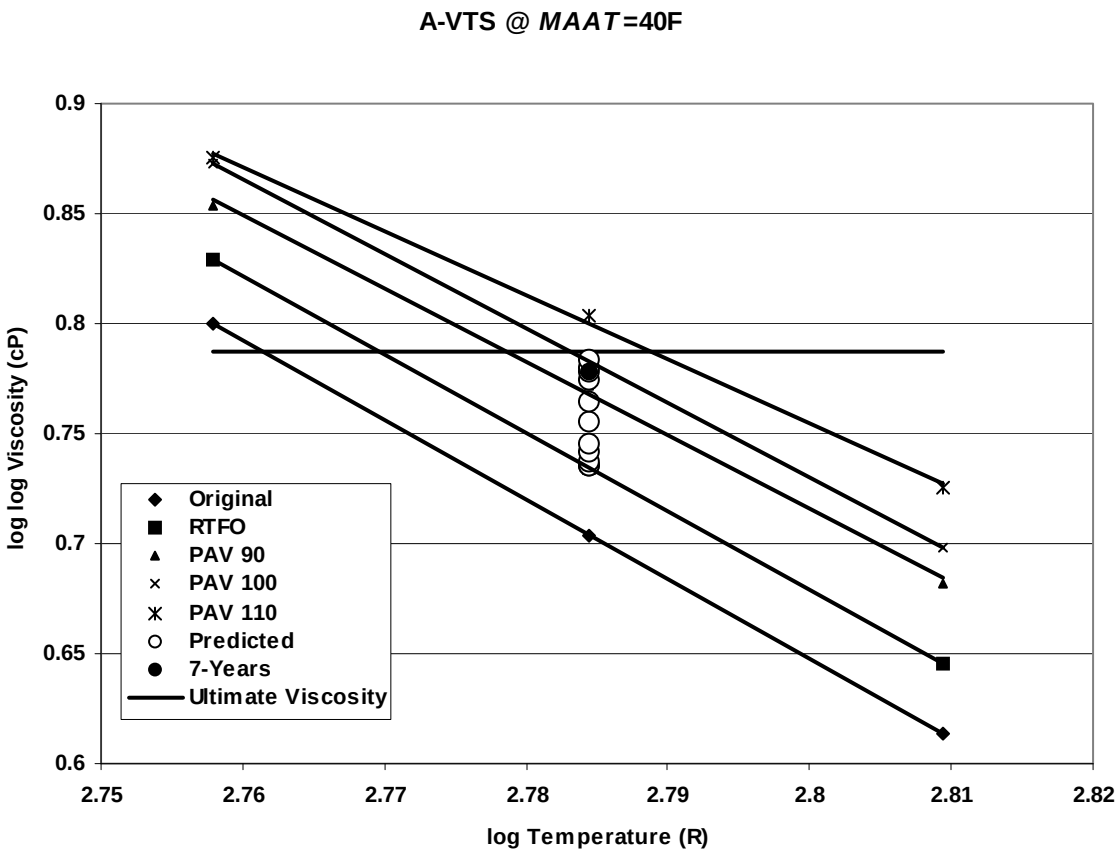

Figure 75
Predicted Viscosities Plotted on A-VTS Plots for MnRoad AC-20

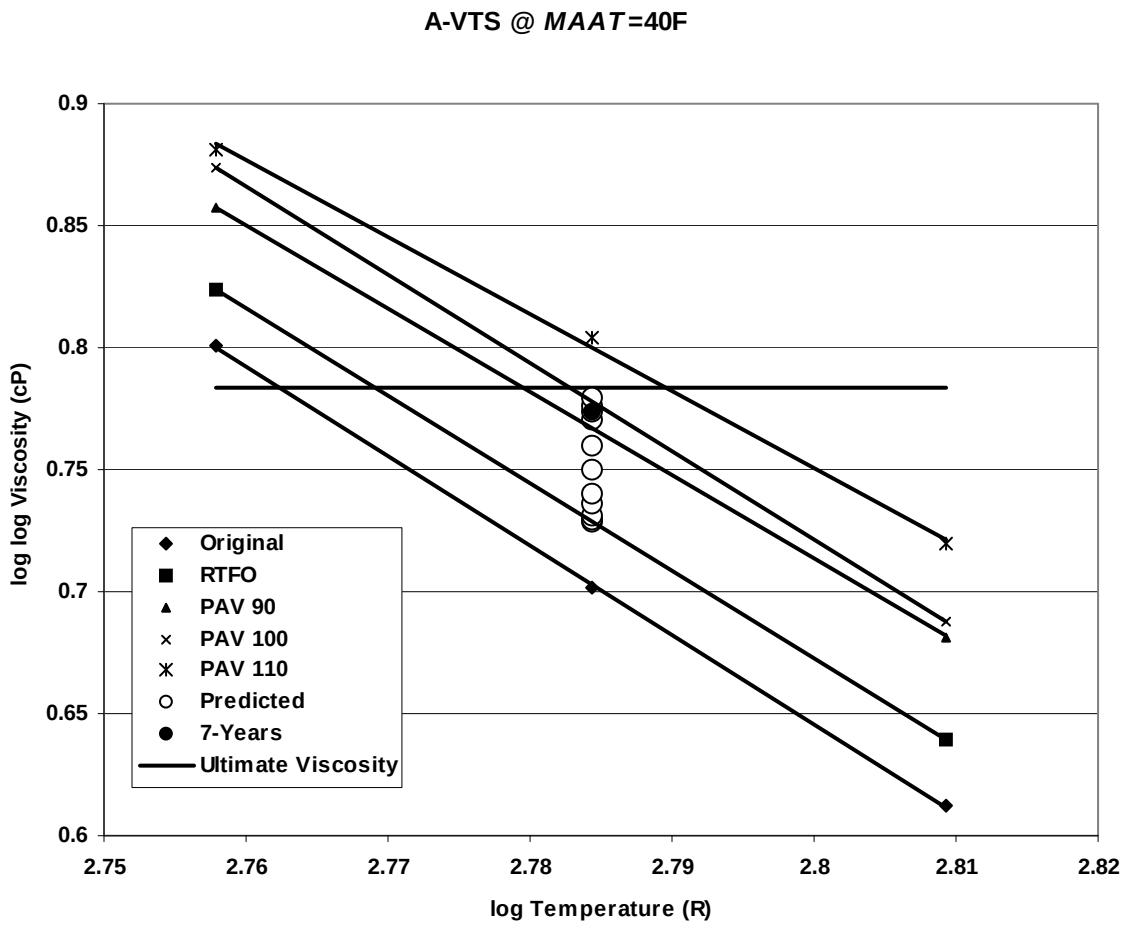

Figure 76
Predicted Viscosities Plotted on the A-VTS Plots for WesTrack AC-20

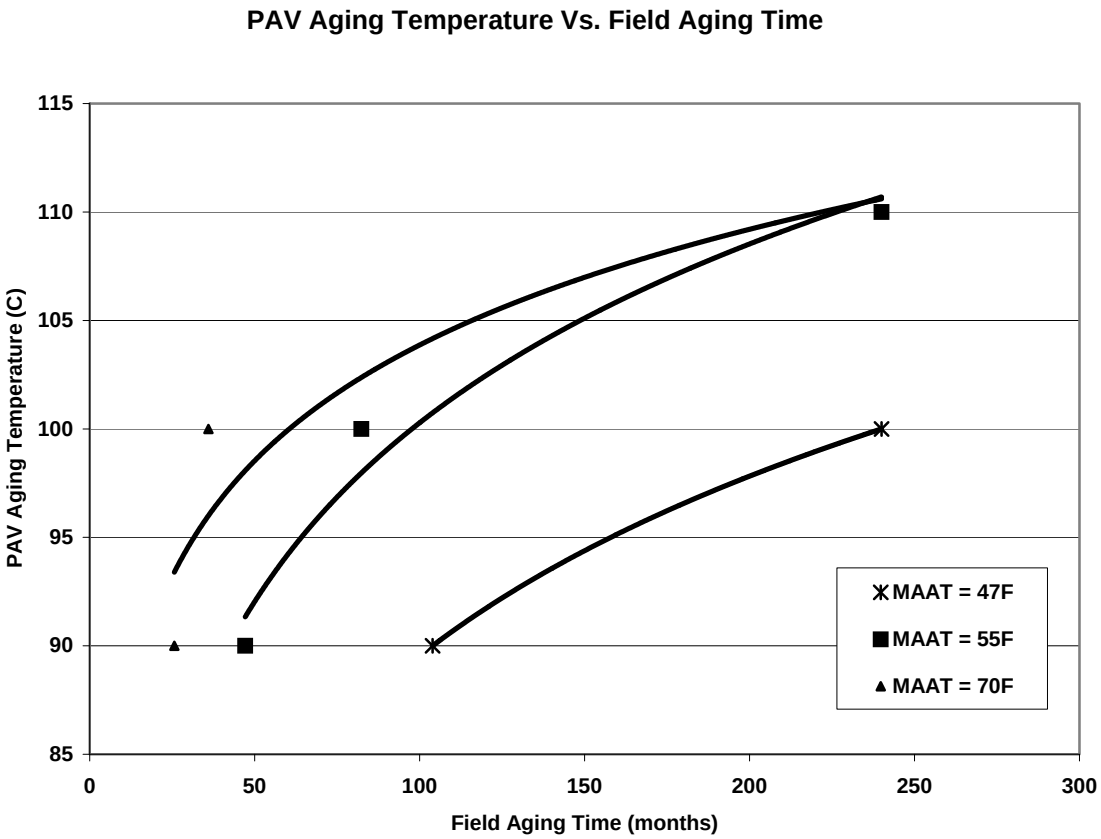

Figure 77
Field Aging Time vs. PAV Aging Temperature for ADOT AC-30

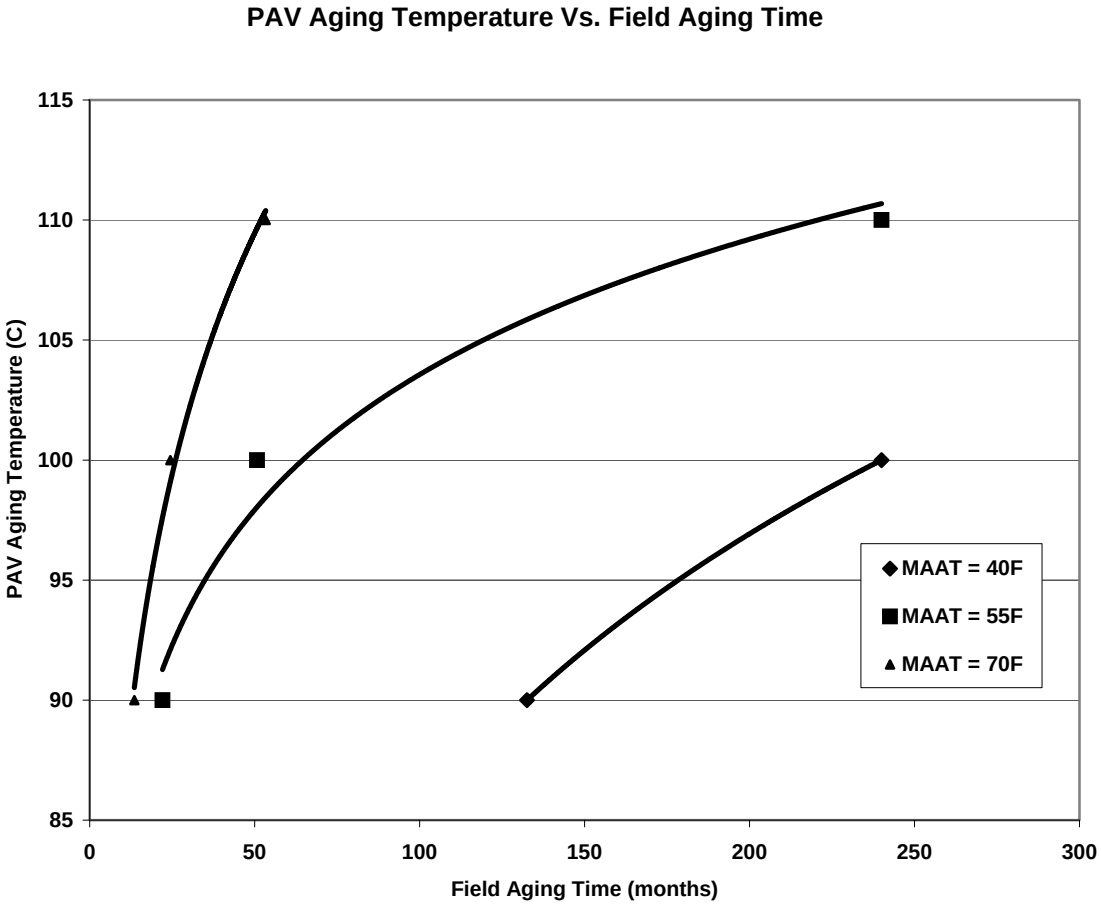

Figure 78
Field Aging Time vs. PAV Aging Temperature for ADOT AC-40

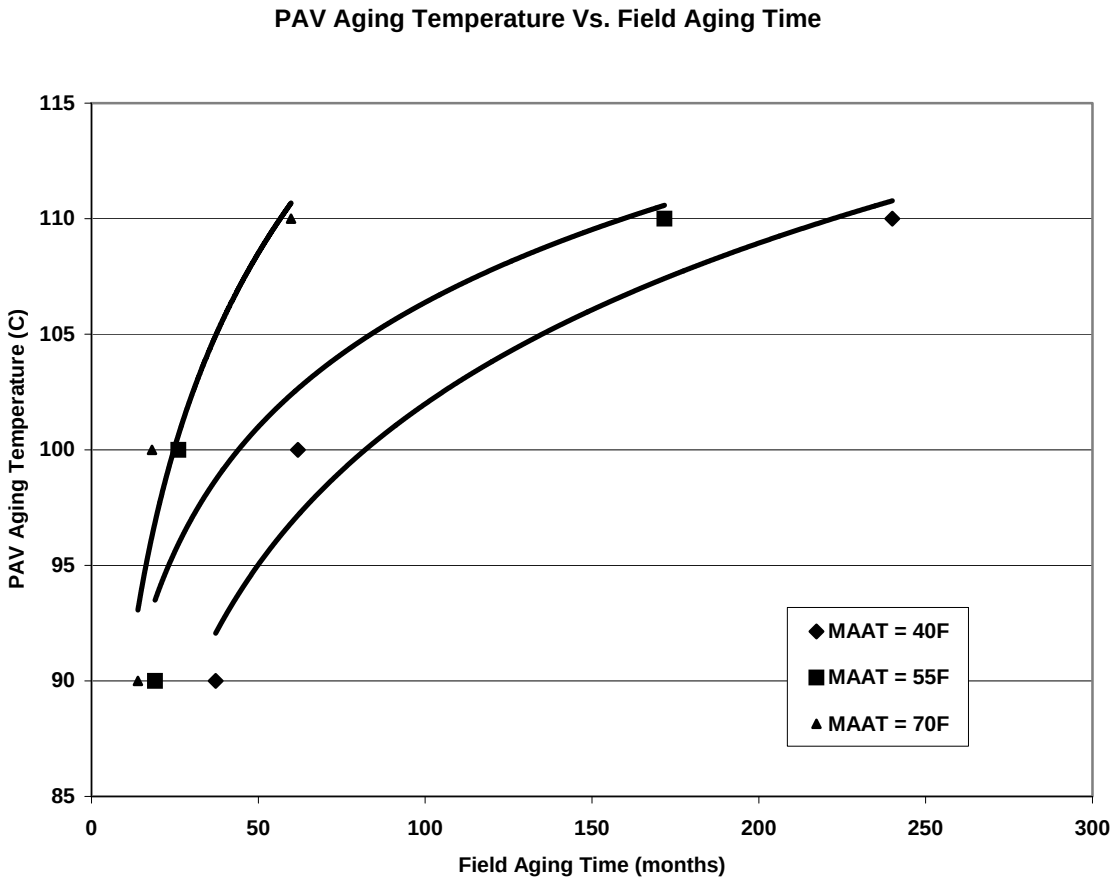

Figure 79
Field Aging Time vs. PAV Aging Temperature for MnRoad AC-120/150

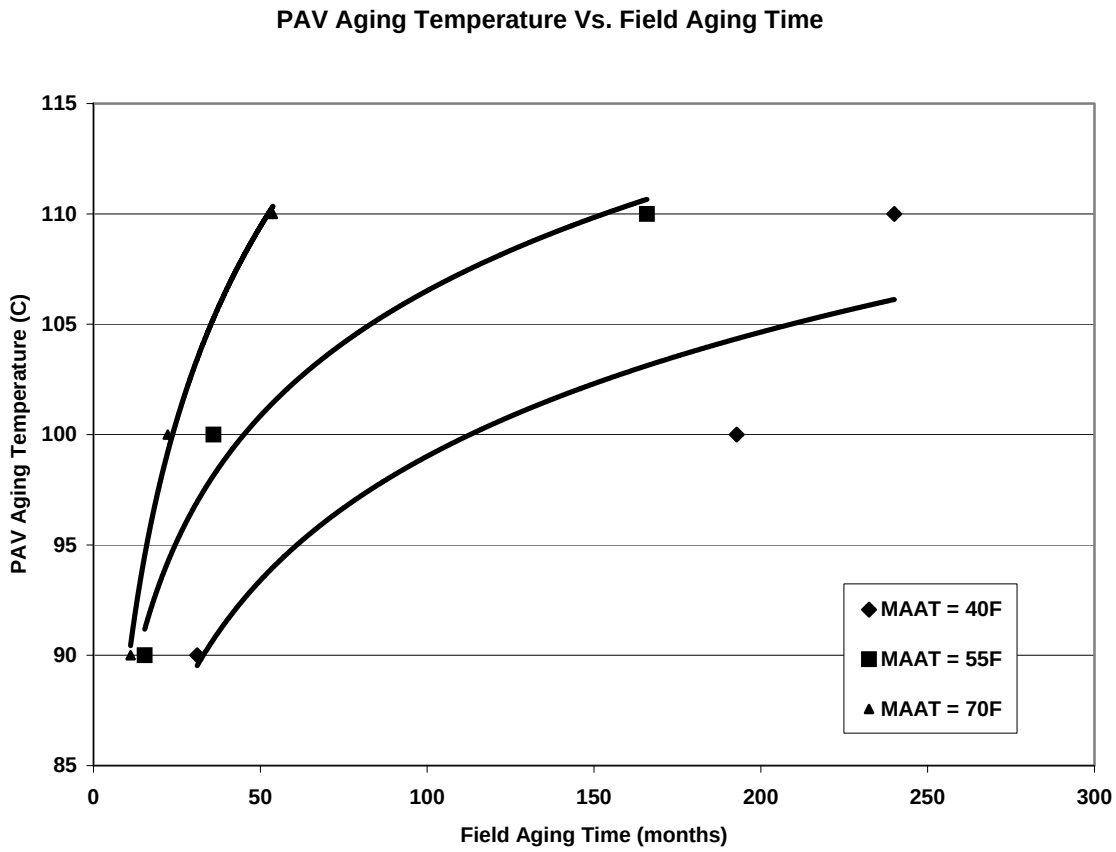

Figure 80
Field Aging Time vs. PAV Aging Temperature for MnRoad AC-20

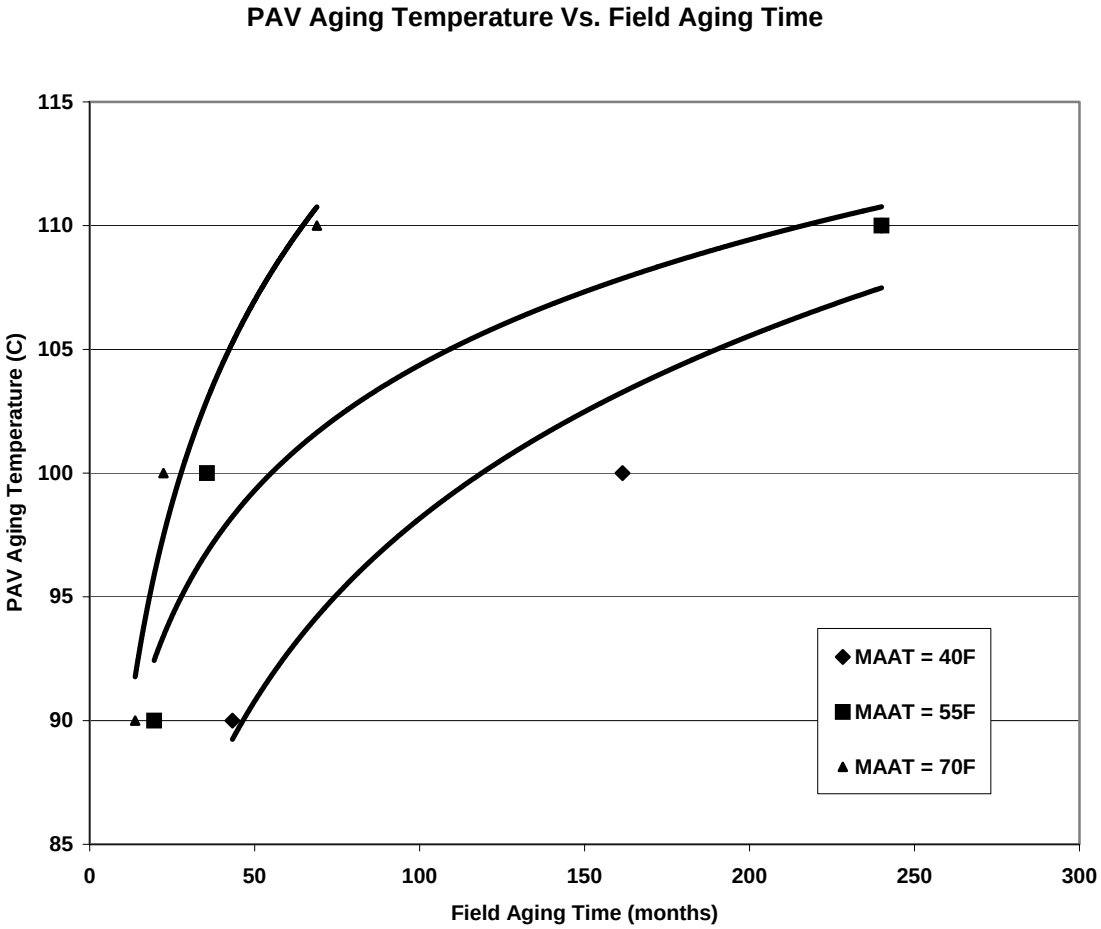

Figure 81
Field Aging Time vs. PAV Aging Temperature for WesTrack AC-20

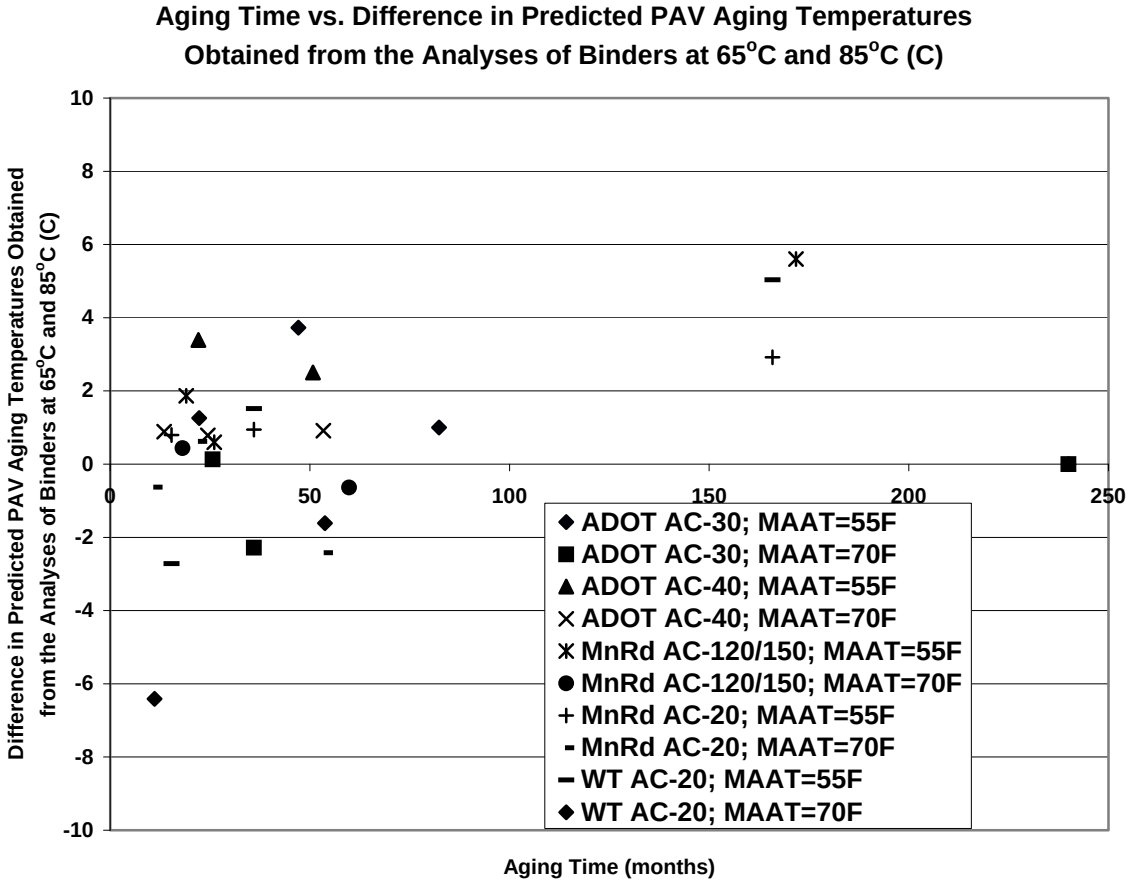

Figure 82
Plot of Difference in PAV Aging Temperatures Estimated from the Analyses of Binders at 65ºC and 85ºC vs. Aging Time

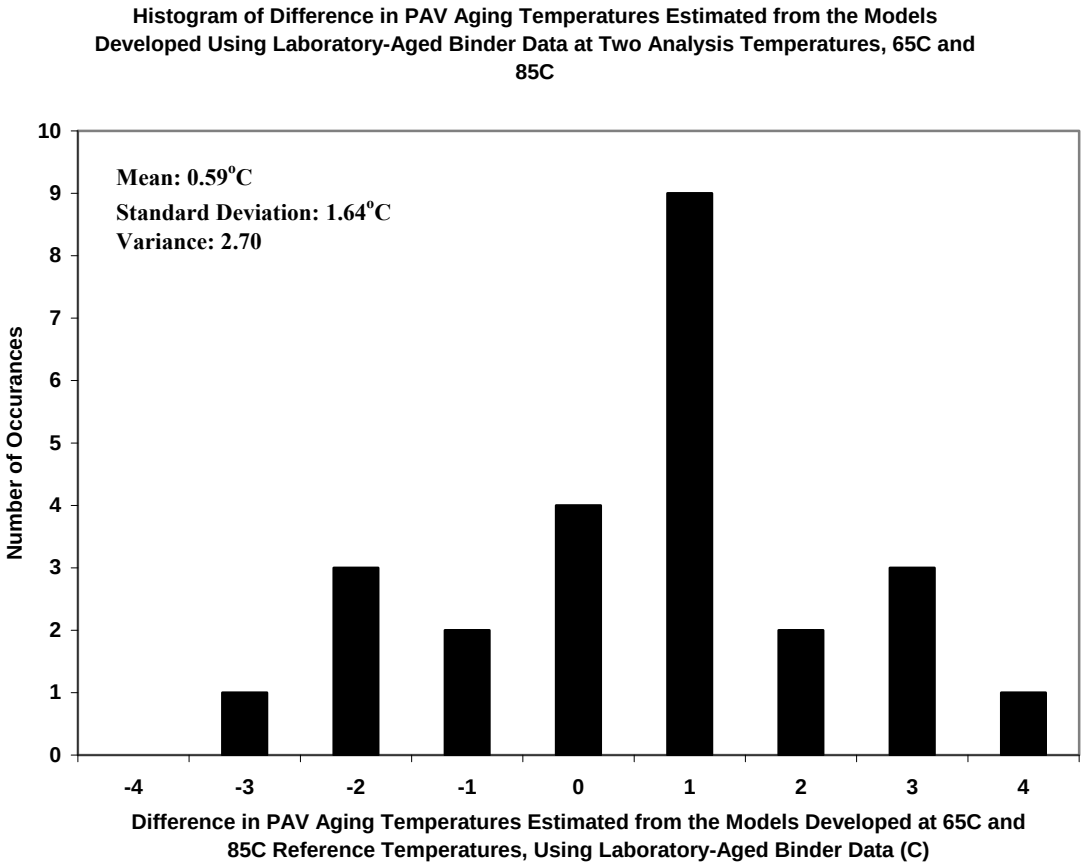

Figure 83
Frequency Distribution of the Difference in PAV Aging Temperatures Estimated from the Analyses of Binders at 65ºC and 85ºC

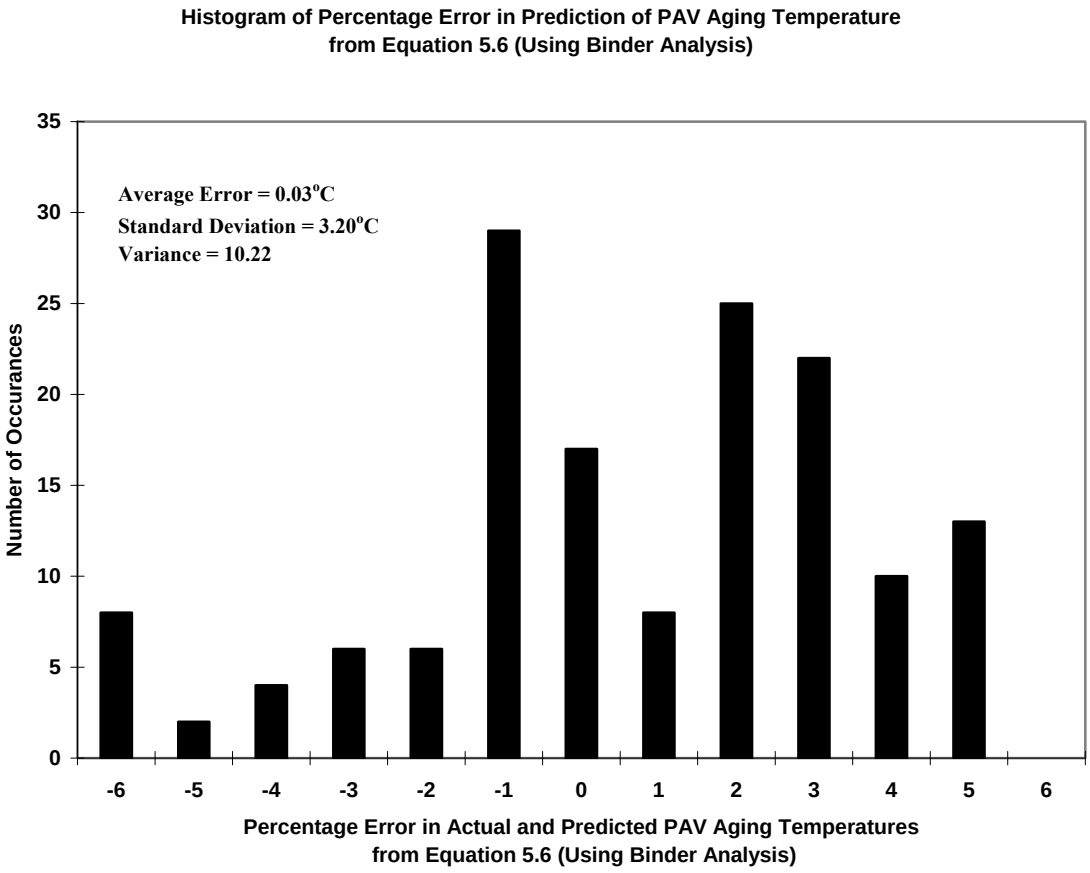

Figure 84
Frequency Distribution of the Percentage Error in Actual and Predicted PAV Aging Temperatures Estimated from Equation 5.6

CHAPTER 6

CALIBRATION OF THE EXPANDED PP1 MODEL WITH FIELD DATA

INTRODUCTION

Up to this point, the PP1 model has been calibrated using only the predictive equation (equation 5.1). This calibration rests on the assumption that the predictive equation provides a good estimate of aging in the field. The predictive equation (equation 5.2) enjoys widespread acceptance in the pavement community, as it has been calibrated extensively using data from 40 field studies. However, it was possible to further calibrate the PP1 equation (equation 5.4) with the field data obtained from the NCHRP 9-23 project study.

MATERIALS USED

In order to achieve this objective, three sites were selected across the United States, which represent different climatic conditions. From these sites, field cores were obtained for the extraction of binder for the calibration of the PP1-98 protocol. The field sites selected are:

- ADOT Sites (Arizona)
- MnRoad Cells (Minnesota)
- WesTrack Sections (Nevada)

BACKGROUND

The age hardening properties of the binders from the above mentioned sites were already evaluated in the previous chapter, *Improvement of the PP1-98 Protocol and Model Development.* Therefore, by using the PP1 equation developed (equation 5.4), the PAV aging temperature, T_{PAV}, required was estimated. DSR testing was conducted on binder extracted from the field cores and field-aged viscosity was obtained. Knowing the aged viscosity, the PAV aging temperature was estimated from the viscosity-temperature relationship (A-VTS plots) of the corresponding binder (Binder characterization). The PAV temperatures obtained were compared to the T_{PAV} values from equation 5.4. This comparison constituted a calibration process. A suitable conclusion was drawn based on the difference between the two PAV temperatures, and a procedure to improve the agreement was developed.

APPROACH

1. Field cores were obtained from the three sites listed above.
2. Field aging conditions such as *MAAT*, age of the pavement and original air-voids were also obtained from databases and interviews with appropriate personnel from the sites selected.

3. Using the PP1 equation (equation 5.4), PAV aging temperatures required to simulate the field aging were estimated for all the field samples obtained.
4. Binders were extracted from the field cores taken from the sites.
5. DSR tests were conducted on the extracted binders to obtain field-aged viscosities.
6. PAV aging temperatures corresponding to field-aged viscosities were estimated using the A-VTS relationships (Binder characterization), at the reference binder temperature of 65ºC.
7. PAV temperatures obtained in Step 3 were compared to corresponding PAV temperatures obtained in Step 6.
8. Based on this comparison, the PP1 equation was further calibrated.

These steps are explained in detail in the following sections.

ESTIMATION OF PAV AGING TEMPERATURE

Information on field-aging conditions obtained from the sites is summarized in Table 21.

PP1 Equation

$$T_{PAV} = \left(2.960435 + 0.183085 \times \left(\log\log \eta_{RTFO,65^oC}\right)^2 \times MAAT\right) \times \ln(t_{aging}) + 111.4301 - 82.7266 \times \left(\log\log \eta_{RTFO,65^oC}\right)^2 \quad (6.1)$$

Where,

T_{PAV} → PAV Aging Temperature, °C
$\eta_{RTFO,\ 65C}$ → RTFO Viscosity at 65°C
$MAAT$ → Mean Annual Air Temperature, °F
t_{aging} → Field Aging Time, months

Using the field aging data summarized in Table 21, in the PP1 equation (equation 6.1), PAV aging temperatures required to simulate field aging were estimated and are summarized in Table 22.

FIELD ANALYSIS

Cores were obtained from the three field sites. The field-cores were sliced into three layers as explained in *Chapter 5*. Binders were extracted separately from each layer. Two cores were used from each site for the binder extraction. DSR testing was conducted on the extracted binders to obtain the field-aged viscosities. The average DSR testing results on the field-cores are summarized in Table 23.

It can be observed from the Figures 85 to 90 that viscosity values at all the three depths, plot nearly on top of each other, i.e. for all practical purposes, there is no significant difference in the viscosity values obtained at different depths in the pavement. This trend

was observed for all the binders extracted from the field cores. Therefore, for the calibration study, the average viscosity of the binder extracted from the top layer (1-inch thickness) was considered to be representative of the site. Furthermore, the field viscosity at a reference binder temperature of 65 ºC was considered in the analysis, to be consistent with the prior analysis. The field-aged viscosity values at 65ºC are summarized in Table 24.

BINDER CHARACTERIZATION

In order to compare the required PAV aging temperature predicted in the laboratory with the measured value in the field, the field-viscosity measured from the cores had to be converted into equivalent PAV aging temperatures. DSR results obtained from PAV aged binders at a reference temperature of 65ºC are summarized in Table 25. Data presented in Table 25 are plotted as shown in Figures 91 to 93.

The binder viscosities as observed in Figures 91 to 93 were also subjected to a minimum of RTFO viscosity at the same reference temperature and a maximum of 2.8 x 10^{12} cP (ultimate viscosity at glassy modulus). Therefore, a sigmoidal relationship was adopted between PAV aging temperature and viscosity. The sigmoid is of the form,

$$T_{PAV} = \frac{a - \ln\left[\dfrac{\log\log\eta_{ult} - \log\log\eta_{RTFO}}{\log\log\eta_{aged} - \log\log\eta_{RTFO}} - 1\right]}{b} \tag{6.2}$$

Where,

η_{ult} → Ultimate viscosity of the binders = 2.8 x 10^{12} cP
η_{RTFO} → RTFO viscosity
η_{aged} → Aged viscosity
a, b → Parameters computed using regression analysis

Parameters a and b computed from the regression analysis are summarized in Table 26. Data presented in Table 26 was re-plotted using the sigmoidal relationship developed and the plots are shown in Figures 94 to 96.

Using the sigmoidal relationships developed, the field-aged viscosities obtained from the cores were converted into equivalent PAV aging temperature values. The equivalent PAV aging temperatures are summarized in Table 27.

Predicted PAV aging temperatures from Table 22 and measured PAV aging temperatures from Table 27 are summarized in Table 28 and are plotted in Figure 97.

It was observed from Figure 97 that there was a poor comparison between predicted PAV aging temperatures and measured PAV aging temperatures. Also, it could be observed that the PP1 equation was over-predicting the temperature in most of the cases. When

source data was analyzed to explain this discrepancy in the data points, it was found that the points that were being over-predicted had lower air-voids and those that were being under-predicted had higher air-voids. Therefore, it was concluded that mix air-voids was a factor that might explain the observed discrepancy.

To overcome the problem and to arrive at a better prediction of PAV temperature, the PP1 equation was corrected using the mix air-voids. The PAV temperatures and the corresponding air-voids are summarized in Table 29.

Figure 98 shows the plot of original air-voids (VA_{orig}) vs. ratio of the predicted and measured PAV aging temperatures.

Using the plot in Figure 98, a relationship was developed between the ratio of measured and predicted PAV temperatures and original mix air-voids,

$$\frac{T_{PAV,measured}}{T_{PAV,predicted}} = 0.445822 \times VA_{orig}^{\ 0.355366} \tag{6.3}$$

Using the relationship given by equation 6.3, a correction factor was developed for the predicted PAV aging temperature that resulted in a relatively accurate prediction,

$$T_{PAV,measured} = T_{PAV,predicted} \times \left(0.445822 \times VA_{orig}^{\ 0.355366}\right) \tag{6.4}$$

The correction factor is applied to the PP1 equation as shown in equation 6.5.

$$T_{PAV} = \left\{ \begin{array}{l} \left(2.960435 + 0.183085 \times \left(\log\log \eta_{RTFO,65^oC}\right)^2 \times MAAT\right) \times \ln(t_{aging}) \\ +111.4301 - 82.7266 \times \left(\log\log \eta_{RTFO,65^oC}\right)^2 \end{array} \right\} \times \left(0.445822 \times VA_{orig}^{\ 0.355366}\right) \tag{6.5}$$

The PAV aging temperatures required, predicted using equation 6.5 are summarized along with measured equivalent PAV aging temperature in Table 30. Figure 99 shows the comparison plot.

It was observed from the plot that the comparison had considerably improved and most of the data points plot very close to the equality line. It was concluded that the PP1 equation with the air-voids correction factor, equation 6.5, was accurate enough for all practical purposes. However, as explained in *Chapter 3, Development of Correction Factor for Binder Extraction*, the aged viscosity values estimated from the PP1 equation, can be used to predict the modulus values using the Witczak et al. equation. Therefore, modulus values were estimated using predicted and measured viscosities and compared. Figure 100 shows the plot of modulus estimated from viscosity equivalent to predicted PAV

aging temperature vs. modulus estimated from viscosity equivalent to measured PAV aging temperature.

It was observed from Figure 100 that most of the modulus values plotted on the equality line or close to the equality line and thus, difference in the modulus values was considered to be insignificant for all practical purposes.

FIELD CALIBRATION AT 85ºC AND 60ºC ANALYSIS TEMPERATURES

The PP1 Equation developed at an analysis temperature of 85ºC (equation 5.5) was also calibrated using the field data. The results obtained were similar to those obtained at 65ºC. Therefore field calibration was carried out at the standard temperature of 60ºC (absolute viscosity). The models calibrated with mix air-voids obtained at 85ºC and 60ºC are shown in equations 6.6 and 6.7 respectively.

$$T_{PAV} = \left\{ \begin{array}{l} \left(4.123608 + 0.167497 \times \left(\log\log \eta_{RTFO,85^oC}\right)^2 \times MAAT\right) \times \ln(t_{aging}) \\ +100.5881 - 72.0334 \times \left(\log\log \eta_{RTFO,85^oC}\right)^2 \end{array} \right\} \times \left(0.468313 \times VA_{orig}^{\ 0.333401}\right) \quad (6.6)$$

$$T_{PAV} = \left\{ \begin{array}{l} \left(2.132432 + 0.193560 \times \left(\log\log \eta_{RTFO,60^oC}\right)^2 \times MAAT\right) \times \ln(t_{aging}) \\ +109.9632 - 78.2945 \times \left(\log\log \eta_{RTFO,60^oC}\right)^2 \end{array} \right\} \times \left(0.445445 \times VA_{orig}^{\ 0.378370}\right) \quad (6.7)$$

The PAV aging temperatures required to predict the field-aged viscosity using equations 6.6 and 6.7 were respectively compared with the PAV aging temperature corresponding to the field-aged viscosities. The comparison plots are shown in Figures 101 and 102. An error analysis was carried out on the PAV aging temperatures estimated from equation 6.7. Figure 103 shows the plot of percentage error between PAV aging temperature obtained from equation 6.7 and PAV aging temperatures corresponding to the viscosities obtained from filed cores at 60ºC. The average error was found to be -0.15%. Therefore, it was concluded that equation 6.7 gives sufficiently accurate prediction of PAV aging temperature for all practical purposes and should be seriously considered as an Addendum to the PP1-98 Protocol.

DISCUSSION OF IMPLEMENTATION

At this point it should be acknowledged that a potential problem exists with the implementation of equation 6.7, although this problem is probably minor. Equation 6.7 yields a continuum of PAV temperatures. However, to the best of the knowledge of the research team, existing PAV chambers operate at only 90ºC, 100ºC, and 110ºC. This discrepancy could possibly be solved with one of the following four approaches.

1. Modify existing PAV chambers to yield a wider range of controlled temperatures.

2. Utilize a new generation of PAV chambers with continuous temperature range, rather than three discrete values.
3. Use equation 6.7 to estimate T_{PAV} and then choose the standard temperature (90, 100, or 110ºC), which is closest to the calculated T_{PAV}. If an unbiased estimate of the aged viscosity is required, use the results reported in Chapters 5 and 6 to approximately correct the results obtained from equation 6.7
4. The new PP1 Protocol will, in general, be used in a predictive mode. It is assumed that, typically, a user would treat the binder in PAV, measure the ensuing viscosity, and then infer future, aged modulus for a given binder, original air-voids, *MAAT*, and assumed field aging time. In this context, the field aging time is usually chosen somewhat arbitrarily. Thus equation 6.7 could either be inverted or used in a trial and error mode to find a field aging time which corresponds to one or more of the following: T_{PAV} = 90, 100, or 110ºC.

Table 21
Field Aging Conditions

Site	Age (years)	*MAAT* (F)	Binder
ADOT Kingman	9	62.6	ADOT AC-30
MnRoad Cell 16	9	46.2	MnRoad AC-20
MnRoad Cell 18	9	46.2	MnRoad AC-20
WesTrack Section 12	7	54.4	WesTrack AC-20
WesTrack Section 15	7	54.4	WesTrack AC-20
WesTrack Section 16	7	54.4	WesTrack AC-20

Table 22
Estimated Required PAV Aging Temperature

Site	PAV Aging Temperature Required (C)
ADOT Kingman	108.8
MnRoad Cell 16	102.0
MnRoad Cell 18	102.0
WesTrack Section 12	104.1
WesTrack Section 15	104.1
WesTrack Section 16	104.1

Table 23
DSR Results for the Field Cores

Temp. (C)	log T (R)	Top		Middle		Bottom	
		Viscosity (Pas)	loglog Visc (cP)	Viscosity (Pas)	loglog Visc (cP)	Viscosity (Pas)	loglog Visc (cP)
ADOT-Kingman							
45	2.757927	59823.5	0.8908049	52980	0.8878486	56689.5	0.8894979
65	2.784403	3745.75	0.8177992	3224	0.8134739	3695.8	0.8174139
85	2.809358	234.15	0.7299334	211.095	0.726277	220.485	0.727816
MnRoad Cell 16							
45	2.757927	18364	0.8611739	18099.5	0.860797	17330.5	0.8596672
65	2.784403	959.075	0.7768357	907.415	0.7750864	884.39	0.7742719
85	2.809358	76.951	0.6889725	70.4335	0.6855428	65.1425	0.6824939
MnRoad Cell 18							
45	2.757927	13808.5	0.8537071	13533.5	0.8531754	11811	0.8495599
65	2.784403	769.49	0.7698352	654.635	0.7646243	588.565	0.7611603
85	2.809358	62.183	0.6806683	59.5635	0.6789716	50.7155	0.6725726
WesTrack Section 12							
45	2.757927	9265.45	0.8430375	6814	0.834637	10667	0.8468344
65	2.784403	436.71	0.751294	312.745	0.7399827	474.555	0.7540643
85	2.809358	37.6575	0.6604719	29.918	0.6508835	42.5975	0.6655232
WesTrack Section 15							
45	2.757927	42259	0.8822922	35195	0.8777445	33114.5	0.8762189
65	2.784403	2008.4	0.799537	1658.5	0.7937705	1494.5	0.7906015
85	2.809358	142.45	0.712116	109.435	0.7023578	101.306	0.6994592
WesTrack Section 16							
45	2.757927	45846.5	0.8843028	37744.5	0.8794889	40226.5	0.8810714
65	2.784403	2177.1	0.8019439	1719.6	0.7948662	1859.95	0.797233
85	2.809358	147.425	0.7133705	120.37	0.705908	127.1	0.7079231

Table 24
Field-Aged Viscosity of the Cores at 65ºC

Site	Field Aged loglog Viscosity (cP) at 65ºC
ADOT Kingman	0.8111672047
MnRoad Cell 16	0.7737159104
MnRoad Cell 18	0.7664438979
WesTrack Section 12	0.7494311224
WesTrack Section 15	0.7959782811
WesTrack Section 16	0.7978828736

Table 25
DSR Results of PAV Aged Binders at 65ºC

Binder	loglog Viscosity (cP) at 65ºC		
	PAV 90	PAV 100	PAV 110
ADOT AC-30	0.805782	0.813024	0.837038
MnRoad AC-20	0.771823	0.782714	0.803691
WesTrack AC-20	0.768548	0.778176	0.804043

Table 26
Parameters *a* and *b* Obtained from Regression Analysis for Various Binders

Binder	*a*	*b*
ADOT AC-30	4.707043	0.032082
MnRoad AC-20	5.460072	0.036415
WesTrack AC-20	5.676990	0.039072

Table 27
Equivalent PAV Aging Temperatures to Simulate Field Aging

Site	Equivalent PAV Temperature (ºC)
ADOT Kingman	95.9
MnRoad Cell 16	92.3
MnRoad Cell 18	86.1
WesTrack Section 12	73.3
WesTrack Section 15	107.1
WesTrack Section 16	108.0

Table 28
Predicted vs. Measured PAV Aging Temperatures

Site	Predicted PAV Temperature Required (ºC)	Measured Equivalent PAV Temperature (ºC)
ADOT Kingman	108.8	95.9
MnRoad Cell 16	102.0	92.3
MnRoad Cell 18	102.0	86.1
WesTrack Section 12	104.1	73.3
WesTrack Section 15	104.1	107.1
WesTrack Section 16	104.1	108.0

Table 29
Summary of PAV Temperatures and Air-Voids

Site	Original Mix Air Voids (%)	Predicted PAV Temp required (C)	Measured Equivalent PAV Temp (C)	Ratio of Measured and Predicted PAV Temperatures
ADOT Kingman	7.00	108.8	95.9	0.881573
MnRoad Cell 16	8.20	102.0	92.3	0.904415
MnRoad Cell 18	5.60	102.0	86.1	0.843431
WesTrack Section 12	4.00	104.1	73.3	0.704613
WesTrack Section 15	8.00	104.1	107.1	1.029347
WesTrack Section 16	12.00	104.1	108.0	1.037779

Table 30
Summary of Predicted and Measured PAV Aging Temperatures

Site	Predicted PAV Temperature Required (°C)	Measured Equivalent PAV Temp (°C)
ADOT Kingman	96.8	95.9
MnRoad Cell 16	96.1	92.3
MnRoad Cell 18	83.9	86.1
WesTrack Section 12	75.9	73.3
WesTrack Section 15	97.1	107.1
WesTrack Section 16	112.2	108.0

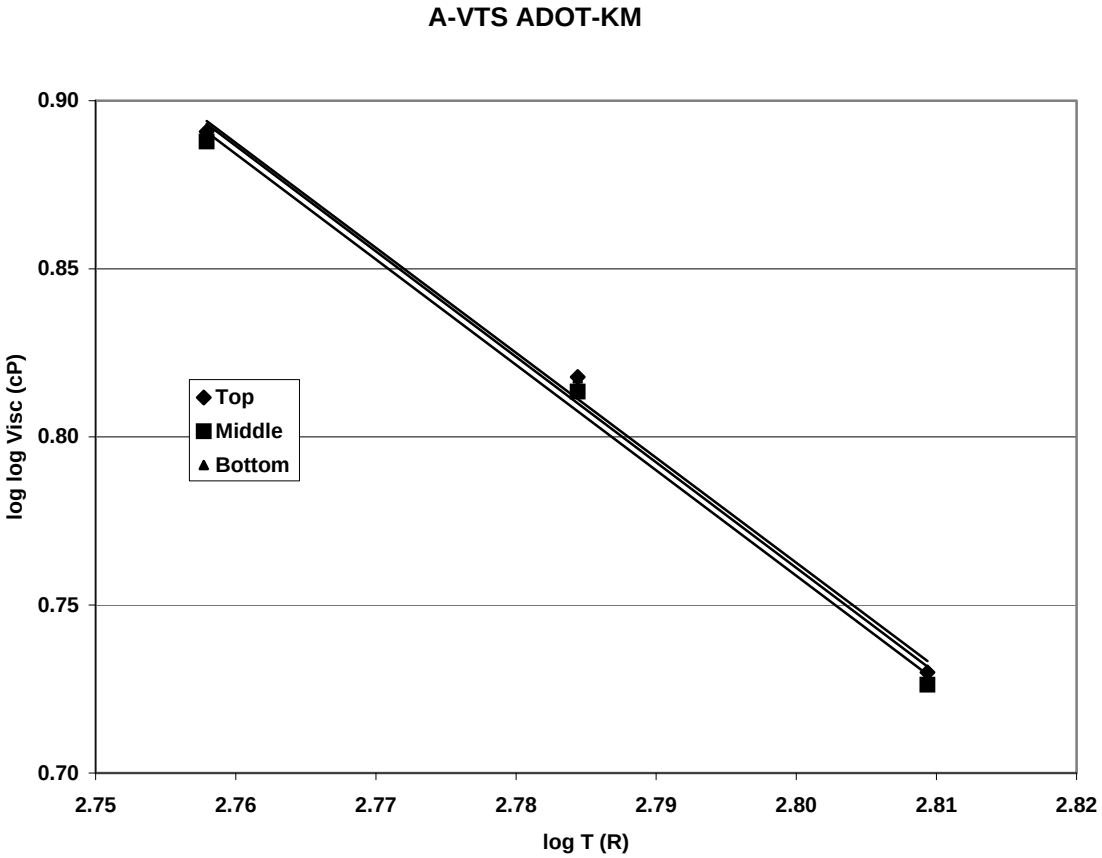

Figure 85
A-VTS Plot for ADOT Kingman Field Core

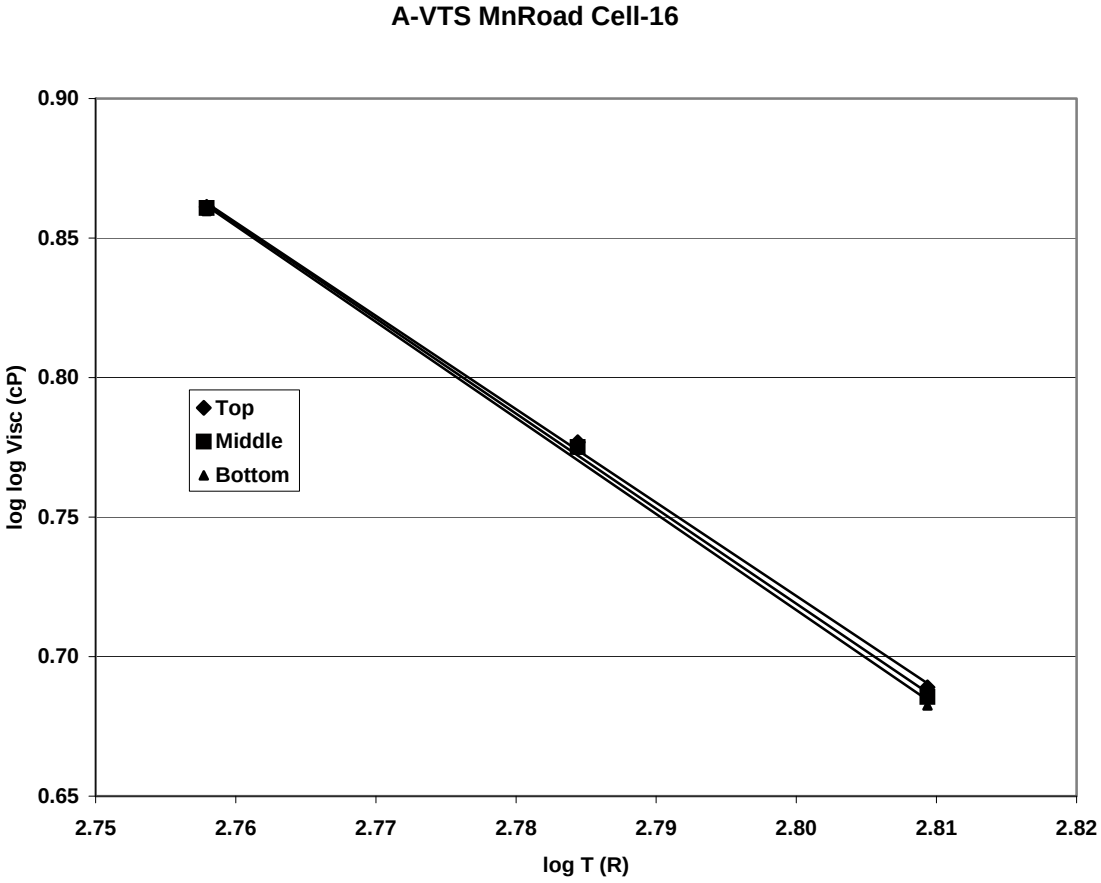

Figure 86
A-VTS Plot for MnRoad Cell 16 Field Core

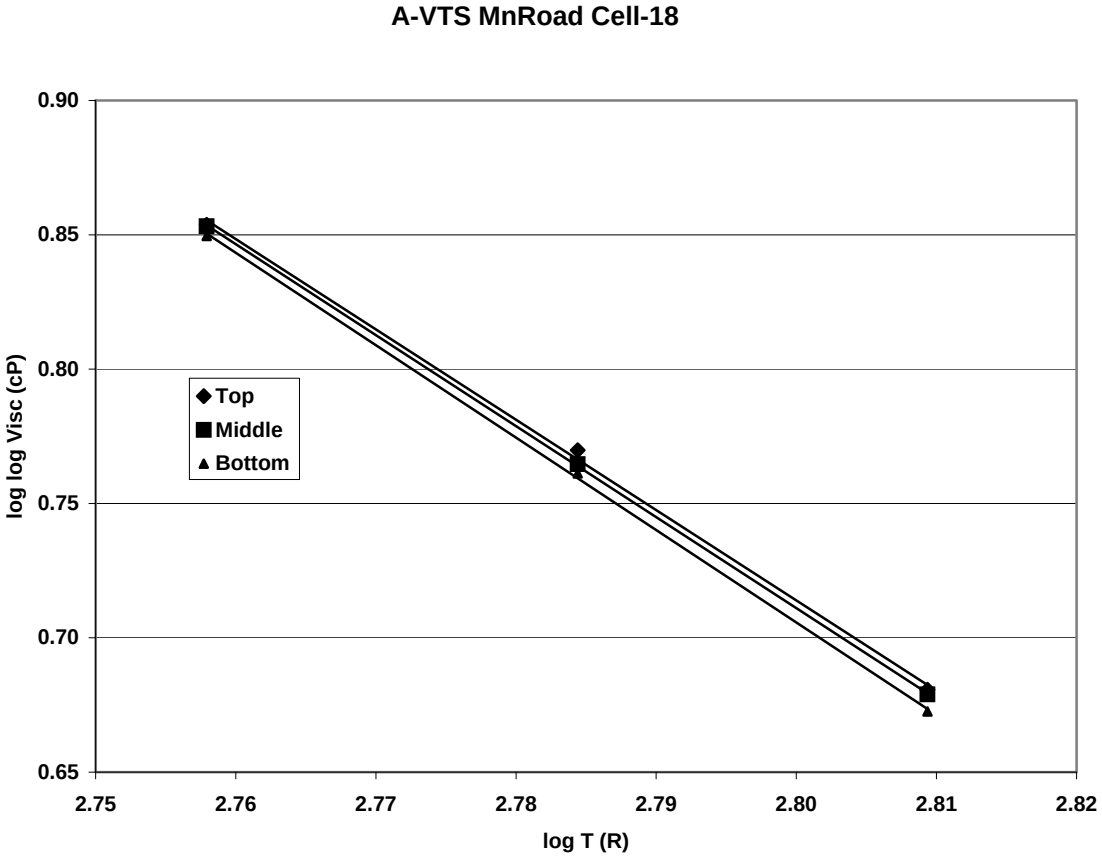

Figure 87
A-VTS Plot for MnRoad Cell 18 Field Core

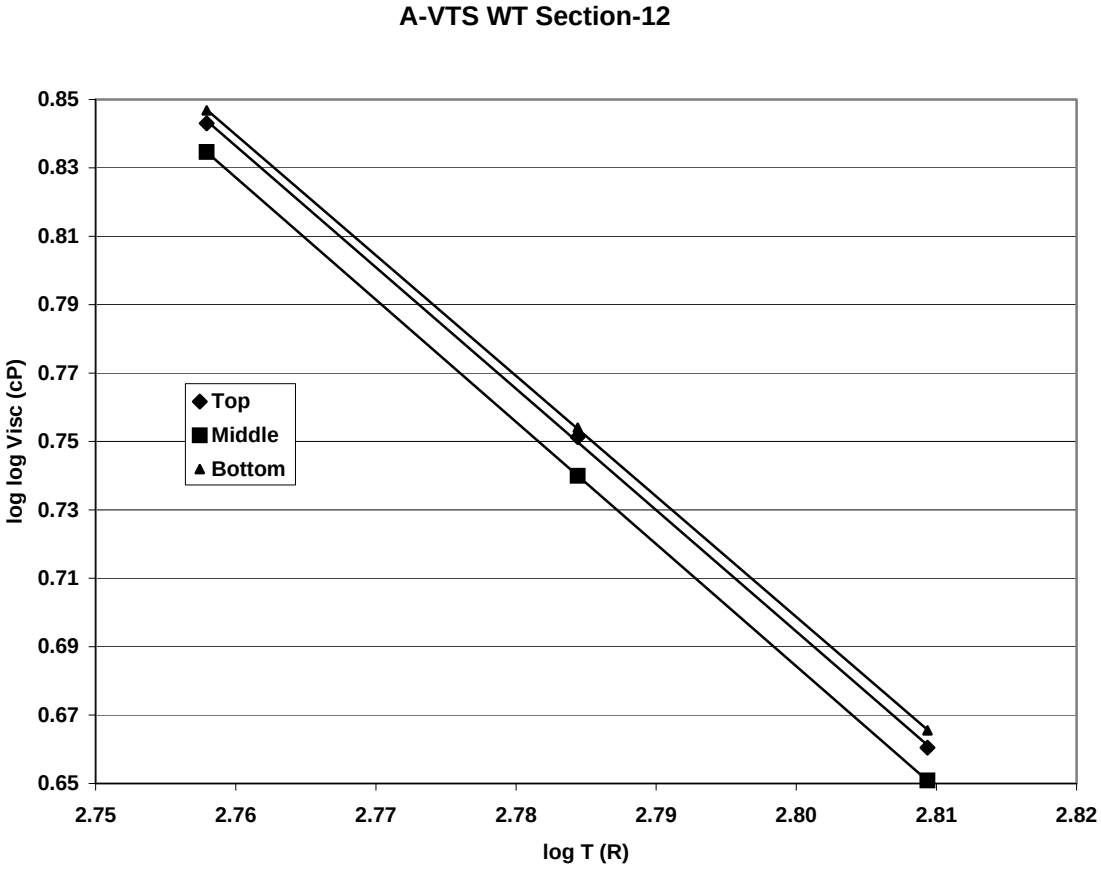

Figure 88
A-VTS Plot for WesTrack Section 12 Field Core

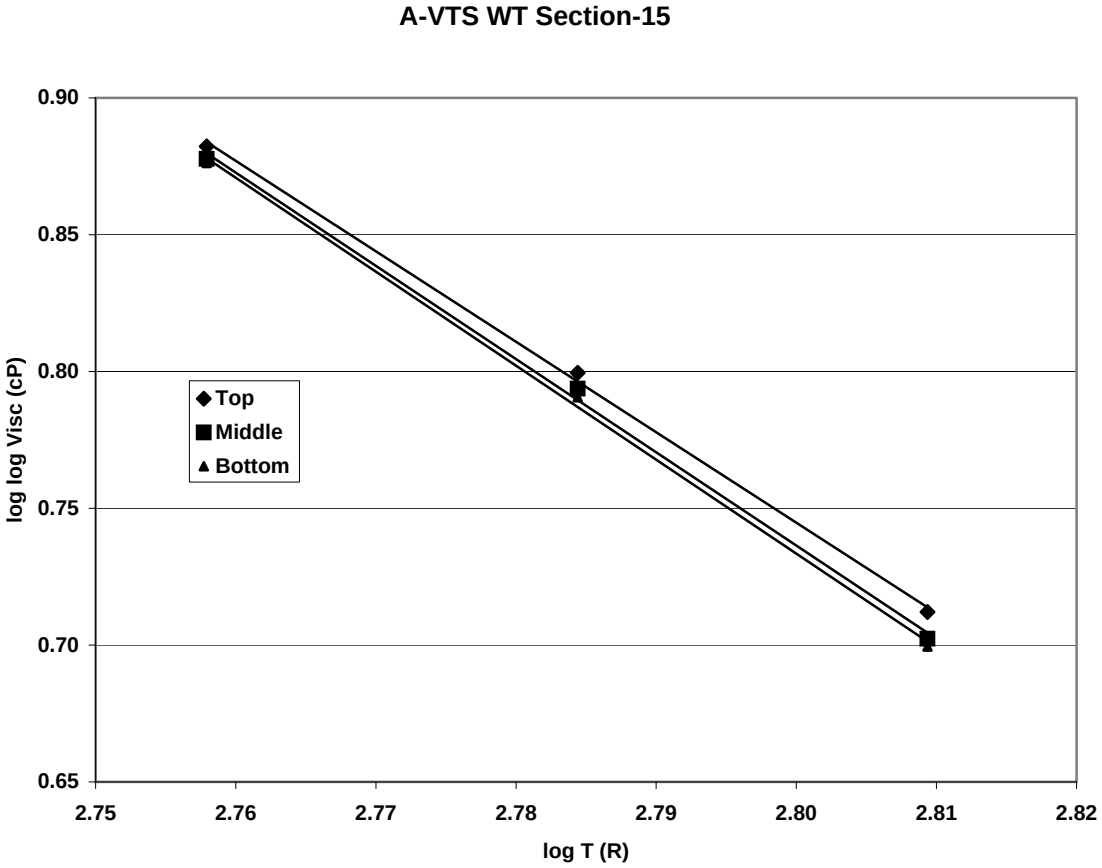

Figure 89
A-VTS Plot for WesTrack Section 15 Field Core

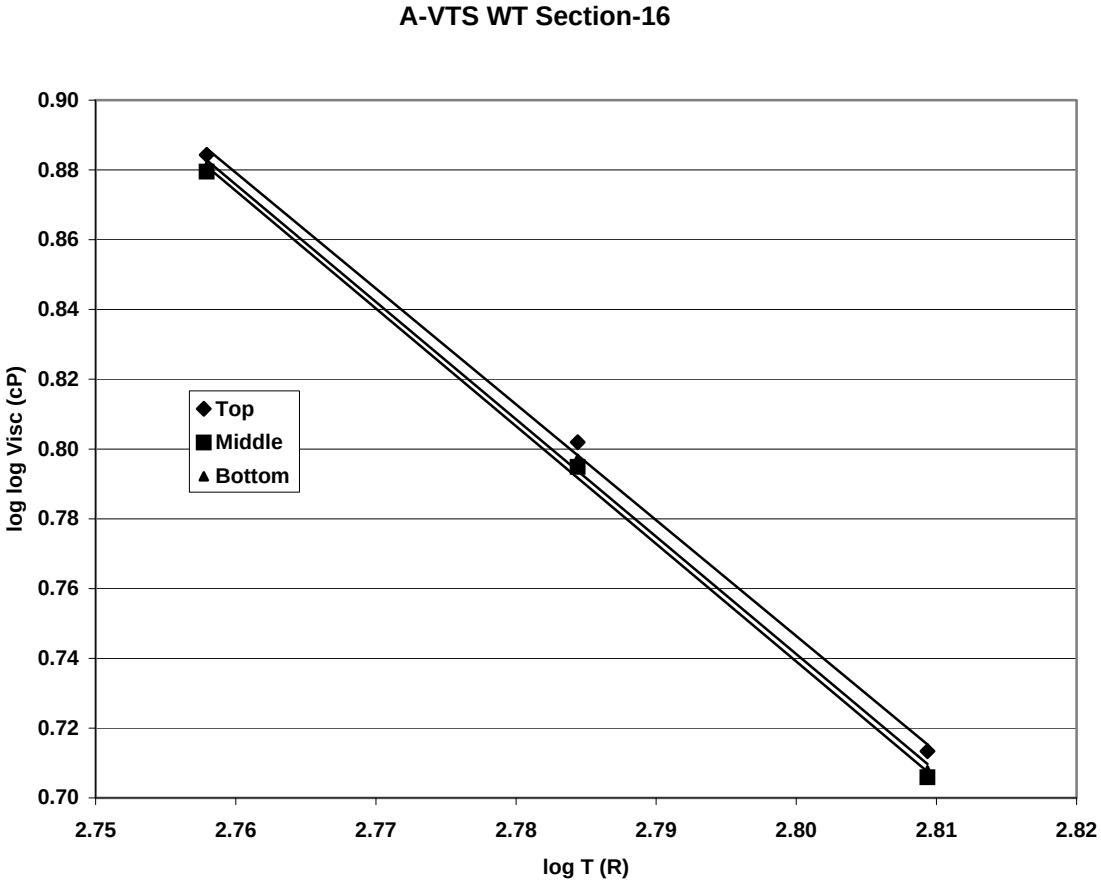

Figure 90
A-VTS Plot for WesTrack Section 16 Field Core

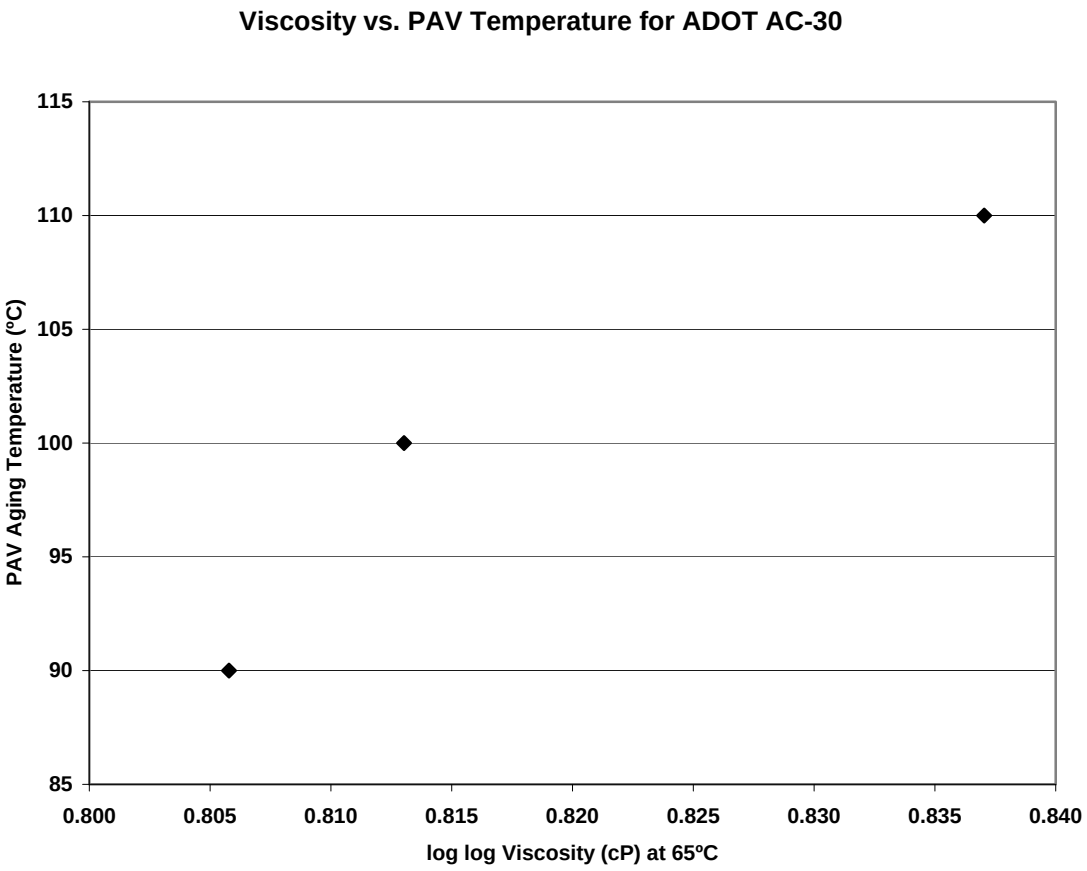

Figure 91
Viscosity at 65ºC vs. PAV Aging Temperature for ADOT AC-30

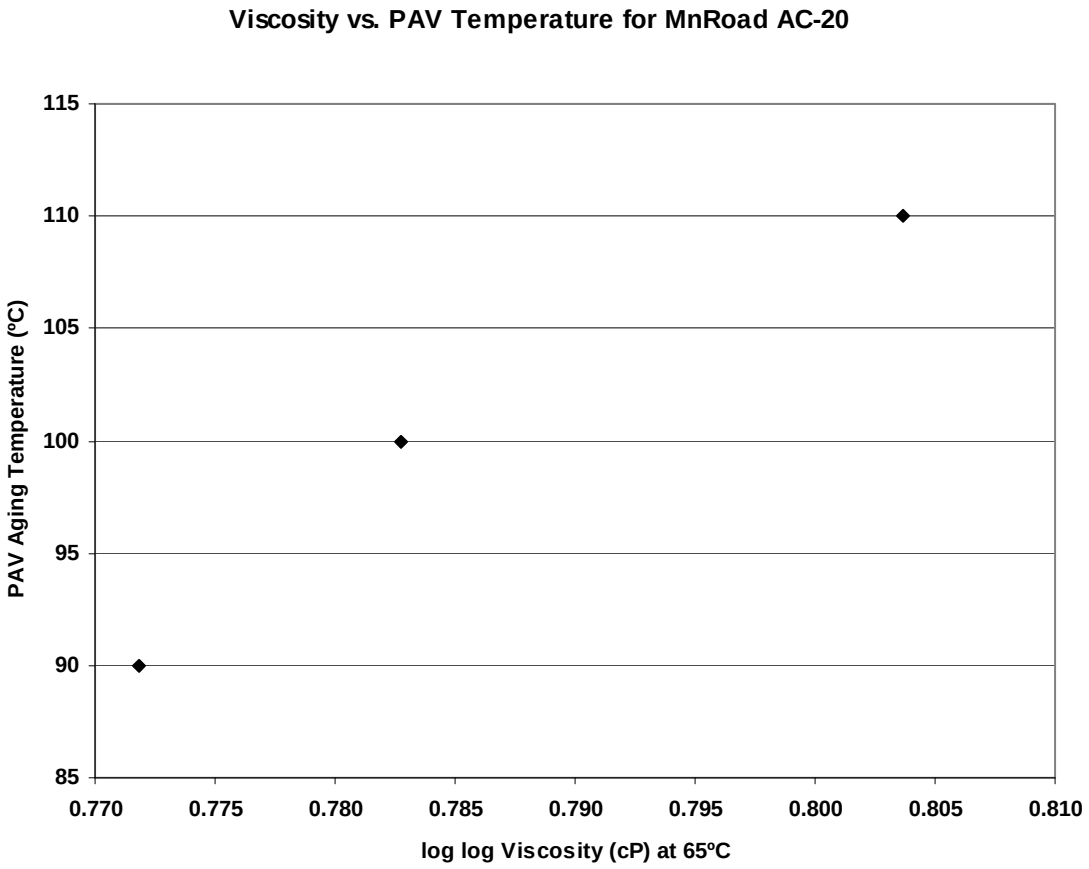

Figure 92
Viscosity at 65ºC vs. PAV Aging Temperature for MnRoad AC-20

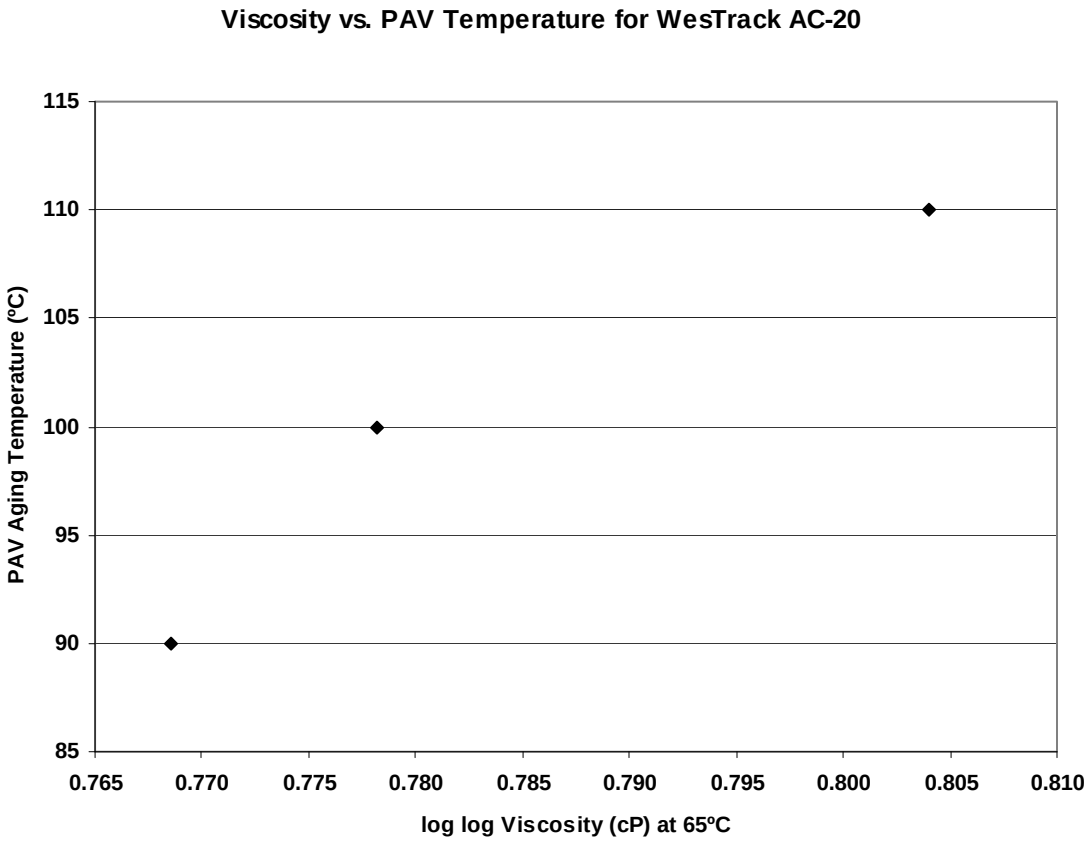

Figure 93
Viscosity at 65ºC vs. PAV Aging Temperature for WesTrack AC-20

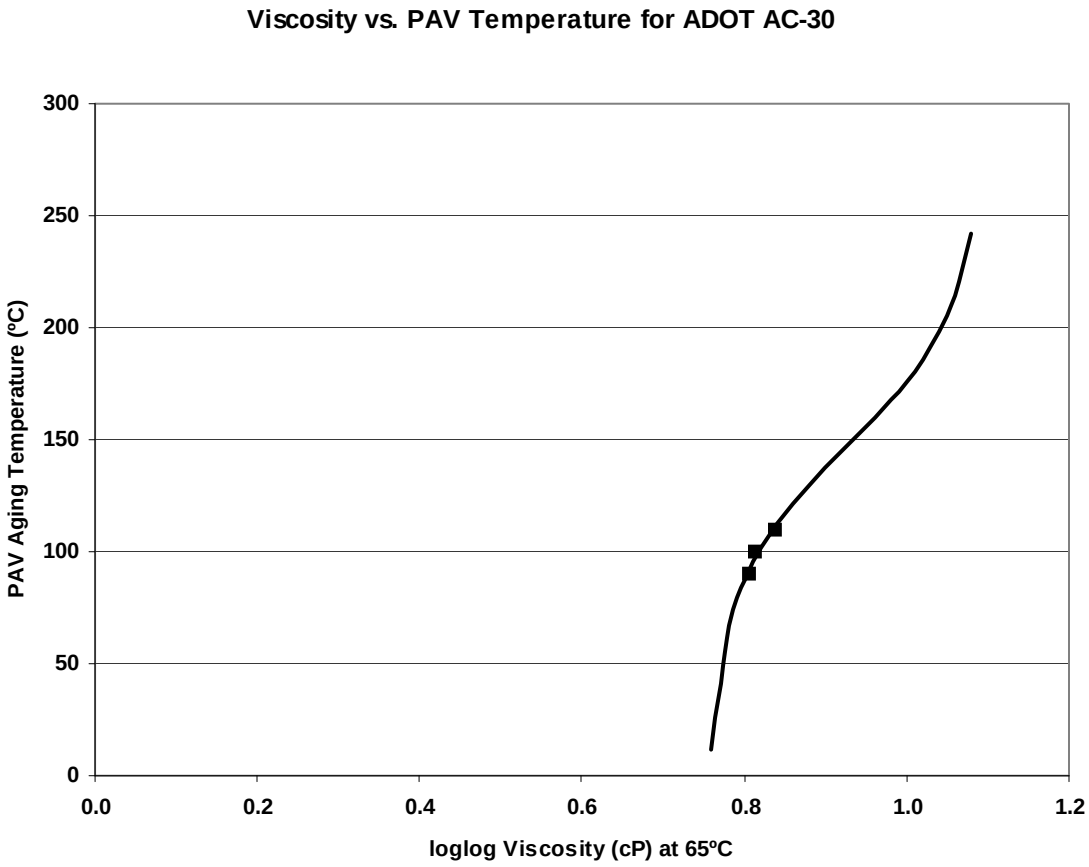

Figure 94
Viscosity at 65ºC vs. PAV Aging Temperature for ADOT AC-30

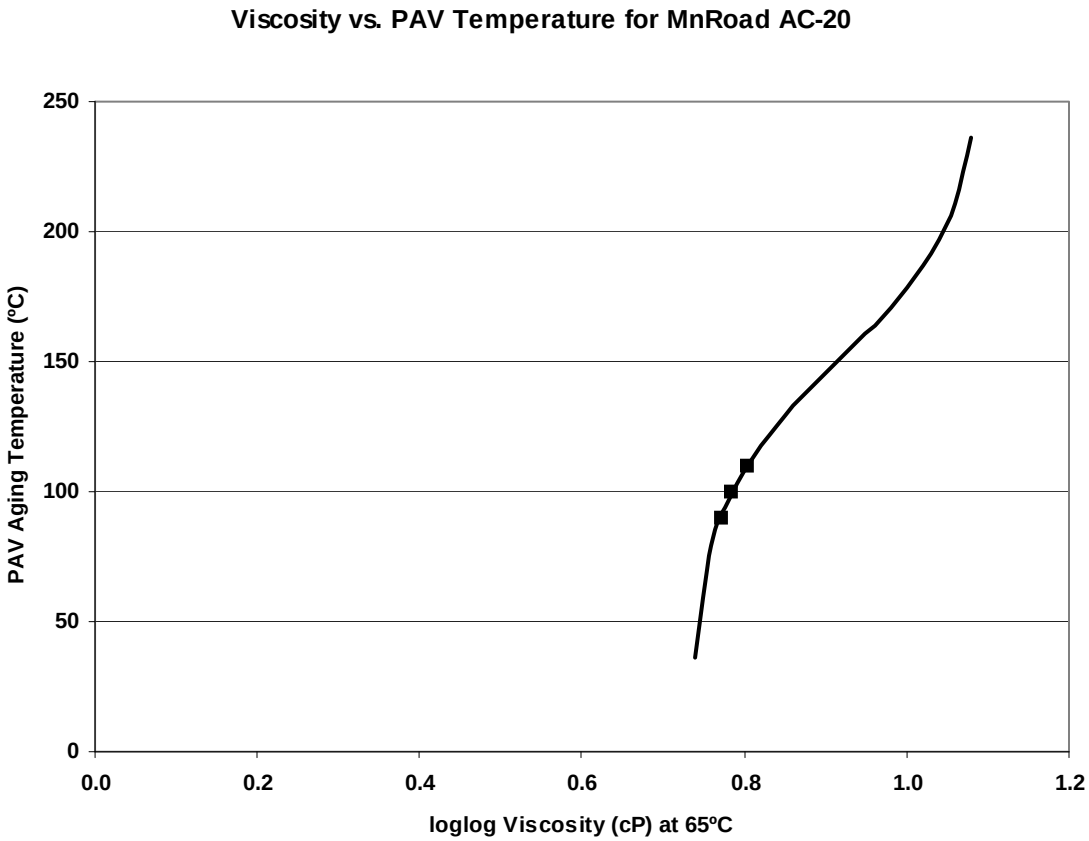

Figure 95
Viscosity at 65ºC vs. PAV Aging Temperature for MnRoad AC-20

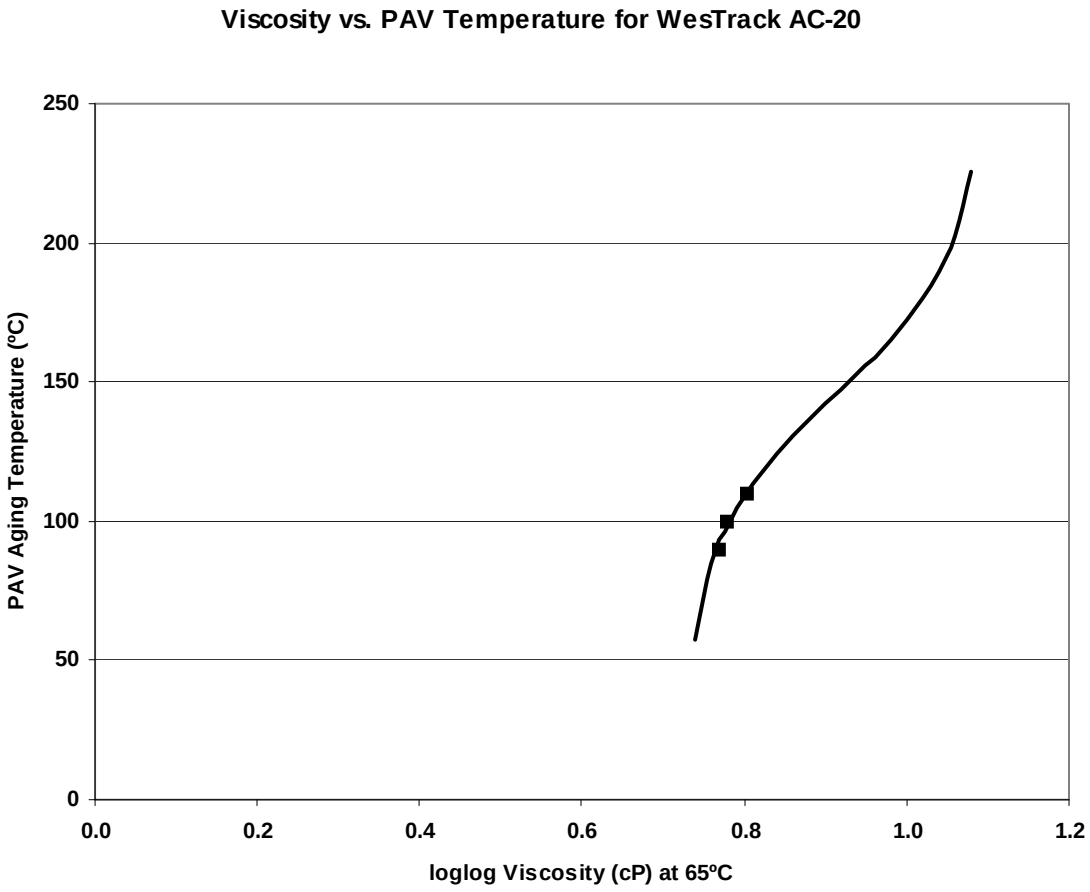

Figure 96
Viscosity at 65ºC vs. PAV Aging Temperature for WesTrack AC-20

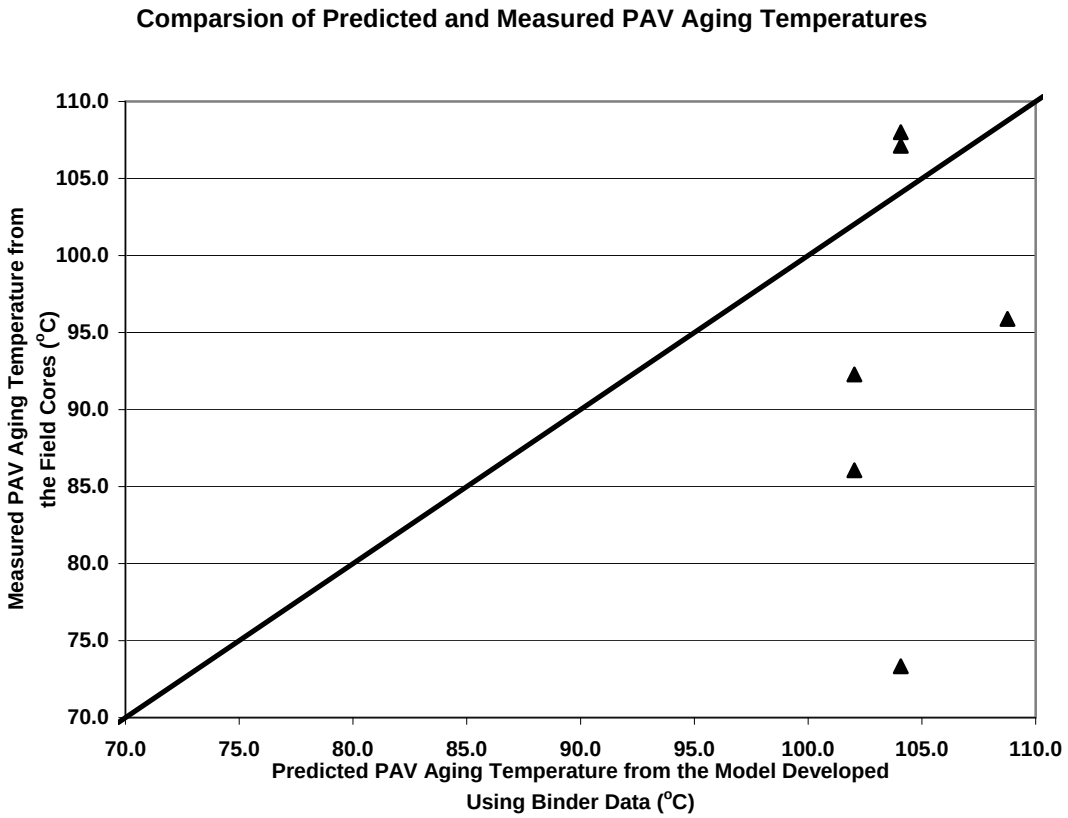

Figure 97
Comparison of Predicted PAV Aging Temperature Required and Measured Equivalent PAV Aging Temperature

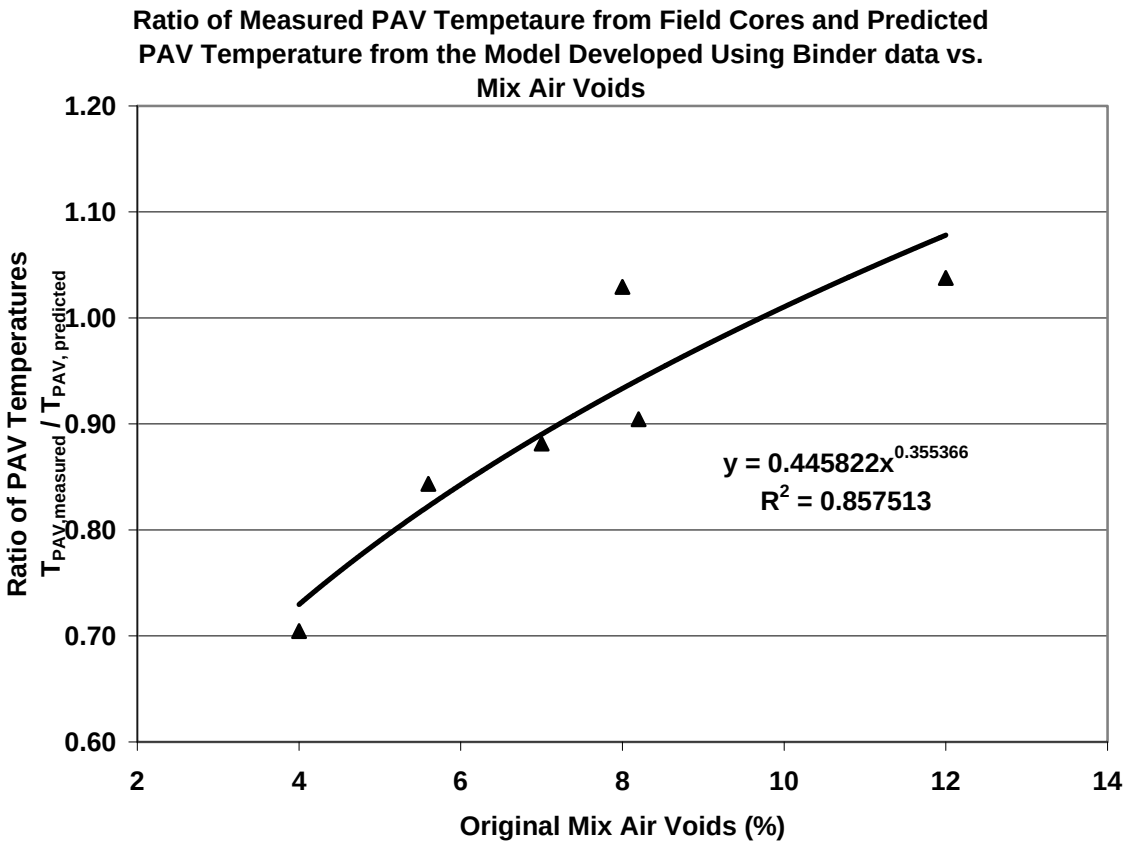

Figure 98
Ratio of Measured and Predicted PAV Aging Temperatures vs. Original Mix Air-Voids

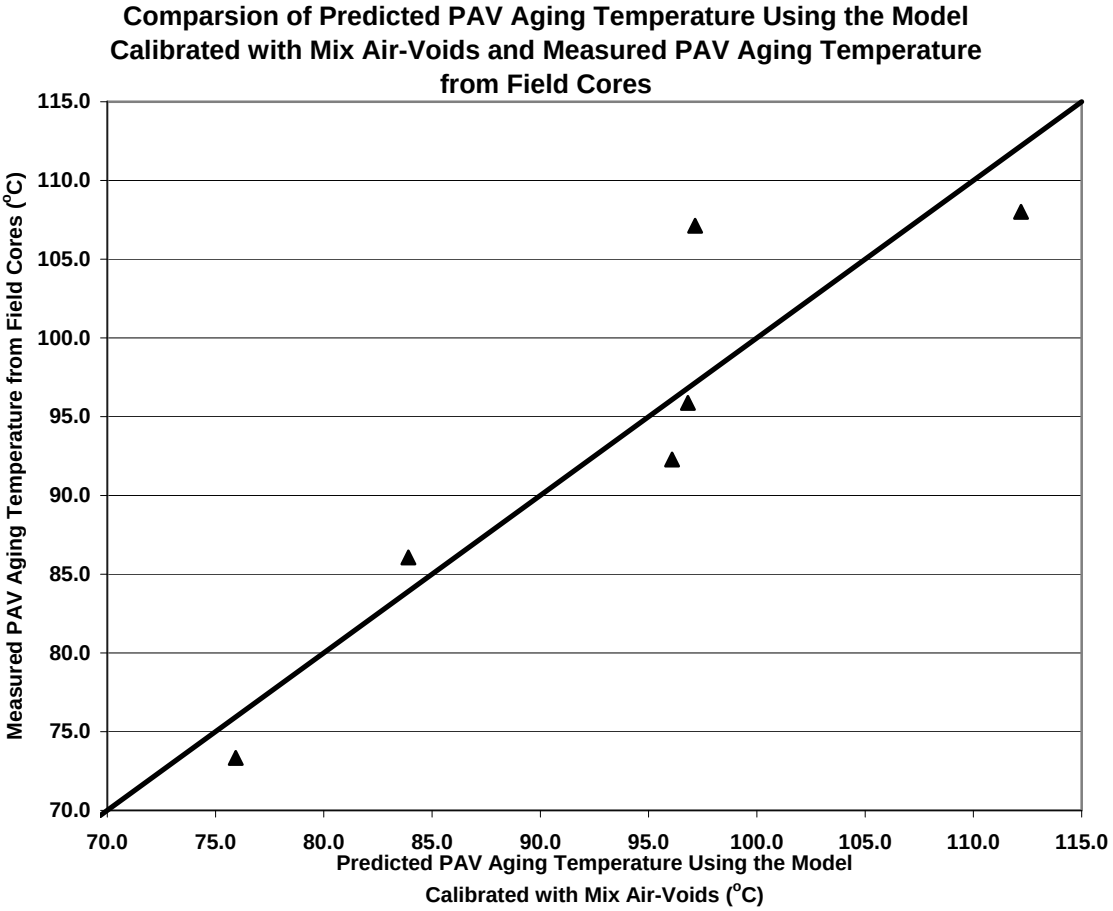

Figure 99
Comparison Plot of Predicted PAV Aging Temperature With Air-Voids Correction Factor and Measured PAV Aging Temperature

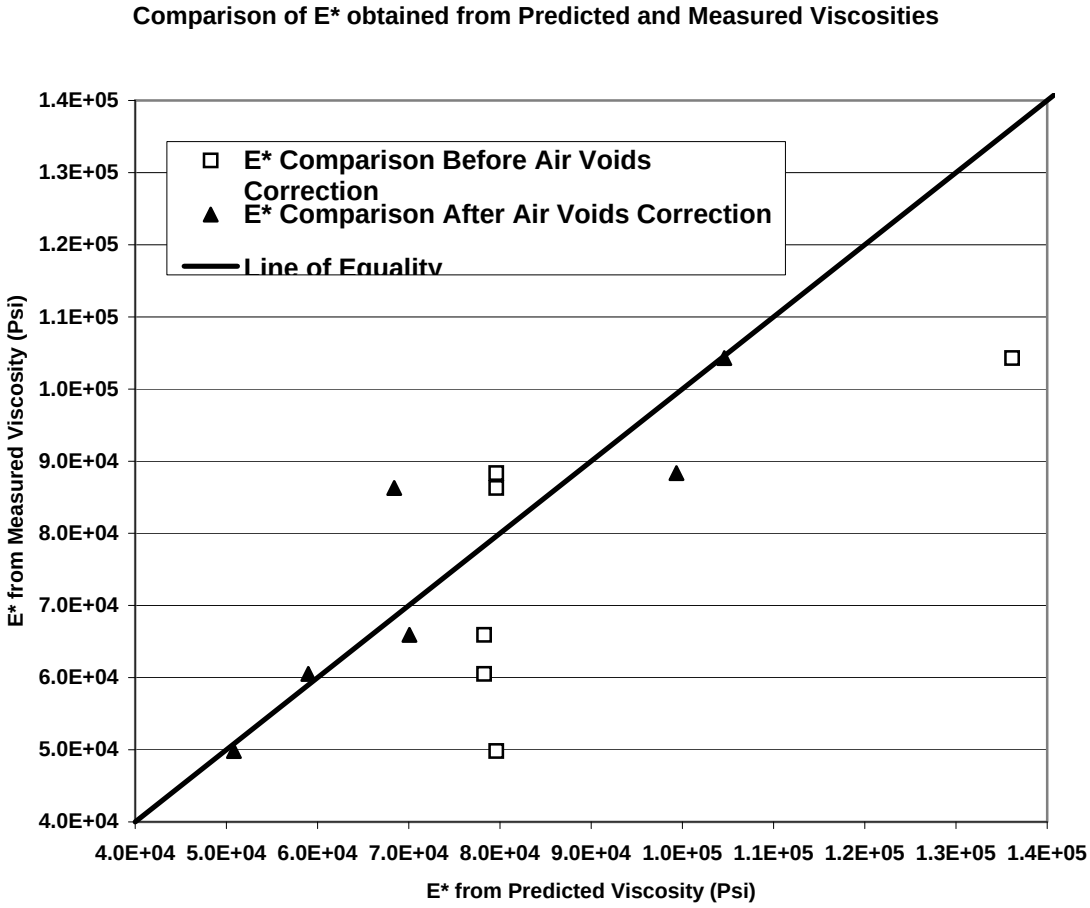

Figure 100
Modulus Equivalent To Predicted PAV Aging Temperature vs. Modulus Equivalent to Measured PAV Aging Temperature

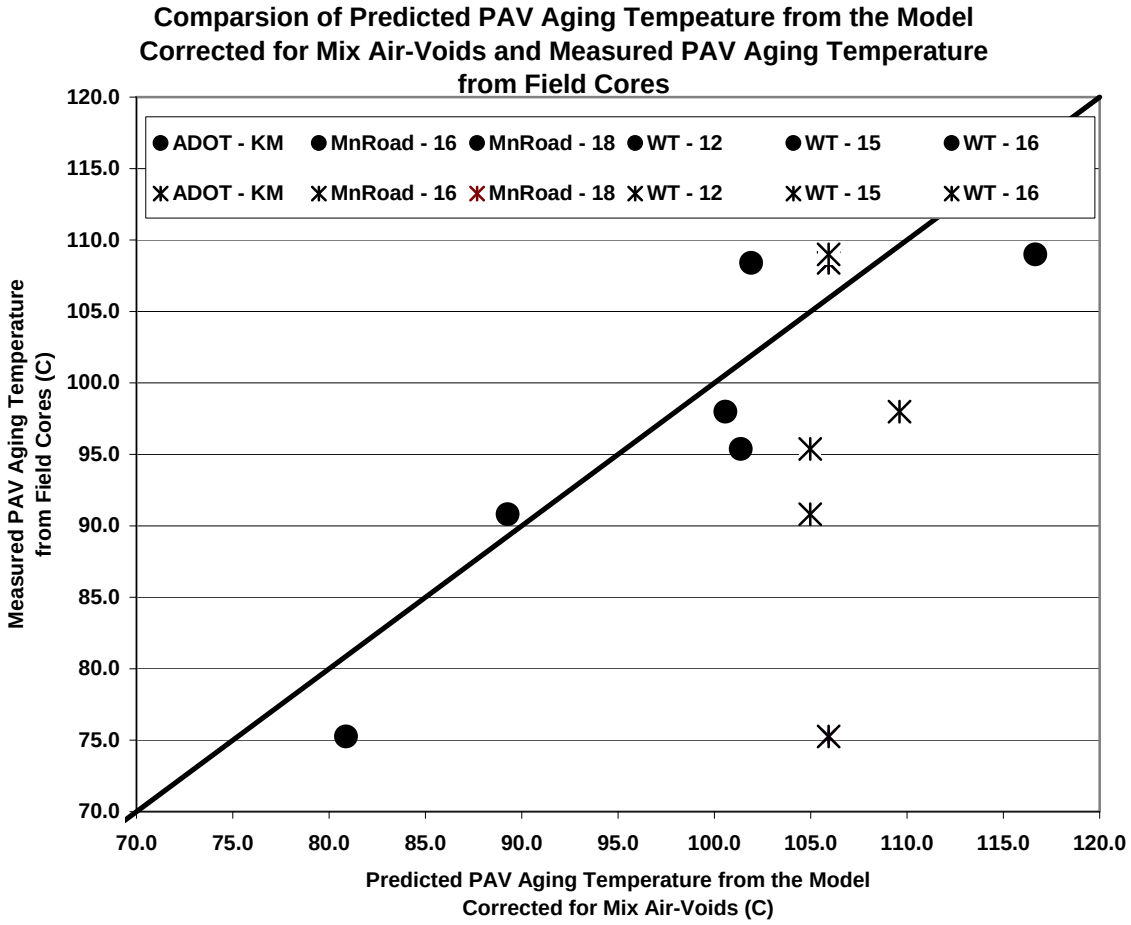

Figure 101
Comparison Plot of PAV Aging Temperatures Obtained from Model Calibrated for Mix Air-Voids At 85ºC and PAV Aging Temperature Corresponding to Field-Aged Viscosity at 85ºC

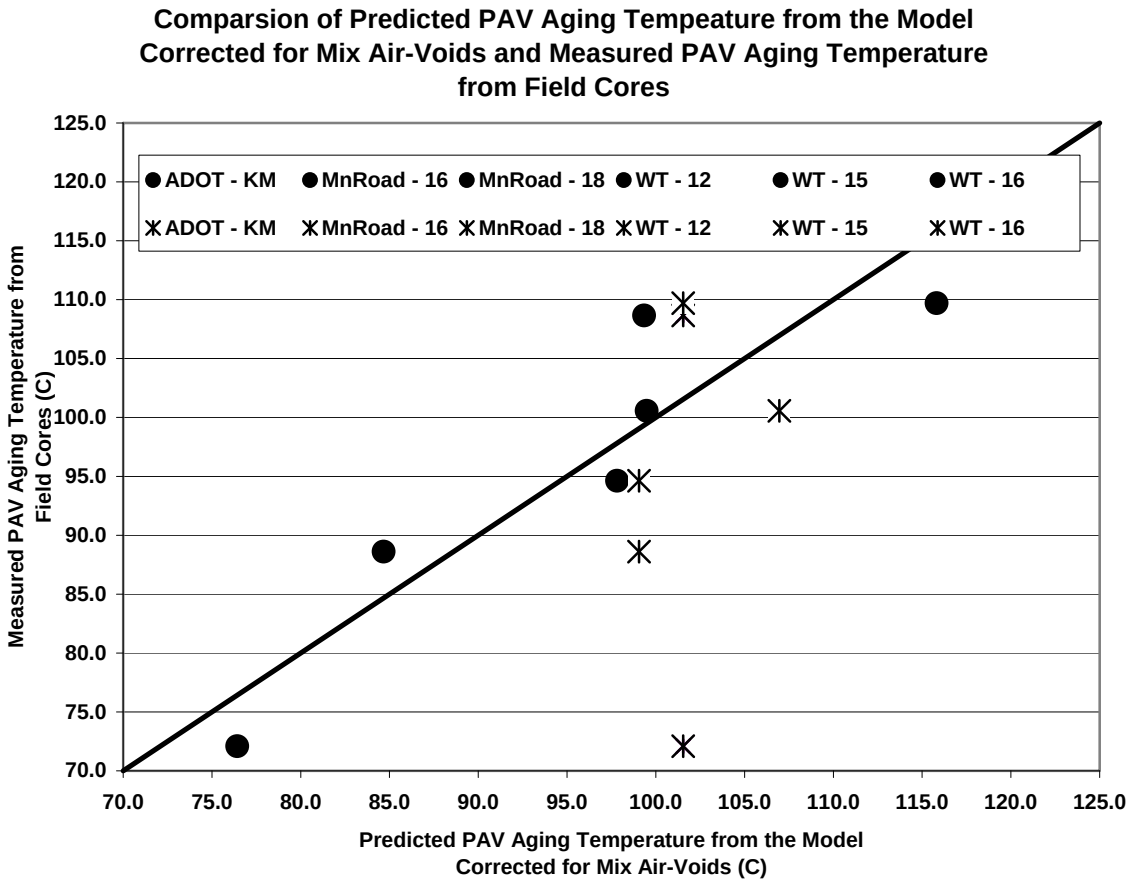

Figure 102
Comparison Plot of PAV Aging Temperature Obtained from Model Calibrated for Mix Air-Voids at 60ºC and PAV Aging Temperature Corresponding to Field-Aged Viscosity at 60ºC

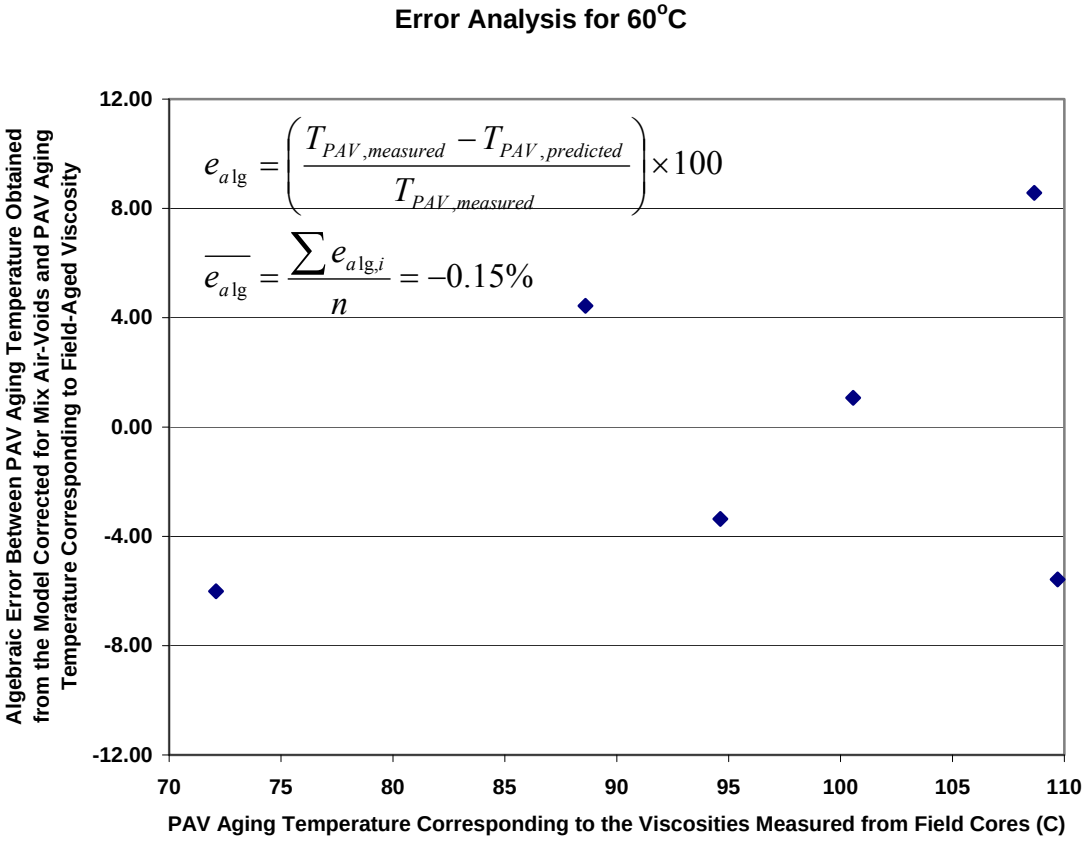

Figure 103
Plot of Percentage Error in PAV Aging Temperature Estimated from the Model Corrected for Mix Air-Voids and PAV Aging Temperature Corresponding to Field-Aged Viscosity

CHAPTER 7

VALIDATION OF THE EXPANDED PP1 MODEL WITH FIELD DATA

INTRODUCTION

A new PP1 equation was developed and presented in *Chapter 5, Improvement of the PP1-98 Protocol and Model Development*. The equation was then calibrated using the field data and extended to include the effect of mix air-voids. This calibration was described in *Chapter 6*. The current chapter deals with validating the final equation (equation 6.7) using the cores obtained from LTPP sites. The procedure adopted for completion of this task is similar to the procedure adopted for Field Calibration. However, original (un-aged) binders were not obtained from the LTPP sites, and the RTFO viscosities were generally not available from the database. Therefore, the RTFO viscosities were estimated using the A-VTS values obtained from the *Mechanistic-Empirical Pavement Design Guide*. The field aging conditions were obtained from the database *DATA PAVE*.

MATERIALS USED

In order to achieve this objective, field-cores were obtained from various LTPP sites across the country. The LTPP sites selected were:

1. 09-1803 located in Groton, Connecticut
2. 50-1681 located in Charlotte, Vermont
3. 30-7066 located in Big Timber, Montana
4. 56-2020 located in Ranchester, Wyoming
5. 56-2019 located in Gillette, Wyoming
6. 08-7035 located in Aurora, Colorado
7. 08-1053 located in Delta, Colorado
8. 53-7322 located in Pullman, Washington

APPROACH

The field aging condition i.e., air-voids and binder grade information were obtained from the LTPP database *DATAPAVE*. *MAAT* data was obtained from the *Mechanistic-Empirical Pavement Design Guide* climate files[8]. Using the PP1 equation (equation 6.7) developed in the previous chapter, the PAV aging temperature, T_{PAV}, required to simulate the field aging was estimated for all the sites. Using the binder characterization developed in *Chapter 5*, the viscosities corresponding to the estimated PAV aging temperatures were predicted. The predicted viscosities were then compared to the field-aged viscosities measured. Based on this comparison, suitable conclusions were drawn.

STEPS USED TO FOLLOW THE AFOREMENTIONED APPROACH

1. Field cores were obtained from the LTPP sites listed above.

2. Field aging conditions such as *MAAT*, age of the pavement and original air-voids were obtained from the LTPP database, *DATAPAVE*.
3. Binders were extracted from the field cores taken from the sites.
4. DSR tests were conducted on the extracted binders to obtain field-aged viscosities.
5. RTFO viscosities were computed using the knowing binder grades and the A-VTS values obtained from the *Mechanistic-Empirical Pavement Design Guide*.
6. Using the PP1 equation (equation 6.7), the PAV aging temperature, T_{PAV} required to simulate the field aging was estimated for all the field samples obtained.
7. Using the binder characterization relationships developed in *Chapter 5, Improvement of the PP1-98 Protocol and Model Development*, the viscosities corresponding to the estimated PAV aging temperatures were predicted.
8. The predicted viscosities were then compared to the measured viscosities and based on this comparison suitable conclusions were drawn.

These steps are explained in detail in the following sections.

LABORATORY TESTING ON FIELD CORES

Cores were obtained from the LTPP field sites. Binder was extracted from the top 1-inch of the core. Two cores were used from each site for the binder extraction. DSR testing was conducted on the extracted binders to obtain the field-aged viscosities. The DSR testing results on the field-cores are summarized in Table 31.

The A-VTS plots obtained from the data presented in Table 31are shown in Figures 104 to 111.

From the A-VTS relationships obtained, the field viscosity at a reference binder temperature of 60ºC was obtained, to be consistent with the prior analysis. The field-aged viscosity values at 60ºC, which corresponds to Log T(R) = 2.7779, are summarized in Table 32.

VISCOSITY PREDICTION

Binder grades of all the binders used in LTPP sites were obtained from the database *DATAPAVE*. A-VTS values corresponding to the RTFO aged condition for these binders were obtained from the *Mechanistic-Empirical Pavement Design Guide*[8]. Using the A-VTS values, RTFO viscosities at 60ºC were computed. Table 33 shows the summary of the binder grades, A-VTS values, and RTFO viscosities at 60ºC for all the LTPP Sites.

ESTIMATION OF PAV AGING TEMPERATURE

Information on Field-aging conditions obtained from the database is summarized in Table 34.

PP1 Equation

$$T_{PAV} = \left\{ \begin{array}{l} \left(2.132432 + 0.193560 \times \left(\log\log \eta_{RTFO,60^oC}\right)^2 \times MAAT\right) \times \ln(t_{aging}) \\ +109.9632 - 78.2945 \times \left(\log\log \eta_{RTFO,60^oC}\right)^2 \end{array} \right\} \times \left(0.445445 \times VA_{orig}^{\ 0.378370}\right) \quad (7.1)$$

Using the data presented in Tables 33 and 34 in the PP1 equation (equation 7.1), the PAV aging temperature, T_{PAV} required to simulate the field aging was predicted and summarized in Table 35.

It can be observed from Table 35 that the PAV aging temperatures predicted are in accordance with the field aging conditions. Higher *MAAT*, air voids and aging times result in higher PAV aging temperatures, and lower *MAAT*, air voids and aging times result in lower PAV aging temperatures. Therefore, it can be concluded that the PP1 equation (equation 7.1) yields satisfactory results.

Viscosities at 60ºC corresponding to these PAV aging temperatures were predicted using the binder characterization and compared with the field-measured values to further validate the PP1 equation (equation 7.1).

A relationship between the aged viscosity at 60ºC and the PAV aging temperature (equation 6.2) was developed in *Chapter 6* under binder characterization,

$$T_{PAV} = \frac{a - \ln\left[\frac{\log\log \eta_{ult} - \log\log \eta_{RTFO}}{\log\log \eta_{aged} - \log\log \eta_{RTFO}} - 1\right]}{b} \quad (7.2)$$

Inverting this equation, an equation for $\eta_{aged,\ 60ºC}$ as a function of T_{PAV} and $\eta_{RTFO,\ 60ºC}$ can be developed as follows,

$$\log\log \eta_{aged} = \left[\frac{\log\log \eta_{ult} - \log\log \eta_{RTFO}}{\exp^{(a - T_{PAV} \times b)} + 1}\right] + \log\log \eta_{RTFO} \quad (7.3)$$

A relationship was developed between the parameters *a* and *b* and $\eta_{RTFO,\ 60ºC}$ from the binders obtained from the calibration sites. Figure 112 shows the plot of parameters *a* and *b* vs. $\eta_{RTFO,\ 60ºC}$ for the binders used in Field Calibration.

Using these relationships, parameters *a* and *b* were computed for the binders used in the validation study, knowing the RTFO viscosity at 60ºC. Substituting all the values in equation 7.2, aged viscosities at 60ºC were computed. Table 36 shows the predicted aged viscosity values at 60ºC. Predicted viscosities from Table 36 are compared with

measured viscosities from Table 32. Summary of the comparison is shown in Table 37 and plot of the comparison is shown in Figure 113.

It can be observed from Figure 113 that the comparison is not a good one. However, the points plot on both sides of the equality line, showing that the results are fairly unbiased. The data points that deviate from the equality line were analyzed. The following factors were identified as the probable causes for that deviation.

1. Binders used in the model development do not represent the entire range of available binders. Binder characterization parameters *a* and *b* were developed based on the binders used in the calibration study. These do not encompass the entire range of binders used in the validation analysis.
2. The A and VTS values obtained from the *Mechanistic-Empirical Pavement Design Guide* were unique for a binder type. However, to a certain extent the A-VTS values are dependent on the source of the binder. In other words, a unique value of A and VTS for a particular binder type may have some variability associated with it, which might have resulted in some error.
3. Field aging conditions used in the viscosity prediction were obtained from the LTPP database *DATAPAVE*. Though this database is fairly accurate, any error in the reported values can cause errors in the perdition.

It is probably reasonable to conclude that if more accurate input data were available the comparison depicted in Figure 113 would have been better. It is also reasonable to expect that when future applications of this revised PP1 ensue, the actual un-aged binder would be available and the RTFO viscosity could be measured directly rather than estimated, as was done for the data points in Figure 113. Furthermore, in future applications, the values of VA_{orig} (original mix air-voids) would generally be known more accurately than the DATAPAVE values which had to be used for Figure 113. In view of these considerations, it can be concluded that equation 7.1 gives a good estimate of the required PAV aging temperature, for all practical purposes.

Table 31
DSR Results from LTPP Field-Cores

Temperature (C)	log T (R)	Core – 1		Core –2		Average	
		Viscosity (Pas)	loglogVisc (cP)	Viscosity (Pas)	loglogVisc (cP)	Viscosity (Pas)	loglogVisc (cP)
Groton, Connecticut							
45	2.757927	10594	0.84665	-	-	-	-
65	2.784403	745.08	0.7688011	-	-	-	-
85	2.809358	70.605	0.6856374	-	-	-	-
Charlotte, Vermont							
45	2.757927	5519.6	0.8287828	6304.5	0.832487	5912.05	0.8307
65	2.784403	441.94	0.7516919	501.8	0.755915	471.87	0.753876
85	2.809358	54.831	0.6756891	52.774	0.674165	53.8025	0.674935
Big Timber, Montana							
45	2.757927	2893.6	0.8103292	2915.1	0.810545	2904.35	0.810437
65	2.784403	342.21	0.7430621	378.77	0.746508	360.49	0.744832
85	2.809358	61.629	0.680316	72.828	0.686842	67.2285	0.683727
Ranchester, Wyoming							
45	2.757927	6145.6	0.8317779	6285.5	0.832403	6215.55	0.832092
65	2.784403	423.52	0.7502672	411.59	0.749308	417.555	0.749791
85	2.809358	54.352	0.6753398	52.872	0.674239	53.612	0.674793
Gillette, Wyoming							
45	2.757927	88055	0.9000805	81932	0.898366	84993.5	0.89924
65	2.784403	4406.4	0.8224351	3599.9	0.816658	4003.15	0.819702
85	2.809358	266.29	0.7344281	201.43	0.724614	233.86	0.72989
Aurora, Colorado							
45	2.757927	26941	0.871013	22378	0.866277	24659.5	0.868761
65	2.784403	1395.7	0.7885072	1143.4	0.782343	1269.55	0.78559
85	2.809358	102.16	0.6997754	84.203	0.692435	93.1815	0.696298
Delta, Colorado							
45	2.757927	2890.3	0.8102959	2949.9	0.810891	2920.1	0.810595
65	2.784403	373.11	0.7459984	393.91	0.747831	383.51	0.746928
85	2.809358	75.048	0.6880048	71.554	0.686156	73.301	0.687093
Pullman, Washington							
45	2.757927	8284.6	0.8399976	10251	0.845765	9267.8	0.843044
65	2.784403	480.11	0.7544508	594.93	0.761512	537.52	0.758185
85	2.809358	43.835	0.6666884	60.422	0.679536	52.1285	0.673673

- Data Not Available

Table 32
Field-Aged Viscosity of the Cores at 60ºC

Site	Field Aged loglog Viscosity (cP) at 60ºC
Groton	0.7854999480
Charlotte	0.7710824605
Big Timber	0.7609482971
Ranchester	0.7703997446
Gillette	0.8357747727
Aurora	0.8034874155
Delta	0.7624691751
Pullman	0.7780077310

Table 33
Binder Grade and RTFO Viscosity of the LTPP Binders at 60ºC

Site	Binder Grade	A	VTS	RTFO loglog Viscosity (cP) at 60ºC
Groton	AC-20	-3.6017	10.7709	0.7656149363
Charlotte	AC 85/100	-3.6210	10.8232	0.7643008092
Big Timber	AC 85/100	-3.6210	10.8232	0.7643008092
Ranchester	AC-20	-3.6017	10.7709	0.7656149363
Gillette	AC-20	-3.6017	10.7709	0.7656149363
Aurora	AC-10	-3.6954	11.0134	0.7478225159
Delta	AC-10	-3.6954	11.0134	0.7478225159
Pullman	AC-5	-3.7914	11.2614	0.7291408472

Table 34
Field Aging Conditions

Site	Age (years)	*MAAT* (F)	Air Voids (%)
Groton	17	51.3	3.1
Charlotte	11	46.5	4.0
Big Timber	11	43.6	4.8
Ranchester	17	45.7	7.8
Gillette	6	48.1	8.7
Aurora	37	50.6	4.0
Delta	18	48.0	3.5
Pullman	3	47.6	3.8

Table 35
Predicted PAV Aging Temperature Required to Simulate Field Aging

Site	Predicted PAV Temperature required (ºC)
Groton	73
Charlotte	76
Big Timber	80
Ranchester	100
Gillette	97
Aurora	85
Delta	76
Pullman	69

Table 36
Predicted Aged Viscosities at 60ºC Corresponding to the Estimated T_{PAV}

Site	PAV Aging Temperature required (ºC)	Predicted loglog Viscosity (cP) @ 60ºC
Groton	73	0.7859256492
Charlotte	75	0.7866115104
Big Timber	79	0.7897314989
Ranchester	98	0.8127876961
Gillette	95	0.8096813506
Aurora	84	0.7792779613
Delta	76	0.7710335785
Pullman	69	0.7483568454

Table 37
Comparison of Predicted and Measured Viscosities at 60ºC

Site	Measured loglog Viscosity (cP) @ 65ºC	Predicted loglog Viscosity (cP) @ 65ºC
Groton	0.7854999480	0.7859256492
Charlotte	0.7710824605	0.7866115104
Big Timber	0.7609482971	0.7897314989
Ranchester	0.7703997446	0.8127876961
Gillette	0.8357747727	0.8096813506
Aurora	0.8034874155	0.7792779613
Delta	0.7624691751	0.7710335785
Pullman	0.7780077310	0.7483568454

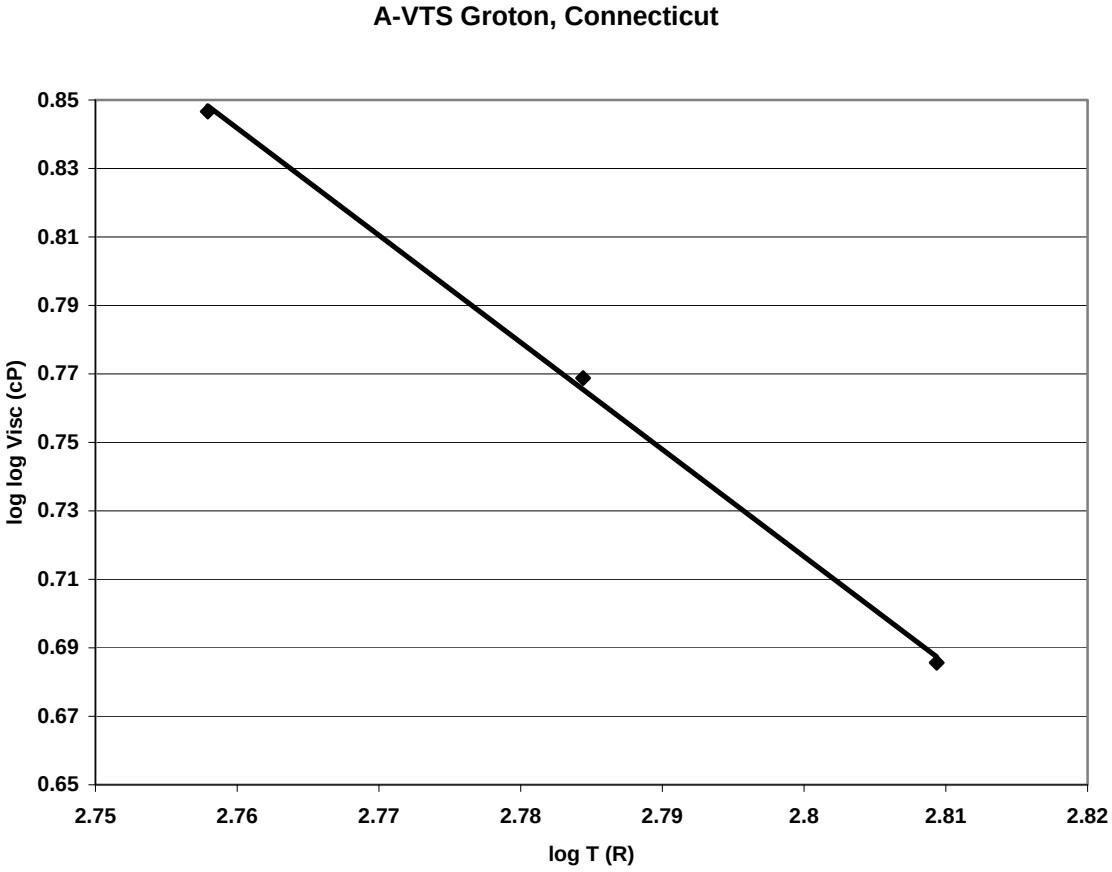

Figure 104
A-VTS Plot for Groton, Connecticut Field Core

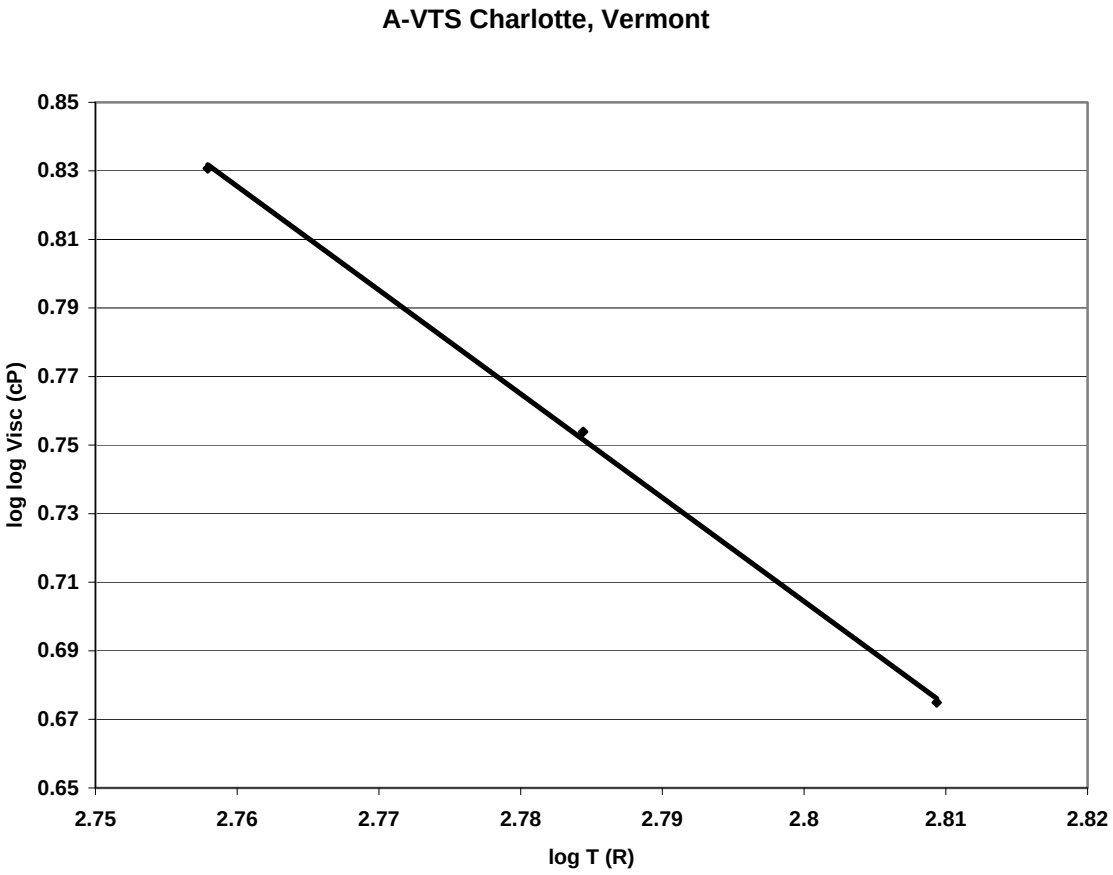

Figure 105
A-VTS Plot for Charlotte, Vermont Field Core

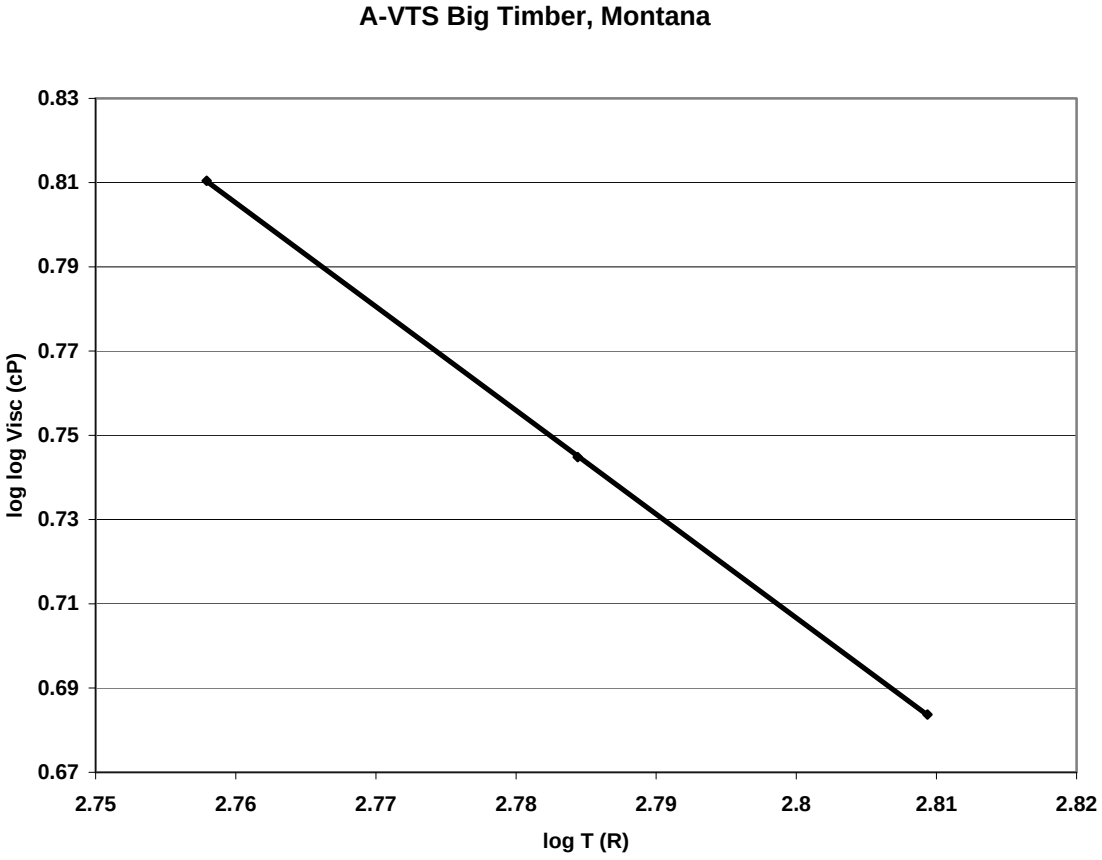

Figure 106
A-VTS Plot for Big Timber, Montana Field Core

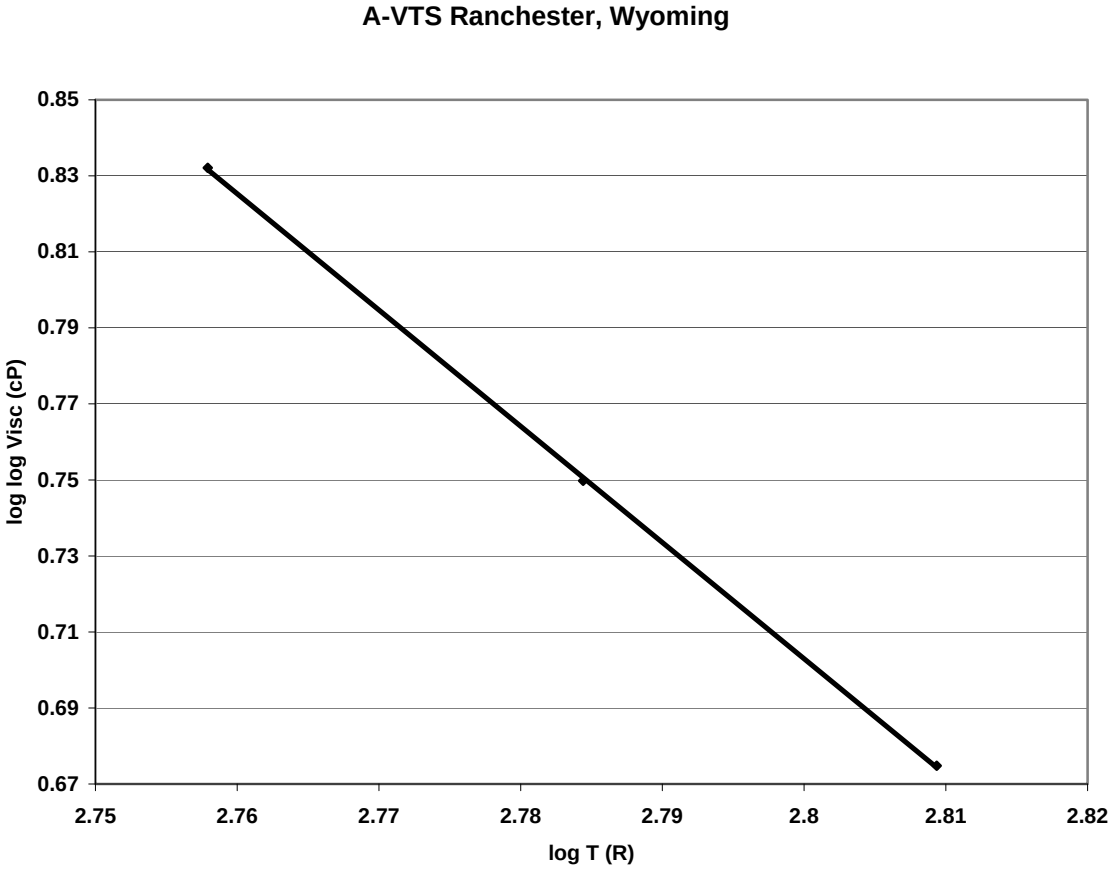

Figure 107
A-VTS Plot for Ranchester, Wyoming Field Core

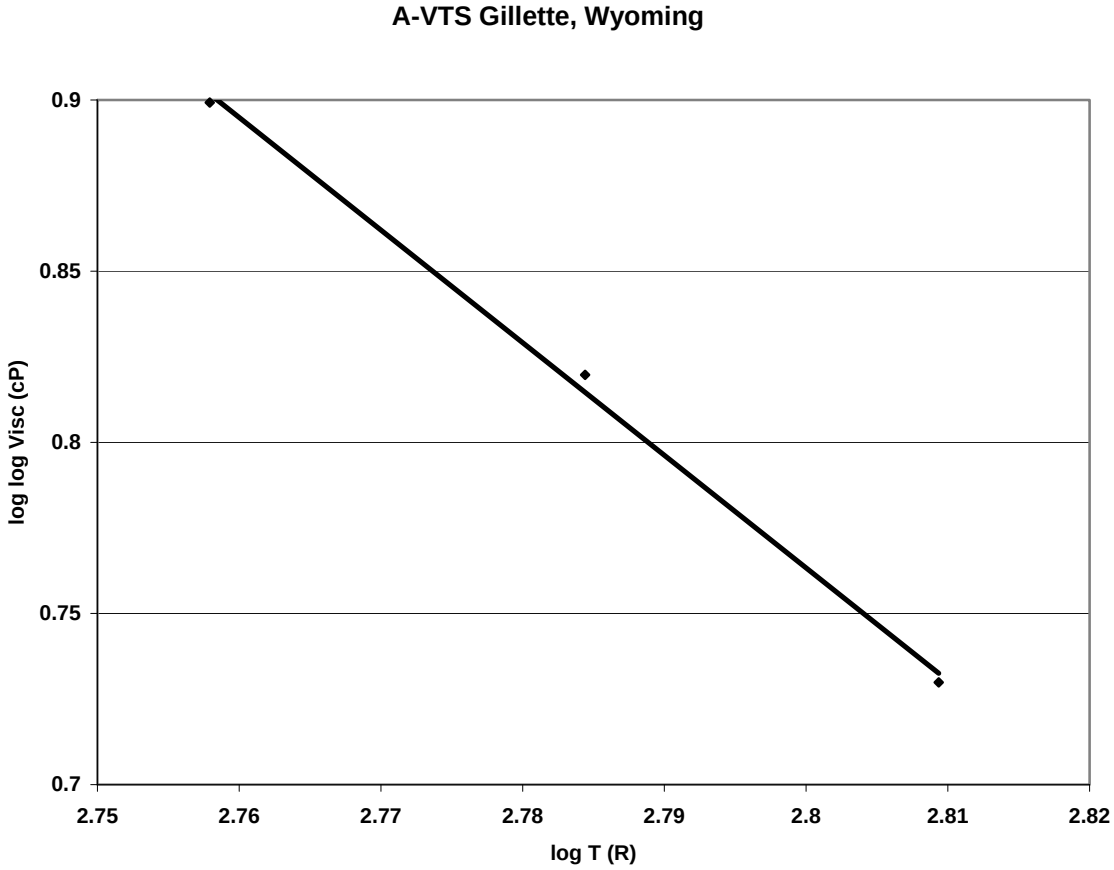

Figure 108
A-VTS Plot for Gillette, Wyoming Field Core

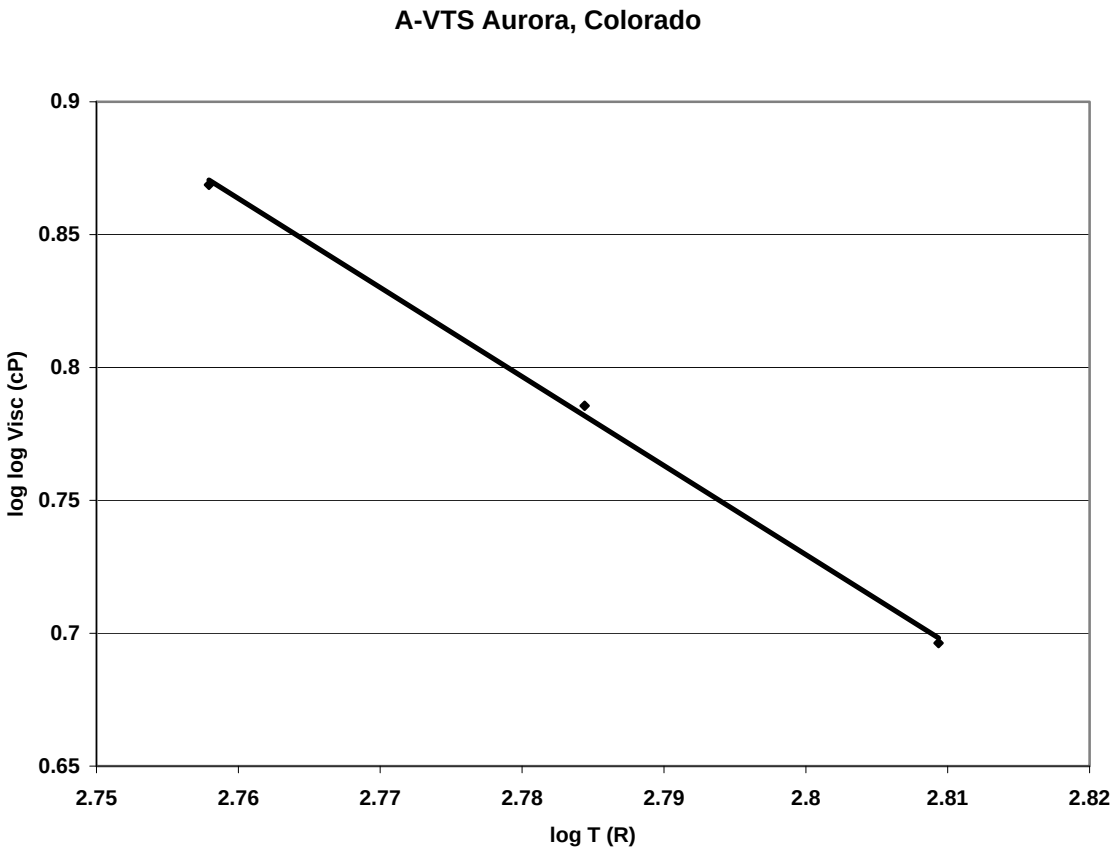

Figure 109
A-VTS Plot for Aurora, Colorado Field Core

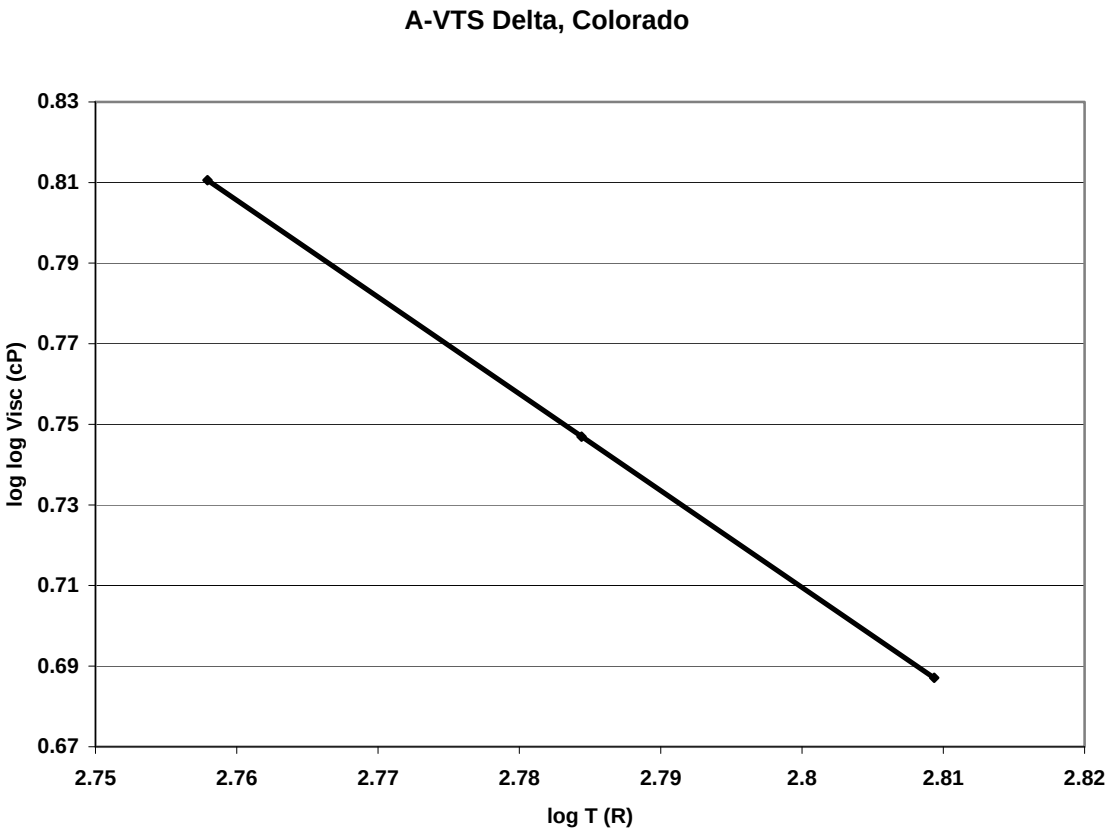

Figure 110
A-VTS Plot for Delta, Colorado Field Core

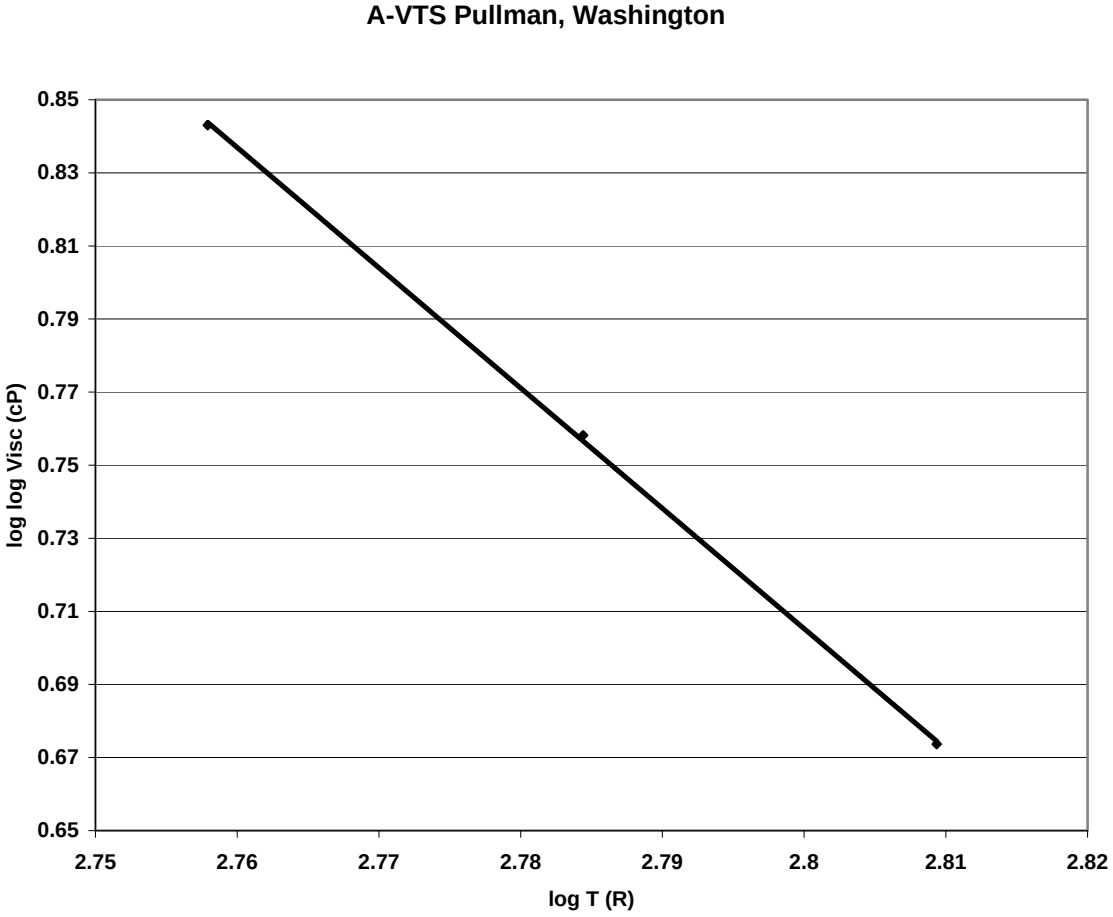

Figure 111
A-VTS Plot for Pullman, Washington Field Core

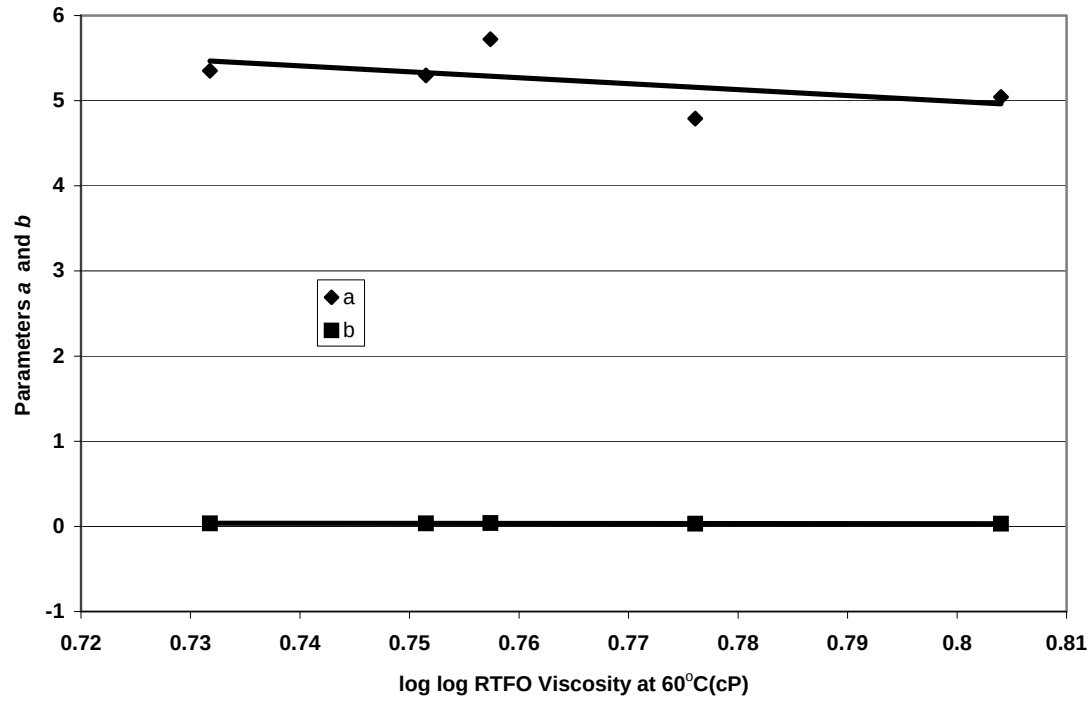

Figure 112
Plot of Parameters *a* and *b* vs. $\eta_{RTFO,\ 60°C}$

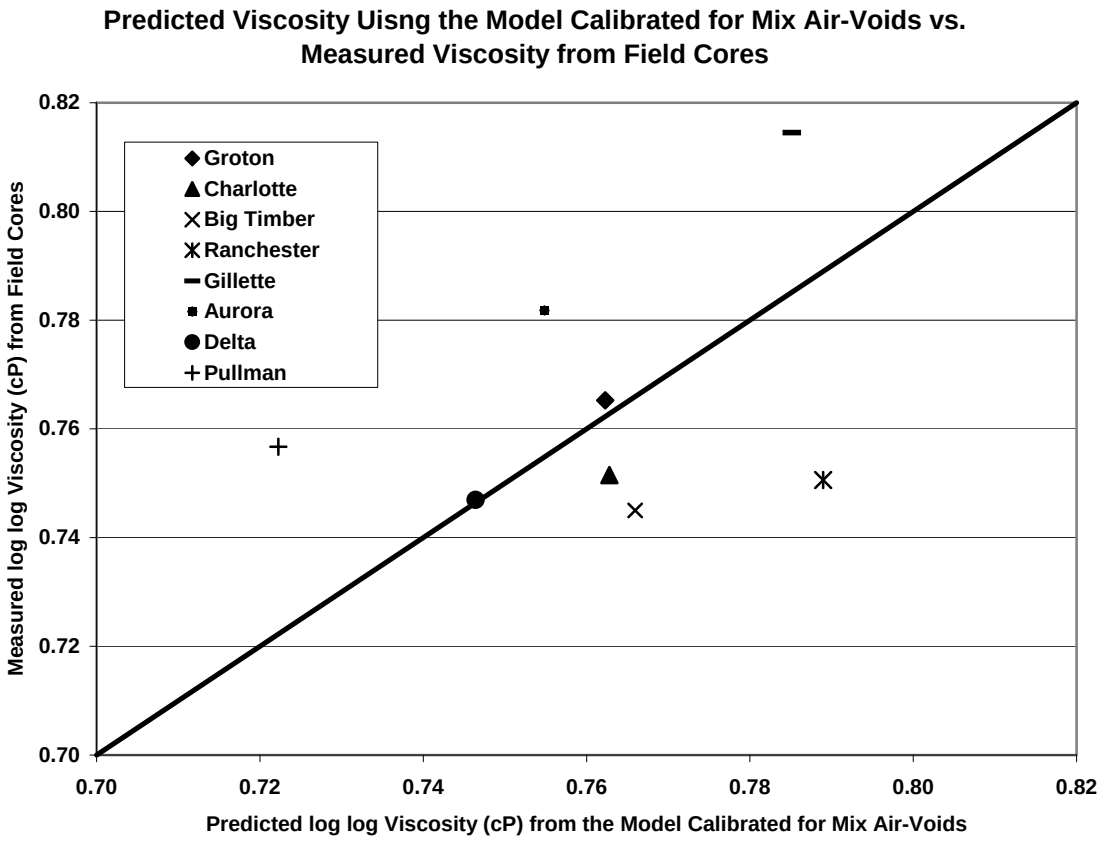

Figure 113
Comparison Plot of Predicted vs. Measured Viscosities at 60ºC

CHAPTER 8

PARAMETRIC STUDY OF THE EXPANDED PP1 EQUATION

INTRODUCTION

The PP1 Equation (equation 6.8) developed in *Chapter 6* was considered to be the final model for the PP1. The current chapter deals with the parametric study of all the parameters involved in that equation. In this chapter, a matrix covering the possible range of input values were used to generate the output, PAV aging temperature. Depending on the output generated, the limitations or constraints on the input parameters were determined.

INPUT MATRIX

Table 38 shows the matrix of input parameters covering the possible range of input values.

PP1 EQUATION

$$T_{PAV} = \left\{ \begin{array}{l} \left(2.132432 + 0.193560 \times \left(\log\log \eta_{RTFO,60^oC}\right)^2 \times MAAT\right) \times \ln(t_{aging}) \\ +109.9632 - 78.2945 \times \left(\log\log \eta_{RTFO,60^oC}\right)^2 \end{array} \right\} \times \left(0.445445 \times VA_{orig}^{\ 0.378370}\right) \quad (8.1)$$

CASE 1: INFLUENCE OF AIR-VOIDS

In this case, the effect of air-voids on the PP1 equation (equation 8.1) was studied. Varying the initial air-voids and keeping the other two parameters constant, the required PAV aging temperature was predicted. The *MAAT* was maintained constant at 55ºF and the binder type selected was AC-20. Air-void values of 3%, 7%, or 10% were input to the PP1 equation (equation 8.1) to predict the PAV aging temperature required to simulate various periods of field aging. The outputs obtained are shown in Figure 114.

It could be observed from Figure 114 that the predicted PAV aging temperature increased with the increase in initial air-voids. This is in agreement with previous theoretical finding that show that higher initial air-voids facilitate higher aging. Therefore, to simulate this higher aging, higher PAV aging temperature is required.

CASE 2: INFLUENCE OF *MAAT*

In this case, the effect of *MAAT* on the PP1 equation (equation 8.1) was studied. Varying the *MAAT* and keeping the other two parameters constant, the required PAV aging temperature was predicted. The initial air-voids value was maintained constant at 7% and the binder type selected was AC-20. Varying *MAAT* value of 40ºF, 55ºF or 70ºF was

input to the PP1 equation (equation 8.1) to predict the PAV aging temperature required to simulate various periods of field aging. The outputs obtained are plotted in Figure 115.

It could be observed from Figure 115 that the predicted PAV aging temperature increased with the increase in *MAAT*. This is in agreement with previous theoretical findings that show that higher *MAAT*s facilitate higher aging. Therefore, to simulate this higher aging, higher PAV aging temperature is required.

CASE 3: INFLUENCE OF BINDER TYPE

In this case, the effect of binder type on the PP1 equation (equation 8.1) was studied. Varying the binder type and keeping the other two parameters constant, the required PAV aging temperature was predicted. The initial air-voids value was maintained constant at 7% and the *MAAT* was maintained at 55ºF. Viscosities corresponding to varying binder types of AC-5, AC-10, AC-20, AC-30, and AC-40 were input to the PP1 equation (equation 8.1) to predict the PAV aging temperature required to simulate various periods of field aging. The outputs obtained are plotted in Figure 116.

It could be observed from Figure 116 that the predicted PAV aging temperature increased with the decrease in binder stiffness. This is in agreement with previous theoretical findings which agrees that under a given set of aging conditions, softer binders undergo higher aging than the harder binders. Therefore, to simulate this higher aging, higher PAV aging temperature is required. It was also observed that the aged viscosity of the stiffer binders remained higher than the aged viscosity of the softer binders at any given aging period. Figure 117 shows the plot of aged viscosity, corresponding to predicted PAV aging temperature vs. aging time.

Furthermore, the range of predicted PAV aging temperatures obtained by changing the binder type was smaller compared to the range of predicted PAV aging temperatures obtained by changing the other two parameters. This phenomenon was presumed to be caused by the interaction between the selection of binder type and the *MAAT* in the field. Therefore, the combined influence of binder type and *MAAT* on the PP1 equation was also considered.

CASE 4: COMBINED INFLUENCE OF BINDER TYPE AND *MAAT*

In this case, the combined effect of binder type and *MAAT* on the PP1 equation (equation 8.1) was studied. Varying the binder type, and *MAAT* simultaneously and keeping the air-voids constant, the required PAV aging temperature was predicted. The initial air-voids value was maintained constant at 7%. Viscosities corresponding to varying binder types of AC-5, AC-10, AC-20, AC-30, and AC-40 and *MAAT*s of 40ºF, 55ºF, or 70ºF were inputted into the PP1 equation (equation 8.1) to predict the PAV aging temperature required to simulate various periods of field aging. The outputs obtained are plotted in Figure 118.

It could be observed from Figure 118 that the range of the predicted PAV aging temperatures increased due to the combined effect of binder type and *MAAT*. The results show the right trends as observed in the field.

It can be concluded that the PAV aging temperatures predicted by the PP1 equation (Equation 8.1) follows the right trends and no limitations or constraints to the input parameters are deem necessary at this point.

Table 38
Matrix of Input Values

Case No.	Original Air Voids (%)	*MAAT* (F)	Binder Type
1	3	55	AC-20
	7		
	10		
2	7	40	AC-20
		55	
		70	
3	7	55	AC - 05
			AC - 10
			AC - 20
			AC - 30
			AC - 40
4	7	40	AC - 05
			AC - 10
		55	AC - 20
		70	AC - 30
			AC - 40

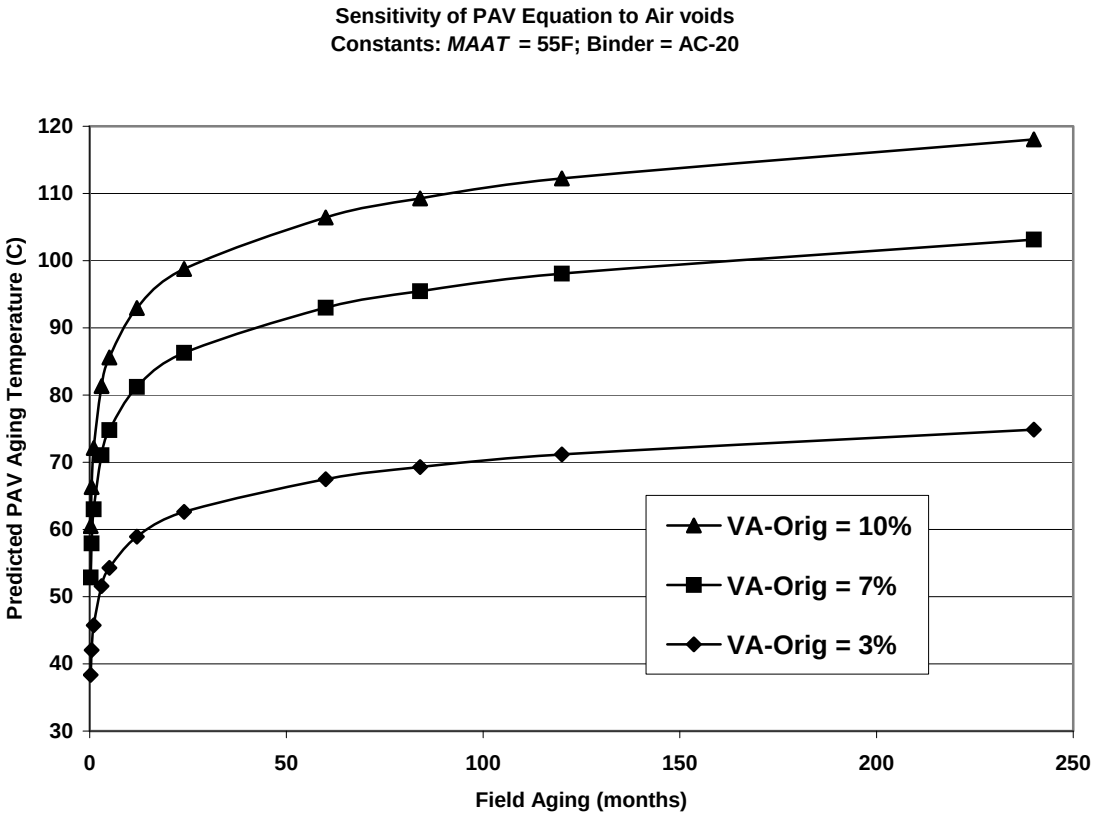

Figure 114
Predicted PAV Aging Temperature with Varying Air-Voids, and Constant *MAAT* and Binder Type

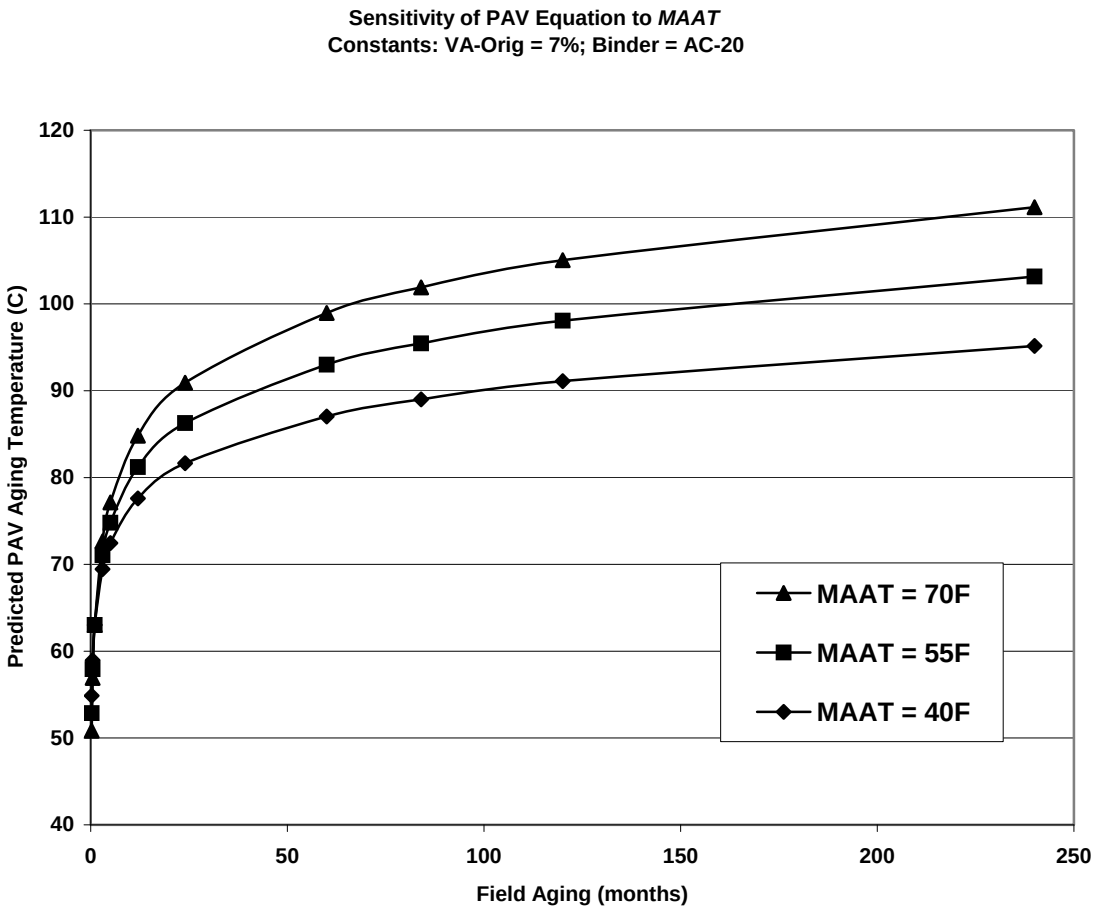

Figure 115
Predicted PAV Aging Temperature with Varying *MAAT*s, and Constant Initial Air-Voids and Binder Type

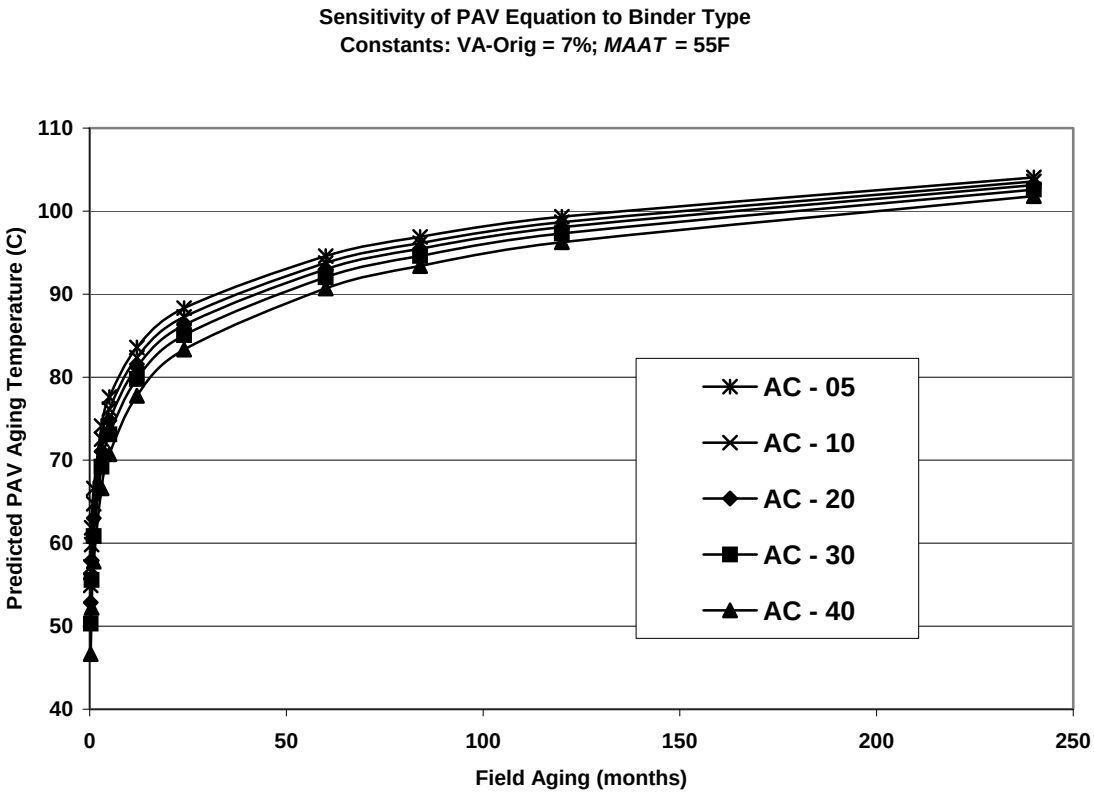

Figure 116
Predicted PAV Aging Temperature with Varying Binder Types, and Constant Initial Air-Voids and *MAAT*

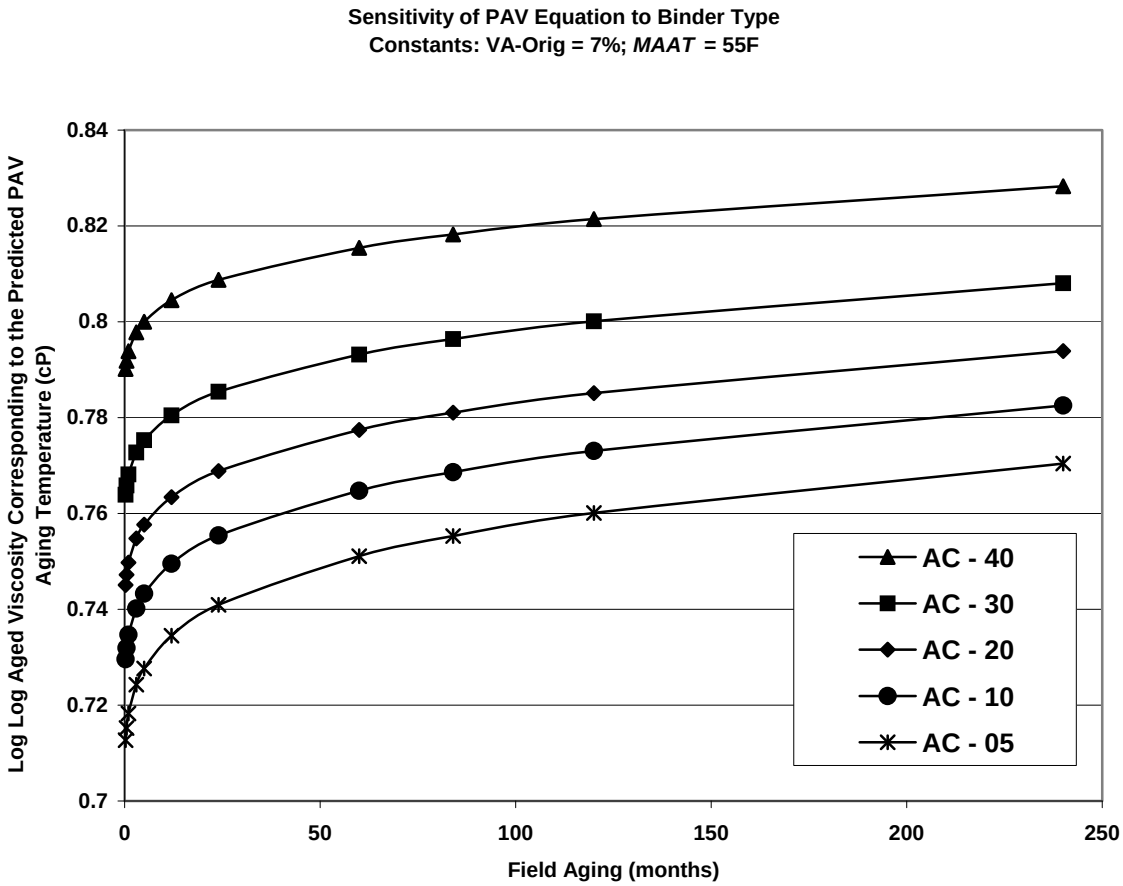

Figure 117
Aged Viscosities Corresponding to Predicted PAV Aging Temperature with Varying Binder Types, and Constant Initial Air-Voids and *MAAT*

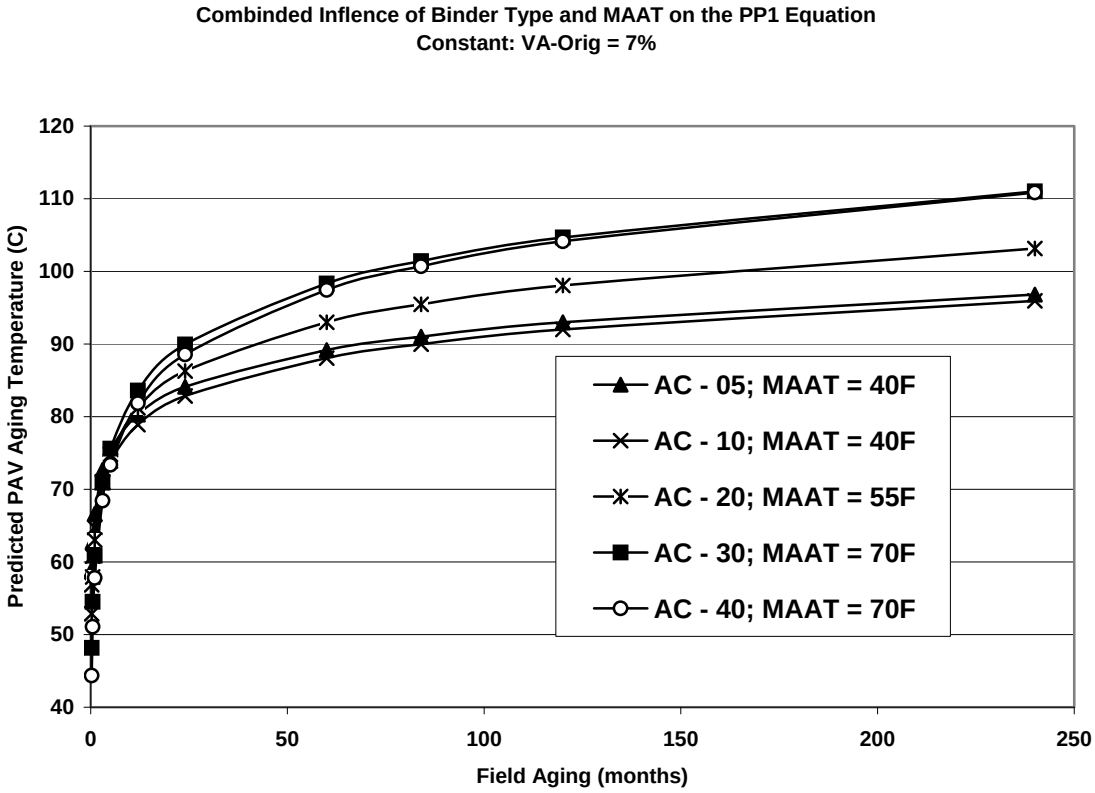

Figure 118
Predicted PAV Aging Temperature with Varying Binder Types and *MAAT*, and Constant Initial Air-Voids

CHAPTER 9

CONCLUSIONS AND RECOMMENDATIONS FOR FUTURE RESEARCH ON PP1 PROTOCOL

This chapter summarizes the conclusions from the chapters related to the PP1-98 Protocol discussed earlier and lists the recommendations for future research.

CONCLUSIONS

Correction Factor for Binder Recovery

- For all practical purposes, there is no significant difference between the viscosities of original and recovered binders. In other words, the particular recovery procedure employed had no significant effect on viscosity.
- Therefore, a correction factor to the recovered binder viscosity is not necessary, or can be construed as one.

Verification of PP1-98 Protocol

- Binder grade (stiffness), *MAAT* and mix air voids are important factors to be considered when deciding the PAV aging temperature required to produce a PAV-aged binder with the same viscosity as a field-aged binder.
- The existing PP1-98 Protocol should be expanded to include the effects of field aging conditions and differences in volumetric properties.
- The field aging simulated by the existing protocol needs to be improved to give a more specific period of aging.
- Other PAV aging conditions such as aging time (currently 20 hours) and pressure (currently 2.1MPa) might be altered to simulate the aging in the field at various mix air-voids and *MAAT*s. Alterations to these conditions were not accomplished in this study.

Calibration of the Expanded PP1 Model with Field Data

- PP1 equation (equation 6.7) appears to give sufficiently accurate prediction of the required PAV aging temperature for all practical purposes and should be seriously considered as an Addendum to the PP1-98 Protocol.

Validation of the Expanded PP1 Model with Field Data

- The required PAV aging temperatures predicted by the PP1 equation (equation 6.7) using actual field-aging conditions were within a reasonable range of values.
- Higher *MAAT*, air voids and aging times resulted in higher PAV aging temperatures.
- The PP1 equation (equation 6.7) yields satisfactory results. This model should be considered to be adequately validated and the new equation (model) should be seriously considered as an Addendum to the PP1-98 Protocol.

Parametric Study of the Expanded PP1 Equation

- The PP1 equation (equation 8.1) has no significant limitations or constraints to be applied to the input values.

RECOMMENDATIONS FOR FUTURE WORK

- Further refinement of the PP1 equation (equation 8.1) can to be accomplished using data from more field sites. If they can be found, it would be preferable to use sites where the RTFO viscosity values were available.
- It was found in this research study that aged viscosity with depth remains more or less constant and the differences found are not significant for practical purposes. This result was unexpected and more research should be conducted to discover the reasons for this outcome.

RECOMMENDATIONS FOR THE IMPLEMENTATION OF THE PP1 MODEL

PP1 equation (equation 6.7) yields a continuum of PAV temperatures. To the best of the knowledge of the research team, existing PAV chambers operate at only 90ºC, 100ºC, and 110ºC. This discrepancy could possibly be solved with one of the following four approaches.

1. Modify existing PAV chambers to yield a wider range of controlled temperatures.
2. Utilize a new generation of PAV chambers with continuous temperature range, rather than three discrete values.
3. Use equation 6.7 to estimate T_{PAV} and then choose the standard temperature (90, 100, or 110ºC), which is closest to the calculated T_{PAV}.
4. The PP1 Protocol will, in general, be used in a predictive mode. It is assumed that, typically, a user would treat the binder in the PAV, measure the ensuing viscosity, and then infer future, aged modulus for a given binder, original air-voids, *MAAT*, and desired field aging time. In this context, the field aging time is usually chosen somewhat arbitrarily. Thus equation 6.7 could either be inverted or used in a trial and error mode to find a field aging time which corresponds to one or more of the following: T_{PAV} = 90, 100, or 110ºC. The inverted form of the equation is shown below.

$$t_{aging} = \exp\left(\frac{\left(\frac{T_{PAV}}{0.445445 \times VA_{orig}^{\ 0.378370}}\right) - 109.9632 + 78.2945 \times \left(\log\log \eta_{RTFO,60^oC}\right)^2}{2.132432 + 0.193560 \times \left(\log\log \eta_{RTFO,60^oC}\right)^2 \times MAAT}\right) \quad (9.1)$$

RECOMMENDED PROVISIONAL PROTOCOL

In order to demonstrate the implementation of the expanded protocol, ten cities representing various climatic regions within the United States were chosen. *MAAT* for these cities were obtained from the *Mechanistic-Empirical Pavement Design Guide*. An original air-voids value of 8% was used in all cases. Typical binder grades were selected based on the maximum and minimum temperatures prevalent in the cities using *LTPPBIND V2.1* (*13*). Using the A-VTS values obtained from the *Mechanistic-Empirical Pavement Design Guide* corresponding to the selected binder PG, RTFO viscosities of the binders were calculated. Using these input values in the PP1 equation developed at 60ºC, the PAV aging temperatures required to simulate 5, 10, 15, and 20 years of aging were predicted. Also, using the inverted PP1 equation (equation 9.1), the field aging time in months simulated by PAV aging temperatures of 90, 100 and 110ºC were estimated. Based on the predictions, a recommended provisional protocol was developed. . Tables 39 to 41 present the summary of the predictions. Table 42 shows the recommended provisional protocol.

Table 39
Summary of Input Data Used in the Prediction

City	*MAAT* (F)	VA_{orig} (%)	Binder PG	loglog RTFO Viscosity cP @ 60°C
Barrow, AK	12.2	8	46 - 46	0.6851
Fargo, ND	42.7	8	58 - 34	0.7289
Billings, MT	47.7	8	58 - 34	0.7289
Chicago, IL	52.8	8	58 - 28	0.7289
Washington D.C	55.2	8	64 - 22	0.7572
San Francisco, CA	56.8	8	58 - 10	0.7265
Oklahoma City, OK	60.6	8	64 - 16	0.7577
Dallas, TX	66.7	8	64 - 16	0.7577
Las Vegas, NV	68.9	8	70 - 10	0.7839
Phoenix, AZ	74.4	8	76 - 16	0.8061

Table 40
Predicted PAV Aging Temperatures

PAV Aging Temperature (°C)			
5 years	10 years	15 years	20 years
85	87	88	89
93	97	100	102
95	100	103	105
97	102	105	107
97	102	106	108
99	104	107	110
99	105	109	111
102	108	112	115
102	109	113	116
104	112	116	119

Table 41
Estimated Field Aging Times

Field Aging Time (months)		
PAV 90	**PAV 100**	**PAV 110**
328	7671	179561
37	179	860
29	123	524
23	88	340
26	90	310
19	69	250
21	66	210
17	49	144
19	50	134
18	43	104

Table 42
Recommended Provisional Protocol

Site	*MAAT* (F)	Recommended PAV Aging Temperature (^{o}C)			
		5 years	10 years	15 years	20 years
Barrow, AK	12.2	85	85	90	90
Fargo, ND	42.7	95	95	100	100
Billings, MT	47.7	95	100	105	105
Chicago, IL	52.8	95	100	105	105
Washington D.C	55.2	95	100	105	110
San Francisco, CA	56.8	100	105	105	110
Oklahoma City, OK	60.6	100	105	110	110
Dallas, TX	66.7	100	110	110	115
Las Vegas, NV	68.9	100	110	115	115
Phoenix, AZ	74.4	105	110	115	120

CHAPTER 10

VERIFICATION OF PP2-99 PROTOCOL

AASHTO DESIGNATION PP2-99: STANDARD PRACTICE FOR MIXTURE CONDITIONING OF HOT MIX ASPHALT

INTRODUCTION

This practice covers the accelerated aging (oxidation) of asphalt mix by means of elevated temperature. The test method is intended to simulate in-service oxidative aging of asphalt mix. The test provides an estimate of the change in the physical or chemical properties of asphalt mix after five to seven years of in-service aging in the field.

CURRENT CONDITIONS FOR THE PP2-99 PROTOCOL

The standard testing procedure under the existing PP2-99 protocol requires asphalt mix samples to be treated under the following conditions:

- Oven aging time = 5 Days
- Aging temperature = 85°C

APPROACH

The following approach was adopted to verify the existing protocol:

1. Plant mixes were obtained from the field sites.
2. The mix was compacted in the gyratory compactor to obtain gyratory plugs of diameter 6 inches and height 8 inches.
3. The gyratory plugs were cored to obtain cores of diameter 4 inches and height 6 inches.
4. These cores were aged in forced draft oven at three aging temperatures (80°C, 85°C, and 90°C).
5. Complex modulus testing was carried out on the aged cores.
6. Modulus plots were developed using the E* values obtained from the testing.
7. Field cores of varying heights (greater than 6 inches) and 10-inch diameter (6-inch in case of ADOT cores) were obtained from existing pavements.
8. These cores were sub-cored to obtain cores of 4-inch diameter and 6-inch height.
9. Cores were subjected to complex modulus testing to obtain field-aged E* values.
10. These field-aged E* values were compared with the lab-aged E* values.
11. Field aging conditions such as mean annual air temperature (*MAAT*) and aging time were previously known for these cores.
12. Observations and conclusions were made based on the comparison plots.

These steps are explained in detail in the following sections.

MATERIALS USED

In order to verify the PP2-99 protocol, plant mixes and field cores were obtained from the following sites:

Flagstaff, Arizona

Flagstaff site is located on Interstate 40 near Walnut Canyon and is about 12 years old. It has a dense graded mix with 4.1% asphalt by weight.

- Field aging time: 12 years
- Binder type: AC-20
- *MAAT*: 50 °F

Kingman, Arizona

Kingman site is located on Highway 93 near Chloride and is about 9 years old. It has a dense graded mix with 4.5% asphalt by weight.

- Field aging time: 9 years
- Binder type: AC-30
- *MAAT*: 62.6°F

MnRoad, Minnesota

The Minnesota Road Research Project is the world's largest and most comprehensive outdoor pavement laboratory. It is located 40 miles northwest of Minneapolis/St. Paul.

The Cells selected from the MnRoad project were Cells 16, 18 and 21. Cell 16 has 197 mm HMA layer and 711 mm base. Cell 18 has base courses of 229 mm and 305 mm and 197 mm HMA layer. Cell 21 has 67 mm HMA layer and 230 mm base.

- Field aging time: 9 years
- Binder type: AC-20
- *MAAT*: 46.2°F

WesTrack, Nevada

WesTrack is located at Nevada Automotive Test Center (NATC), 60 miles southeast of Reno and 35 miles from Carson City. The climate is dry, no frost penetration, although the LTPP database has catalogued this site as dry and subject to freezing action.

The sections selected in WesTrack were Sections 12, 15 and 16. These sections were designed for 4% 8% and 12% design air voids, respectively. They are of fine and fine-plus gradation type.

- Field aging time: 7 years
- Binder type: AC-20
- *MAAT*: 54.4°F

MINI – STUDY ON COMPACTED SPECIMENS

One of the major issues with regard to the PP2-99 protocol was to further consider the issue of whether aging of the mix should be performed in the loose state or the compacted condition. This is considered a major deviation from the existing protocol, which requires aging the compacted specimen for the determination of the long-term aging of the mix in the field. Because of the much longer oven time required to achieve a given degree of laboratory aging when compacted specimens are oven-treated instead of loose mixes, because of concerns over specimen uniformity and homogeneity, and because of the relatively large mechanical property variation reported in the literature when the aging is carried out on compacted specimens, it was initially decided to age the mixes in the loose condition. The long-term properties are then obtained by compacting the aged mix. The merits of this aspect of the plan were debated extensively between the panel and the research team, and, indeed, within the research team.

It is relevant to the debate to cite certain important factors, including the shift from the SST (simple shear test) to the Complex Modulus test (E*). The Complex Modulus requires a much taller specimen compared to the SST device. This much larger specimen requires much longer oven treating to achieve a given degree of aging, perhaps by as much as a factor of 5 to 10. Likewise, the gradients in degree of aging within the E* specimen are likely to be somewhat greater than in the SST specimen. Testing a non-uniform specimen complicates the interpretation of Complex Modulus testing, which typically utilizes relatively uniform specimens.

A mini-study on compacted specimens was carried out in the ASU laboratories in an effort to provide data that would help to move this debate off of dead center. The findings are reported in this section.

In connection with the PP2-99 protocol, the plant mix should be aged in the forced draft oven at different temperatures and aging times. The research team had initially proposed that the long-term aging be conducted on loose mixes instead of compacted specimens as recommended in the current protocol developed under the SHRP program. The PP2-99 protocol, originally developed for the SST evaluation on specimen sizes 4" to 6" in diameter and 1 ½" to 2" thick is not likely to be applicable or appropriate for the larger E* specimens. Therefore, it was envisioned that long-term aging would be more meaningful and easily interpreted if performed on loose mixes; furthermore, and more importantly, it would be much faster.

During the course of the project, the panel recommended further study of the aging of compacted specimens, before embarking on the aging of loose mixes. Following the panel discussion, an experimental study was executed to evaluate the feasibility using compacted gyratory specimens, compacted first and then aged in the forced draft oven and then used in the evaluation of the E* response of AC mixtures.

The following testing sequence was carried out to provide additional data relative to the use of specimens compacted prior to aging.

1. Section # 12 from WesTrack site was selected as a candidate mix. A total of six specimens were prepared using the gyratory compactor. All of the specimens were compacted at the construction air voids level.
2. The gyratory compacted specimens were aged at 1, 5, and 10 days in the forced draft oven at 85°C. Each condition had one replicate resulting in a total of 6 specimens.
3. Immediately after compaction, the height of the specimen was measured to quantify the slump during the oven aging process of the compacted specimen. The slump measurements are shown in Table 43. As it can be observed in Table 43, the value of slump increased with increased in aging time, thereby possibly/probably changing the air voids in the specimen. Possibly even more important than any change in the air voids is the substantial strains associated with slumping, which are occurring in an essentially unconfined condition and therefore represent "specimen disturbance".
4. The gyratory plugs were then cored to obtain 4-inch diameter specimens for the complex modulus testing.
5. Complex modulus testing was carried out on all the six plugs. The tests were conducted at two temperatures: 70° F and 130° F. The results of the complex modulus tests are shown in Figure 119.
6. An indication of the aging profile of the binder within the specimen was obtained by extracting the binder from the following portions as shown in the sketch below:

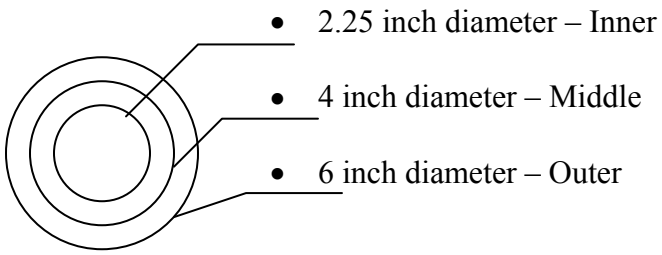

The above configuration was used to obtain the viscosity profile in the radial direction. In order to quantify the viscosity profile in the vertical direction, the inside core (2.25 inch in diameter) was sawed into three lifts, as shown below:

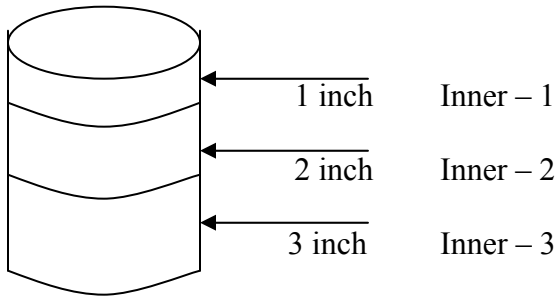

This resulted in a total of five extractions for each specimen to determine the aging profiles in terms of viscosity within each of them.

As stated earlier, two specimens were prepared for each aging condition. The aging conditions were 1, 5 and 10 days at 85^{o}C and were carried out in a forced draft oven. Each specimen was then sawed into segments to study the viscosity profile within the specimen. Because sufficient

material for binder extraction and recovery could not be obtained from each segment of the specimen, the corresponding segments from the two specimens were combined for binder extraction and recovery. This resulted in a single extraction and recovery at each aging condition. The DSR testing on the extracted binder was carried out at 25, 45, 65 and 85°C.

The results obtained are summarized below:

1. Figure 120 shows the results of the binder viscosity obtained using the DSR versus the aging time in days. Figures 120(a) through 120(d) show the radial variation within the specimen at 25, 45, 65, and 85°C respectively. It can be observed that generally the outer shell aged faster than the middle and inner portions.
2. No definite conclusion could be made with regards to the variation between the aging that occurs in the middle and inner cores of the specimen. The variation between these two radial locations seemed to be random and no consistent trend was observed. It was concluded that the radial variation between the middle and the inner core was not significant.
3. Figures 121(a) through 121(d) show the vertical profile or viscosity variation within the specimen at 25, 45, 65, and 85°C respectively. The maximum variation was observed at day five aging when compared to the variation at day one and day ten. The results at day one were as expected since no significant aging occurs initially; however, the results at day ten had no logical explanation. Decrease in stiffness is not possible from day five to day ten, and could only be explained by random variation of the test results.
4. Figure 122 shows the percent difference between the viscosities obtained on the outer shell and the middle shell. It can be observed that the maximum difference occurred at day five. This result was expected since not much aging had occurred at day one.
5. Figure 123 shows the percent difference in the DSR results between the middle and the inner cores at the four temperatures. Lesser percent difference was observed compared to Figure 122 for all temperatures and aging times.
6. Finally, Figure 124 shows the percent difference in the vertical profile. The two locations that were compared were inner 1 and inner 2. These were compared since they provided the maximum difference in the vertical direction. It was observed that the difference was as high as 30%.

Based upon the data obtained, it was concluded that some measurable difference in horizontal and vertical aging profile existed, if the aging was carried out on compacted specimens. The aging profile in the vertical direction was found to be more significant than the horizontal profile.

The results of the DSR testing on the aged binder are shown in Table 44.

LABORATORY AGING

The plant mixes obtained were heated to the appropriate compaction temperature. The heated mix was compacted using a gyratory compactor. Gyratory plugs were prepared making sure to achieve the in-situ air voids. In total 54 plugs were compacted: (3 Sites x 3 Sections x 3 Aging conditions x 2 replicates). The gyratory plugs were of 6-inch diameter and 8-inch height. These plugs were allowed to cool down to room temperature and were cored to obtain E* testing cores of 4-inch diameter and 6-inch height.

The aging was done on the 4-inch by 6-inch cores. The cores were aged in the forced draft oven at three temperatures (80, 85, 90°C) for 5 days (as per the existing protocol).

To avoid or minimize the slump that was observed when the samples were aged in the forced draft oven for extended periods of time (5 days) various methods such as using sand as a confining medium during aging; drilling holes in a plastic cylinder and aging the samples confined in those cylinders; and using chicken wire mesh jackets with 3 clamps fastened around the top, middle and bottom of the core, were discussed and tested.

The use of the chicken wire mesh was found to be the most practical of all, to the point that it demonstrated the elimination of the slump almost completely, with an average value of less than 1 mm. Table 45 presents the height measurements taken at 6 different places on the core before and after the aging process. As a result, the slump observed was considered to be negligible.

Test cores were wrapped in wire mesh. Three steel clamps were used to hold the mesh in place. This method facilitated the highest amount of air circulation (more than 90% of the surface area being exposed) without allowing for any slump. The cores were then aged in the forced draft oven for 5 days at 80˚C, 85˚C and 90˚C. Figure 125 shows the encasing of cores in wire mesh and clamps.

COMPLEX MODULUS E* TESTING ON LABORATORY AGED CORES

Complex modulus testing was conducted on the aged cores. Figures 126 to 134 show the plots of complex modulus vs. frequency of loading obtained from the complex modulus testing.

COMPLEX MODULUS E* TESTING ON FIELD CORES

The field cores obtained were of 10-inch diameter (6 inches in case of ADOT cores) and of varying heights exceeding 6 inches. From these cores, sub-cores of 4-inch diameter and 6-inch height were cored. Complex modulus testing was conducted on three cores taken from each site. Two of these cores were used for the E* testing. This resulted in one replicate for each E* testing on the field-aged cores.

The E* test results on the field-aged cores were plotted on the plots obtained from the lab-aged cores for comparison. Figures 135 to 142 show the E* comparison plots of field-aged and lab-aged cores.

ANALYSIS AND CONCLUSIONS

Discussion on the Mini – Study on Compacted Specimens Results

The mini – study on compacted specimens work was carried out at ASU and LAW Engineering Laboratories and the results obtained indicate that viscosity gradients do exist both in the vertical and the radial directions within the plug, as shown by the data presented. However, these profiles do not show nearly as much gradient in aging profile as was expected by the research team. Nevertheless, significant and measurable non-uniformity is indicated, even though the patterns of variation were not always consistent. Based on the statistical variations observed it was difficult to quantify the gradients with any precision.

The most interesting results to the research team are those shown in Table 43 and Figure 128. To begin with, Figure 119 shows that E* for 5 days aging consistently exceeded E* for 10 days aging. This result is most surprising, given that more aging obviously occurs in 10 days than in 5. The answer to this puzzle lies in Table 43, which shows slump. The large strains associated with 9 mm of slum apparently “softened up” the structural arrangement of the framework of aggregate particles. The "disturbing" effect of the strain on the specimen is heightened by the unconfined state (zero radial normal stress) during slumping. The effect of the slumping had an overriding effect for the 10-day specimens.

Finally, the curves of Figure 119 suggest that at least 5 days, and may be 10 to 15 days, of oven time might be needed to simulate 15 to 20 years of field aging in a warm climate. Added to this oven time is the additional technician time required to prevent slump. These very long times are to be compared to a probable few hours up to perhaps 15 hours for the aging of loose mixes. The long time required for aging compacted specimens means that the (modified) PP2-99 protocol would essentially never be used in a production laboratory, if we compacted first and then aged.

A concern with the prospect of aging loose mixes was raised within the research team, relative to the potential difficulty of compacting specimens with the aged loose mix. It was feared that loose mix aging in the oven would result in hardened coatings on the aggregate, with a net result that higher compaction energy would be required and possible crushing of aggregate might occur and difficulty in achieving the target air voids might occur. Furthermore, there was concern that the hard coatings might lead to an unusual "structure" of the aggregate framework of particles, wherein the aggregate particles rarely actually touched. These concerns turned out to be unfounded because they were based on the tacit assumption that the gyratory compaction would be performed at room temperature. It was subsequently pointed out that room temperature compaction was not necessary, or even appropriate. Current compaction protocols for differing grades of binder call for compaction at different temperatures; with the objective being to bring the viscosities of the binders all to the same target value at the time of compaction. The same would be done for the aged loose mixes in the (modified) PP2-99. The temperature would be elevated so as to target the standard compaction viscosity and the ease of compaction should be comparable to all other mixes, previously aged or not. Likewise, there would be no reason to assume that the "structure" of the aggregate framework would be unusual.

Another issue rose related to the desire to "match field conditions". Although the matching of field conditions is a very common goal in connection with material testing; for the case in hand, it was neither practical nor necessary. Even if it were possible, it would be less convenient and slower to do so. The aspect of matching the field that is being discussed here refers to the profile of modulus with depth and laterally. Although the radial and vertical variations for compacted specimen by the mini-study described above suggested modest but measurable variation in both viscosity and E*, these variations are probably much less than those typically found in the field for vertical profiles. The variation in stiffness with depth in the field is quite pronounced, with the top inch or so showing much, much higher stiffness, which then decreases rapidly with depth. The field profile is no doubt driven heavily by UV attack of the top inch; whereas, the compacted "lab" specimen may have a profile that is driven heavily by simply elevated temperature, with the absence of UV. For the compacted lab specimen the elevated temperature quickly becomes

uniform throughout the test specimen and stays uniform throughout aging. The results of this mini-study and what we know about typical field profiles suggests that the compacted specimen may typically be much more uniform than corresponding elements in the field and perhaps closer to a perfectly uniform specimen than to a "field" element. To the extent that this is true, neither the perfectly uniform specimen nor the compacted-then-aged specimens are good matches for the field profile. Probably the only way to get a very good match for a 15-year-old field profile is to subject an element of our AC to the appropriate temperature history and likewise subject it to 15 years of sunshine and UV. Obviously, this is impractical.

Fortunately, we had chosen to use a different methodology. We used the lab testing to provide a relationship between stress and strain (the modulus) and we evaluated this modulus for a particular time and temperature history. The value of the modulus was considered to be a property and this property was allowed to vary as appropriate as the point of consideration moves through the prototype. Thus the modulus was considered to be the property of a point or a small element, or a small layer. The behavior of a larger non-homogeneous mass in the field is ascertained with a numerical model of some type, which integrates the response of all the small elements, while ensuring compatibility. An example of such a numerical model is the finite element method.

The bottom line of the preceding discussion is that it is not legitimate to be concerned about having the lab test specimen match the heterogeneity of the prototype. This heterogeneity (in the field) gets taken care of later in the analysis when the numerical model is employed. The purpose of the lab test program was to evaluate the relationship between stress and strain (the modulus) and the more homogenous the test specimen was, the easier the test interpretation. In fact, we not only strived to make the test specimen as uniform as possible, we also tried to make the applied stress fields as uniform as possible. One of the advantages the triaxial apparatus enjoys over other types of apparatus is that it has a more nearly uniform stress state than other types of shear loading apparatus.

Summary and Conclusions Relative to the Mode of Aging Issue

Our investigations show that the aging of specimens after compaction entailed two disadvantages:

1. The first was a major, overriding disadvantage in that aging of large compacted E* specimens require much, much more time than the aging of loose mix. Furthermore, steps to prevent slump required considerable more technician time. The test specimens were aged at 89°C (185°C) and the slump was excessive and must be dealt with. If a higher temperature were used – to accelerate the aging – the slump would be worse and would add to these problems. If a lower temperature were used, the time required to simulate field aging would be even more, and it was already excessive.
2. The second disadvantage was that the compacted specimens were somewhat more non-uniform than loose-mix-aged specimens, which complicated data interpretation somewhat. This disadvantage appeared to be only minor to moderate, as the degree of non-uniformity for these compacted-then-aged specimens was much less than what was anticipated by the research team.

By contrast, the loose mix aging plan possesses no disadvantages that could be identified by the research team. Accordingly, the research team recommended to proceed with the aging of loose mix and the subsequent compaction of E* specimens. However, the panel recommendation after analyzing the findings of this mini-study came to the conclusion that the aging should be carried out on the compacted cores.

Summary of Laboratory Aging Results

It was observed from the graphs shown that field-aged E* plotted at different positions relative to the lab-aged E*. However, as listed in the limitations, the existing protocol predicts the same degree of aging for all aging conditions.

It was observed from the ADOT, Flagstaff results that the field value plotted between 80˚C and 85˚C lab values. On the other hand, in case of ADOT, Kingman the field value plotted below 80˚C lab value. This was attributed to differences in aging conditions. Flagstaff field core had undergone 3 more years of aging than Kingman field core. Also, the binder in Flagstaff core was softer than the binder in Kingman core. As a result Flagstaff core had aged to a greater degree than Kingman core.

In case of MnRoad, the field values plotted below the lab-aged values in all the cells. This was attributed to the low *MAAT*. As discussed in the earlier sections of this report, *MAAT* plays an important role in asphalt mix aging.

WesTrack Sections showed higher degree of aging with increase in air-voids. In Section 12 with lowest air-voids (4%), the field-aged E* plotted below the 80˚C lab value. However, in Sections 15 and 16 with air-voids of 8% and 12% respectively, the field value plotted close to the 90˚C lab value.

It was observed from all the plots that the field E* value plotted below the 80˚C lab value, with the exception of WesTrack Sections 15 and 16 (having high mix air-voids). However, the existing protocol specifies 85˚C as the aging temperature.

Based on the above observations, the following conclusions were drawn:

1. PP2-99 protocol cannot be verified in its current condition.
2. Binder grade (stiffness) and mix air voids are important factors to be considered in simulating field aging.
3. Other aging conditions such as oven aging time (currently 5 days) and temperature (currently 85˚C) might be altered to simulate more accurate aging in the field.

Table 43
Slump Measurements

Specimen No.	Original height after gyratory compaction (mm)	Aging time (days)	Final height after oven aging (mm)	Difference in height, slump due to aging (mm)
W1208	170.00	1	168.00	2.00
W1212	170.00		167.00	3.00
W1206	169.98	5	165.00	4.98
W1207	169.72		165.00	4.72
W1210	170.00	10	162.00	8.00
W1211	169.84		161.00	8.84

Table 44
DSR Testing Results on the Aged Binder

Aging Profile with Days of Aging:

10 – Day aging												
Temp ©	Complex Viscosity, (cP)											
	Outer	loglog(V)	Middle	loglog(V)	Inner – 1	loglog(V)	Inner – 2	loglog(V)	Inner – 3	loglog(V)	Avg Inner	loglog(V)
25	379720000	0.93346	334880000	0.930689	300280000	0.928269	342560000	0.93119	327180000	0.930174	323340000	0.929912
45	34616000	0.87733	28946000	0.872831	23126000	0.86712	26729000	0.870812	25939000	0.87005	25264667	0.869379
65	1751000	0.795413	1519800	0.791114	1237700	0.784804	1344300	0.787354	1262400	0.785415	1281466.7	0.785878
85	126810	0.707839	111170	0.702946	87693	0.693988	101480	0.699524	93199	0.696305	94124	0.69668
5 – Day aging												
Temp ©	Complex Viscosity, (cP)											
	Outer	loglog(V)	Middle	loglog(V)	Inner – 1	loglog(V)	Inner – 2	loglog(V)	Inner – 3	loglog(V)	Avg Inner	loglog(V)
25	356700000	0.932083	307540000	0.9288	345520000	0.93138	295270000	0.927895	337910000	0.930888	326233333	0.93011
45	33866000	0.876781	25916000	0.870027	32589000	0.875817	22802000	0.866758	28370000	0.872323	27920333	0.871918
65	1675400	0.794078	1312200	0.786609	1670100	0.793982	1111400	0.781459	1379000	0.788138	1386833.3	0.788312
85	118900	0.705452	104450	0.700609	123690	0.706917	89303	0.694681	104830	0.700746	105941	0.701142
1 – Day aging												
Temp ©	Complex Viscosity, (cP)											
	Outer	loglog(V)	Middle	loglog(V)	Inner – 1	loglog(V)	Inner – 2	loglog(V)	Inner – 3	loglog(V)	Avg Inner	loglog(V)
25	302700000	0.928448	298990000	0.928173	243840000	0.923612	289080000	0.927423	295120000	0.927883	276013333	0.92639
45	19992000	0.863374	17768000	0.860316	13841000	0.853769	17925000	0.860545	18848000	0.861849	16871333	0.858967
65	940090	0.776205	856450	0.773253	676920	0.765709	835950	0.772482	864900	0.773565	792590	0.770782
85	68228	0.684303	68562	0.684494	56510	0.676888	69279	0.684899	72841	0.686849	66210	0.68313

Table 44, cont'd

Aging Profile with DSR Test Temperature:

Complex Viscosity, (cP) at 25 C												
Aging time (days)	**Outer**	**loglog(V)**	**Middle**	**loglog(V)**	**Inner - 1**	**loglog(V)**	**Inner - 2**	**loglog(V)**	**Inner - 3**	**loglog(V)**	**Avg Inner**	**loglog(V)**
10	379720000	0.93346	334880000	0.930689	300280000	0.928269	3.43E+08	0.93119	3.27E+08	0.930174	323340000	0.929912
5	356700000	0.932083	307540000	0.9288	345520000	0.93138	2.95E+08	0.927895	3.38E+08	0.930888	326233333	0.93011
1	302700000	0.928448	298990000	0.928173	243840000	0.923612	2.89E+08	0.927423	2.95E+08	0.927883	276013333	0.92639
45C												
	Complex Viscosity, (cP)											
Aging time (days)	**Outer**	**loglog(V)**	**Middle**	**loglog(V)**	**Inner - 1**	**loglog(V)**	**Inner - 2**	**loglog(V)**	**Inner - 3**	**loglog(V)**	**Avg Inner**	**loglog(V)**
10	34616000	0.87733	28946000	0.872831	23126000	0.86712	26729000	0.870812	25939000	0.87005	25264667	0.869379
5	33866000	0.876781	25916000	0.870027	32589000	0.875817	22802000	0.866758	28370000	0.872323	27920333	0.871918
1	19992000	0.863374	17768000	0.860316	13841000	0.853769	17925000	0.860545	18848000	0.861849	16871333	0.858967
65 C												
	Complex Viscosity, (cP)											
Aging time (days)	**Outer**	**loglog(V)**	**Middle**	**loglog(V)**	**Inner - 1**	**loglog(V)**	**Inner - 2**	**loglog(V)**	**Inner - 3**	**loglog(V)**	**Avg Inner**	**loglog(V)**
10	1751000	0.795413	1519800	0.791114	1237700	0.784804	1344300	0.787354	1262400	0.785415	1281466.7	0.785878
5	1675400	0.794078	1312200	0.786609	1670100	0.793982	1111400	0.781459	1379000	0.788138	1386833.3	0.788312
1	940090	0.776205	856450	0.773253	676920	0.765709	835950	0.772482	864900	0.773565	792590	0.770782
85 C												
	Complex Viscosity, (cP)											
Aging time (days)	**Outer**	**loglog(V)**	**Middle**	**loglog(V)**	**Inner - 1**	**loglog(V)**	**Inner - 2**	**loglog(V)**	**Inner - 3**	**loglog(V)**	**Avg Inner**	**loglog(V)**
10	126810	0.707839	111170	0.702946	87693	0.693988	101480	0.699524	93199	0.696305	94124	0.69668
5	118900	0.705452	104450	0.700609	123690	0.706917	89303	0.694681	104830	0.700746	105941	0.701142
1	68228	0.684303	68562	0.684494	56510	0.676888	69279	0.684899	72841	0.686849	66210	0.68313

Table 45
Core Height Measurements

Height of the Core (mm)							
	H1	**H2**	**H3**	**H4**	**H5**	**H6**	**Average H**
Before Aging	148	149	147	147	147	148	147.67
After Aging	147	147	148	148	149	148	147.83

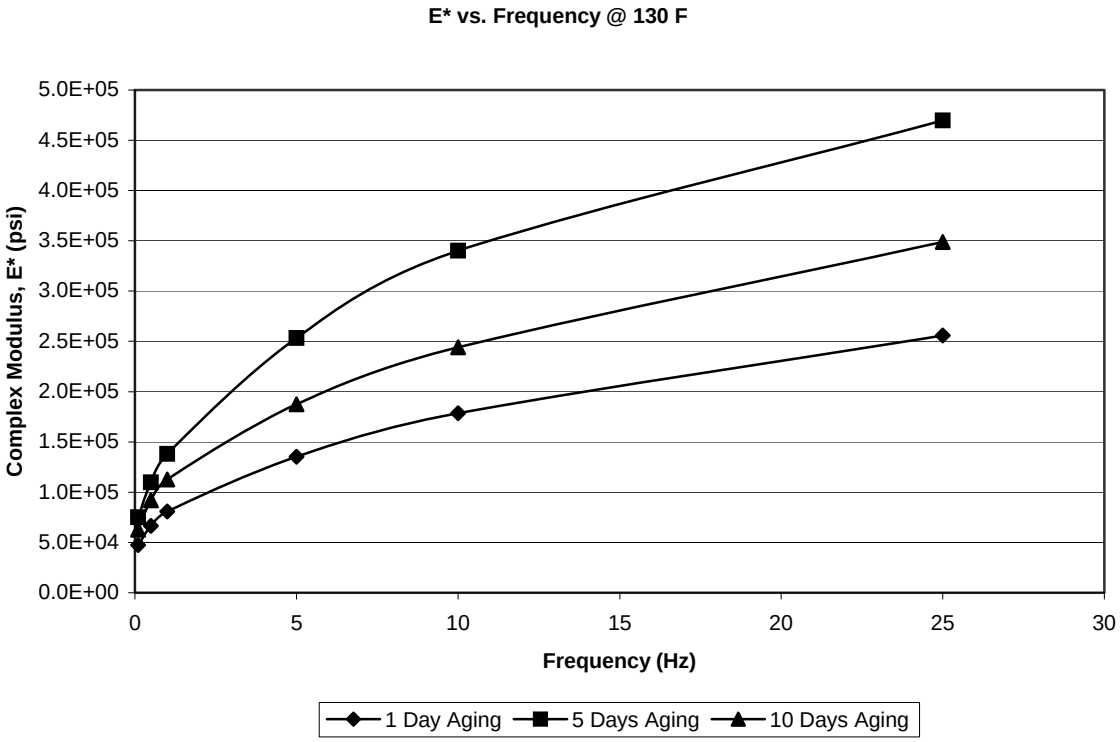

Figure 119
Complex Modulus Test Results

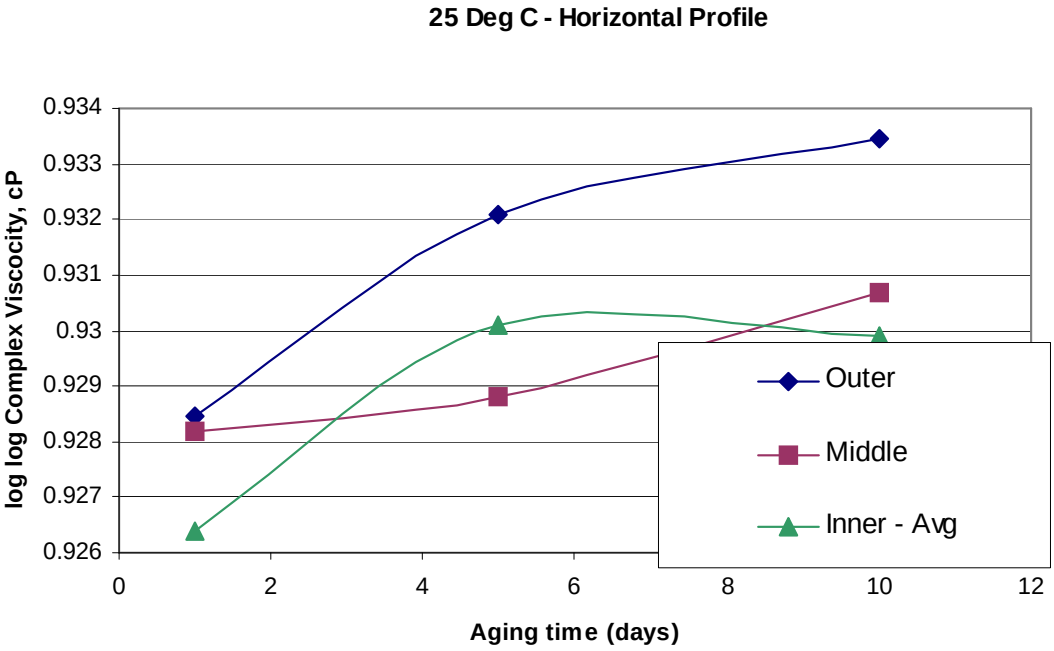

(a)

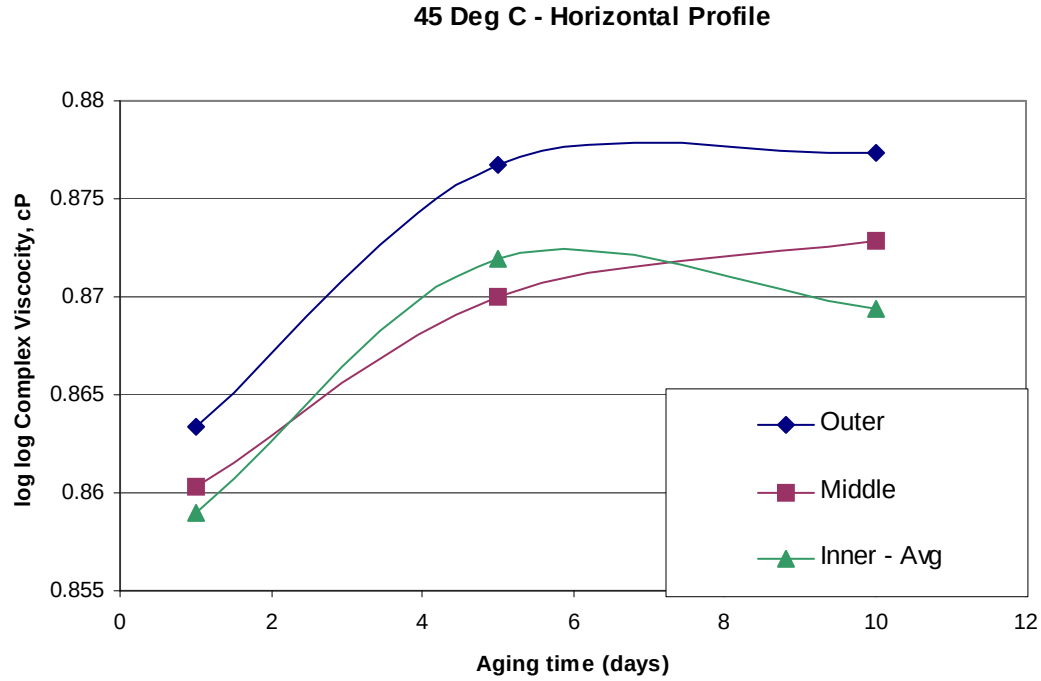

(b)

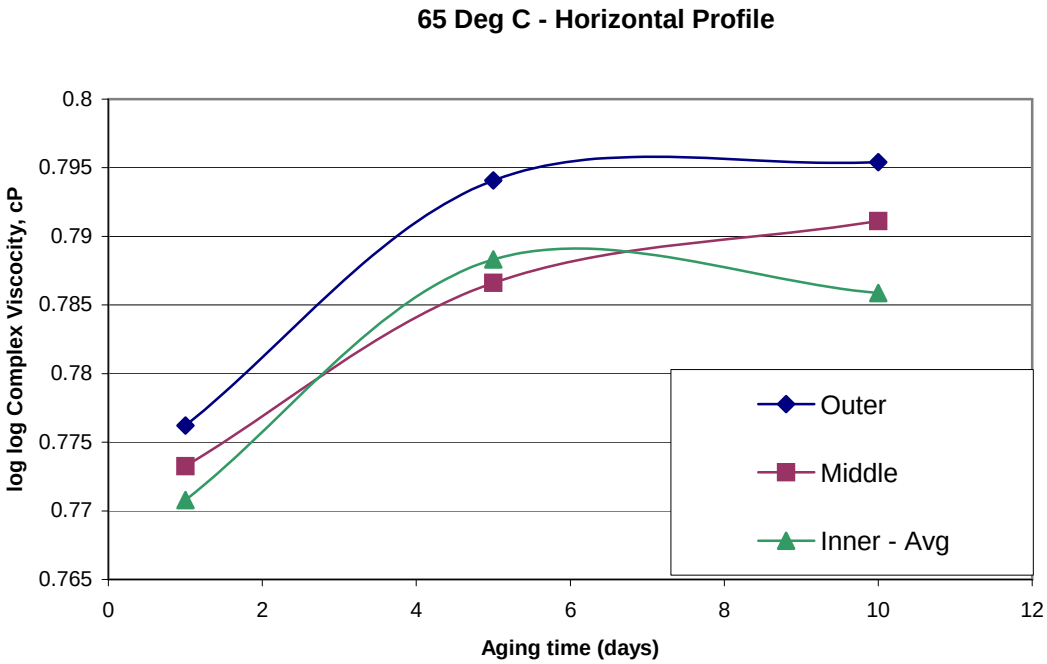

(c)

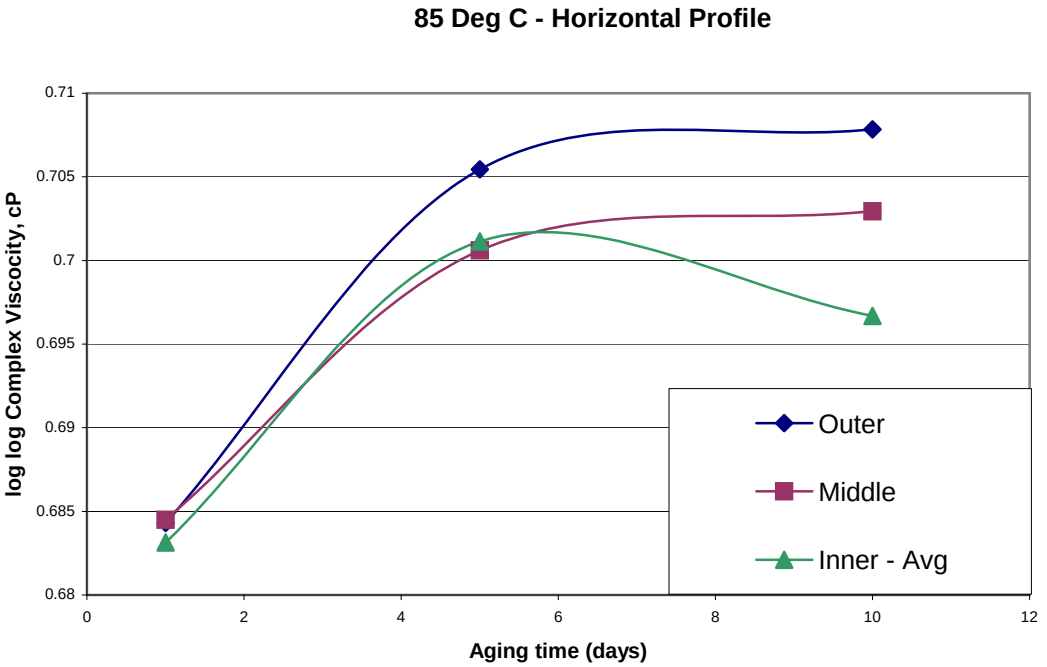

(d)

Figure 120
Binder Viscosity – Radial Profile

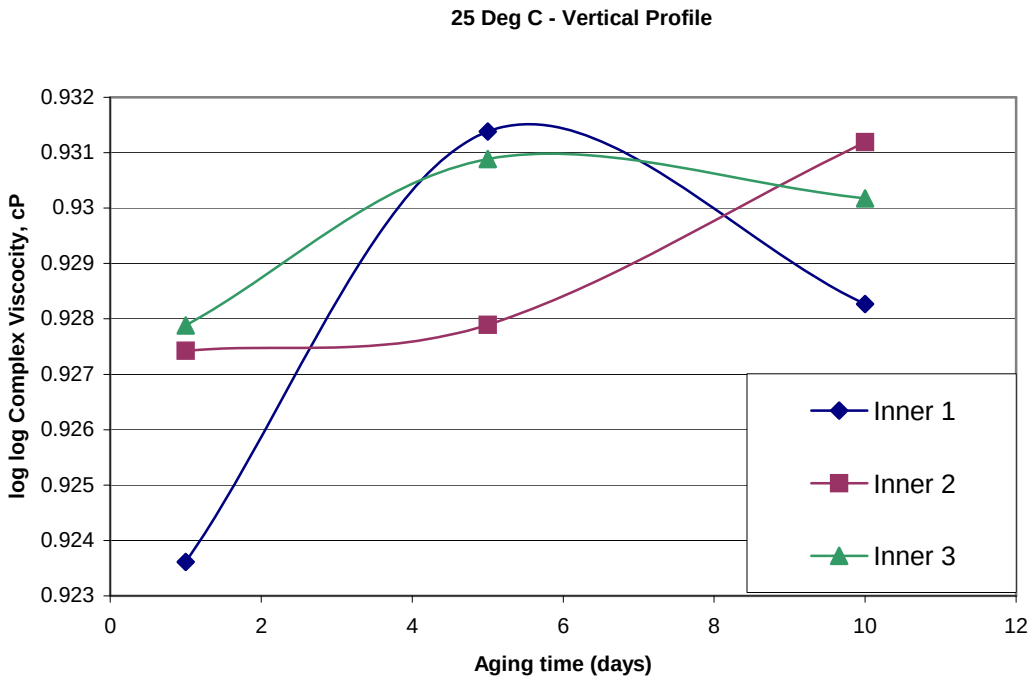

(a)

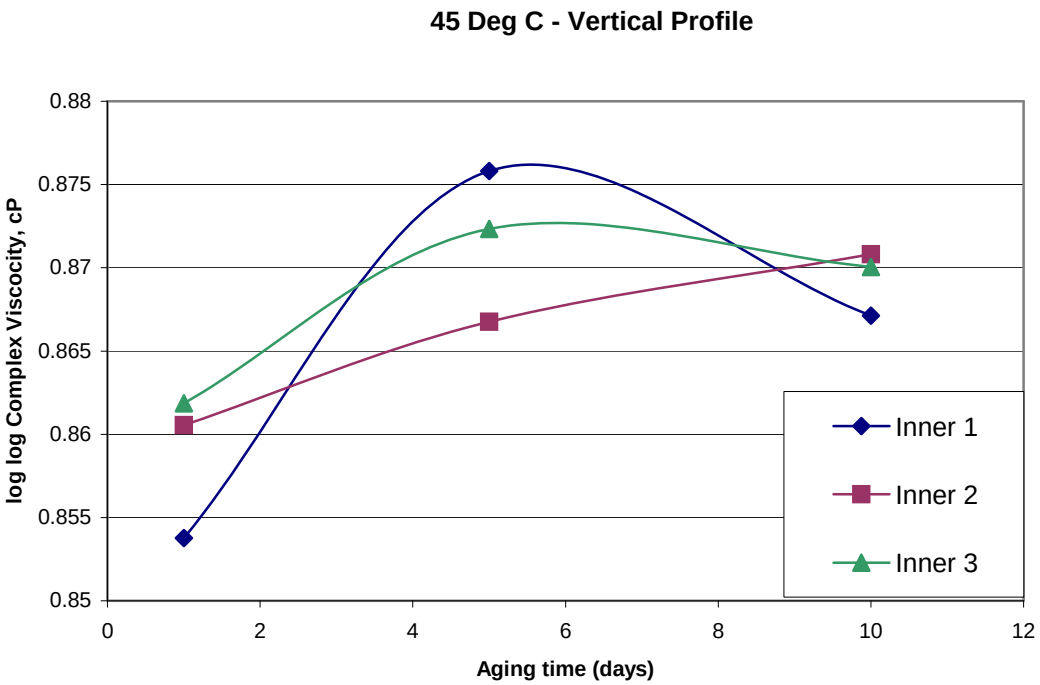

(b)

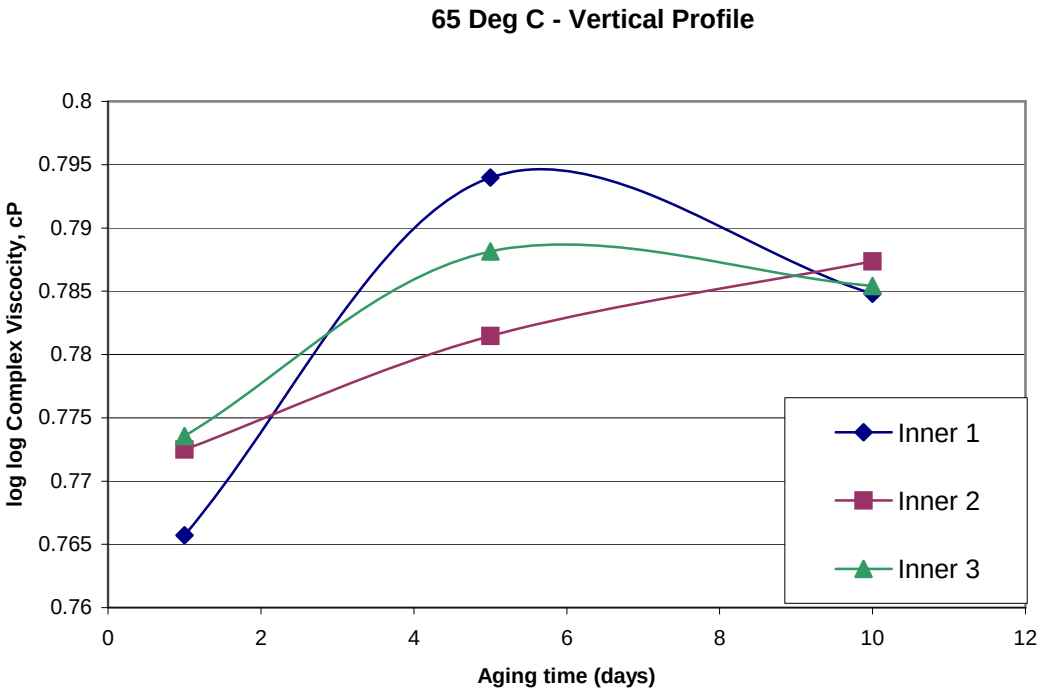

(c)

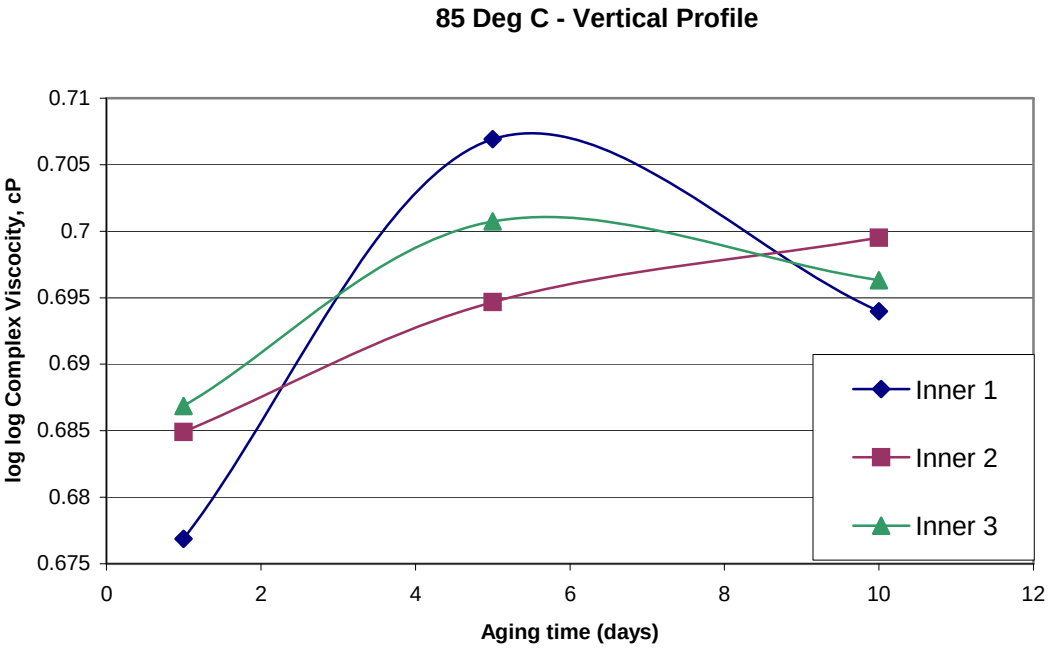

(d)

Figure 121
Binder Viscosity – Vertical Profile

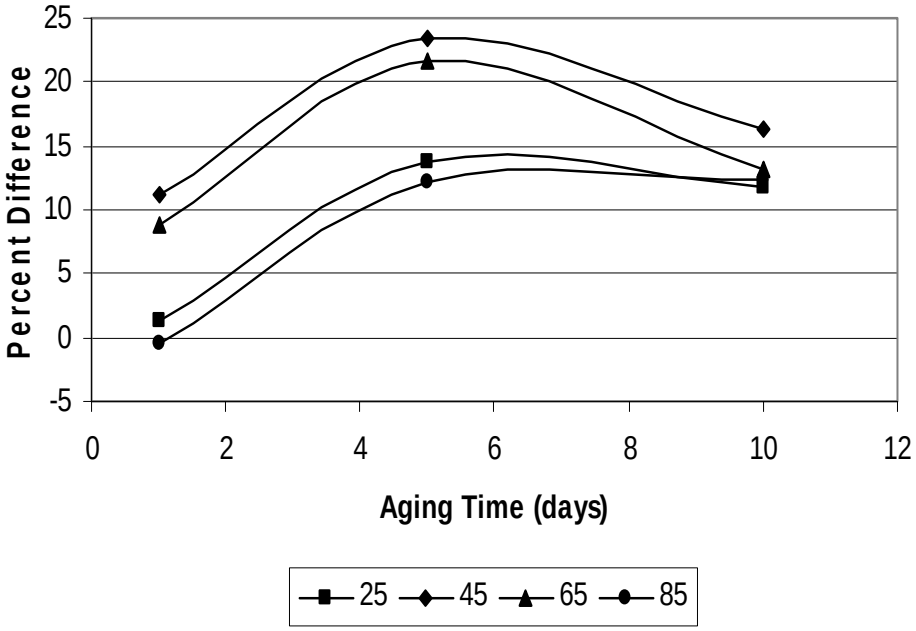

Figure 122
Percent Difference between the Outer Shell and the Middle Shell

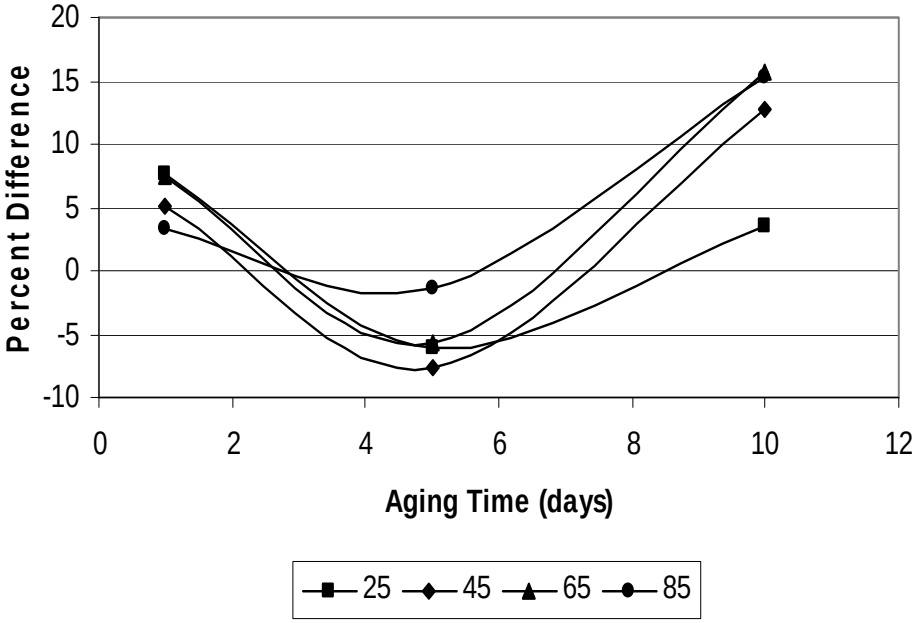

Figure 123
Percent Difference between the Middle Shell and the Inner Core

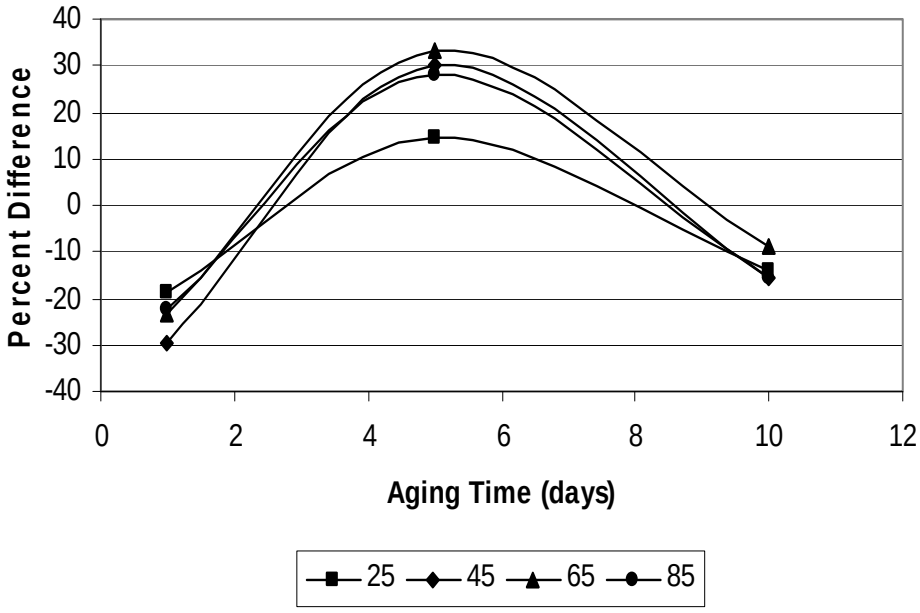

Figure 124
Percent Difference between Inner 1 and Inner 2 (middle of sample)

Figure 125
E* Test Cores Encased in Wire Mesh and Clamps to Eliminate Slump During Aging

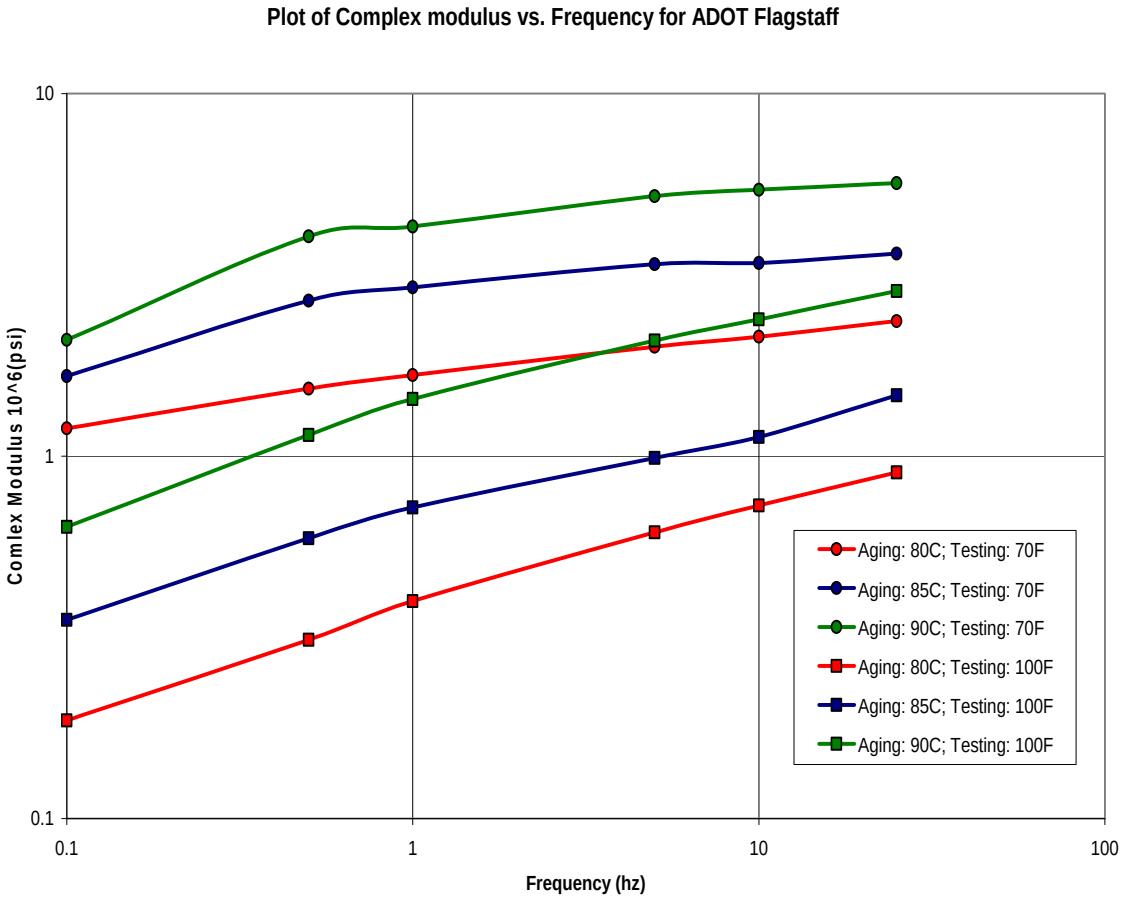

Figure 126
Plot of Complex Modulus vs. Loading Frequency for ADOT Flagstaff

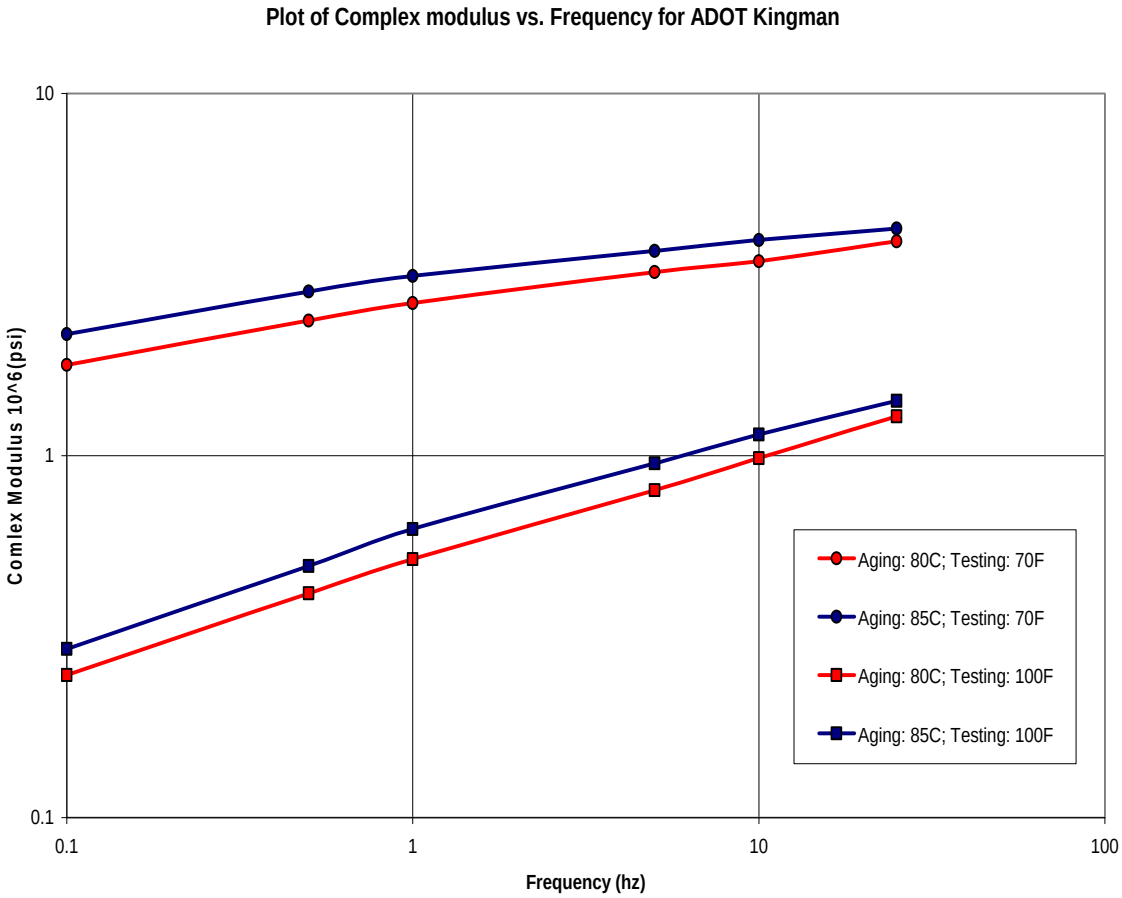

Figure 127
Plot of Complex Modulus vs. Loading Frequency for ADOT Kingman

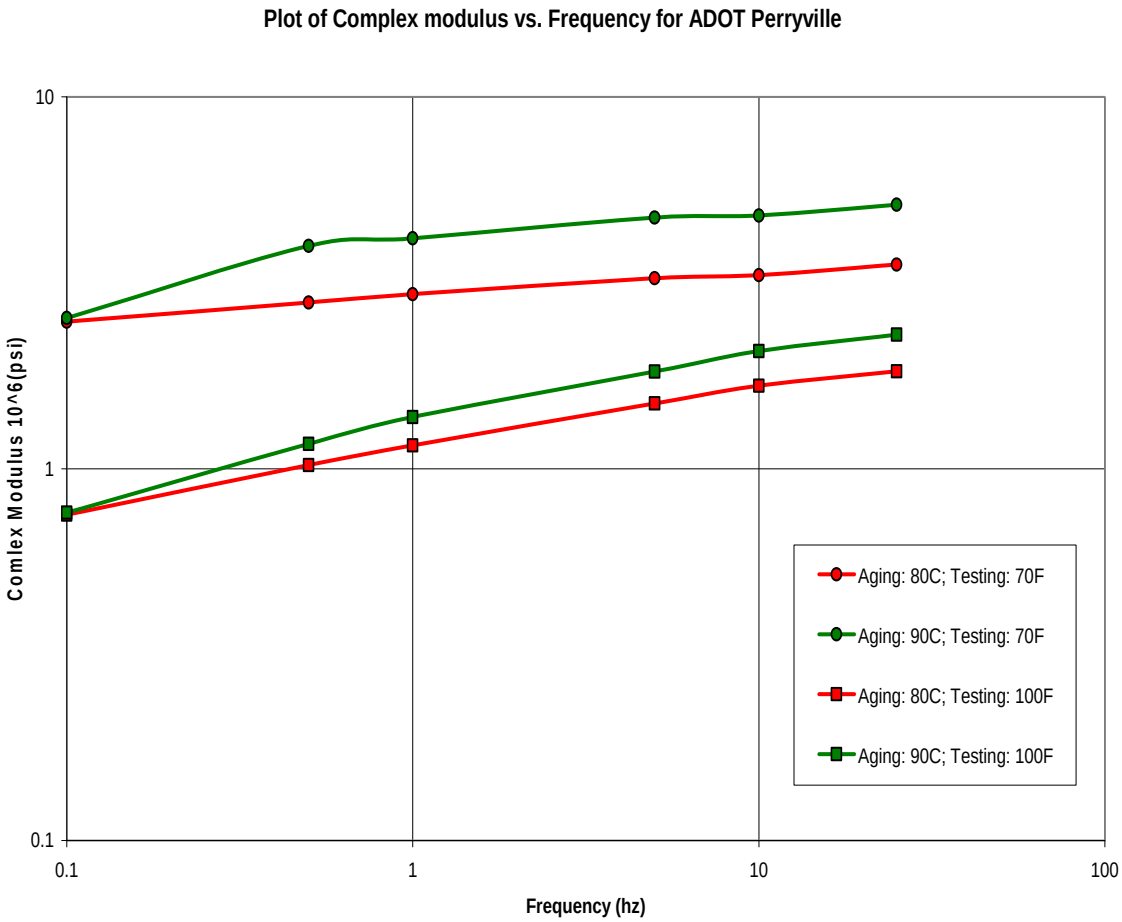

Figure 128
Plot of Complex Modulus vs. Loading Frequency for ADOT Perryville

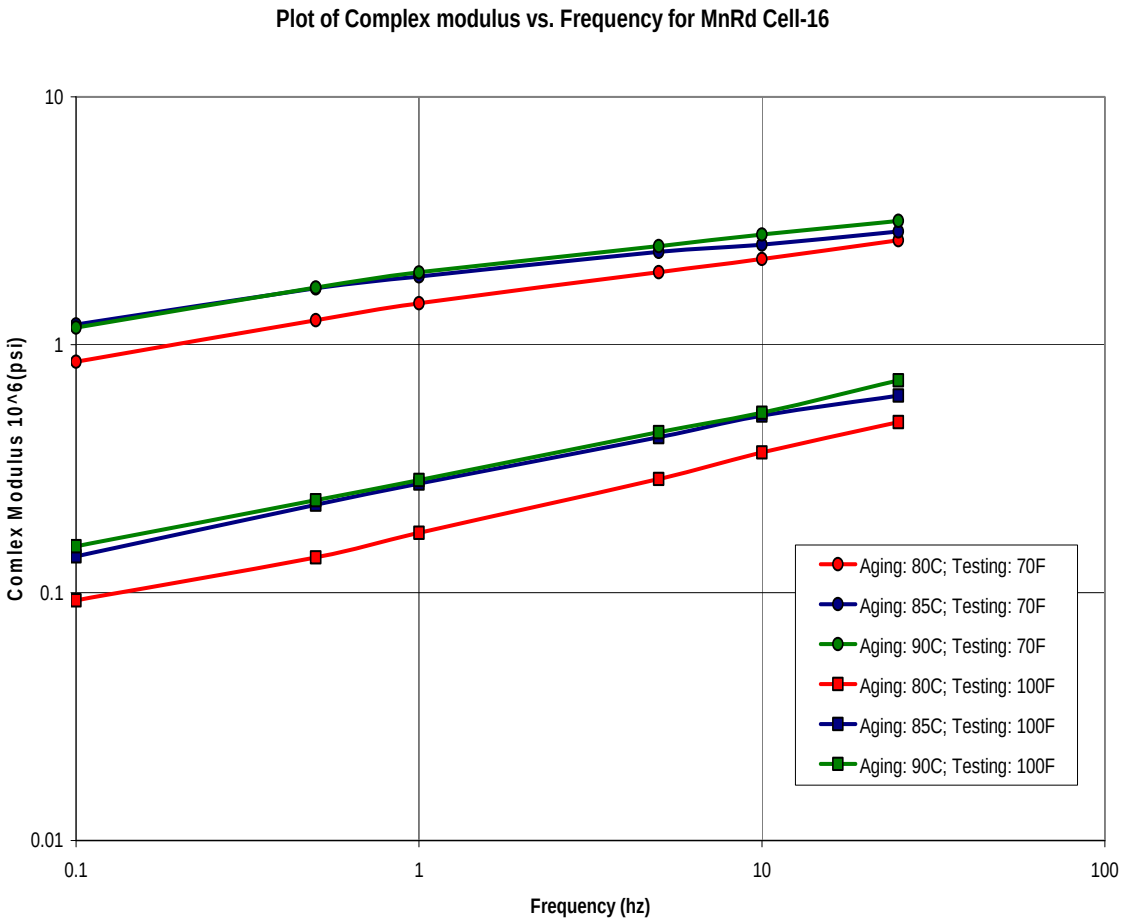

Figure 129
Plot of Complex Modulus vs. Loading Frequency for MnRoad Cell 16

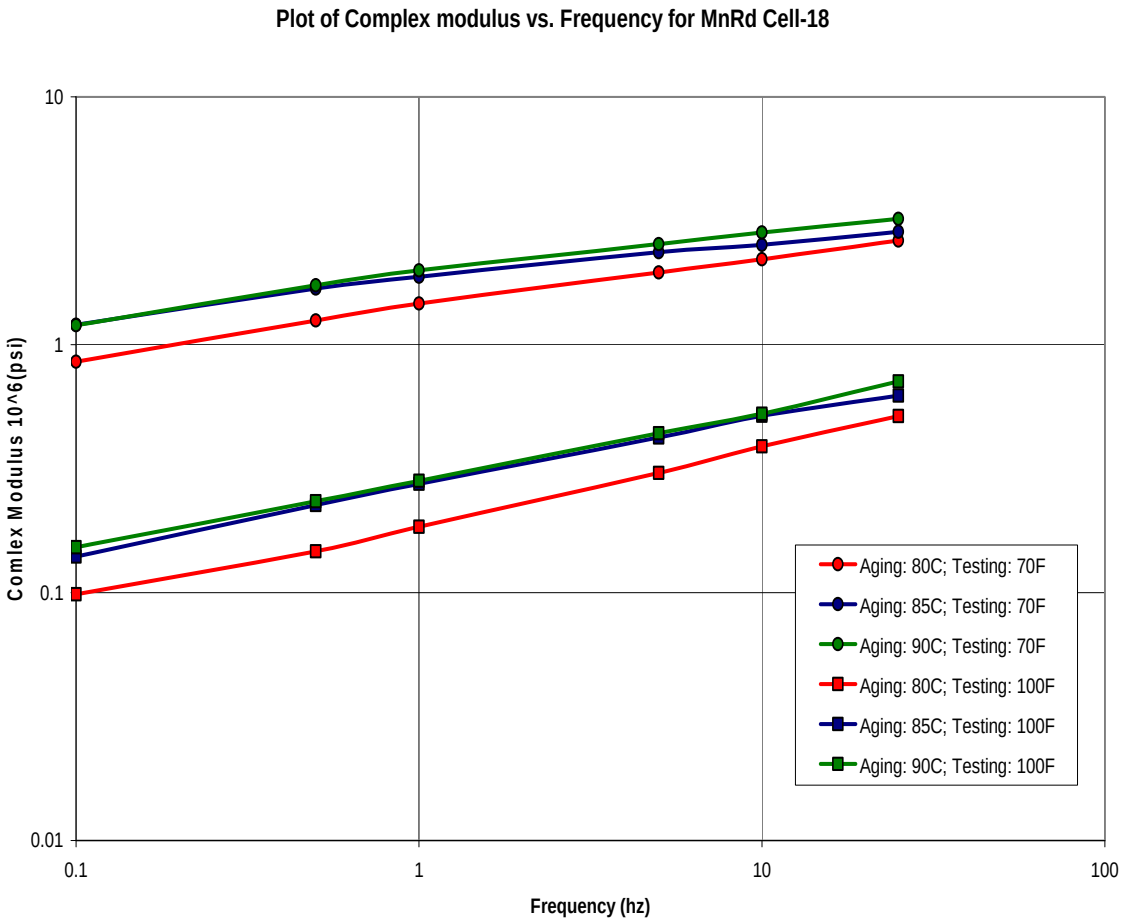

Figure 130
Plot of Complex Modulus vs. Loading Frequency for MnRoad Cell 18

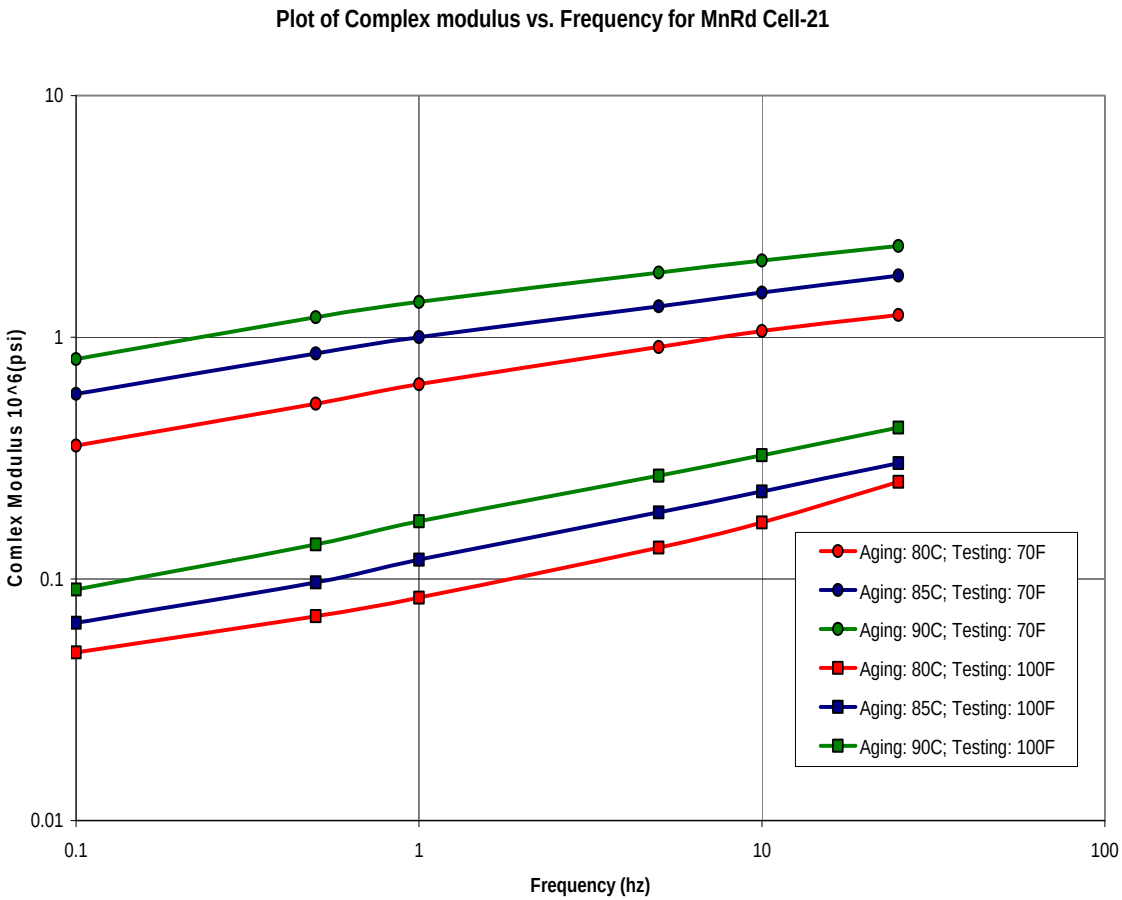

Figure 131
Plot of Complex Modulus vs. Loading Frequency for MnRoad Cell 21

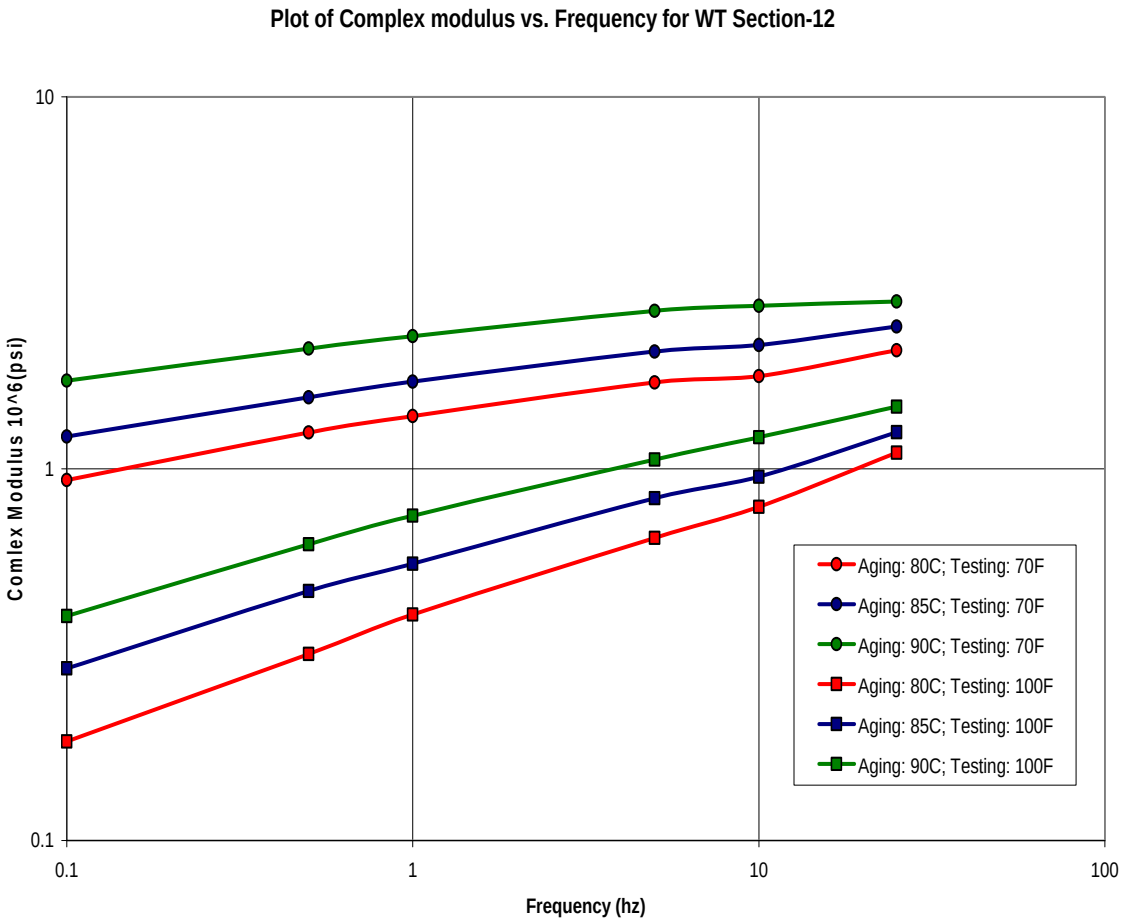

Figure 132
Plot of Complex Modulus vs. Loading Frequency for WesTrack Section 12

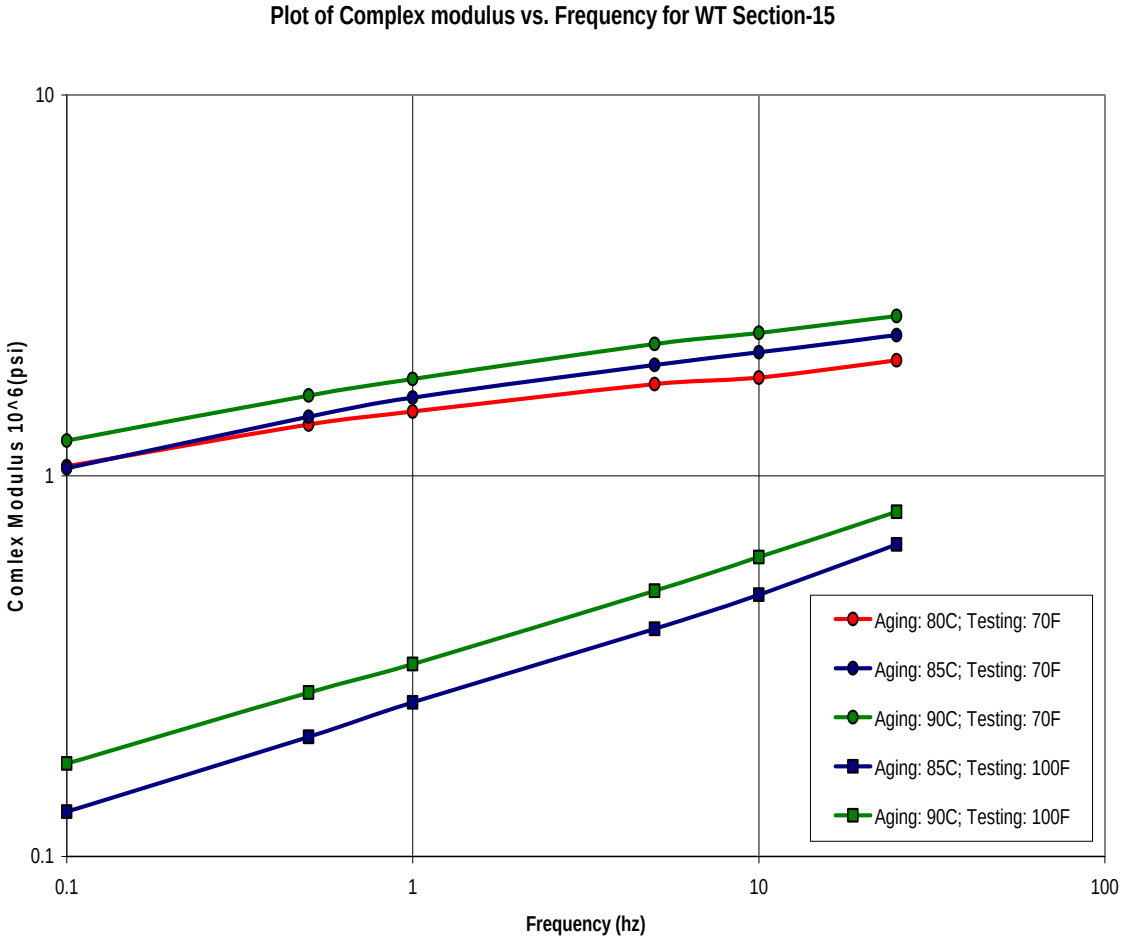

Figure 133
Plot of Complex Modulus vs. Loading Frequency for WesTrack Section 15

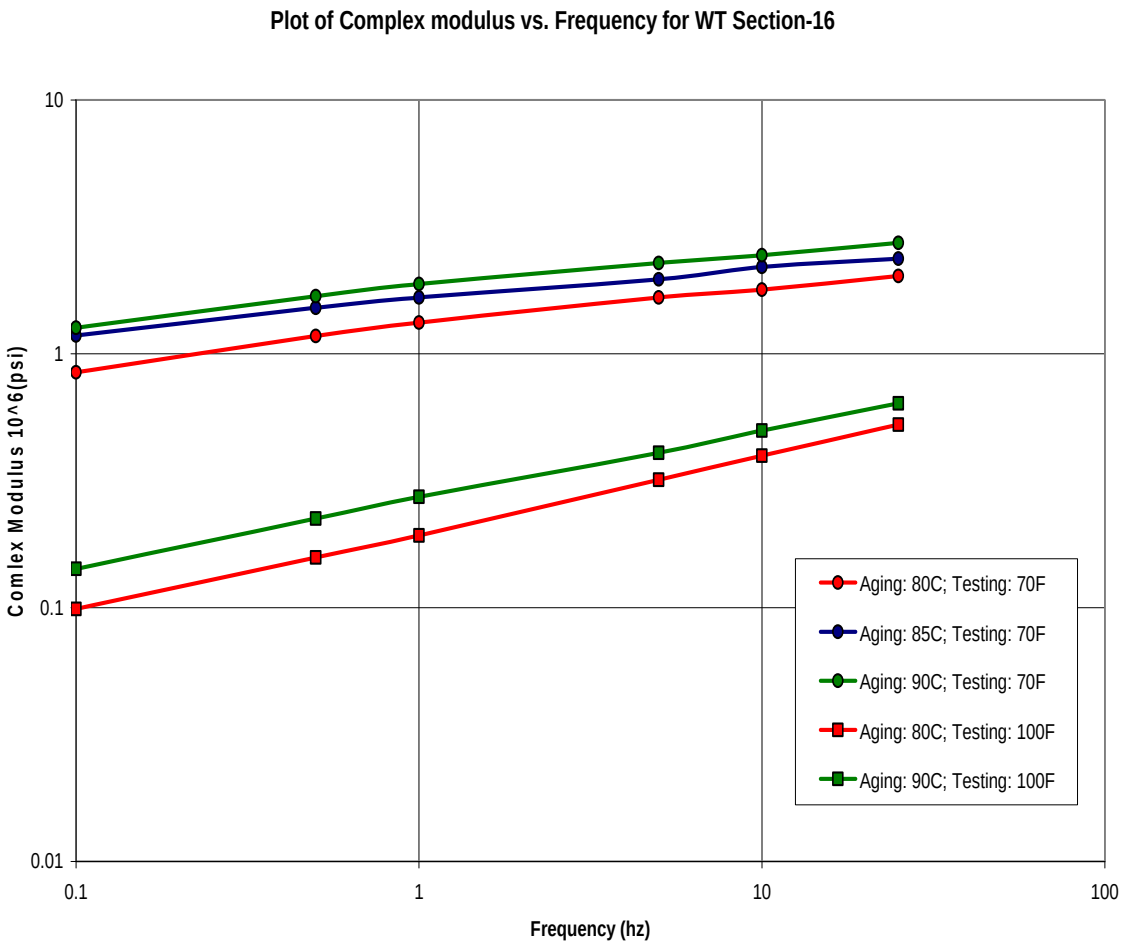

Figure 134
Plot of Complex Modulus vs. Loading Frequency for WesTrack Section 16

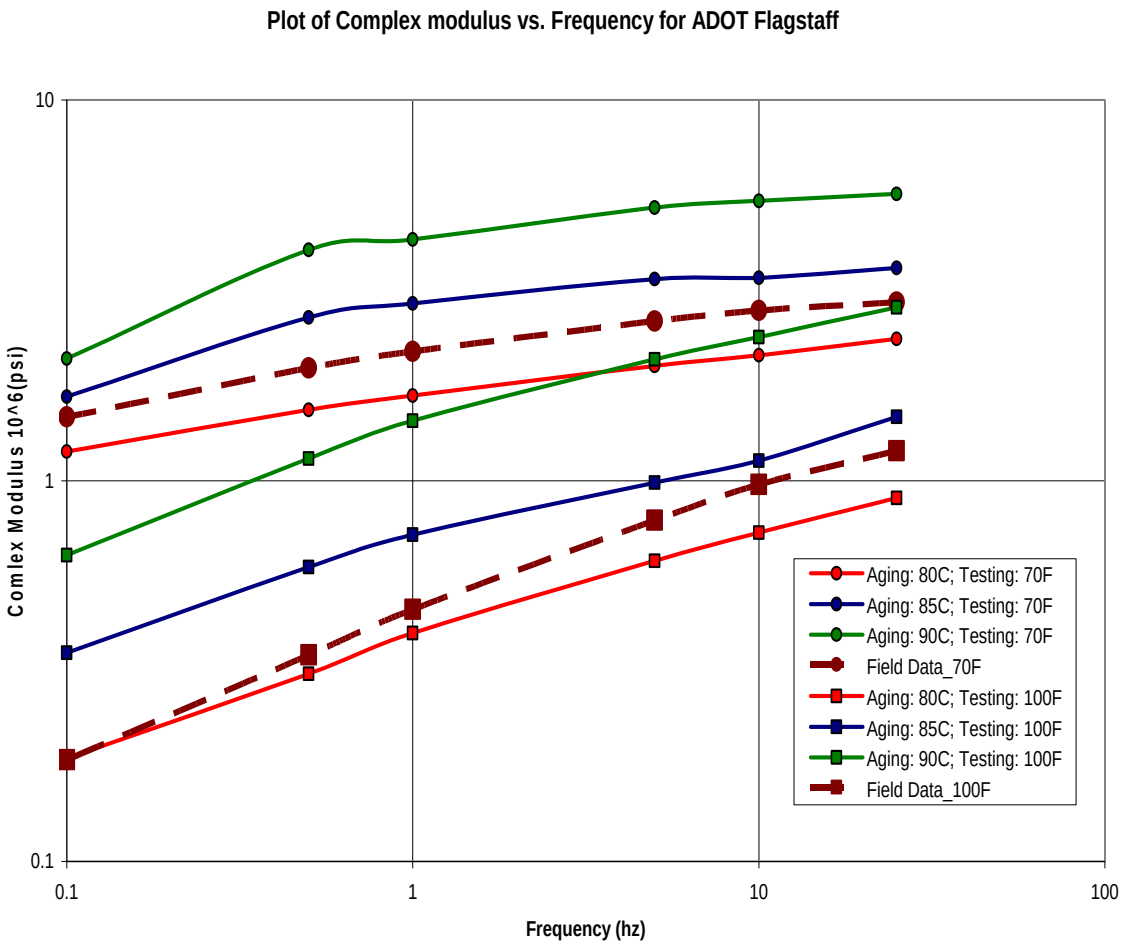

Figure 135
E* Comparison of Lab-aged and Field-aged Cores for ADOT, Flagstaff

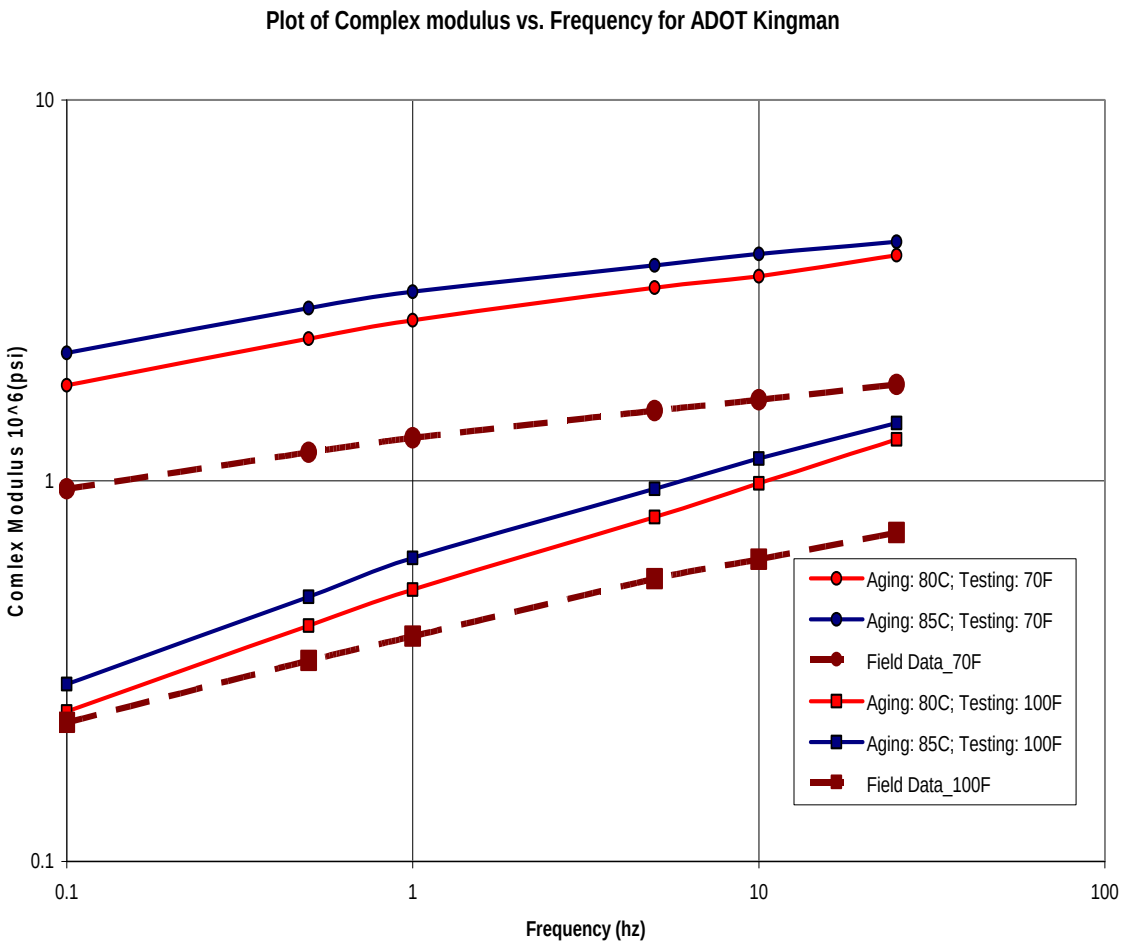

Figure 136
E* Comparison of Lab-aged and Field-aged Cores for ADOT, Kingman

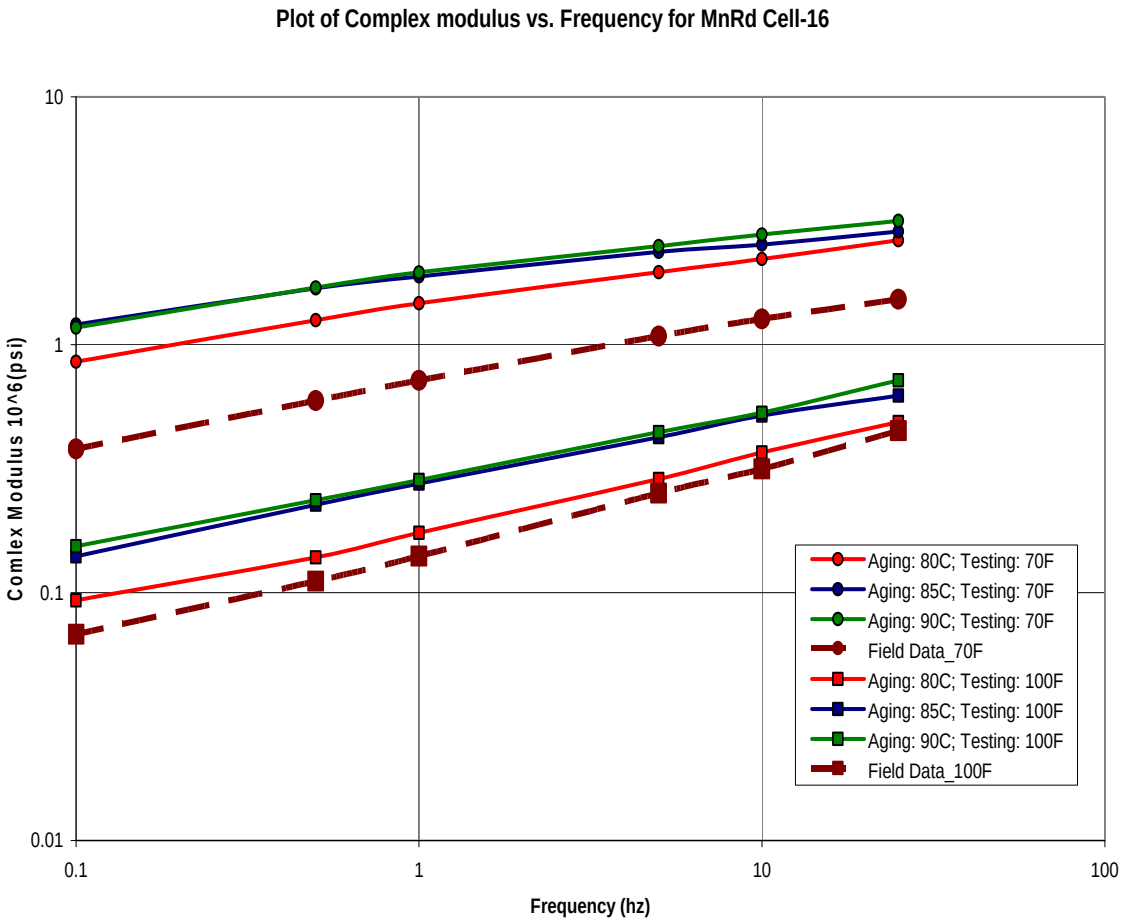

Figure 137
E* Comparison of Lab-aged and Field-aged Cores for MnRoad Cell 16

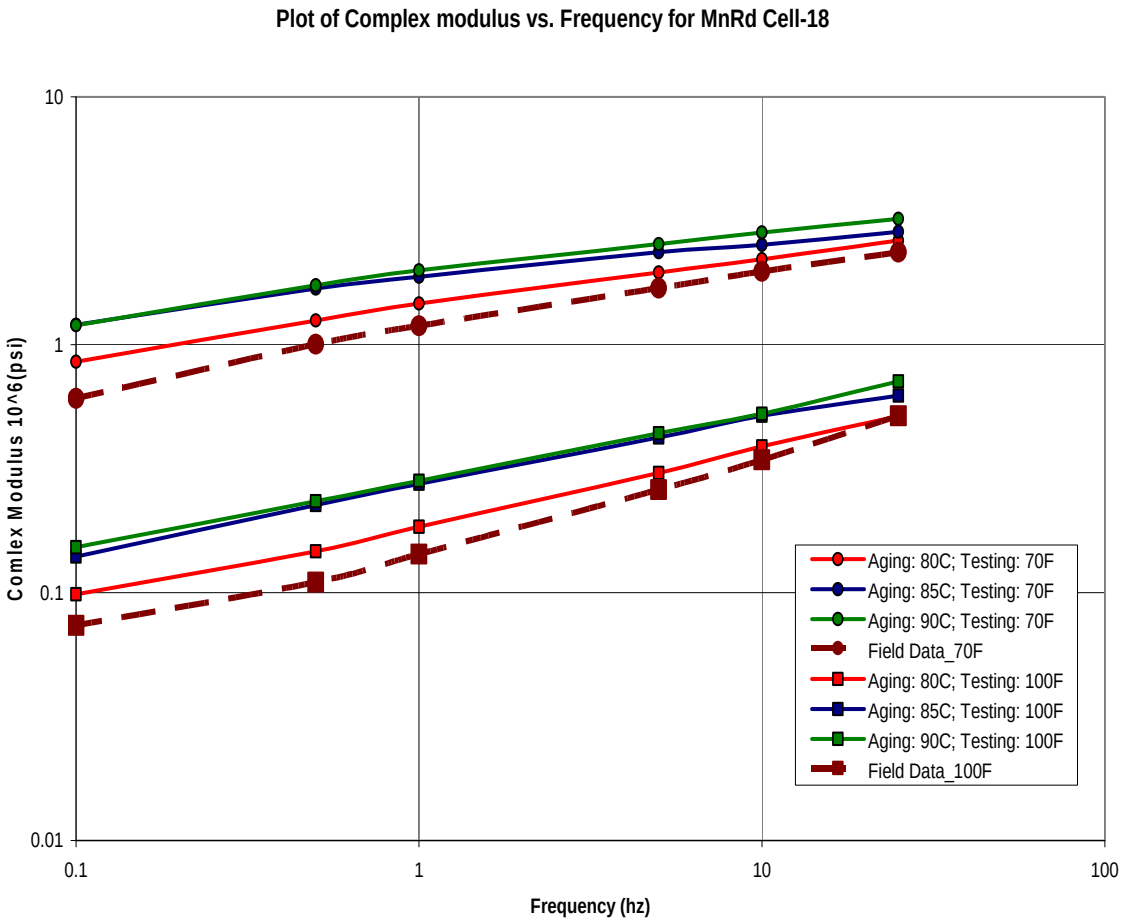

Figure 138
E* Comparison of Lab-aged and Field-aged Cores for MnRoad Cell 18

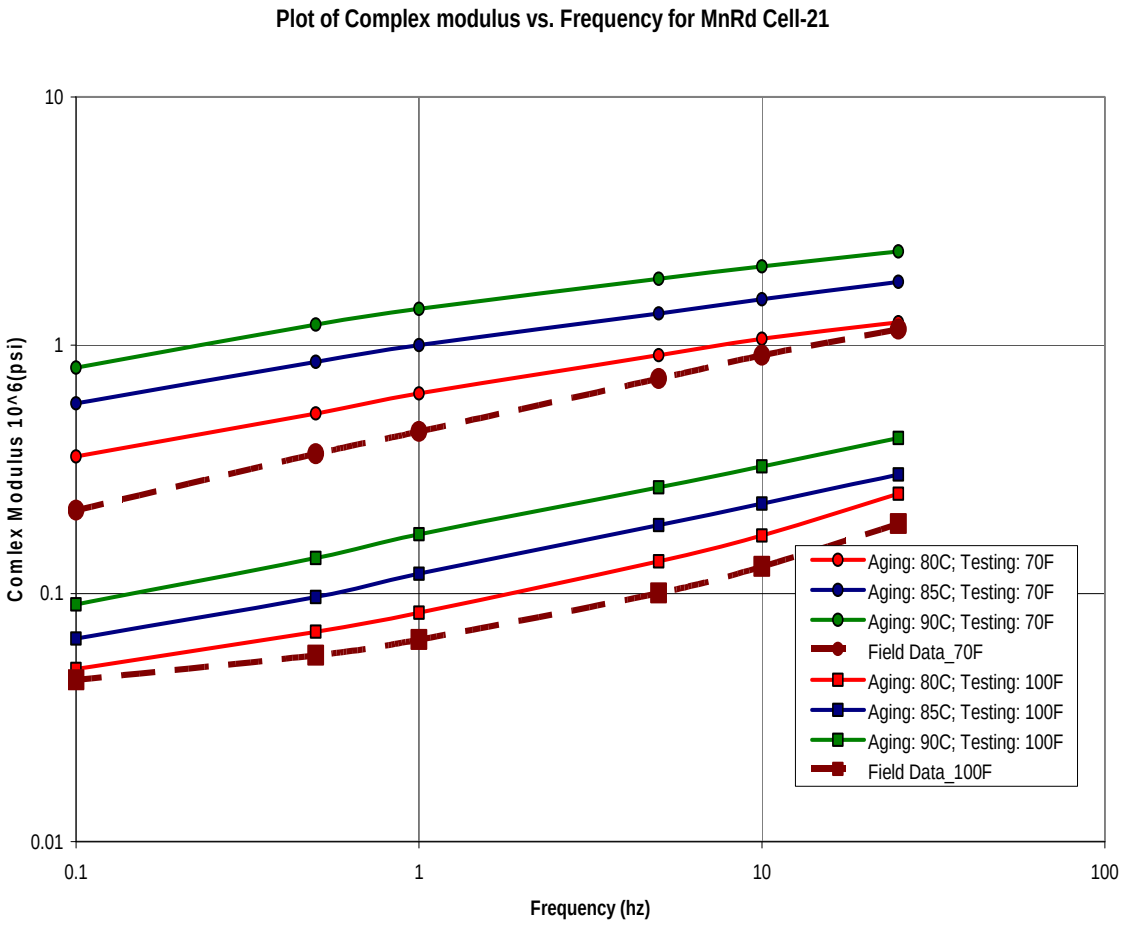

Figure 139
E* Comparison of Lab-aged and Field-aged Cores for MnRoad Cell 21

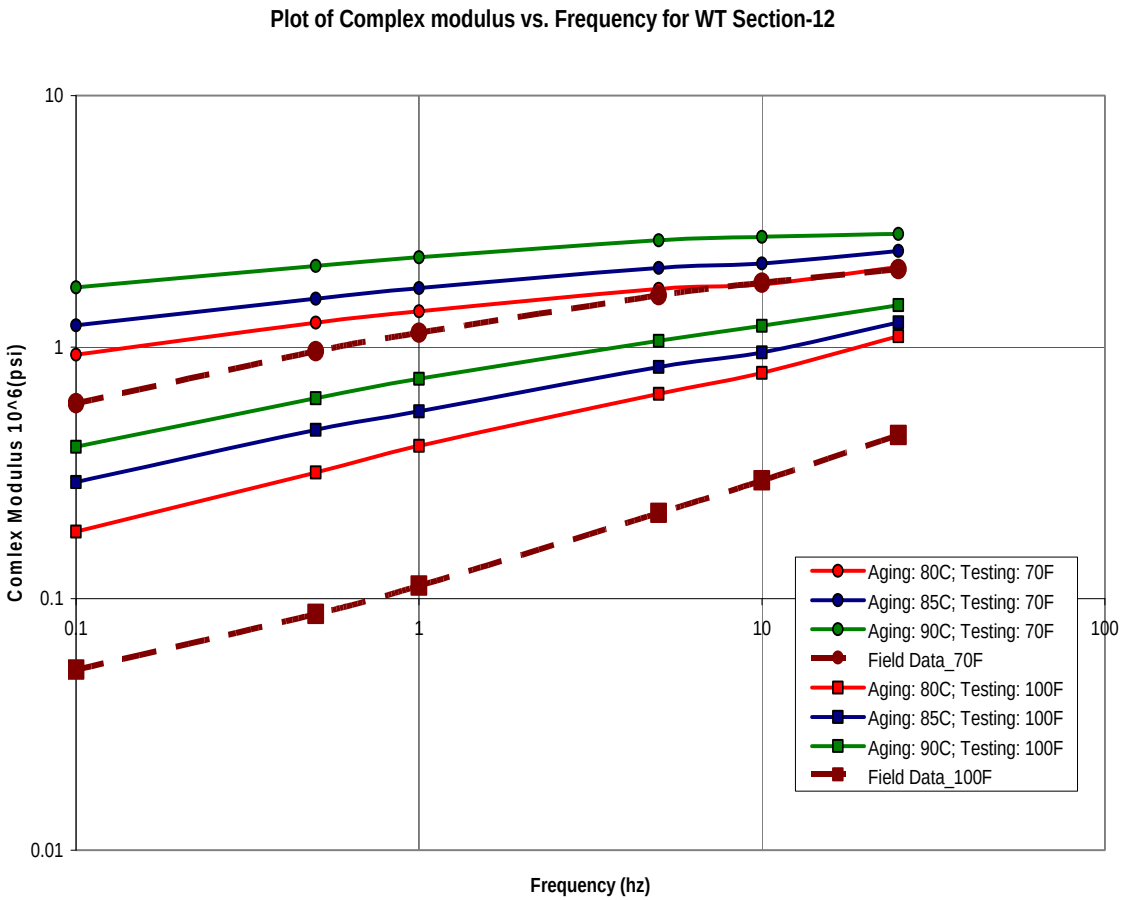

Figure 140
E* Comparison of Lab-aged and Field-aged Cores for WesTrack Section 12

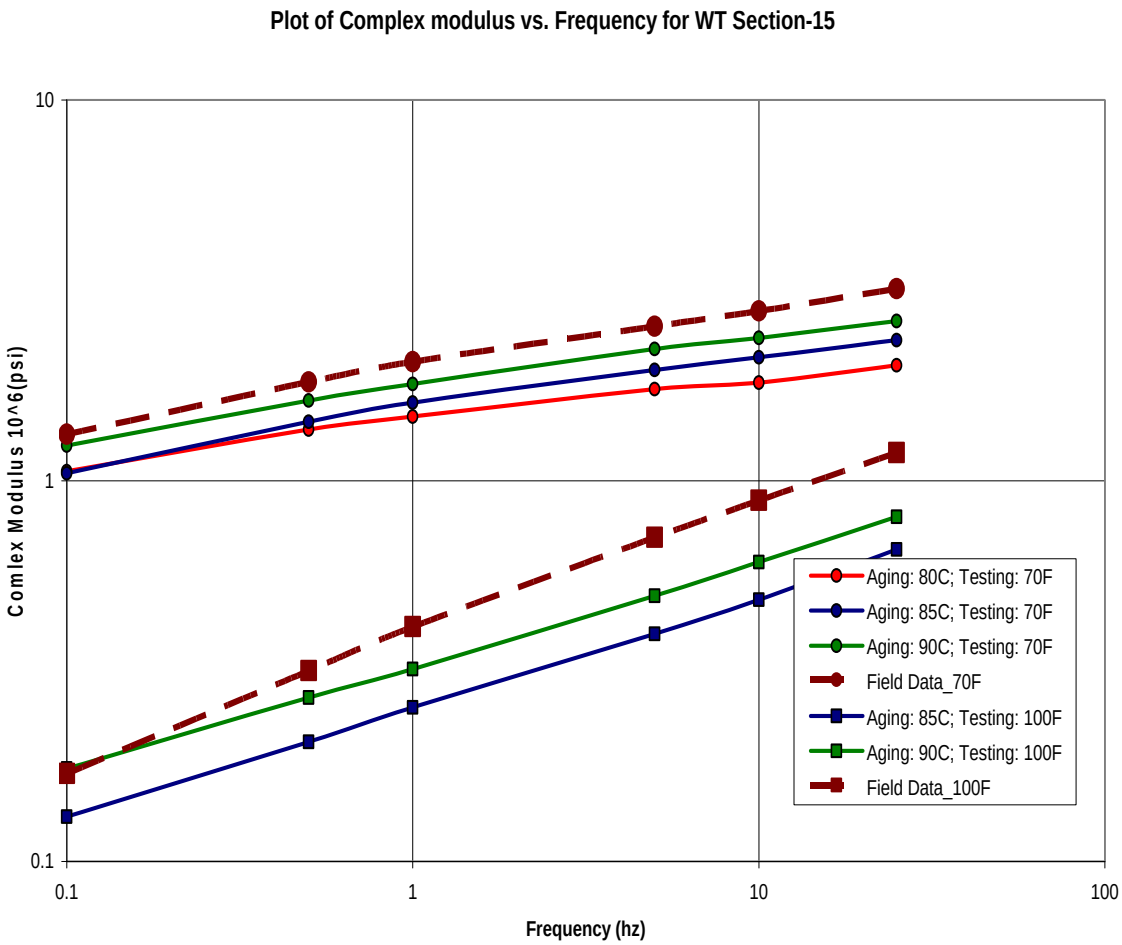

Figure 141
E* Comparison of Lab-aged and Field-aged Cores for WesTrack Section 15

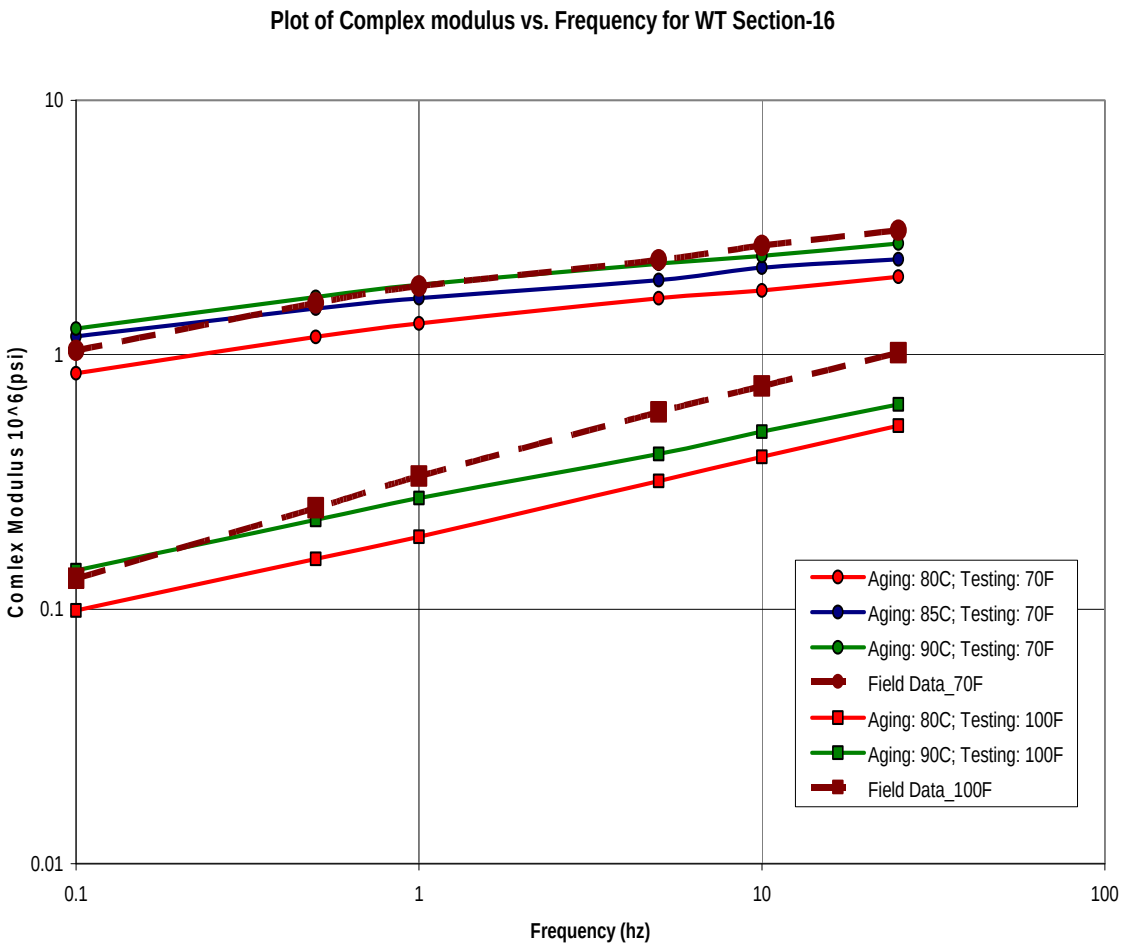

Figure 142
E* Comparison of Lab-aged and Field-aged Cores for WesTrack Section 16

CHAPTER 11

ANALYSIS AND CORRELATION OF LABORATORY AGED AND FIELD AGED CORES DATA

INTRODUCTION

This chapter presents the analysis of E* test results obtained from the lab-aged and field-aged cores. Based on the analysis, it was intended to develop an improved model for the PP2-99 protocol. However, as presented in *Chapter 10, Verification of PP2-99 Protocol*, the data was inconclusive and hence an improved model could not be developed.

TEST RESULTS OF LABORATORY-AGED CORES

Laboratory Aging

Plant mixes were obtained from the field sites mentioned earlier. Mixing and compacting temperatures for the mixes were determined based on the binder grade used. Plant mixes were heated in the forced draft oven to a few degrees more than the compaction temperature. The heated mix was poured into the gyratory moulds, which were preheated. The mix was compacted in the gyratory compactor to obtain plugs of 8-inch diameter and approximately 10-inch height. These plugs were cut and cored to obtained cores of 4-inch diameter and 6-inch height.

As mentioned in *Chapter 10*, various alternatives were studied to reduce the slump during aging. Finally, an arrangement using wire mesh and clamps was desired as it produced practically no slump. The cores were aged at three temperatures 80˚, 85˚, and 90˚ C for 5 days. As in the case of PP1, only one parameter was chosen as the variable while keeping other parameters as constants. As a result, the aging time of 5 days as specified by the existing protocol was not altered; but the aging temperatures of 80˚ and 90˚ C were used in addition to the currently specified temperature of 85˚ C.

Laboratory-Aged Cores Data

Complex modulus testing was conducted on the aged cores. Figures 143 to 151 show the plots of complex modulus vs. frequency of loading obtained from the complex modulus testing.

TEST RESULTS OF FIELD-AGED CORES

The field cores obtained were of 10-inch diameter (6 inches in case of ADOT cores) and of varying heights exceeding 6 inches. From these cores, sub-cores of 4-inch diameter and 6-inch height were obtained. Complex modulus testing was conducted on these cores. Three cores were obtained from each site. Two of these cores were used for the E* testing, resulting in one replicate for each E* testing on the field-aged cores.

The E* test results on the field-aged cores were plotted on top of the plots obtained from the lab-aged cores for comparison. Figures 152 to 159 show the E* comparison plots of field-aged and lab-aged cores.

ANALYSIS AND CONCLUSIONS

It can be observed from the plots that although aging periods are within the specified limits of the exiting protocol, the aged-modulus values correspond to different lab-aging temperatures. This observation, as mentioned in *Chapter 10*, is a result of environmental conditions prevalent in the field during aging. Due to the limited amount of data available, the PP2-99 protocol could not be improved, as it was the case for the PP1-98 protocol.

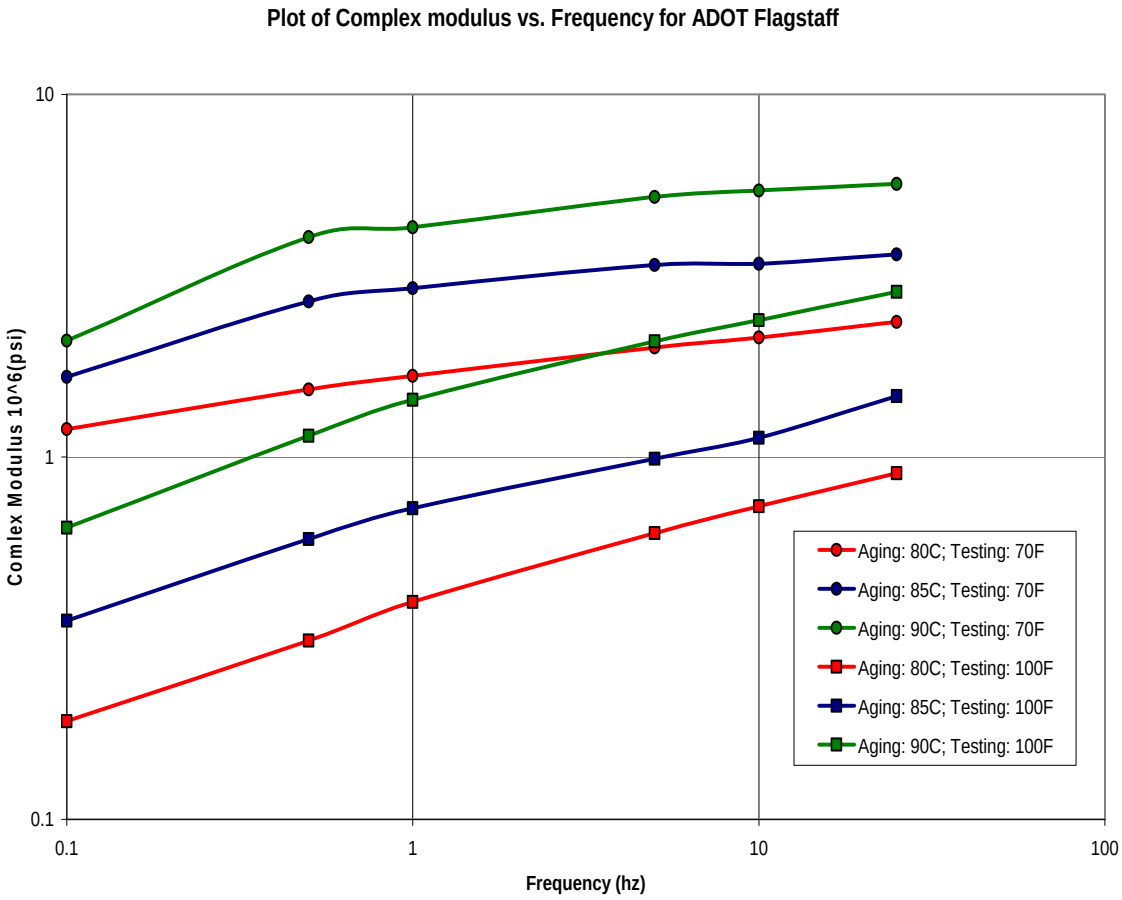

Figure 143
Plot of Complex Modulus vs. Loading Frequency for ADOT Flagstaff

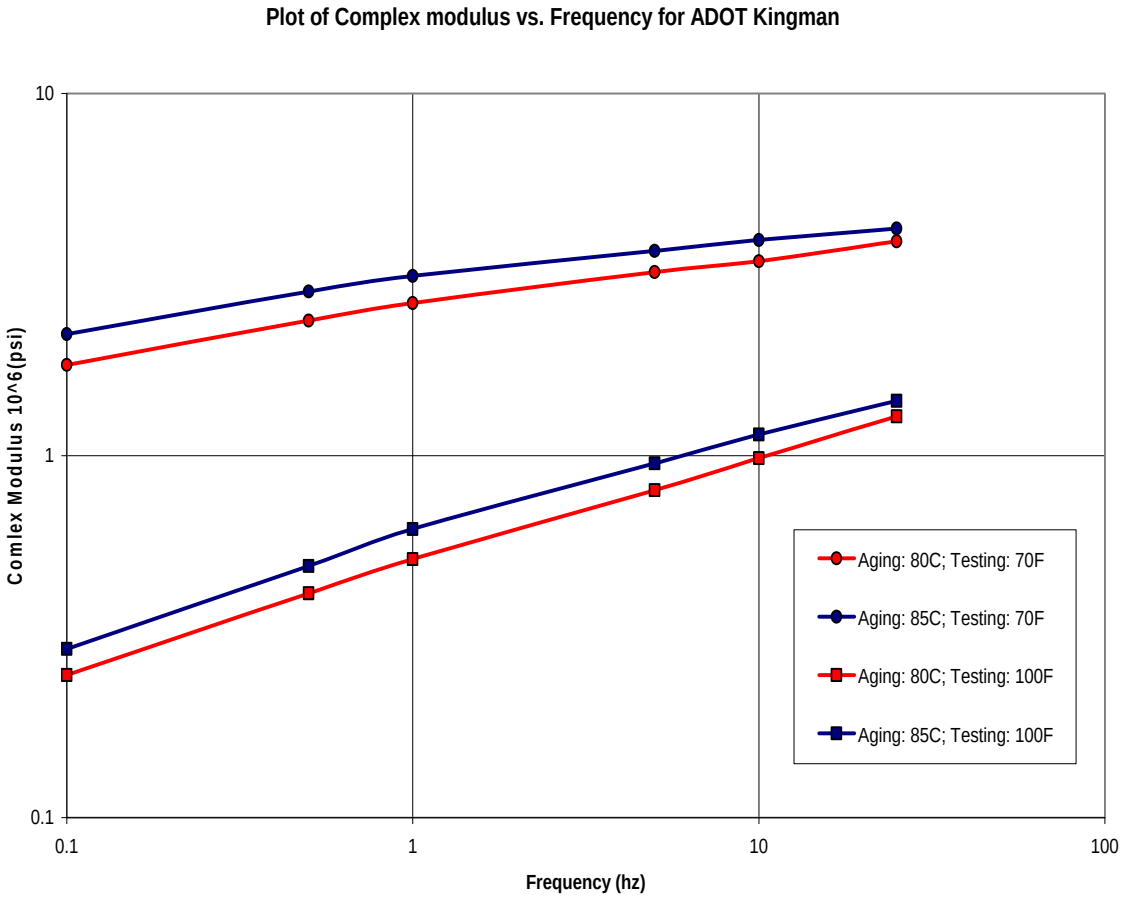

Figure 144
Plot of Complex Modulus vs. Loading Frequency for ADOT Kingman

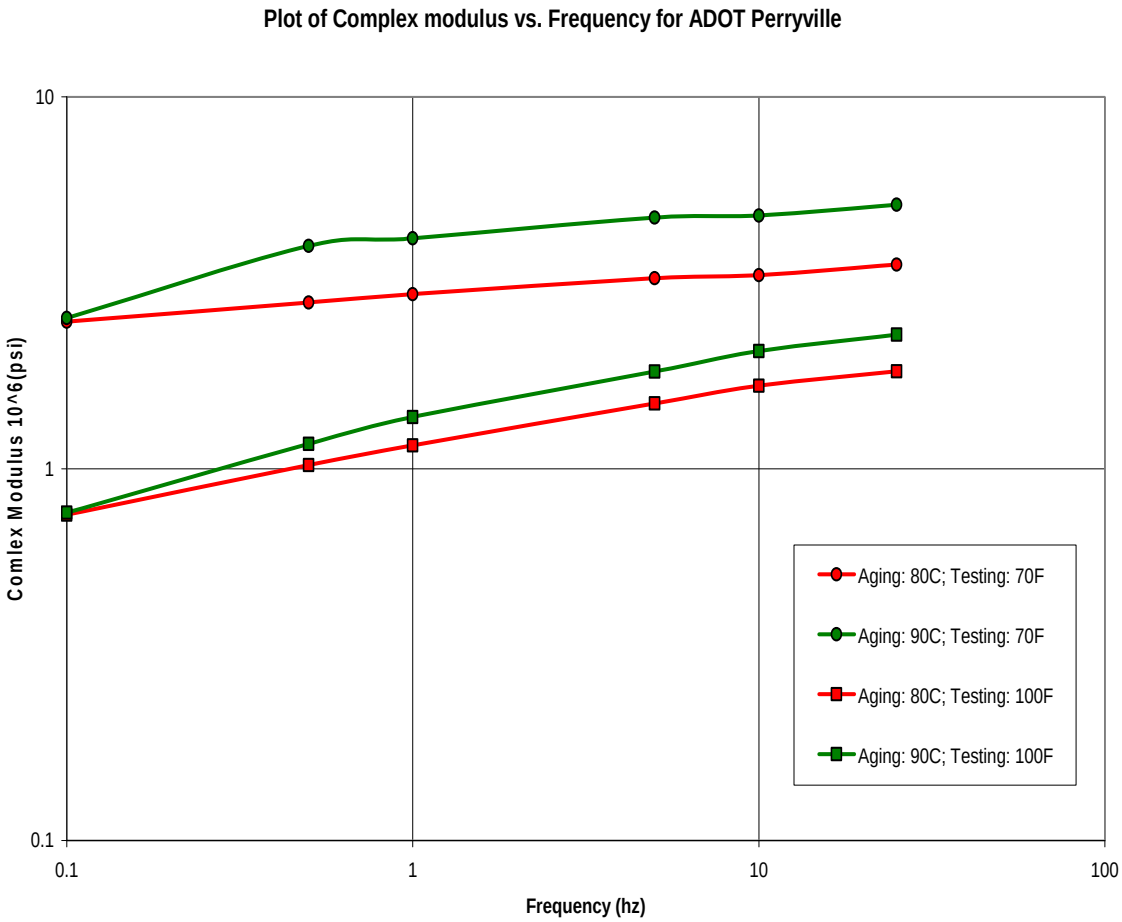

Figure 145
Plot of Complex Modulus vs. Loading Frequency for ADOT Perryville

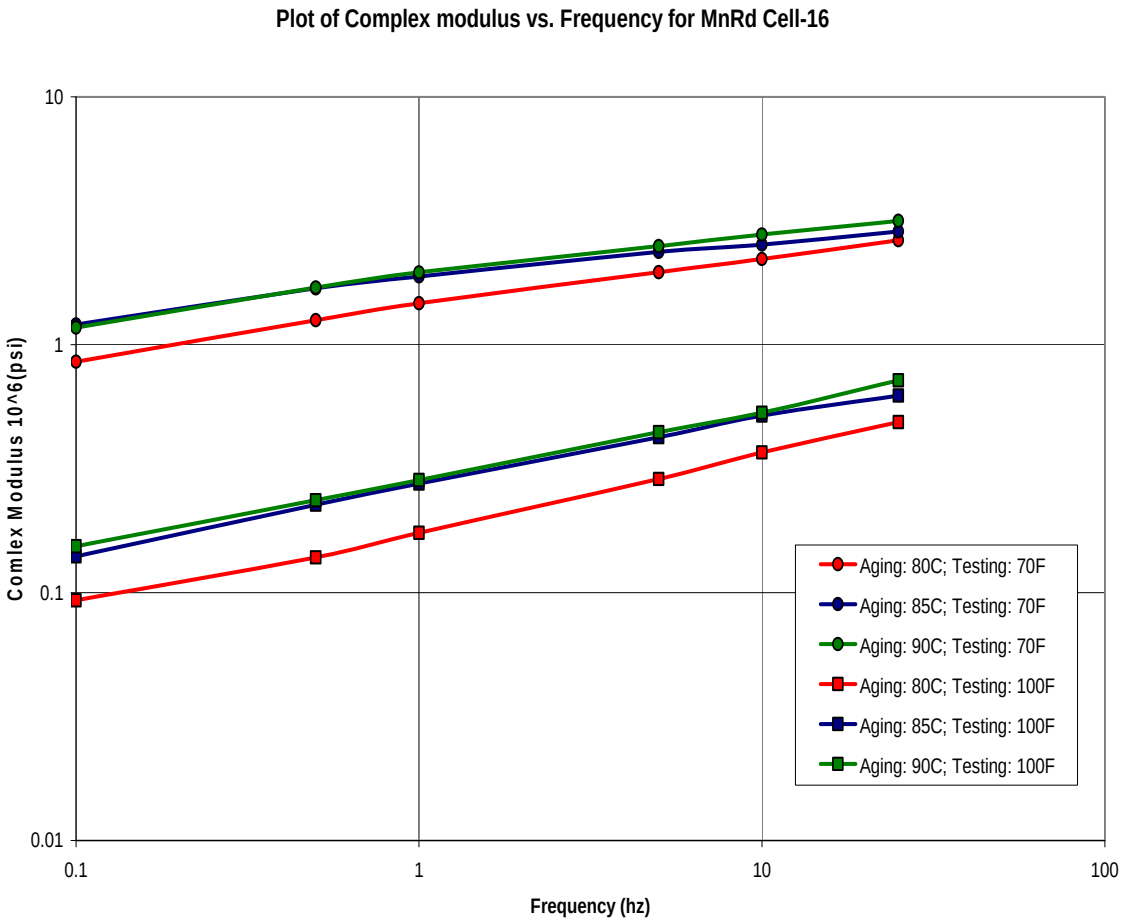

Figure 146
Plot of Complex Modulus vs. Loading Frequency for MnRoad Cell - 16

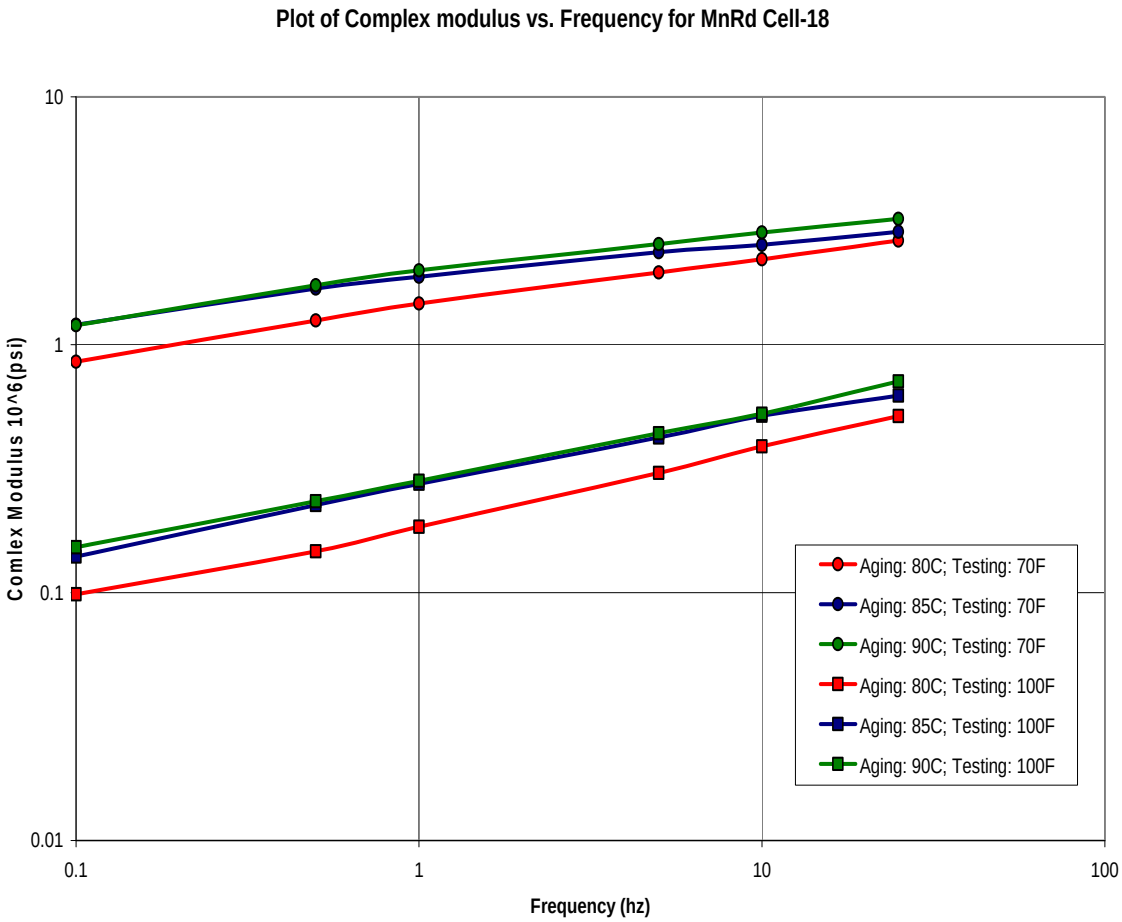

Figure 147
Plot of Complex Modulus vs. Loading Frequency for MnRoad - Cell 18

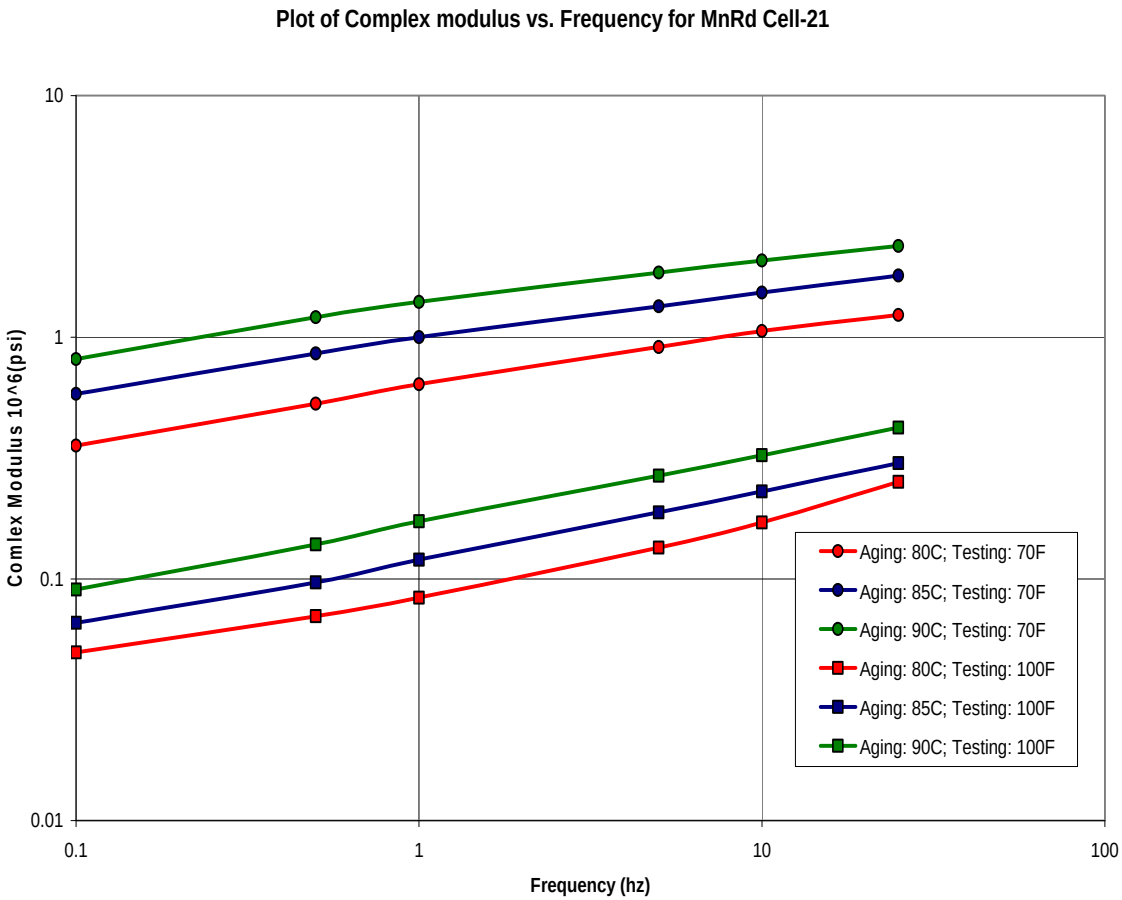

Figure 148
Plot of Complex Modulus vs. Loading Frequency for MnRoad - Cell 21

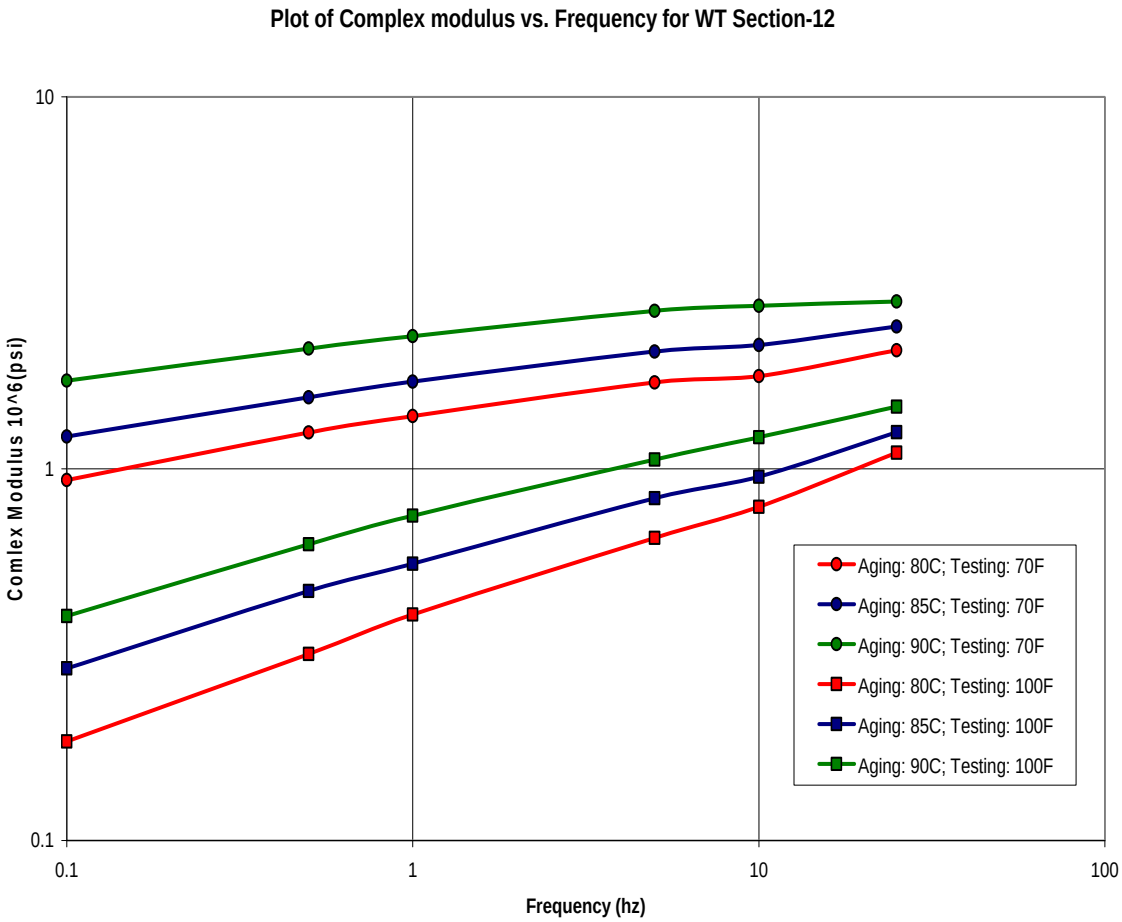

Figure 149
Plot of Complex Modulus vs. Loading Frequency for WesTrack Section 12

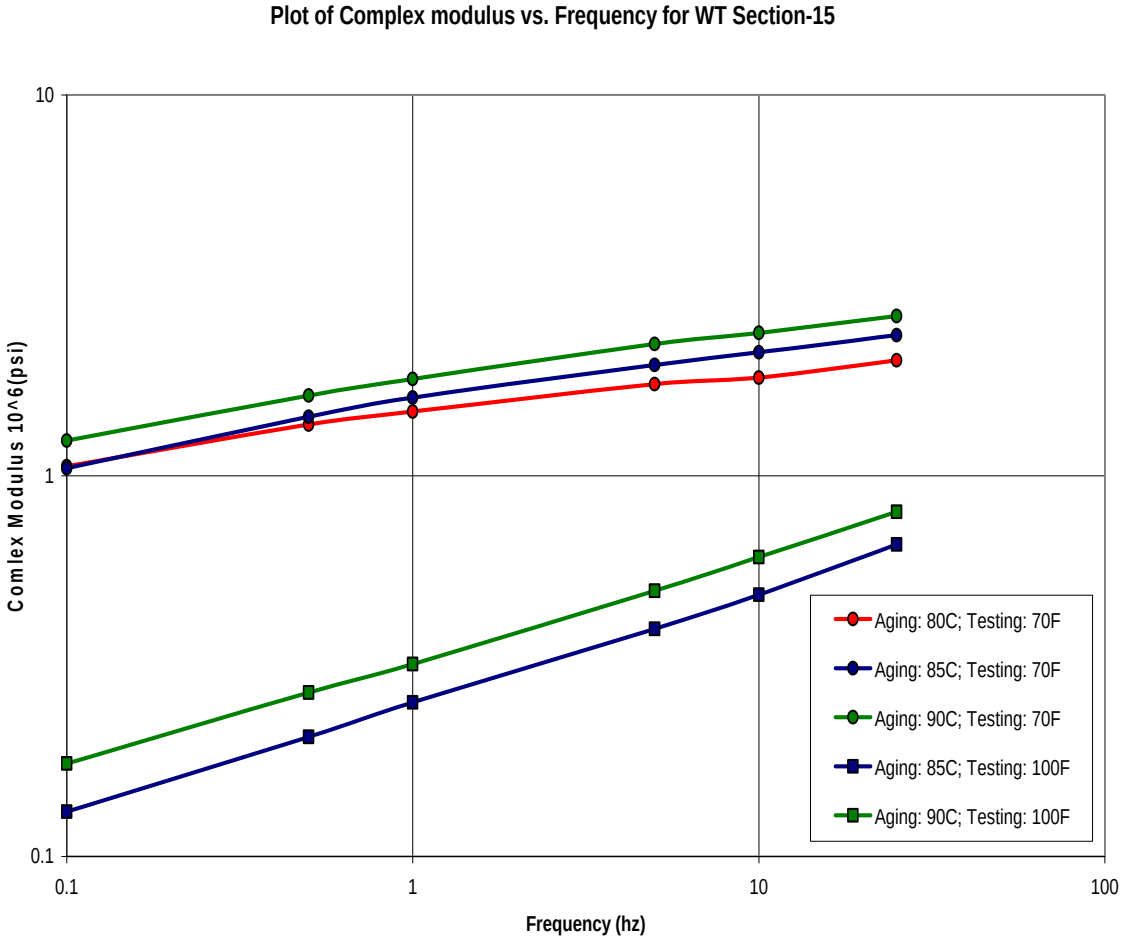

Figure 150
Plot of Complex Modulus vs. Loading Frequency for WesTrack Section 15

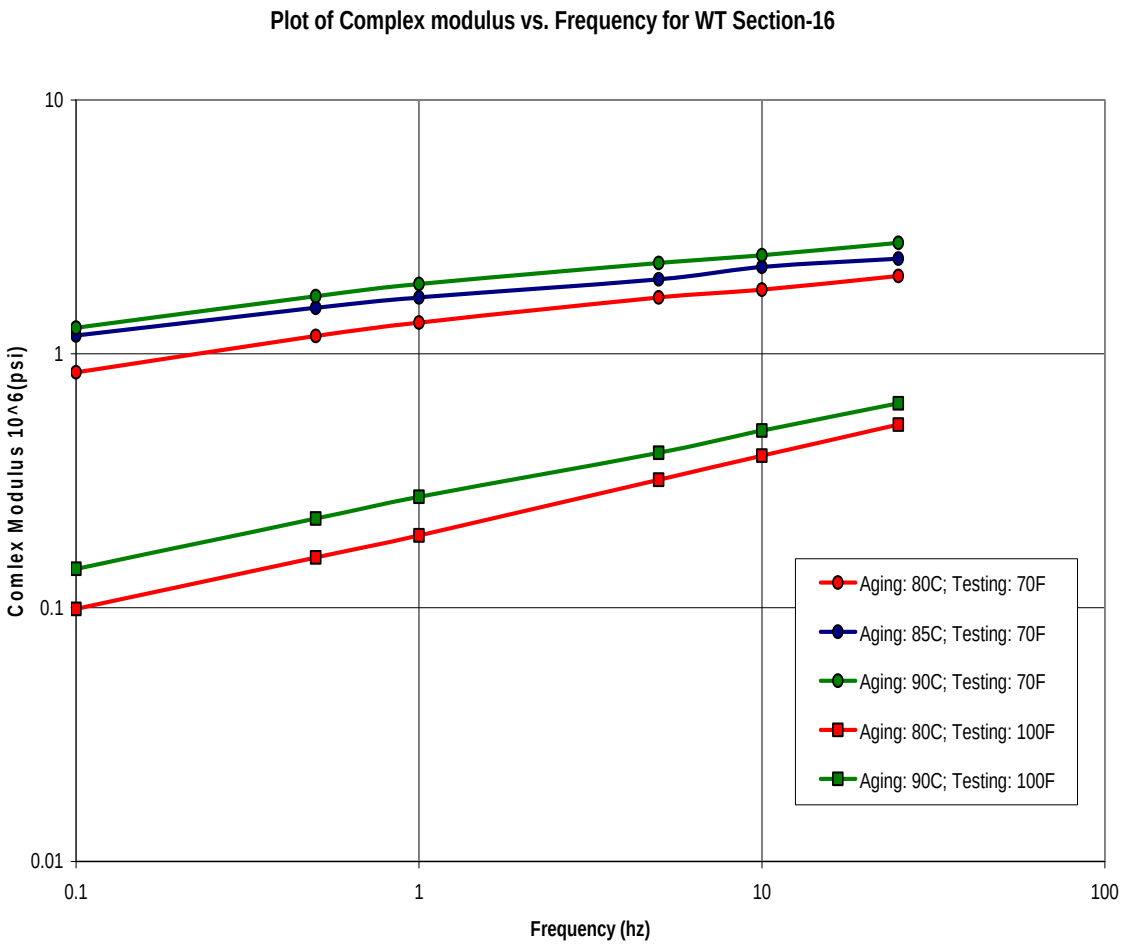

Figure 151
Plot of Complex Modulus vs. Loading Frequency for WesTrack Section 16

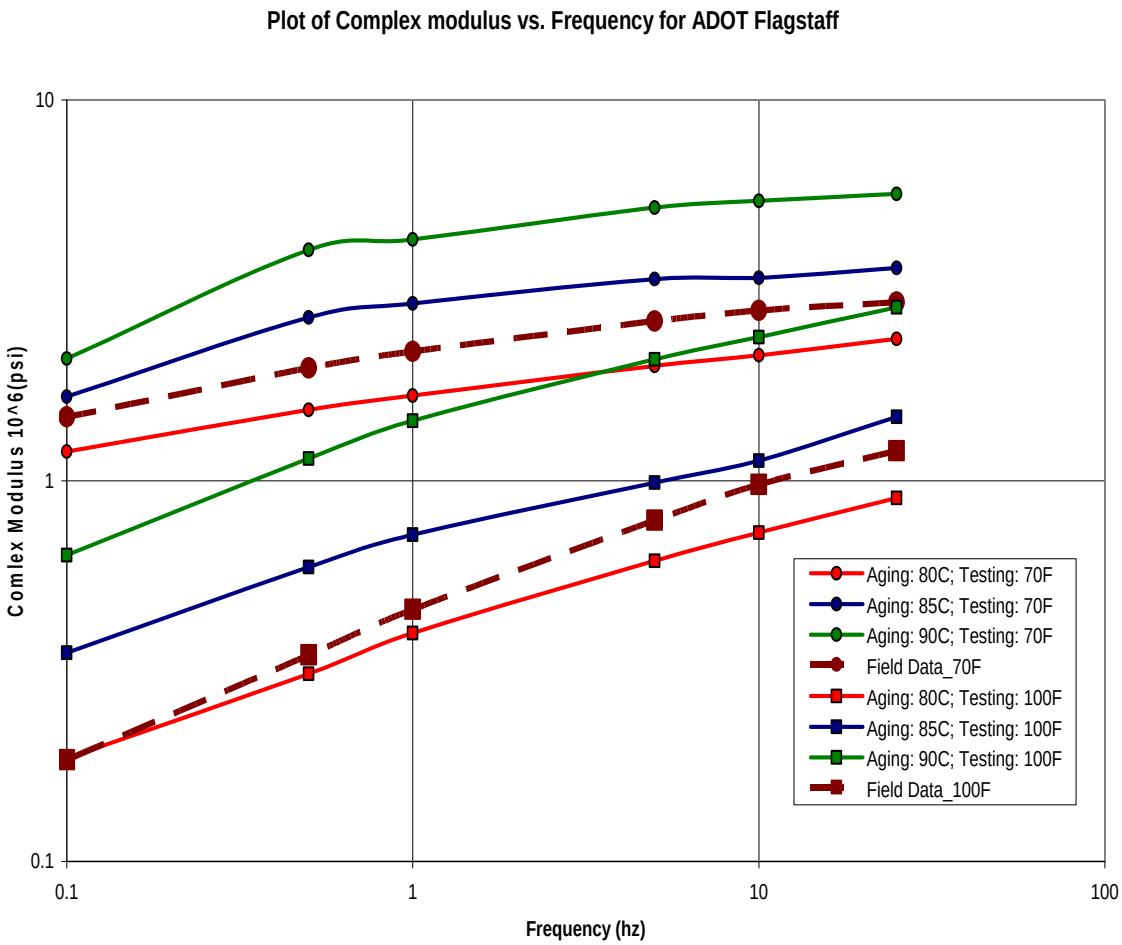

Figure 152
E* Comparison of Lab-aged and Field-aged Cores for ADOT, Flagstaff

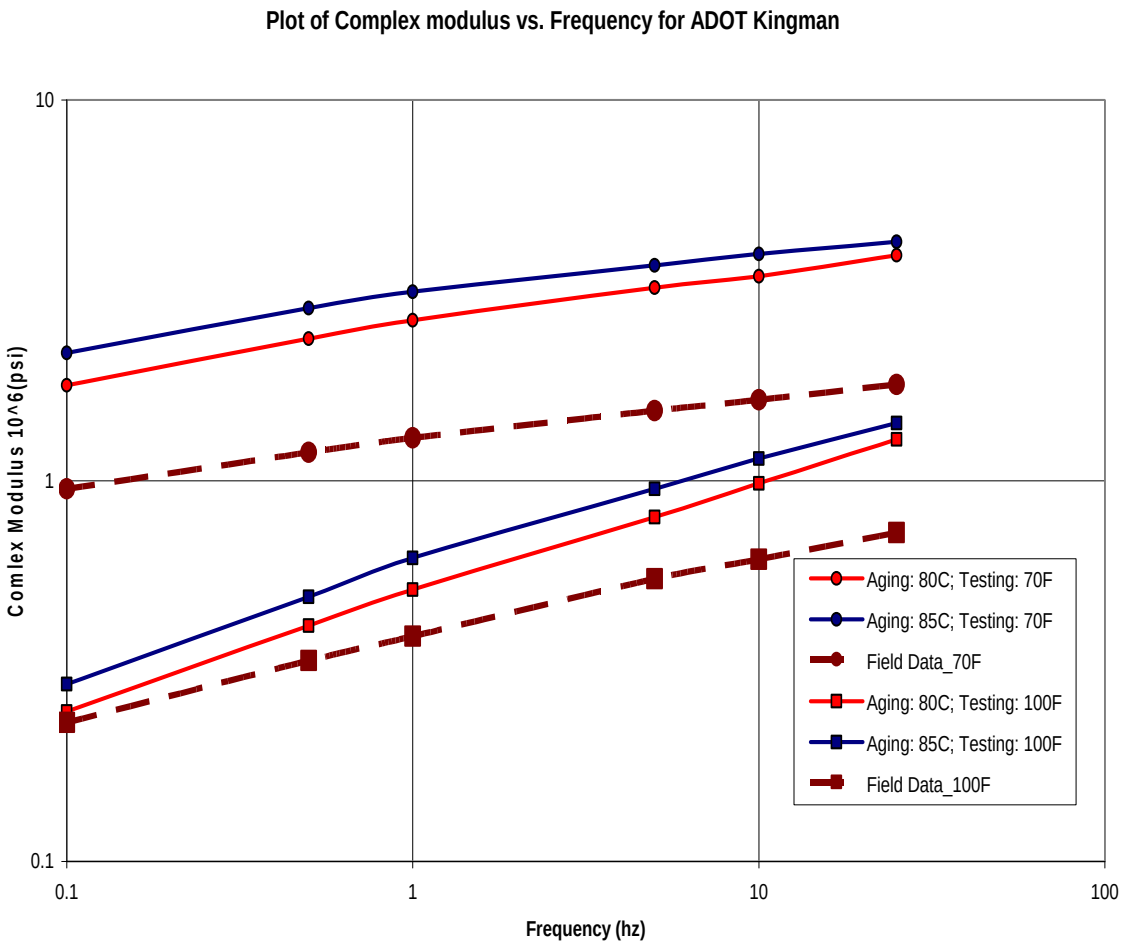

Figure 153
E* Comparison of Lab-aged and Field-aged Cores for ADOT, Kingman

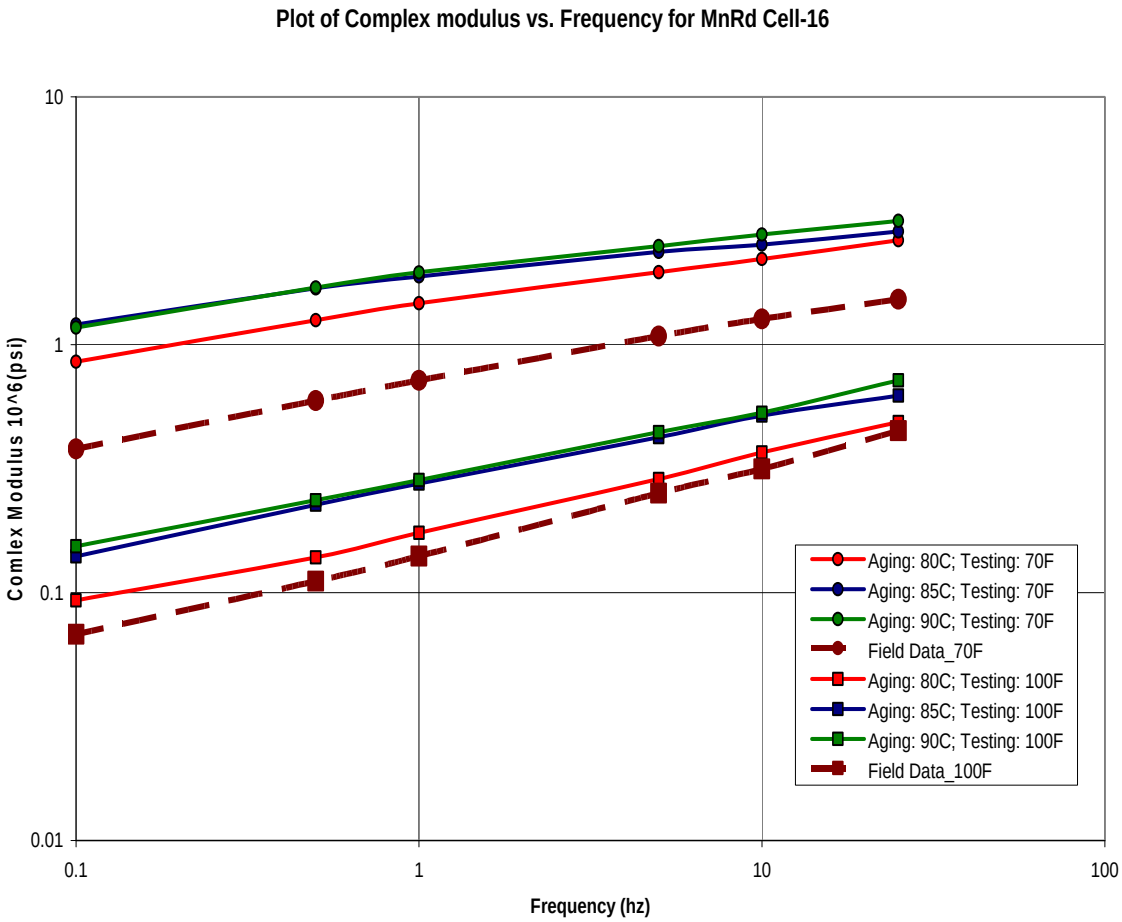

Figure 154
E* Comparison of Lab-aged and Field-aged Cores for MnRoad - Cell 16

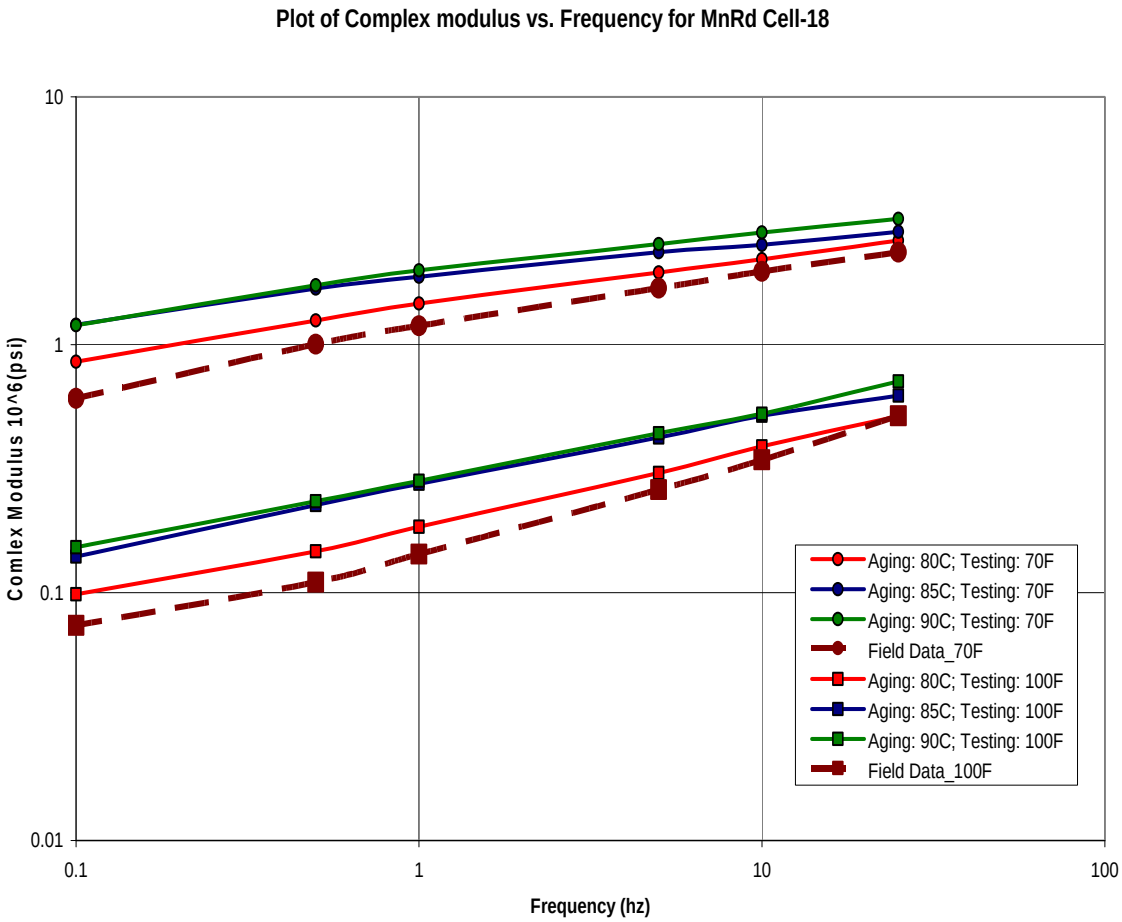

Figure 155
E* Comparison of Lab-aged and Field-aged Cores for MnRoad - Cell 18

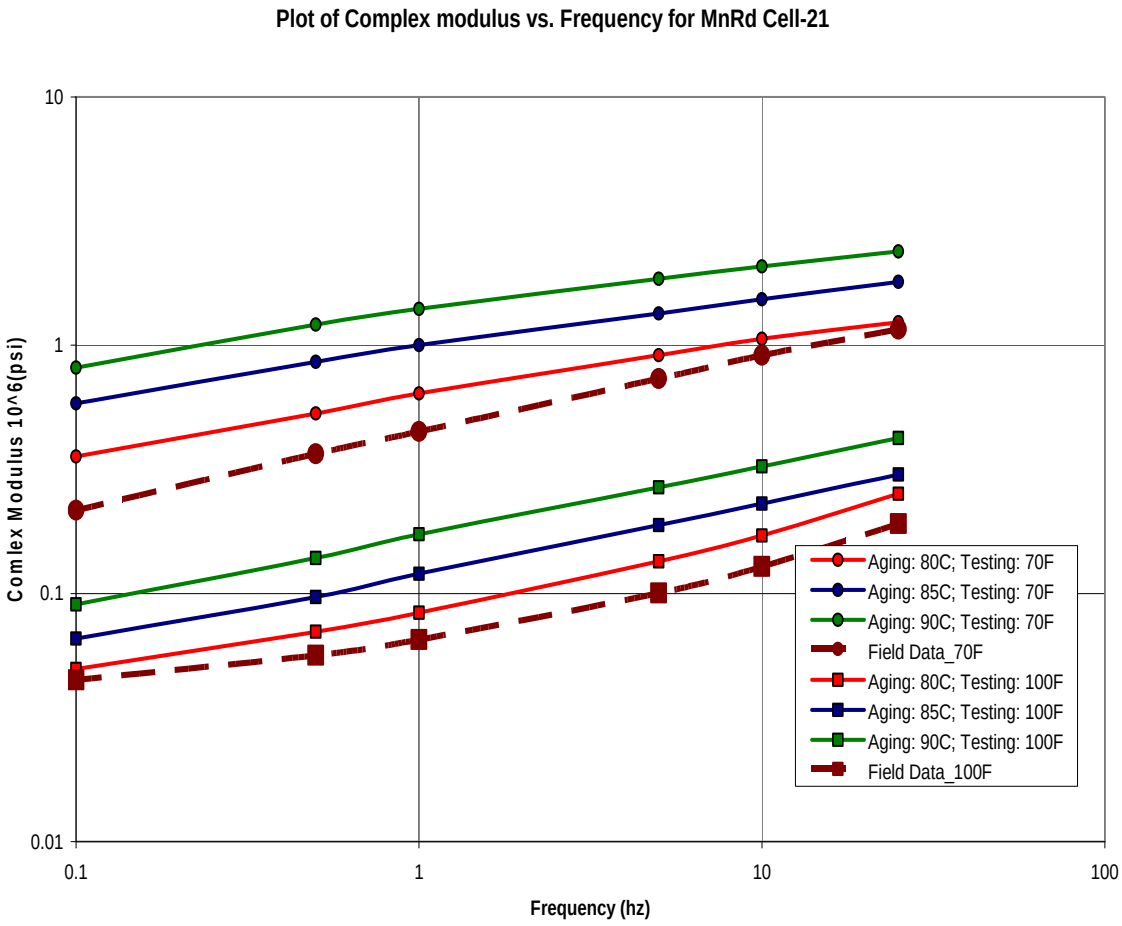

Figure 156
E* Comparison of Lab-aged and Field-aged Cores for MnRoad - Cell 21

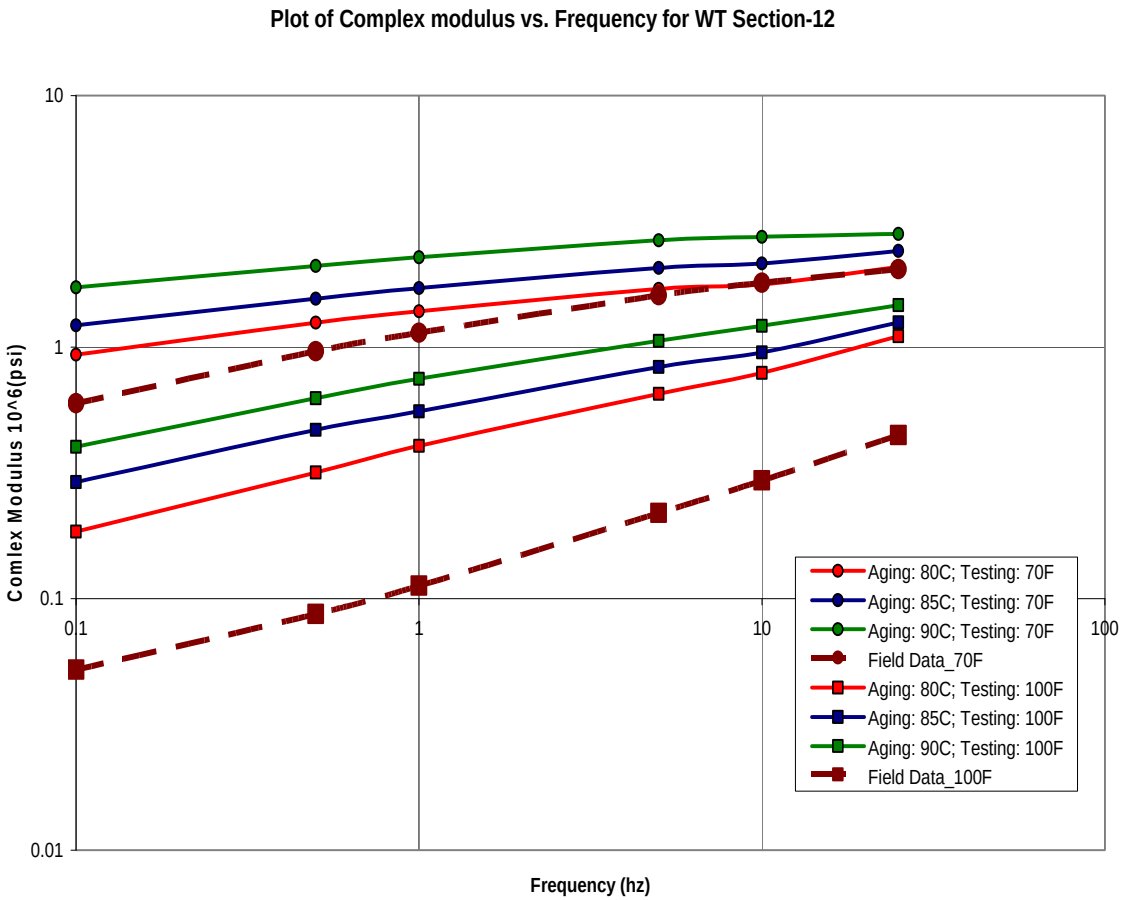

Figure 157
E* Comparison of Lab-aged and Field-aged Cores for WesTrack Section 12

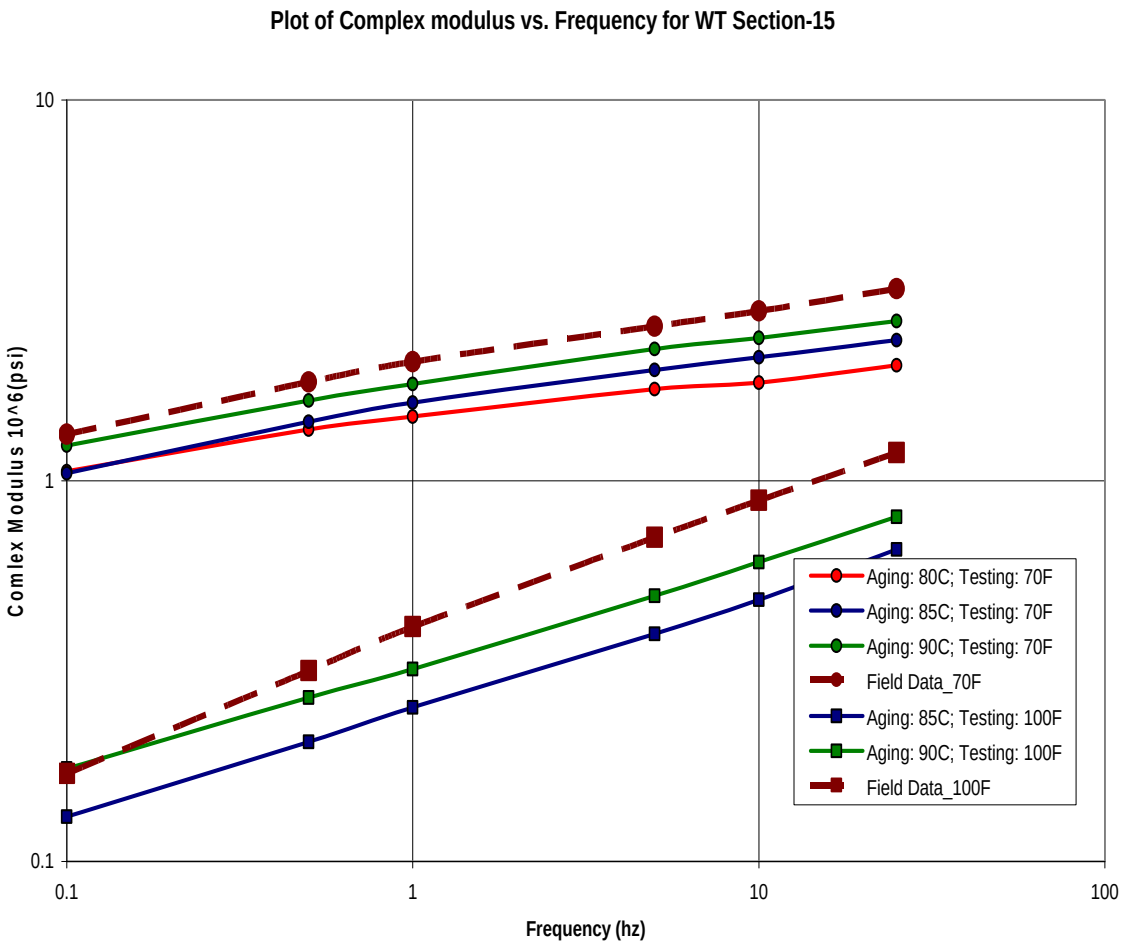

Figure 158
E* Comparison of Lab-aged and Field-aged Cores for WesTrack Section 15

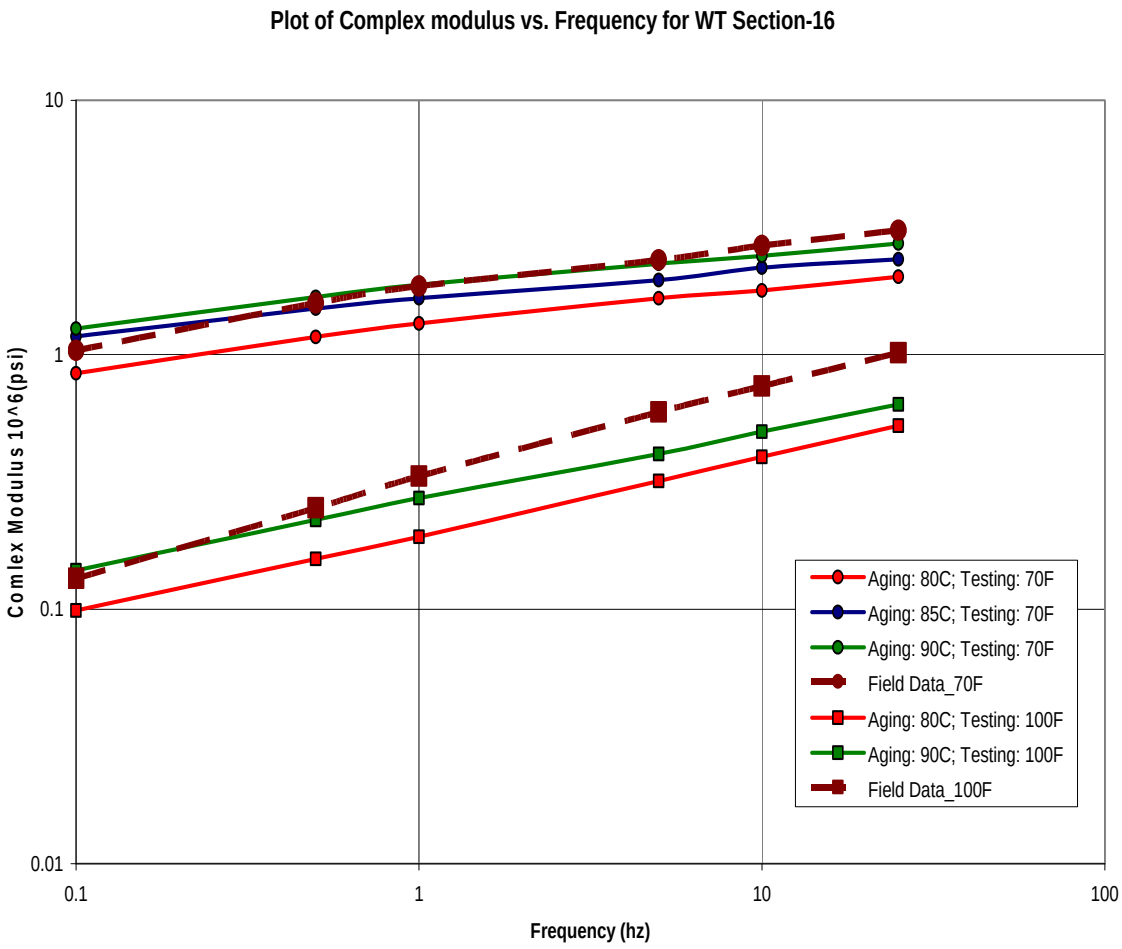

Figure 159
E* Comparison of Lab-aged and Field-aged Cores for WesTrack Section 16

CHAPTER 12

CONCLUSION AND RECOMMENDATIONS FOR FUTURE RESEARCH WORK ON PP2-99 PROTOCOL

In the last fifty years, a significant amount of research has been focused upon the use and behavior of asphalt cements/mixes within pavement applications. While enormous advances have been made in the general state of the art; the problem of asphalt mix durability and its tendency to age (harden) with time due to oxidation in both the plant mix process and in-service conditions remain one area where further studies are warranted.

Hardening, or aging of the original asphalt cement binder or the asphalt mix, due to the plant mix/laydown process (sometimes referred to as short term aging) and normal in-situ aging (sometimes referred to as long term aging) are extremely complex phenomena due to the numerous factors which influence the rate of aging for any particular construction project. One of the most complex factors affecting aging is the chemical composition of the original asphalt cement itself. While asphalt cements have historically been "graded" by specifications based on ranges or groupings of consistency values at one or more temperatures; two or more asphalt cements having similar "grades" or "consistency values" may have entirely different chemical compositions resulting from differences in crude oil source, refining process and levels of additives (volatile oils) present. In addition, the complexity in aging rates is amplified during the mixing process by such factors as mix type, mixing temperature and time, as well as the general type of plant (batch versus continuous).

Long-term aging is a complex process and is influenced by several factors. Among the various factors responsible for in-situ aging, mix properties and environmental factors are among the critical ones that need to be considered when simulating the aging behavior in the laboratory. Warmer temperatures are generally associated with increased rates of oxidation, all other factors being identical. Similarly, higher air voids in the mix will result in higher oxidation rate, because more mix is in contact with the circulating air. In addition, it is not only the design air voids but also the change in air voids due to traffic that can significantly change the aging characteristics of the mix. This change in air voids can be directly attributed to the mix type and the level of traffic.

While the mechanism of aging is complex and is not fully accounted with the current state of knowledge, its impact upon pavement performance is generally understood. The short and long term aging processes result in a hardening of the asphalt cement binder with time. Thus, the overall response (i.e. dynamic modulus) of the asphalt mixture also gradually increases in rigidity with time. This in turn, leads directly to a variable set of changing stress, strain and deflection patterns within the pavement structure as the pavement system "ages". As the asphalt mix becomes more rigid with the aging process,

an increased susceptibility to cracking and fracture occurs. This cracking or fracture helps in the development of other distress types, which may ultimately lead to failure of the pavement system.

Because of the importance of aging and its close relationship to the durability of asphalt cements or asphalt mixes, it is a major concern of asphalt technologists. In view of this, Strategic Highway Research Program (SHRP) proposed a procedure to simulate long-term aging of the asphalt mixes in the laboratory. The approach was later adopted by AASHTO under Protocol PP2-99; "Standard Practice for Mixture Conditioning of Hot Mix Asphalt". According to the existing protocol (AASHTO Designation: PP2-99), the proposed procedure ages the asphalt mixes in the laboratory corresponding to 7 to 10 years of aging in field. In this procedure, mix properties and environmental factors are not taken into account. Inability to account for the mix properties and environment has prompted this research effort.

The major objective of this study has been directed towards the verification of the approach developed under the Strategic Highway Research Program (SHRP) to simulate long-term aging of the asphalt mixes. In addition, make recommendations for future research required for the improvement of the existing protocol, if the current research fails to verify the exiting protocol.

In order to fulfill the objectives of this study, the verification for the long-term age hardening of the asphalt mix (Protocol PP2-99) was carried out in a similar manner as in the case of PP1-98. Field samples were obtained from three sites in the United States. The sites selected were Arizona, Minnesota (MnRoad) and Nevada (WesTrack). These sites were selected as they represented a broad range of environmental conditions. In addition, all these sections were constructed with strict quality control standards and further; each site had multiple sections representing different binder and mix properties. Based upon the laboratory work carried out, the following conclusions were made.

CONCLUSION

1. The sites selected were considered to be sufficient for verification purposes, but were not enough to develop or modify the existing laboratory process to simulate the age hardening behavior in the laboratory. This was due to the observed variability in the data from these sites and the inability to account for all the significant variables. However, research carried out did meet the required objective to verify the existing protocol (AASHTO Designation: PP2-99).
2. Plant mixes obtained from the three sites were compacted in the laboratory and were aged at 80^{o}C, 85^{o}C and 90^{o}C for 5 hours. The laboratory-aged samples were tested at two test temperatures and six loading frequencies for Complex modulus evaluation. For all the mixes tested, increased in the aging temperature resulted in higher Complex modulus values. This result was expected, as higher temperatures will result in relatively more aging and thus increase in the mix stiffness. Based upon this observation, it can be concluded that warmer climates

will result in more aging compared to the cooler climatic regions. This result contradicts the existing protocol that requires only one standard aging temperature to simulate the aging condition irrespective of the climatic region.

3. In general, the laboratory aged samples resulted in higher stiffness compared to field aged samples. This may be due to the fact that more pronounced stiffness profile existed in the field samples compared to the laboratory-aged samples. That is, aging or hardening in the field is more pronounced at the surface because the asphalt mix is in direct contact with the air resulting in higher rate of hardening and thus lower effective stiffness of the entire core. In case of the laboratory cores, aging profile is relatively more uniform resulting in hardening of the entire sample. This resulted in higher stiffness of the laboratory cores.
4. The existing protocol (PP2-99) suggests that laboratory aging corresponds to 7 to 10 years of aging in field irrespective of the environmental and mix properties. For this study all sites selected were 7-10 years and the air voids varied from 4 percent to 12 percent. Based on the limited data collected, it was observed that in most situations the laboratory stiffness values were higher than the field stiffness except for the WesTrack sections that had 8 and 12 percent air voids. This result suggests that for air voids less than 8 percent the laboratory aging is more severe compared to field aging. On the other hand, higher air voids resulted in more severe field aging, which in time resulted in higher stiffness for the field samples compared to laboratory prepared samples. Based on this observation, it can be concluded that a simple linear relationship may not exist for the air voids between the field samples and samples that are compacted in the laboratory to simulate field aging. It should be realized that in the existing protocol, the laboratory samples were all compacted approximately at the initial design air voids content.
5. Based upon the work carried out under this research study, it can be concluded that the existing protocol is not sufficient to accurately predict the aging of asphalt mixes in the field. As a minimum, the samples prepared should be a function of environmental conditions and some parameters that describe the mix properties.

RECOMMENDATIONS FOR FURTHER RESEARCH

1. As suggested, modifications to the existing protocol are needed to more accurately predict the aging characteristics of the asphalt mixes in the laboratory as the existing protocol is not sufficient to simulate the age hardening in the laboratory. Detailed analyses and additional data are needed from controlled field site/sections. The data obtained from the specific sites should be preferably taken at different intervals of time. For this study, verification of the existing protocol was based upon the cores obtained at one time that corresponded to an aging time between 7 to 10 years.
2. Due to the stiffness profile that exists in the field, it is recommended that the aging prediction should be a function of the thickness of the asphalt layer. That is, thicker pavements will result in less effective modulus compared to the thin layers that are more uniformly aged with depth. For example, a 50 mm thick asphalt layer will age differently than a 150 mm asphalt layer under the same

conditions. Thus, the laboratory simulation procedure should account for the asphalt layer thickness in the laboratory simulation process.

3. Air voids is a critical factor that needs to be considered when upgrading the protocol to simulate the long-term field aging of the asphalt mixes. The sites selected for further variations should include sections with wider range in air voids values than the one used in the current study. This is necessary since the behavior of the asphalt mix might change beyond a certain air voids level. It was further found that field stiffness values were generally larger than the laboratory compacted samples for air voids level greater than 8 percent. A reverse phenomenon was observed for air voids less than 8 percent.
4. The study was only carried out for conventional asphalt binders. It is recommended that future studies include modified asphalts such as polymer modified and rubber asphalt. In addition, Reclaimed Asphalt Pavement (RAP) should also be part of future studies as the use of modified asphalts and RAP is probably going to increase with time to meet future transportation needs.

REFERENCES

1. Mirza, M. W., and Witczak, M.W. Development of a Global Aging System for Short and Long Term Aging of Asphalt Cements. *Journal of the Association of the Asphalt Paving Technologists*, Vol. 64, 1995, pp. 393-424.
2. NCHRP 9-23. Environmental Effects in Pavement Mix and Structural Design Systems. Interim Report, August 2001.
3. Dickson, E. J. The hardening of Middle East Petroleum Asphalts in Pavement Surfacing. *Journal of the Association of Asphalt Paving Technologists*, Vol. 49, 1980, pp. 30-63.
4. Corbett, L. W., and Merz, P. E. Asphalt Binder Hardening in the Michigan Test Road After 18 Years of Service. *Transportation Research Record 544*, TRB, National Research Council, Washington, D.C., 1975.
5. Hubbard, P., and Gollomb, H. The Hardening of Asphalt with Relation to the Development of Cracks in Asphalt Pavements. *Journal of the Association of Asphalt Paving Technologists*, Vol. 9, 1937, pp. 165-194.
6. AASHTO. *Provisional Standards, May 1999 Interim Edition*. American Association of State Highway and Transportation Officials, Washington, D.C., 1999.
7. Price, R. P., and Burati, Jr., J.L. A Quantitative Method Using HP-GPC to predict Laboratory Results of Asphalt Cement Tests. *Journal of the Association of Asphalt Paving Technologists*, Vol. 58, 1989, pp. 182-219.
8. NCHRP 1-37A. Development of the 2002 Guide for the Design of New and Rehabilitated Pavement Structures. Draft Unpublished, December 2003.
9. Epps, J., Witczak, M., Decker, D., and Acott, M. *Hot Mix Asphalt Visions – 2000 and Beyond*, National Asphalt Pavement Association (NAPA), NAPA Building, 5100 Forbes Blvd. Lanham, Maryland, 2000.
10. Jones, D. R. “An Asphalt Primer: Understanding how the Origin and Composition of Paving-Grade Asphalt Cements Affects their Performance”, SHRP Asphalt Research Program, Technical Memorandum #4, The University of Texas, Austin, Texas.
11. Peterson, J. C. Chemical Composition of Asphalt as Related to Asphalt Durability: State of the Art, Transportation Research Record, No. 999, TRB, National Research Council, Washington D.C., 1984.
12. Plancher, H., Green, E. L. and Petersen, J. C. Reduction of Oxidative Hardening of Asphalts by Treatment with Hydrated Lime – A Mechanistic Study., Proc., Association of Asphalt Paving Technologists, Vol. 45, 1976, pp. 1-24.
13. Schweyer, H.E. and Traxler, R.N. "Separating Asphalt Material, Butanol-Acetone Method," *Oil Journal*, Vol. 52, 1953, pp. 133.
14. Corbett, L.W. "Composition of Asphalt Based on Generic Fractionation Using Solvent Deaphaltering, Elution-Adsorption Chromatography and Densimetric Characterization," *Analytical Chemistry*, Vol. 41, 1969, pp. 576-579.
15. Corbett, L.W. and Schweyer, H. E. "Compositional and Rheology Considerations in Age Hardening of Bitumen," *Proceedings, The Association of Asphalt Paving Technologists*, Vol. 50, 1981, pp. 571-582.

16. Rostler, F.S. and Sternberg, H.W. "Compounding Rubbee with Petroleum Products," *Industrial and Engineering Chemistry*, Vol. 41, 1949, pp. 598-608.
17. Peterson, J.C. "Quantitative Functional Group Analysis of Asphalt Using Differential Infrared Spectrometry and Selective Chemical Reactions – Theory and Application," *Transportation Research Record*, No. 1096, TRB, National Research Council, Washington D.C., 1986, pp. 1-11.
18. Corbett, L.W. "Relationship between Composition and Physical Properties of Asphalt." *Proceedings, The Association of Asphalt Paving Technologists*, Vol. 39, 1970, pp. 481-491.
19. Traxler, R. N. and Schweyer, H. E. "How to Make Component Analysis," Oil and Gas Journal, 52, 158 (1953).
20. Traxler, R. N. "Relation Between Hardening and Composition of Asphalt," American Chemical Society, Division of Petroleum Chemistry, 5, A71-A77 (1960).
21. Rostler, F. S. and White, R. M. "Influence of Chemical Composition of Highway Asphalts, 85-100 Penetration Grade", *Proceedings, The Association of Asphalt Paving Technologists*, Vol. 31, 1962, pp. 35-89.
22. Bullin, J. A., Davison, R. R., Glover, C. J., Chaffin, J., Liu, M. and Madrid, R. "Development of Superior Asphalt Recycling Agents – Final Technical Progress Report". U.S. Department of Energy, Office of Industrial Technologies, Washington DC, 1997.
23. Corbett, L. W. and Merz, P. E. "Asphalt Binder Hardening in the Michigan Test Road After 18 Years of Service", Transportation Research Board, 544, 1975, pp. 27-34.
24. Petersen, J. C., Branthaver, J. F., Robertson, R. E., Harnsberger, P. M., Duvall, J. J. and Ensley, E. K. "Effect of Physicochemical Factors on Asphalt Oxidation Kinetics", Transportation Research Record, 1391, 1993, pp. 1-10.
25. Lau, C. K., Lunsford, K. M., Glover, C. J., Davison, R. R. and Bullin, J. A. "Reaction Rates and Hardening Susceptibilities as Determined from POV Aging of Asphalts", Transportation Research Record, 1342, 1992, pp. 50-57.
26. Lunsford, K. M. "The Effect of Temperature and Pressure on Laboratory Oxidized Asphalt Films with Comparison to Field Aging", PhD Dissertation, Texas A&M University, Department of Chemical Engineering, College Station, TX, 1994.
27. Bright, R. and Reynolds, E.T. "Effect of Mixing Temperature on Hardening of Asphalt binder in Hot Bituminous Concrete", *Highway Research Board*, Bulletin No. 333, 1962.
28. Lund, J. W. and Wilson, J. E. "Evaluation of Asphalt Aging in Hot Mix Plants," *Proceedings, The Association of Asphalt Paving Technologists*, Vol. 53, 1984, pp. 1-18.
29. Price, R.P. and Burati, Jr, J.L. "A Quantitative Method Using HP-GPC to predict Laboratory Results of Asphalt Cement Tests," *Proceedings, The Association of Asphalt Paving Technologists*, Vol. 58, 1989, pp. 182-219.

30. Kemp, G.N. and Predoehl, N.H. “A Comparison of Field and Laboratory Environments on Asphalt Durability,” *Proceedings, The Association of Asphalt Paving Technologists*, Vol. 50, 1981, pp. 492-537.
31. Zube, E. and Shok, J. "Final Report on Zaca-Wigmore Asphalt Test Road", *Proceedings, The Association of Asphalt Paving Technologists*, Vol. 38, 1969, pp. 1-38.
32. The Asphalt Institute, "Research and Development of The Asphalt Institute's Thickness Design Manual," Research Report No. 82-2, Manual Series No. 1 (MS-1), Ninth Edition, August 1982.
33. Hubbard, P. and Gollomb, H. "The Hardening of Asphalt with Relation to the Development of Cracks in Asphalt Pavements," *Proceedings, The Association of Asphalt Paving Technologists*, Vol. 9, 1937, pp. 165-194.
34. Lewis, R.H. and Welborn, J.Y. "A Study of the Effect of Characteristics of Asphalt on the Physical Properties of Bituminous Mixtures," *Proceedings, The Association of Asphalt Paving Technologists*, Vol. 17, 1948, pp. 228-263.
35. Kandhal, P.S. and Koehler, W.C. "Significant Studies on Asphalt Durability: Pennsylvania Experience," *Transportation Research Record*, No. 999, TRB, National Research Council, Washington D.C., 1984, pp. 41-50.
36. Petersen, J. C. "A Thin Film Accelerated Aging Test for Evaluating Asphalt Oxidative Aging”, *Proceedings, The Association of Asphalt Paving Technologists*, Vol. 58, 1989, pp. 220-237.
37. Lee, D. Y. "Asphalt Durability Correlation in Iowa", Highway Research Board, Record 468, 1973, pp. 43-60.
38. Vallerga, B. A., Monismith, C. L. and Granthem, K. "A Study of Some Factors Influencing the Weathering of Paving Asphalt", *Proceedings, The Association of Asphalt Paving Technologists*, Vol. 26, 1957, pp. 126-150.
39. Hugo, F. and Kennedy, T. W. "Surface Cracking of Asphalt Mixtures in Southern Africa", *Proceedings, The Association of Asphalt Paving Technologists*, Vol. 54, 1985, pp. 454-501.
40. Quintus, H. V., Scherocman, J., Kennedy, T. and Hughes, C. S. "Asphalt Aggregate Mixture Analysis System", Final Report NCHRP, 1988.
41. Kumar. A. and Goetz, W. H. "Asphalt Hardening as Affected by Film Thickness, Voids and Permeability in Asphaltic Mixtures", *Proceedings, The Association of Asphalt Paving Technologists*, Vol. 46, 1977, pp. 571-605.
42. Kim, O. K., Bell, C. A., Wilson, J. and Boyle, G. "Effect of Moisture and Aging on Asphalt Pavement Life, Part 2 – Effect of Aging", FHWA-OR-RD-86-01-2, Final Report to Oregon Department of Transportation and Federal Highway Administration, 1986.
43. Hveem, F. N., Zube, E. and Skog, J. "Proposed New Tests and Specifications for Paving Grade Asphalts", *Proceedings, The Association of Asphalt Paving Technologists*, Vol. 32, 1963, pp. 247-327.
44. Tia, M., Ruth, B. E., Charai, C. T., Shiau, J. M., Richardson, D. and Williams, J. "Investigation of Original and In-Service Asphalt Properties for the Development of Improved Specifications – Final Phase of Testing and Analysis", Final Report,

Engineering and Industrial Experiment Station, University of Florida, Gainesville, FL, 1988.
45. Andrei, D., Witczak, M. W. and Mirza, M. W. "Development of a Revised Predictive Model for the Dynamic (Complex) Modulus of Asphalt Mixtures", Development of the 2002 Guide for the Design of New and Rehabilitated Pavement Structures – Inter Team Technical Report, University of Maryland, 1999.
46. Rada, G. R., Elkins, G. E. Henderson, B., Van Sambeek, R. J. and Lopez, Jr., A. FHWA-RD-94-110, LTPP Seasonal Monitoring Program: Instrumentation Installation and Data Collection Guidelines, April 1994, United States Department of Transportation, Federal Highway administration
47. Galal, K. A., White, T. D. and Hand, A. J. Second Phase Study of Changes in In-Service Asphalt. *Joint Transportation Research Program*. Purdue University, Indiana, 2000.
48. Burr, B. L., Glover, C. J., Davison, R. R. and Bullin, J.A. New Apparatus and Procedure for the Extraction and Recovery of Asphalt Binder from Pavement Mixtures. *Transportation Research Record 1391*, TRB, National Research Council, National Academy Press, Washington, D.C., 1993.
49. Burr, B. L., Davison, R. R, Glover, C. J. and Bullin, J. A. Solvent Removal from Asphalt. *Transportation Research Record 1269*, TRB, National Research Council, Washington, D.C., 1990.
50. Andrei, D., Witczak, M. W. and Mirza, M. W. Development of a Revised Predictive Model for the Dynamic (Complex) Modulus of Asphalt Mixtures. *NCHRP 1-37A Inter Team Technical Report*, University of Maryland, College Park, Maryland, 1999.
51. LTPPBIND Version 2.1. A Software for Determining SUPERPAVE Performance Grades Based on LTPP and SHRP Pavement Temperature Models and Data from 7928 Weather Stations in North America. FHWA, Turner – Fairbank Highway Research Center, Virginia, 1999.